The Effect of Loading Frequency on Tenocyte Metabolism

Chineye Princess Udeze-Jyambere

Submitted in partial fulfilment of the requirements of the
Degree of Doctor of Philosophy

SUPERVISORY TEAM: Prof. Hazel Screen
Dr. Dylan Morrissey
Dr. Graham Riley

May 2017

Queen Mary University of London
School Of Engineering and Material Science

An orthopaedic research UK supported project

STATEMENT OF ORIGINALITY

I, Chineye Princess Udeze-Jyambere, confirm that the research included within this thesis is my own work or that where it has been carried out in collaboration with, or supported by others, that this is duly acknowledged below and my contribution indicated. Previously published material is also acknowledged below.

I attest that I have exercised reasonable care to ensure that the work is original, and does not to the best of my knowledge break any UK law, infringe any third party's copyright or other Intellectual Property Right, or contain any confidential material.

I accept that the College has the right to use plagiarism detection software to check the electronic version of the thesis.

I confirm that this thesis has not been previously submitted for the award of a degree by this or any other university.

Signature: C.P. Udeze-Jyambere

Date: 22/12/2016

ACKKNOWLEDGEMENTS

I would like to appreciate my supervisor, Professor Hazel Screen, for her guidance, support, encouragement and faith in my abilities. I could not have asked for a more dedicated supervisor, whose support has allowed me to develop as a researcher. Her enthusiasm, depth of knowledge and ability to stay on top of things despite her busy schedule never ceases to amaze me. She is an inspiration.

I would also like to thank Orthopaedic Research UK for funding this research project and thank all the collaborators involved. I would also like to thank Graham Riley and Eleanor Jones, University of East Anglia, UK, for your guidance and help in performing gene expression analysis and analysing the data.

I would like to appreciate my husband, Pierre Jyambere, for his utmost support, encourage and faith in me. I would also like to acknowledge my family for their support. And lastly my friends and colleagues at Queen Mary, University of London, who made every day at Queen Mary an enjoyable experience.

Finally, I would like to dedicate this thesis to my God, for His wisdom, knowledge, grace and favour all the way. I am forever grateful.

ABSTRACT

Achilles tendinopathy is a prevalent, highly debilitating condition. It is believed to result from repetitive overuse, which creates micro-damage tendon, and initiates a catabolic cell response. The aetiology of tendinopathy remains poorly understood, therefore appropriate treatment remains unclear.

Current data support the use of shock wave therapy and eccentric exercise as some of the more effective treatment options for tendinopathy. Studies have shown that these treatments generate perturbations within tendon at a frequency of approximately 8-12Hz. Consequently, it is hypothesised that 10Hz loading initiates increased anabolic tenocyte behaviour promoting tendon repair. The primary aim of this thesis is to investigate the effects of 10Hz perturbations on tenocyte metabolism, comparing tenocyte gene expression in response to a 10Hz and 1Hz loading profile.

A variety of *in vitro* models for mechanically stimulating cells were explored, comparing tissue explants with isolated cells on a 2D or within a 3D collagen gel. The mechanical environment of each model was investigated, in addition to cell viability and gene stabilisation following strain, as needed for future cell studies. 3D collagen gels arose as the most suitable model. Human tenocytes from healthy semitendinosus and tendinopathic Achilles tendons were seeded into 3D collagen gels and subjected to cyclic strain at 10Hz and 1Hz to establish cell response. Tenocyte gene expression was characterised using qRT-PCR.

Healthy tenocytes showed increased expression of all analysed genes in response to loading. Furthermore, the increase was significantly larger in the 10Hz loading group. Tendinopathic tenocytes showed a more varied response, possibly indicative of an early healing response. Nevertheless, the response to 10Hz loading was consistently greater than seen with 1Hz loading. Analysis of the signalling pathways involved suggested that the IL1 signalling pathway may be involved in the strain response reported.

This study has demonstrated for the first time that loading at a frequency of 10Hz may enhance metabolic response in healthy tenocytes.

TABLE OF CONTENTS

LIST OF TABLES

Chapter 1

Chapter 2

Chapter 3

Chapter 4

LIST OF FIGURES

Chapter 1

Chapter 2

Chapter 3

Chapter 4

LIST OF ABBREVIATIONS

18s	18s Ribosomal Ribonucleic Acid
2D	Two Dimensional
3D	Three Dimensional
ACAN	Aggrecan
ADAMTs	A Disintegrin and metalloproteinase with Thrombospondin Motifs
AMH	Anti-Mullerian Hormone
AT	Achilles tendon
ATP	Adenosine Triphosphate
BCA	Bicinchoninic Acid
BDNF	Brain-Derived Neutrophic Factor
bFGF	Basic Fibroblast Growth Factor
BGN	Biglycan
BLC	B-Lymphocyte Chemoattractant
BMRC	Bio-Medical Research Centre
C-terminal	Carboxyl Terminal
cDNA	Complimentary Deoxyribonucleic Acid
Ckβ	Chemokine Beta
COL1A1	Collagen Type I, Alpha 1
COL2A1	Collagen Type II, Alpha 1
COL3A1	Collagen Type III, Alpha 1
COL4A1	Collagen Type IV, Alpha 1
COL5A1	Collagen Type V, Alpha 1
COL6A1	Collagen Type VI, Alpha 1
COL9A1	Collagen Type IX, Alpha 1
COL11A1	Collagen Type XI, Alpha 1
COL12A1	Collagen Type XII, Alpha 1
COL14A1	Collagen Type XIV, Alpha 1
COMP	Collagen Oligomeric Matrix Protein
COX-2	Cyclooxygenase-2
cPLA2	Cytosolic Phospholipase A2

CS	Chondroitin Sulphate
Ct	Cycle Threshold
CTGF	Connective Tissue Growth Factor
DAG	Diacylglycerol
DCN	Decorin
DMEM	Dulbecco's Modified Eagle Medium
DMSO	Dimethyl Sulfoxide
DNA	Deoxyribonucleic Acid
dBTP	Deoxy-nucleotide Triphosphate
DPBS	Dulbecco's Phosphate-Buffered Saline
DS	Dermatan Sulphate
DTT	Dithiothreitol
ECM	Extracellular Matrix
EGF	Epidermal Growth Factor
ENA	Epithelial Neutrophil-Activating Protein
ERK	Extracellular Signal-Regulated Kinase
ES	Energy Storing
ESWT	Extracorporeal Shock Wave Therapy
FACIT	Fibril Associated Collagen with Interrupted Helix
FBS	Fetal Bovine Serum
FGF	Fibroblast Growth Factor
FMOD	Fibromodulin
FN1	Fibronectin
GAG	Glycosaminoglycan
GAPDH	Glyceraldehyde 3-phosphate dehydrogenase
GCP	Granulocyte Chemoattractant Protein
GCSF	Granulocyte Colony Stimulating Factor
GDF	Growth and Differentiation Factor
GDNF	Glial Cell-Line Derived Neurotrophic Factor
GM-CSF	Granulocyte Macrophage Colony Stimulating Factor
GRO	Growth Regulated Oncogene
HEPES	4-(2-hydroxyethyl)-1-piperazineethanesulfonic acid
HGF	Hepatocyte Growth Factor

HS	Heparin/Heparan Sulphate
I-309	Inflammatory Cytokine
IFM	Interfascicular Mattrix
IGF	Insulin Growth Factor
IGFBP	Insulin Growth Factor Binding Protein
IkB	Nuclear Factor Kappa-B Inhibitor
IKKb	Inhibitor of Nuclear Factor Kappa-B Kinase Subunit Beta
IL	Interleukin
IL-1Ra	Interleukin 1 Receptor Antagonist
IL-1RAP	Interleukin-1 Receptor Accessory Protein
IP	Interferon Gamma-Induced Protein
IP_3	Inositol Trisphospate
IRAK	Interleukin-1 Receptor-Associated Kinase
JNK	c-Jun N-terminal Kinases
KOOS	Knee Injury and Osteoarthritis Outcome Score
KS	Keratan Sulphate
LAP	Latency Associated Peptide
LIF	Leukaemia Inhibitory Factor
LLC	Large Latent Complex
LTBP	Latent Transforming Growth Factor Protein
MAPK	Mitogen-Activated Kinases
MCP	Monocyte Chemoattractant Protein
MCSF	Macrophage Colony-Stimulating Factor
MDC	Macrophage –Derived Chemokine
MEM	Minimum Essential Medium
MIF	Macrophage Migration Inhibitory Factor
MIG	Monokine Induce by Interferon
MIP	Macrophage Inflammatory Protein
MKK	Mitogen-Activated Kinase Kinase
MMP	Matric Metalloproteinase
mRNA	Messenger Ribonucleic Acid
mTORC	Mammalian Target of Rapamycin
MYD88	Myeloid Differentiation Primary Response Gene 88

N-terminal	Amino Terminal
NAP	Neutrophil-Activating Protein
NFkB	Nuclear Factor Kappa-B Kinase
NSAIDS	Non-Steroidal Anti-Inflammatory Drugs
NT	Neurotrophin
OPG	Osteoprotegerin
PARC	Pulmonary and Activation-Regulated Cytokine
PC	Plastic Compression
PCR	Polymerase Chain Reaction
PDGF	Platelet-Derived Growth Factor
PEG	Polyethylene Glycol
PGE2	Prostaglandin E2
PBS	Phosphate Buffered Saline
PG	Proteoglycan
PI3K	Phosphoinositol 3-Kinase
PIGF	Placenta Growth Factor
P(LLA-CL)/collagen	Poly(L-Lactide-co-ε-Caprolactone)/Collagen
PRG4	Proteoglycan 4
PS	Penicillin Streptomycin
qRT-PCR	Quantitative Real Time Polymerase Chain Reaction
RANTES	Regulated on Activation, Normal T Cell Expressed and Secreted
RER	Rough Endoplasmic Reticulum
RNA	Ribonucleic Acid
ROCK	Rho/Rho Associated Protein Kinase
rRNA	Ribosomal Ribonucleic Acid
SCF	Stem Cell Factor
SCDF	Stromal Cell-Derived Factor
SCX	Scleraxis
SHC	Src Homology 2 Domain-containing Transforming Protein
SLC	Small Latent Complex
SLRPs	Small Leucine Rich Proteoglycan
SSC	Stretch-Shortening Cycles

TAB	Transforming Growth Factor Beta Activated Kinase Binding Protein
TAK	Transforming Growth Factor Beta Activated Kinase
TARC	Thymus and Activation-Regulated Chemokine
TDSC	Tendon Derived Stem Cell
TGFβ	Transforming Growth Factor Beta
TGFβRI	Inhibitor of Transforming Growth Factor Beta Receptor 1
TIMP	Tissue Inhibitor of Metalloproteinase
TIR	Toll-/Interleukin-1 Receptor
TLDA	Taqman Low Density Array
TNC	Tenascin C
TNF	Tumour Necrosis Factor
TNMD	Tenomodulin
TOLLIP	Toll-Interacting Protein
TOP1	Topoisomerase 1
TRAF6	Tumor Necrosis Factor Receptor-Associated Factor 6
tRNA	Transfer Ribonucleic Acid
Tsp	Thrombospondin
UEA	University of East Anglia
VAS	Visual Analogue Scale
VCAN	Versican
VEGF	Vascular Endothelial Growth Factor
VISA-A	Victorian Institute of Sports Assessment

CHAPTER ONE

BACKGROUND LITERATURE

1.1 INTRODUCTION

Tendons are fibrous connective tissues, composed of cells within a complex extracellular matrix (ECM) containing collagens, glycoproteins and water. Tendons connect muscle to bone and are passive structures concerned with the function of force transmission [Witvrouw et al., 2007]. They can be classified into two major groups, depending on the characteristics of the tendon and type of activities they perform, as either energy storing (ES) tendons or positional tendons [Thorpe et al., 2013a]. Positional tendons are those which simply act to position limbs, while ES tendons are high strain tendons with an additional function to stretch, to store and then release elastic potential energy during locomotion (i.e. running, walking, jumping and hopping). ES tendons are more prone to injury and micro-damage because of their function. They are exposed to higher stresses and strains during use and require a greater ability to stretch and recoil under load to ensure efficient return of stored potential energy [Thorpe et al., 2013b]. The high strains these tendons must withstand makes them prone to highly debilitating and painful injuries known as tendinopathies.

Tendinopathies are a range of diseases associated with impaired tendon function and pain, and represent a substantial proportion of the musculoskeletal injuries referred to general practitioners [Institute of Sport Exercise and Health, 2014]. Although these conditions do not have an immediate risk of mortality, patients suffer with a decrease in quality of life, involving pain and decreased mobility, which lead to numerous other health problems, including cardiovascular disease and obesity. Characteristic symptoms of tendinopathy include chronic pain, swelling, localised tenderness and impaired movement [Koutouris and Cook, 2007; Birch et al., 1998]. Vascular profusion, impingement, trauma and repetitive unequally distributed strain have all been implicated in the development of tendinopathy [Cook and Purdam, 2009]. However, we have very limited understanding of the aetiology and pathophysiology of tendinopathy [Kader et al., 2002]. This makes the condition very difficult to treat, despite an increase in prevalence [Cassel et al., 2014].

1.2 TENDON HIERARCHICAL STRUCTURE AND FUNCTION

Tendon vary widely in shape from wide and flat to cylindrical/rounded cords, encompassing strap-like bands, flattened ribbons and fan shapes [Sharma and Maffulli, 2006; Devkota, 2006]. Tendon contains 60-80% water, while the remaining dry matter is composed mainly of type I collagen that is arranged in a hierarchical structure [Kannus, 2000] (Figure 1.1).

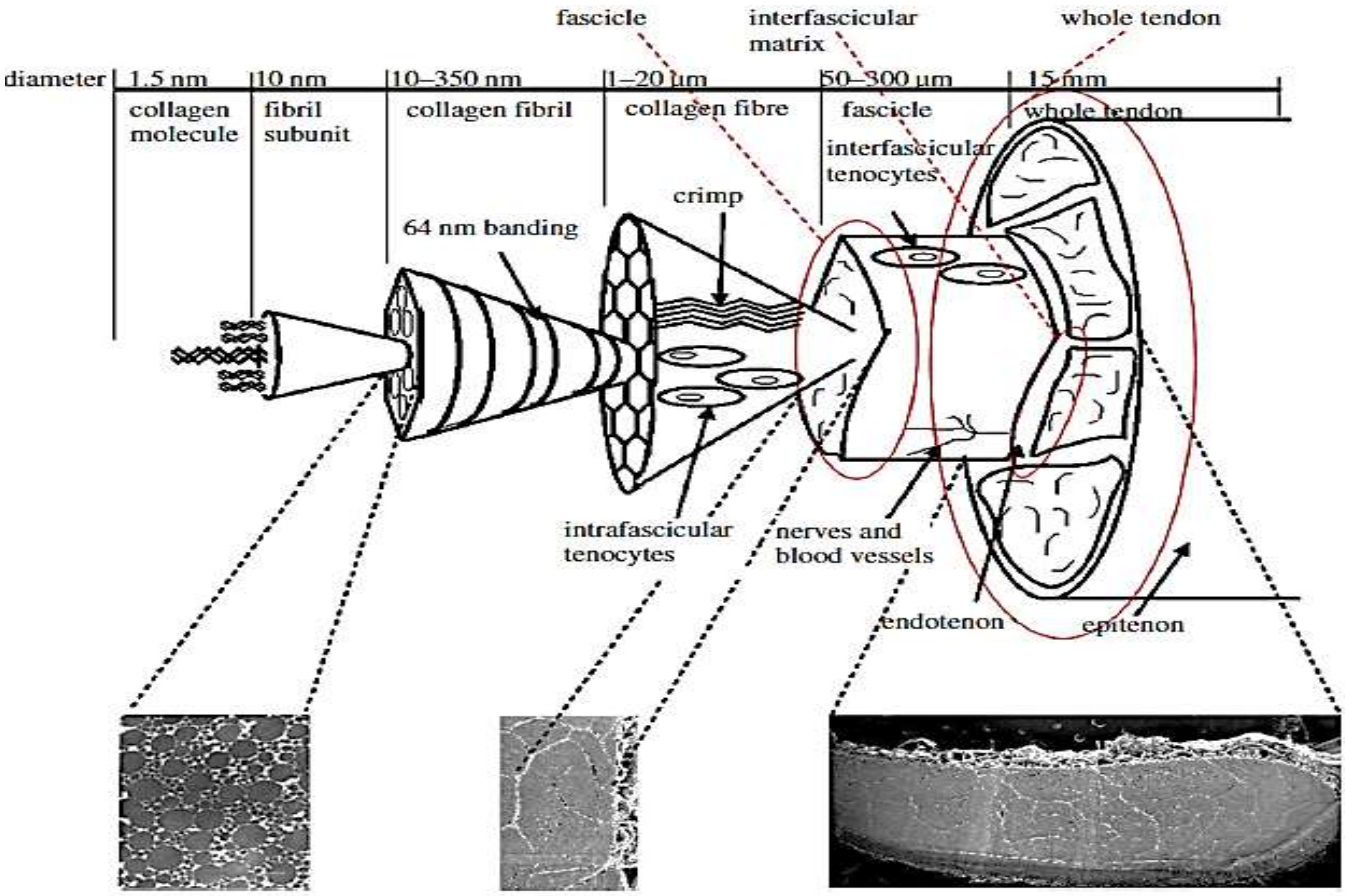

Figure 1.1: *Schematic showing the hierarchical structure of tendon. Triple helical collagen molecules are arranged in a highly ordered, quarter-stagger pattern to form fibrils, which are grouped together to form fibres, fascicles, and finally tendon. Proteoglycan-rich matrix intersperses collagen at each hierarchical level of tendon. [Thorpe et al., 2012; Kastelie et al., 1978]*

The hierarchical structure of tendon begins with collagen molecules, grouped together in a highly ordered fashion to form fibrils, which in turn aggregate into fibres surrounded by non-collagenous matrix. Fibres further aggregate to form fascicles surrounded by interfascicular matrix, a loose connective tissue that binds them together to form a whole tendon [Thorpe et al., 2016a; Thorpe et al., 2015a].

As an aligned fibre composite material, the hierarchical structure of tendon enables it to withstand high tensile forces, but also results in complex anisotropic and viscoelastic mechanical characteristics. The ability of tendon to carry out its function of force transfer is determined by the composition and organization of the matrix at each structural level and the way in which each structural level contributes to tensile loading [Thorpe et al., 2012]. However, the relationships between structure and function throughout the tendon hierarchy remain unclear. A number of studies have characterised some of the structure-function mechanics of the hierarchical collagenous matrix that makes up the majority of the tendon substance [Cheng and Screen, 2007; Sharma and Maffulli, 2006; Devkota, 2006; Kannus, 2000], with the most recent work focused on how the interfascicular matrix contributes to the mechanics of the whole tendon. Recent studies by Thorpe et al. [2012], suggest that the interfascicular matrix functions mainly to facilitate the high strain characteristics of ES tendons by controlling sliding between adjacent fascicles when tendon is strained.

The interfascicular matrix, also referred to as endotenon, is a thin reticular network of connective tissue, composed of collagen type III, proteoglycans, glycoproteins, blood vessels, lymphatics and nerves, and is synthesized and maintained by the population of interfascicular fibroblasts [Sharma and Maffulli, 2006; Devkota, 2006]. Similarly, the whole tendon is bounded by a sheath of a fine loose connective tissue also containing blood vessels, lymphatics, nerves, collagen fibrils (type I and III), and some elastic fibrils [Sharma and Maffulli, 2006;Devkota, 2006]. The tendon sheath is often subdivided into layers. The upper layer is called the paratenon, which is a loose areolar connective tissue. Underneath the paratenon is the epitenon, a dense fibrillar network of collagen, and finally the inner most layer is called the endotenon, which is a thin reticular network of connective tissue [Kannus, 2000]. These sheaths help reduce friction between the tendon and adjacent tissues thereby facilitating tendon sliding during use [Wang, 2006].

1.2.1 GROSS ANATOMY OF ACHILLES TENDON

The Achilles tendon (AT) is the strongest, thickest and largest human tendon, connecting the triceps surae muscle group (two heads of the gastrocnemius and the soleus) to the calcaneus (Figure 1.2) [Ranson and Young, 2011]. The gastrocnemial parts of the tendon (11-26cm long), are broad and flat near their origin, and become more round and narrow distally, while the soleus part (3-11cm long), begins as a band proximally on the posterior surface of the soleus muscle and becomes the anterior part of the tendon, ending medially to the soleus muscle at

the insertion (calcaneal bone). The AT is 15cm long on average but can be up to 26cm in humans while the width varies longitudinally from around 6.8cm (range 4.5-8.6cm) at the origin, to 1.8cm (range 1.2-2.6cm) in the mid portion [Doral et al., 2010].

The AT can experience forces of up to 12.5 times body weight during activities such as running leaving it susceptible to both acute and chronic injuries [Doral et al., 2010; Nunley, 2009].

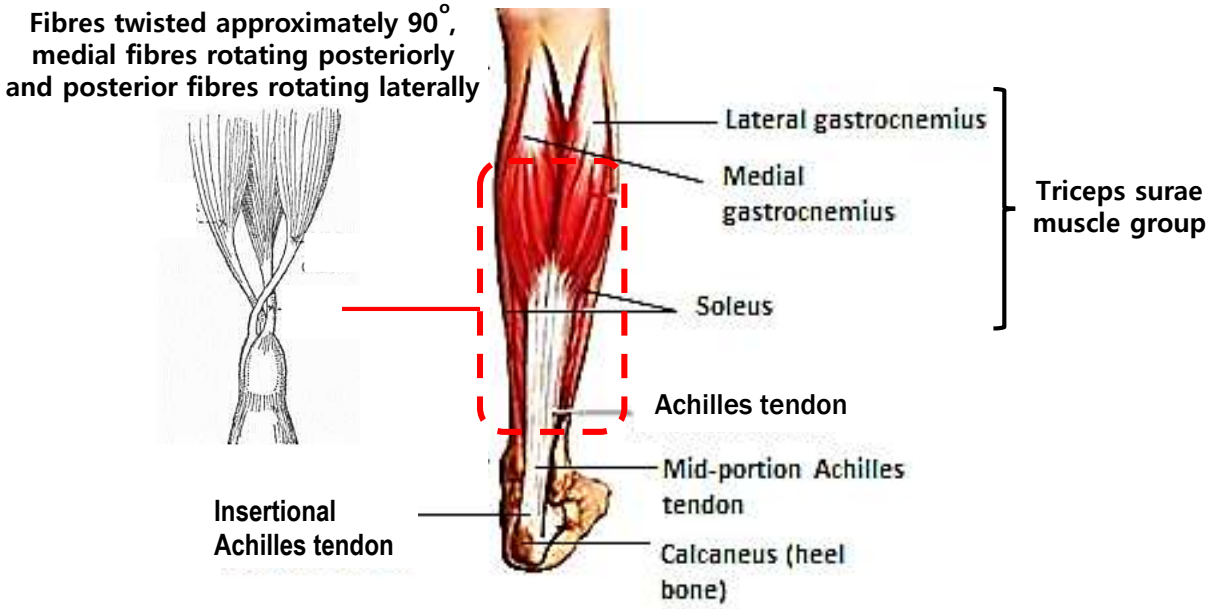

Figure 1.2: *Gross anatomy and structure of the Achilles tendon, showing the tendon emerge from the distal confluence of the gastrocnemius and the soleus muscles and insert into the calcaneus, with the fibres twisting as it descend. [Adapted from Freedman et al., 2014]*

The gastrocnemius muscle is activated when jumping and running and is composed predominantly of fast-twitch (type II) muscle fibres [Fugle-Meyer et al., 1979]. In contrast, the soleus muscle has more of a stabilizing function, especially when standing, and consists predominantly of slow-twitch (type I) muscle fibres [Garret et al., 1984]. The triceps surae muscle undergoes both eccentric (lengthening) and concentric (shortening) contractions during walking and running [Teitz et al., 1997].

The fibers of the AT are not vertically aligned but rotate by roughly 90 degrees when descending from the proximal muscle attachment to the calcaneal bone insertion. Accordingly, the soleus fibres insert medially at the calcaneus whereas the gastrocnemius fibres insert laterally [Root et al., 1977]. Doral et al. [2010] noted that the extent of angular rotation in the Achilles tendon depends on the position of the fusion between the two muscles i.e. a more

distal fusion, result in a tighter rotation. The fibre twisting is necessary for vascular network constriction and also means less fibre buckling when the tendon is lax and less deformation of individual fascicles during tension [Doral et al., 2010].

1.2.2 TENDON BIOMECHANICS

Tendon is a viscoelastic composite material consisting of collagen components embedded in a softer non-collagenous matrix throughout the hierarchy [Puxkandl, et al., 2002]. The elastic component is provided mainly by the collagenous matrix whereas viscosity is provided largely by the non-collagenous fraction of the matrix [Puxkandl, et al., 2002]. The collagen fibres are crimped in the unloaded state, but crimping is lost when the stretch exceeds ~2% while macroscopic rupture occur between 8-22% [Maganaris et al., 2008; Maffulli, et al., 2004] (Figure 1.3). The huge range in reported mechanical properties stems from the different behaviours of functionally distinct tendons, in addition to the effects of different testing protocols on resulting mechanical parameters.

The human Achilles tendon, an energy storing tendon, experiences peak stresses of between 42 and 110 MPa and strains of between 6.2 - 10.3% *in vivo* [Birch, 2007; Lichtwark and Wilson, 2005; Wren et al., 2001]. In contrast, positional tendons like the anterior tibalis tendon have been observed to have much lower *in vivo* stresses and strains of ~30MPa and ~3.1% respectively [Wren et al., 2001; Maganaris and Paul, 2000].

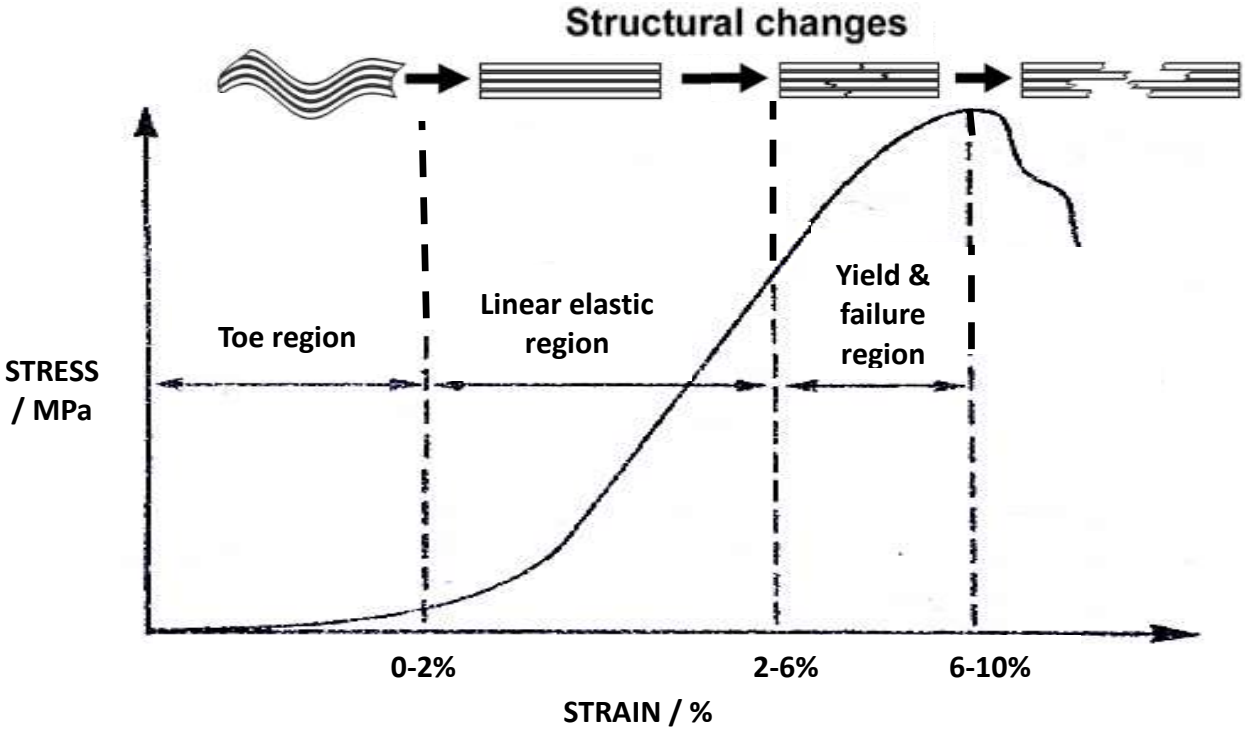

Figure 1.3: *Graphic representation of tendon mechanical behaviour. The curve is generally considered to consist of three regions, for which different structural behaviours can be accredited: Toe region – the nonlinear region of the curve where the collagen un-crimps and orients in the direction of the load and stretch; Linear elastic region – the physiological load region where the collagen fibrils continues to orient themselves in the direction of the load and stretch; Yield and failure region – the region where the tendon stretches beyond its physiological limit and fails.*

1.3 COMPOSITION OF TENDON

By dry weight, tendon tissue is composed primarily of collagen type I (approximately 70-90%), but also contains collagen types III and V (approximately 3-5%), and trace amounts of types II, IV, VI, IX, X, XI, XII and XIV [Hampson et al., 2008; Graham, 2007; Devkota, 2006]. Tendon also contains a range of glycoproteins, the most abundant of which are proteoglycans (approximately 1-5%), and also elastin (approximately 1-2%), cells (less than 10%) and inorganic components (of approximately 0.2%), which include copper, magnesium, manganese, cadmium, cobalt, zinc, nickel, lithium, lead, fluoride, phosphor and silicon [Rumian et al., 2007; Wang, 2006; Nordin and Frankel, 2001; Kannus, 2000; Kastelic et al., 1978].

1.3.1 COLLAGENS

To date, 29 different collagen types have been described in the literature with different structures, functions and tissue distributions [Pingel et al., 2013; Jelinsky et al., 2011; Nagase et al., 2006; Ireland et al., 2001]. Collagens are generally composed of a triple helix formed of homo or heterotrimers polypeptides chains (α-chains) that play a vital role in tissue architecture and strength [Kadler et al., 1996]. Of the different collagen types in tendon, type I collagen is by far the most abundant. The type I collagen molecule triple helix is made of two α1 chains and one α2 chain. Each chain has approximately 1000 amino acids and is rich in glycine, which can be found at every third amino acid residue [Lodish et al., 2000]. The Type I collagen molecule is about 280-300nm long and 1.5nm thick [Jozsa and Kannus, 1997].

Type III collagen is the second most abundant collagen in the tendon, comprising about 1-5% tendon dry weight and is made up of three α1 chains and forms smaller, less organized fibrils, which may result in decreased mechanical strength in tendon [Wang, 2006]. However, Type III collagen is essential for normal fibrillogenesis and regulation of type I collagen fibril size [Kadler *et al.*, 1990]. Type V collagen consist of two α1 and one α2 chains, and also provides an essential template for fibrillogenesis [Wenstrup et al., 2004; Kadler et al., 1996]. Collagen is constantly turned over in human tendon, enabling the ECM to adapt to changes in the mechanical environment [Kjær et al., 2005]. Collagen turnover rates in tendon are generally thought to be low, however, it could be hypothesised that collagen turnover will be faster in ES tendons because they experience higher levels of micro-damage due to the higher stresses and strains they are exposed to, thus requiring a greater capacity for matrix turnover.

Unexpectedly, findings by Heinemeier et al. [2013] proves otherwise, suggesting that healthy human Achilles tendons experience limited collagen turnover, being practically inert during adult life.

Table 1.1: Collagen types found in the tendon ECM (Sutmuller et al., 1997)

Collagen	Structure formed	Structure / Type	Location and Function	Reference
Type 1	Quarter staggered fibrils	Fibrillar forming collagen. Two α1(I) and one α2(I).	Main constituent of tendon (~95% of total collagen). Provide little flexibility and high mechanical strength.	Franchi et al., 2007
Type II	Quarter staggered fibrils	Fibrillar forming collagen. Three α1(II).	Abundant at the fibrocartilage of the tendon. Provides tensile strength.	Maffulli et al., 2005
Type III	Quarter staggered fibrils	Fibrillar forming collagen. Three α1(III).	Normally restricted to the interfascicular matrix. Essential for fibrillogenesis.	Kadler *et al.*, 1990; Liu et al., 1997
Type IV	Basement membrane	Forms meshwork. Two α1(III), α1-6(III).	Structural support.	Borchiellini et al., 1996
Type V	Quarter staggered fibrils	Fibrillar forming collagen. α1(V), α2(V) and α3(V).	Core of type I collagen fibril. Regulation of fibril diameter. Essential for collagen fibril nucleation.	Wenstrup et al., 2004
Type VI	Beaded filaments	Non-fibrillar collagen. α1(VI), α2(VI), α3(VI).	Cell-associated found in 'seams' between fibrils.	Sutmuller et al., 1997; Riley, 2005
Type IX	FACIT	Non-fibrillar collagen. α1(IX), α2(IX) and α3(IX).	Mediates cell–matrix interactions with type II collagen fibril surface.	Sutmuller et al., 1997; Riley, 2005
Type X	Hexagonal lattices (short chains)	Non-fibrillar collagen. Forms meshwork. Three α1(X).	Restricted to insertion fibrocartilage. Maybe associated with mineralisation.	Sutmuller et al., 1997; Riley, 2005
Type XI	Quarter staggered fibrils	Fibrillar forming collagen. α1(XI), α2(XI) and α3(XI)	Core of type II collagen fibril forms template for fibrillogenesis.	Sutmuller et al., 1997; Riley, 2005
Type XII	FACIT	Non-fibrillar collagen. Three α1(XII).	Integrates adjacent extracellular matrices	Zhang et al., 2005

Type XIV	FACIT	Non-fibrillar collagen. Three α1(XIV).	Regulating the entry of fibril intermediates into lateral fibril growth. Functions in the integration of fibrils into fibres.	Ansorge et al., 2009

Abbreviation: FACIT – Fibril Associated Collagen with Interrupted Helix

1.3.1.1 COLLAGEN SYNTHESIS

Collagen synthesis occurs within the cell in a precursor form known as preprocollagen consisting of a three-dimensional stranded structure with the amino acids glycine and proline as its principal components. The procollagen undergoes hydroxylation by the addition of hydroxyl groups to the amino acids proline and lysine, catalysed by lysyl-oxydase enzyme. This step is imperative for later glycosylation and collagen formation [Hutson and Canty, 2011]. Collagen synthesis involves steps both inside and outside of the cell (Figure 1.4). All 29 types of collagens are triple helical structures, but their differences depend on the alpha peptides.

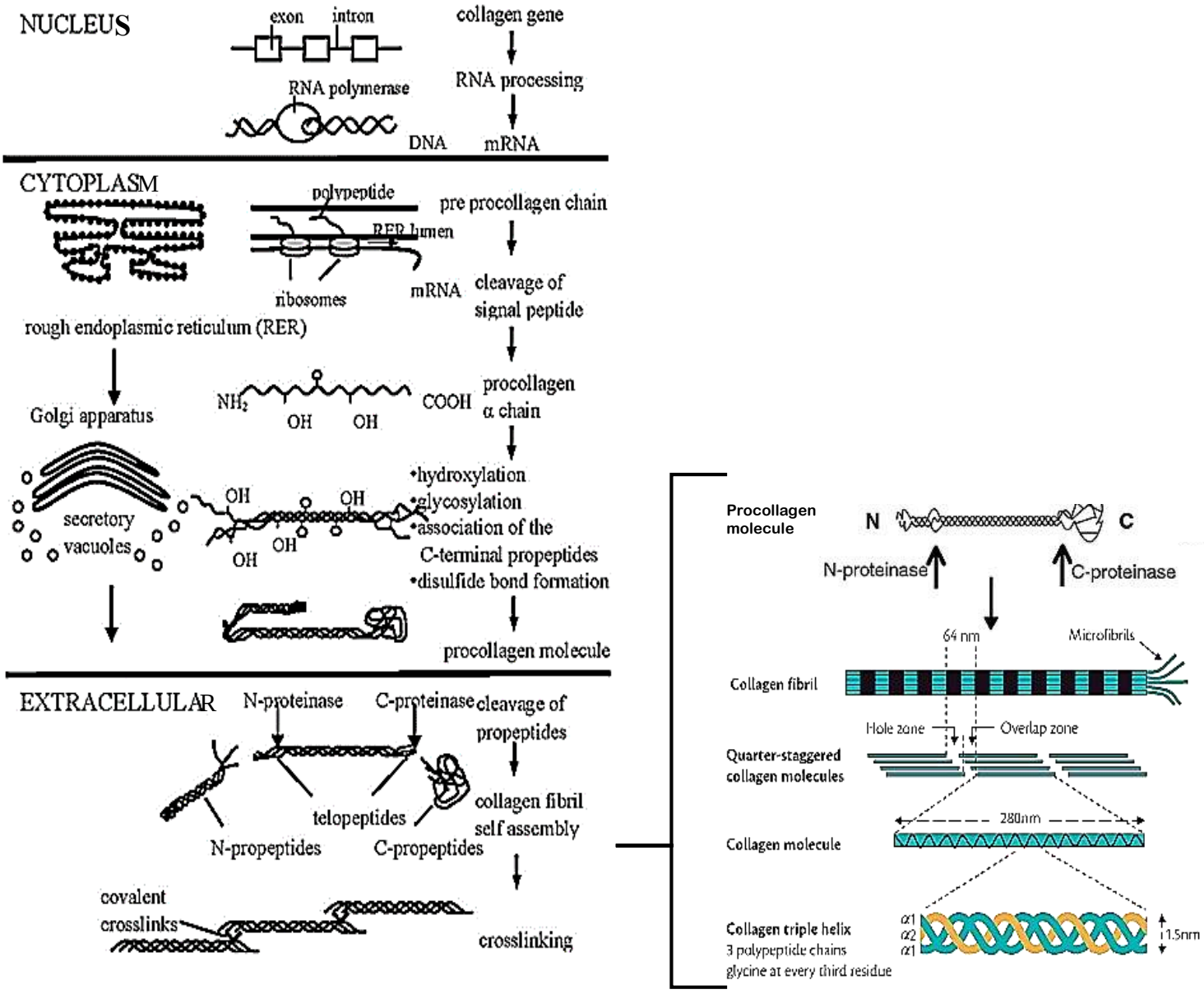

Figure 1.4: *Overview of the steps involved in the production of collagen fibrils from procollagen to a single collagen fibril [adapted from Holmes et al.(2001); Canty and Kadler, (2005); Hutson and Canty, (2011) and Chhabra, (2013)].*

Within the nucleus, a number of genes are associated with collagen formation, each coded with a specific mRNA sequence. DNA are unwound by RNA polymerase to form mRNA. This process is referred to as mRNA transcription. The mRNA that codes for preprocollagen enters into the cytoplasm of the cell, where it is detected by signal peptides and directed to the rough endoplasmic reticulum (RER) of the cell [Riley, 2005]. This process is referred to as the translation process.

Transcription and Translation

The process of transcription begins when an enzyme called RNA polymerase attaches to the template DNA strand and begins to catalyse production of complementary RNA. RNA polymerase reads the template DNA strand and adds nucleotides from the DNA upstream five-prime (5') of the gene at a specialized sequence called a promoter to the three-prime (3') end of a growing RNA transcript [Gelse et al., 2003]. When RNA polymerase reaches a termination sequence on the DNA template strand, the pre-mRNA transcript and RNA polymerase are released from the complex. The pre-mRNA contains introns and exons which are either spliced or included, giving rise to several different possible mRNA products in a process called RNA splicing [Rossert et al., 2002].

The process of translation involves transportation of the mRNA out of the nucleus, into the cytoplasm, to the ribosome (rRNA and proteins). The ribosome binds to the mRNA at a specific area and starts matching tRNA anticodon sequences to the mRNA codon sequence to form a polypeptide chain [Clancy et al., 2008]. The ribosome continues until it hits a stop sequence, then it releases the polypeptide and the mRNA. The polypeptide chain is translated into a protein, in this case a preprocollagen molecule which protrude into the lumen of the rough endoplasmatic reticulum with the help of a signal recognition domain recognized by the corresponding receptors [Gelse et al., 2003].

Post-translational Modifications of Collagen

Within the lumen of the RER, the signal peptides that direct the preprocollagen to the RER are removed to form a procollagen chain. This process is referred to as post-translational processing. The procollagen chain undergoes hydroxylation, which is catalysed by two different enzymes: prolyl-4-hydroxylase and lysyl-hydroxylase to form specific residues (so proline and lysine form hyroxyproline and hydroxylysine) to aid cross-linking of the alpha peptides (Gly-X-Y). Procollagen is made up of a repeating sequence of Gly-X-Y, Gly is Glycine, while the X and Y can be any amino acid but are usually proline and hyroxyproline respectively (with amino acid polypeptide extensions at the C- and N- terminals). The hydroxylated procollagen chain then forms a triple helix by forming intra/inter-chain disulphide bonds within the C-propeptides and intra-chain disulphide bonds within the N-propeptides [Bullied et al., 1997]. The C-propeptides are essential for the early stage of procollagen assembly and in ensuring the correct association of the individual procollagen

chains to form a trimeric molecule, but are not in essential in triple helix nucleation and alignment of the α-chains [Bulleid et al., 1997]. Glycosylation occurs by adding either glucose or galactose monomers onto the hydroxy groups that are placed onto lysines, but not on prolines. The hydroxylated and glycosylated propeptides twist to form a triple helix [Lamande and Bateman, 1999].

The procollagen chain is translocated to the Golgi apparatus where it is converted into a procollagen molecule with an inter-chain disulphide bond within the N-propeptide. This process is referred to as nucleation, and alignment of the trimerised α-chains occurs by a sequence of propagation/folding from the C- to the N- terminus [Buchner and Moroder, 2009].

Following nucleation of the triple-helix, the procollagen is secreted into the extracellular matrix (ECM) where the C- and N- terminals are cleaved by enzymes carboxyproteinase and aminoproteinase and ADAMTS 2, 3 and 14 respectively [Buchner and Moroder, 2009]. The cleaving of the procollagen ends with the release of the triple helical collagen molecule.

Fibrillogenesis

In the extracellular space, the resulting collagen molecules assemble instinctively into quarter-staggered fibrils in a process known as fibrillogenesis. This assembly is stimulated by the presence of clusters of hydrophobic residues and of charged amino acids on the surface of the molecules [Rossert et al., 2002]. During fibrillogenesis, some lysyl and hydroxylysyl residues are deaminated by oxiadation, which deaminates the $–NH_2$ group, giving rise to aldehyde derivatives [Rossert et al., 2002]. These aldehydes associate with adjacent lysyl or hydroxylysyl residue spontaneously, by the $–NH_2$ groups, forming interchain cross-links. These cross-links increase the tensile strength of the fibrils considerably.

1.3.2 NON-COLLAGENOUS COMPONENTS

The non-collagenous matrix components of the ECM are thought to play a vital role in ensuring tendon viscoelasticity and lubrication, as well as allowing spacing for fibre gliding and cross-tissue interactions [Maffulli et al., 2005]. They are also vital membrane proteins, essential for cell-cell interactions [O'Brien, 1997]. The most abundant non-collagenous matrix molecules are glycoproteins and proteoglycans. The non-collagenous matrix also include the fibrous protein elastin that forms part of elastic fibres (see table 1.2 for summary).

1.3.2.1 ELASTIN

Elastin is a hydrophobic protein with an ability to stretch to over 100% of its original length with fully elastic recovery [Grant et al., 2013]. Elastin is formed from tropoelastin and becomes insoluble and stable once fully formed into elastic fibres.

Elastin is the major component of the elastic fibre, which has been hypothesised to be essential for tendon strength and elasticity during movement as well as the preservation of the crimp [O'Brien, 1997]. Studies have reported the presence of elastin in tendon at about 1-2% by dry weight [Hutson and Speed, 2011]. The distribution of elastin is yet to be fully determined, but may vary across a tendon depending on the mechanical environment that the tendon is exposed to [Thorpe et al., 2013c]. Some studies have reported that elastic fibres in tendon are found within the tenocytes and between fascicles localised to the interfascicular matrix (IFM) where the presence of elastin in the IFM is thought to influence fascicle sliding and recoil [Thorpe et al., 2016b; Grant et al., 2013; Thorpe et al., 2013c]. By contrast, some data suggests that elastic fibre concentration is highest at the insertional regions, due the high tension the area undergoes, whilst it is minimal at the fibrocartilageous areas [Grant et al., 2013].

1.3.2.2 GLYCOPROTEINS

Glycoproteins are large macromolecules that consist of a large protein component and small carbohydrate component. There are numerous glycoproteins, of which proteoglycans are the most abundant. Of other glycoproteins, the most abundant in tendon are cartilage oligomeric matrix protein (COMP), tenascin-C, fibrillin, fibronectin, laminin, thrombospondin (Tsp) and tenomodulin [Juneja and Veillette, 2013].

1.3.2.3 PROTEOGLYCANS

Proteoglycans (PGs) are a specific class of glycoproteins, and are the most abundant non-collagenous proteins in tendon. PGs are composed of a core protein attached to one or several polysaccharide chains which contain amino sugars. The polysaccharide chains are called glycosaminoglycan (GAG) side chains and are linked to the core protein by covalent bonds (Figure 1.5) [Nordin and Frankel, 2001; Clark, 1996]. Sulphated GAGs such as heparin/heparan sulphate (HS), chondroitin sulphate (CS), dermatan sulphate (DS), keratan sulphate (KS) and hyaluronan can form part of a proteoglycan molecule [Varki et al., 2009]. Tendons have different total GAG percentages according to their function. GAG content is

known to be highest in compressive regions of tendon (about 3.5%) relative to about 0.2% in the tensile regions within tendon [Yoon and Halper, 2005].

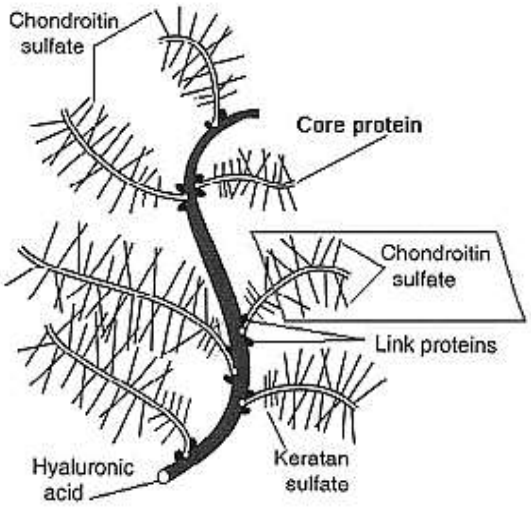

Figure 1.5: *The proteoglycan complex [adapted from Gupta, 2012]*

PGs are negatively charged hydrophilic molecules that can hold water up to 50% of their weight [Hutson and Speed, 2011]. The ability of PGs to attract water is useful in maintaining fluid and electrolyte balance within a tissue, thereby keeping the ECM and resident cells hydrated, and providing high resistance to compression forces. However, PGs not only function as structural features of tendon but are also essential for cellular processes like cell-cell, cell-matrix and ligand-receptor interactions, and also signal transduction processes [Perrimon and Bernfield, 2001]. PGs can be categorised as small leucine rich proteoglycans (SLRPs) or large aggregating proteoglycans.

It has been proposed that PGs may play a role in functions such as fibrillogenesis and fibre lubrication, which may be the reason for the presence of PGs in the IFM of the tendon [Thorpe et al., 2015a]. However, some studies also suggest that PGs play a mechanical role, modulating tendon mechanics. Due to the hydrophilic nature of PGs and their non-covalent bond to the fibrils, PGs can associate and dissociate along the fibrils causing them to break and reform [Cribb and Scott, 1995]. This promote fibril elongation and decrease in diameter under tension demonstrating that the PGs promote deformation, and stiffening of tendon matrix [Cribb and Scott, 1995]. The mechanical role of PGs in tendon remains controversial, with some studies demonstrating an important role and others reporting no role [Matuszewski et al., 2012].

❖ *Small Leucine Rich Proteoglycans (SLRPs)*

The SLRPs are named owing to their small core proteins (~40kDa) and long 20-30 amino acids chains containing high levels of leucine [Matuszewski et al., 2012; Merline et al., 2009]. The SLRPs present in tendon are decorin, biglycan, fibromodulin and lumican, with decorin and biglycan being the most abundant [Stanton et al., 2011]. Decorin consists of a core protein bound to just one GAG chain of CS or DS which is nearly always one DS in tendon [Watanabe, et al., 2012; Yan et al., 2011]. The role of decorin in tendon function remains controversial but it is thought to assist in maintaining tendon tensile strength mechanically link adjacent collagen fibrils and enabling inter-fibril load sharing [Rigozzi et al., 2012; Parkinson et al., 2011]. Biglycan consists of a core protein with two GAG chains of either CS or DS; two CS chains are more common in tendon [Yan et al., 2011]. Fibromodulin consists of a core protein bound to 100 KS or 21 CS GAG chains, while lumican is a core protein bound to 21 CS GAG chains [Parkinson et al., 2011].

Decorin, biglycan, fibromodulin and lumican are able to bind to fibrillar collagens (type I and II), and via interaction with their core proteins regulate collagen fibrillogenesis [Matuszewski et al., 2012]. These PGs play a key role in the fibril formation process by timing fibril alignment and aggregation, which ultimately alters the thickness of the fibrils [Milan et al., 2005].

❖ *Large Proteoglycans*

Aggrecan and versican are both members of the family of large aggregating PGs. Aggrecan (~250kDa) contains large numbers of CS and KS GAG chains and is located in compressive areas of tendon [Matuzewski et al., 2012]. Versican (~380kDa) consist of a large CS GAG chain, located in fibrous, tensile-load bearing regions [Hutson and Speed, 2011; Theocharis et al., 2002]. In the Achilles tendon, versican was identified as the major large PG in the tendon mid-substance whilst there was more aggrecan at the insertion. Site-specific variation in PGs are related to the mechanical history and function of the tendon [Hutson and Speed, 2011], and the capacity to resist the high compressive and tensile forces associated with loading and mobilization [Yoon and Halper, 2005].

Proteoglycans Synthesis

The literature describing proteoglycan synthesis is not as extensive as that for collagen. However, the synthesis process follows the same route from the RER to the Golgi apparatus and finally to the ECM [Zhang et al., 1995]. Within the RER, the protein is synthesized, and glycosylation begins (protein folding, N-linkage). Glycosylation is an enzyme-directed chemical process involving the addition and subsequent processing of carbohydrate [Lodish et al., 2000]. The presence of the carbohydrate residue on the protein acts as a marker, facilitating protein movement from the RER to the Golgi. At the Golgi where glycosylation ends, the protein folding is completed by the addition of further N-linkages and O-linkages held by glycosidic bonds (Figure 1.6). After the linkage, GAGs attach to the Ser residue by a tetrasaccharide link to the core protein, forming a primer for polysaccharide growth [Gupta, 2012]. The Ser residue is generally in the sequence -Ser-Gly-X-Gly- (where X can be any amino acid residue), although not every protein with this sequence has an attached GAG [Gupta, 2012; Zhang et al., 1995]. Carbohydrates are added one at a time by glycosyl transferase to form a complete PG [Lairson et al., 2008]. The PG is then secreted to the ECM.

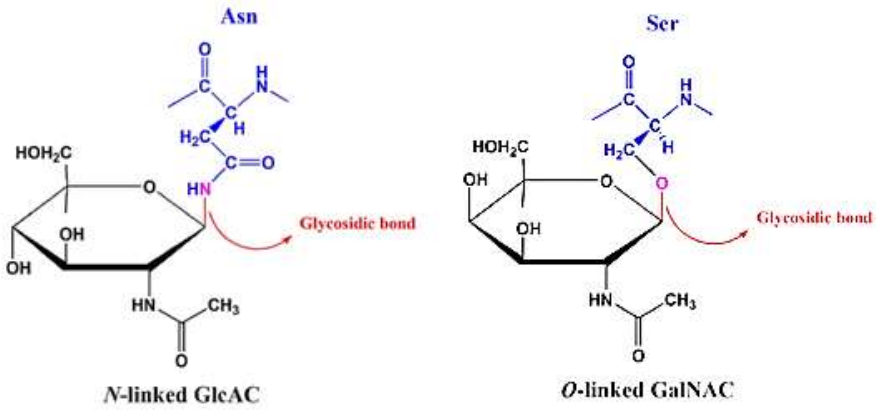

Figure 1.6: *Representation of the N- and O- linkage that occurs during protein glycosylation [adapted from Zhang et al., 1995]*

Table 1.2: Non-Collagenous components of tendon ECM (Juneja and Veillette, 2013)

	Structure	Type	Function	Reference
Glycoprotein				
Collagen oligomeric matrix protein (COMP)	~524kDa Oligomer composed of five subunits connected by disulphide bonds	Large pentameric protein.	Mediates interaction with collagen, cells and other matrix proteins. Maybe involved in fibrillogenesis	Hutson and Speed, 2011
Tenascin-C	Disulfide linked protein with subunits of between 200-300kDa	Hexameric protein.	May help improve mechanical strength provides elasticity.	Hutson and Speed, 2011
Fibrillin	-	Linear arrays	Essential for the formation of elastic fibres (elastogenesis)	Omelyanenko et al., 2014
Fibronectin	~250kDa	Modular protein	Mediates interactions between cell and surrounding matrix in normal tissues as well as in repair and pathology	Riley, 2005
Laminin	~400kDa	Modular protein	Found in vascular walls of tendon and myotendinous junction. Essential for cell differentiation, migration and adhesion.	Kannus, 2000; Riley, 2005
Thrombospondin (Tsp)	-	Modular protein	Mediates interactions between cell-cell and cell-matrix. Essential for formation of integrins-mediated myotendinous junction.	Riley, 2005
Tenomodulin	317 amino acid residues	Transmembrane protein.	Essential for normal tenocyte proliferation and formation of regular collagen. Involved in fibril alignment and organisation.	Omelyanenko et al., 2014

GAG				
Chrondrontin Sulphate (CS)	15-70kDa of 20-100 attached GAG chains	Linear polymer	Located in pressure / insertional zone of tendon accounts for~65% of the GAG content. Binds biglycan, aggrecan and versican.	Yoon and Halper, 2005; Riley, 2005
Dermatan Sulphate (DS)	15-55kDa of 2-8 attached GAG chains	Linear polymer	Located in tensional zone of tendon accounts for~ 60% of the GAG content. Binds decorin.	Yoon and Halper, 2005; Riley, 2005
Keratan Sulphate (KS)	2-20kDa	Linear polymer	Binds fibromodulin and aggrecan.	Riley, 2005
Hyaluronan	-	Linear polymer	Located at the myotendinous junction accounts for~6% of the total GAG.	Yoon and Halper, 2005
PGs				
Decorin	~36-40kDa with 10 LRRs and one or two CS or DS chains	Small leucine-rich PG	Maintains and regulates collagen fibril structure. Regulates cell proliferation. Stimulates immune response. Directs tendon remodelling due to tensile forces	Yoon and Halper, 2005; Riley, 2005
Biglycan	~38-42kDa with 10 LRRs and two DS chains	Small leucine-rich PG	Interacts with type I collagen. Important in formation of mature collagen fibrils.	Yoon and Halper, 2005
Fibromodulin	~42kDa with 10 internal repeats of 25 amino acid	Small leucine-rich PG	Modulates collagen fibrogenesis and tendon strength. Binds type I and II collagen but at different site on each collagen molecule. Promotes formation of mature large collagen fibrils.	Yoon and Halper, 2005
Lumican	~38kDa with 10 LRRs	Small leucine-rich PG	Similar function to fibromodulin.	Yoon and Halper, 2005

Aggrecan	~42kDa of CS and KS chains attached to a large core protein	Large aggregating PG. Modular (lectican).	Low levels in tensional zone compared to compressive zone (fibrocartilage). Interacts with collagen. Contributes to tendon viscoelasticity. Acts as a lubricant by allowing fascicle sliding.	Yoon and Halper, 2005
Versican	~265-370kDa	Large aggregating PG. Modular (lectican).	Also contributes to tendon viscoelasticity. Support cell shape necessary for cell proliferation and migration.	Yoon and Halper, 2005

1.3.3 TENDON CELLS

Tendon cells, called tenocytes, are responsible for the synthesis and maintenance of the tendon ECM. The cells adhere to the ECM through specific cell surface receptors, particularly integrins [Franchi et al., 2007]. Through these receptors, mechanical signals are transmitted between the ECM and the cells [Franchi et al., 2007].

Tendon has a comparatively low cell content at less than 10% of the tendon composition. Around 90% - 95% of the cells are tenocytes and tenoblasts [Franchi et al., 2007]. The remaining 5% -10% of cells are of variable origin, with chondrocytes at the insertion sites and in the areas which undergo compression, and synovial and vascular cells (such as capillary endothelial cells and smooth muscle cells) in the endo- and epitenon, as well as myofibroblast-like contractile cells (responsible for the modulation of contraction-relaxation of the muscle-tendon complex) [Hampson et al., 2008; Kannus, 2000]. In pathological conditions, cells such as inflammatory cells, progenitor cells and macrophages can also be found in tendon tissue, contributing to healing [Dyment, et al., 2014; Kannus, 2000]. Tenocytes and tenoblasts both have a mesenchymal origin and the terms appear to be used interchangeably in the literature. However, they can be differentiated based on their shape. Tenocytes are elongated, spindle shaped cells with elongated nuclei, which reside on collagen fibers. In contrast, tenoblasts are more variable in shape (i.e. elongated, rounded or polygonal) and size (i.e. from 20µm to 70µm in length and 8µm to 20µm in width) [Cowin and Doty, 2007]. Tenoblasts are mainly found in immature/young tendon and are transformed into tenocytes with age or injury [Maffulli et al.,

2005]. Tenoblasts are thought to have increased metabolic activity compared to tenocytes. Nonetheless, the different roles that tenocytes and tenoblasts may play are unclear.

1.4 TENDON INJURY

In most everyday activities, the loads measured in tendons are comparatively low and well below the tissue's ultimate tensile strength. Conversely, in fast eccentric movements like running and hopping where a limb must be rapidly decelerated, more significant stresses can be measured [Schechtman & Bader, 1997]. As a result of these high in vivo loads, tendons such as the Achilles and patellar are particularly prone to overuse injuries, often referred to as tendinopathies (Fung et al., 2010). However, mechanical loading can create not only structural damage, but can also initiate a cell response to remodel the matrix [Kjær et al., 2009; Franchi et al., 2007; Wang, 2006]. This is because an intimate interplay exists between mechanical loading, cell response and biochemical changes within the tendon extracellular matrix, resulting in adaptations in tendon morphology, structure and material properties in response to applied loads [Kjær et al., 2009]. This interplay between mechanically induced and cell induced matrix changes is poorly understood and has led to considerable debate concerning the aetiology of tendon injuries.

1.4.1 TENDINOPATHY

Birch et al., [1998] highlighted how tendinopathy is frequently preceded by degenerative changes to the extracellular matrix rather than occurring as a result of a single overload event. However, the factors that cause the initial degradation remain unclear. Kountouris and Cook [2007] state that tendinopathy might be due to overuse and other additional factors such as inefficient lower limb biomechanics and musculoskeletal function. Nevertheless, they went on to highlight that the exact aetiology of this condition is unknown. There is also some debate as to genetic factors influencing tendinopathy. Cook and Purdam [2009] referred to tendinopathy as failed healing, and a degenerative response, in which overload may be a contributing factor. However, they argue that the pathology (cell and matrix changes) observed in a tendon with tendinopathy are the same whether the tendon was unloaded (stress-shielded) or overloaded, indicating an important cellular role.

Tendinopathy can certainly be described as a painful condition occurring in and around the tendon, most frequently encountered in the Achilles tendon [Alfredson and Cook, 2007]. To summarise the current view point, tendinopathy is thought to occur due to one, or a combination of the following;

- A failed healing response.
- Breakdown of the normal maintenance of the tissue.
- Excessive repetitive overload
- Load following a period of no load or under load.

Achilles tendinopathy is a common injury amongst athletes and non-athletes. It accounts for about 30-50% of all sport injuries; particularly sports incorporating high stretch-shortening cycles (SSC) such as found in running related sports like tennis (40% injuries), basketball (32% injuries) and volleyball (45% injuries) [Wilde, et al., 2011; Sharma and Maffulli, 2006; Lian et al., 2005]. However, tendinopathy is not only limited to those participating in sporting activities but is also common among sedentary populations, with 33% of patients with tendon injuries participating in no sports [Samiric et al., 2009; Kingma et al., 2007].

1.5 TENDINOPATHY TREATMENT

There remains no clear evidence-based treatment for tendinopathy due to the limited understanding of the underling aetiology and pathogenesis of the condition.

Prior to the 1990s, tendinopathy was consistently referred to as tendinitis (also spelt tendonitis) which would imply inflammatory processes in and around the lesion [Rees et al., 2013; Stanish et al., 1986]. This was because the condition was associated with pain in response to overuse [Khan et al., 2002]. Not surprisingly, most of the treatment modalities proposed at this time aimed at controlling the inflammation, such as non-steroidal anti-inflammatory drugs (NSAIDS) and corticosteroid injections [Alfredson and Cook, 2007]. However, these treatment options reported limited success. As the understanding of tendinopathy evolved, a number of studies began providing evidence to support the ideology that tendinopathy was a degenerative process that did not demonstrate an inflammatory response, thus eliminating the term tendinitis and instead using tendinosis [Khan et al., 1999; Jozsa et al., 1997; Astrom and Rausing, 1995]. Some of the evidence supporting a diagnosis of tendinosis were the presence of collagen separation, thinning, and disruption with the absence of inflammatory cell infiltrate [Khan et al., 1999]. In addition, researchers also noted that the characteristics of inflammation seen in other inflammatory diseases such as rheumatoid disease, were not seen when a tendinopathic tissue was observed [Astrom and Rausing, 1995]. These findings resulted in research into new treatment methods to target the degeneration, including

- Treatment using blood and blood products aimed at improving healing and remodelling. These include stem cell or gene therapy, or bone marrow-derived cells [Young, 2012; Gaida and Cook, 2011].
- Treatments aimed at reducing pain rather than healing the tendon itself, such as sclerosant or high volume injections, or the application of glyceryltrinitrate patches (GTN) [Wilde, et al., 2011; Gaida and Cook, 2011].
- Extracorporeal shock wave therapy [Waugh et al., 2015; Alfredson and Cook, 2007].
- Exercise-based physical therapy which includes eccentric and concentric exercises for the associated muscle [Lorenz and Reiman, 2011].

Currently, the term tendinopathy is preferred to describe tendon injury, a term that assumes no knowledge about the underlying pathology. This is because the importance of inflammation in both the pathogenesis of tendon injury and the healing process has been contentious in recent

years and remains poorly understood. Recent studies suggest that a finely balanced inflammatory response is necessary for tendon healing, at least at the early stage of the healing process [Dakin, et al., 2014].

Injections of blood or platelet-rich plasma, as well as stem cell or gene therapy have been reported to 'regenerate connective tissues' [Young, 2012; Gaida and Cook, 2011]. However, these treatment options are unproven and still in the experimental stages. The injections contain saline solution and also a local anaesthetic, with or without cortisteroid, which may influence outcome. Further, the act of injecting a solution can separate the tendon sheath from the tendon and disrupt surrounding vessels and nerves, also thought to improve tendinopathy [Wheeler, 2014]. Indeed, this approach is often adopted directly, and sclerosing injections and high volume injections have demonstrated a positive outcome in a number of studies, and are hypothesised to work on the principle that tendinopathy is associated with pain and neovascularisation which the injections prevent [Wilde, et al., 2011; Gaida and Cook, 2011]. However, there was no significant association between a decrease in neovascularisation and functional outcome [O'Neill et al., 2015; Tol et al., 2012]. Thus, evidence pertaining to these treatment is insufficient, requiring more investigation and randomised trials to support their efficacy [Lohrer et al., 2016; Scott et al., 2013; Magnussen et al., 2009].

The use of extracorporeal shock wave therapy has more recently been suggested as an option in treating several tendon and fascial injuries, with some evidence of success [Alfredson and Cook, 2007]. However, according to Sems et al., [2006] the efficacy of shock wave therapy remains controversial. This could be as a result of the multiple variables associated with this therapy, such as the amount of energy delivered, the method of focusing the shock waves, the frequency and timing of shockwave delivery, and whether or not anaesthetics are used alongside treatment [Wilson and Stacy, 2011; Sems et al., 2006]. However, over the last twenty years, the one treatment that has consistently been promoted and has the strongest evidence of efficacy has been eccentric exercise [Lorenz and Reiman, 2011]. Eccentric exercise has been consistently effective in improving tendon function and reducing pain. These two treatments are now considered in greater detail.

1.5.1 EXTRACORPOREAL SHOCK WAVE THERAPY (ESWT)

In a clinical setting, extracorporeal shock wave therapy (ESWT) involve a device that passes kinetic energy in the form of acoustic shockwaves through tissues. Shockwaves are pressure waves, characterised by a rapid rise in positive pressure and high peak pressure amplitude, followed by a fall in pressure below ambient, i.e. negative pressure (Figure 1.7). The waves are concentrated on the area of pain and pathology, therefore applying mechanical forces to the tissue [Waugh e al., 2015]. There are three methods through which shock wave can be generated; electrohydraulic, electromagnetic, and piezoelectric / pneumatic [Wang, 2012; Wilson and Stacy, 2011]. Although the methods of generating the shock wave may vary, the principles of how they interact with tissue remain same. The electrohydraulic method of shock wave application uses an underwater explosion with a high-voltage electrode spark discharge to produce a vaporization bubble of high-energy pressure waves. The electromagnetic method uses a coil that induces a strong magnetic field in a metallic membrane which is then transferred to a fluid medium to produce shock waves. Finally, the piezoelectric method uses piezocrystals mounted in a sphere to produce a rapid electrical discharge.

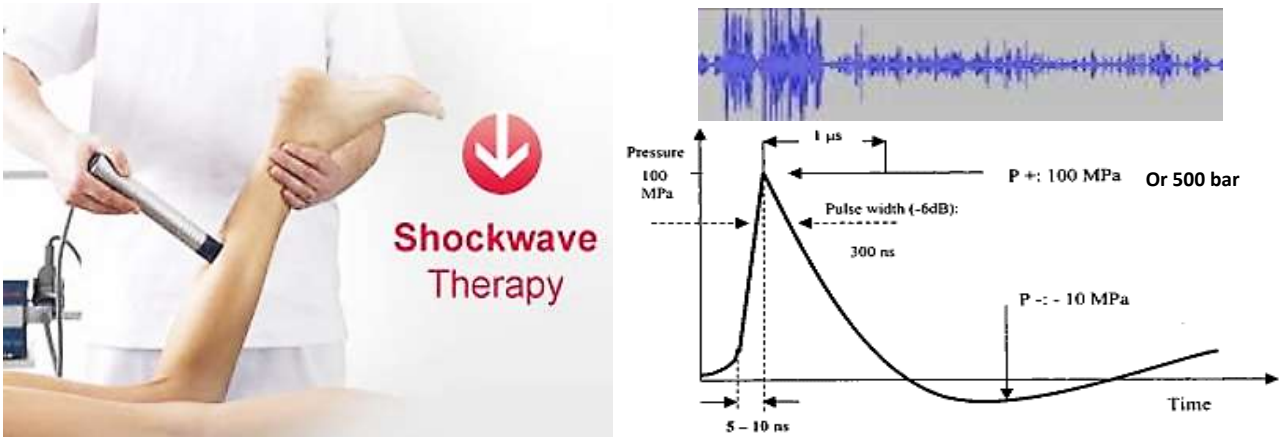

Figure 1.7: *A typical shock wave therapy machine, with details of the pressure pulse it generates. There is a rapid rise in positive pressure and high peak pressure amplitude, which is eventually followed by a variable negative pressure. This generates shock waves at a frequency of around 10Hz in the tissue [adapted from Ogden et al., 2001].*

Shock waves produce two basic effects in tissues. The primary effect is where direct mechanical forces of pulse energy are directed to the tissue target point [Wang et al., 2012]. However, ESWT also causes cavitation, characterised by the formation of gas bubbles. The implosion of the bubbles with the rise in pressure from the subsequent shock wave produces a secondary energy wave, which also provides a mechanical stimulus [Wang et al., 2012; Ogden

et al., 2001]. Shock waves augment tissue density as a result of the positive and negative phases of the propagating wave passing through it, and in doing so deliver direct mechanical perturbations to the tissue at around 8-10Hz [Waugh et al., 2015].

There is considerable research evidence concerning the effectiveness of shock wave in treating tendinopathy demonstrating decreased pain and improved tissue function post ESWT [Mani-Babu et al., 2014; Al-Abbad and Simon, 2013; Wang, 2012; Wilson and Stacy, 2011; Rompe et al., 2007]. Generally, most applications of shockwave for Achilles tendinopathy takes about 3-4 sessions of approximately 30 minutes treatment depending on the severity of the condition [Wilson and Stacy, 2011]. A study by Wang et al., [2003], stated that EWST promoted pain relief and tissue repair at the tendon-bone junction of the Achilles tendon in rabbits. The study demonstrated that EWST induced the in-growth of neovascularization within the tendon and enhanced angiogenesis, which may play a role in improving blood supply and in turn promote tissue regeneration. Another study by Chen et al., [2004], demonstrated that ESWT promoted cell proliferation and tissue regeneration in rat Achilles tendon with increased expression of growth factors such as TGFβ1. In addition, a study by Bosch et al., [2009], demonstrated that ESWT prompted collagen metabolism in the equine superficial digital flexor tendon. Short-term studies by Rompe et al., [2007] compared eccentric exercise, ESWT, and a wait-and-see policy for the treatment of midportion Achilles tendinopathy in humans over a 4 months period. At the end of the 4 months, the Victorian Institute of Sports Assessment – Achilles Questionnaire (VISA-A) scores of patients' improvements were 60% for eccentric exercise, 52% for ESWT and 24% for the wait-and-see policy.

Some studies show no effect, hence, more clinical trials are needed to fully evaluate efficacy of ESWT. In addition, the in vivo mechanism by which ESWT may promote tendon healing is yet to be understood.

1.5.2 EXERCISE BASED TREATMENT

The concept of exercise based treatment for the rehabilitation of tendon injuries was introduced in the mid-1980s by Stanish et al. [1986], after which it became embedded in rehabilitation regimes by Alfredson a decade later [Alfredson et al., 1998]. Ever since then, exercise therapy has been continually reviewed and developed to try and maximize its effectiveness. Muscles can undergo eccentric, concentric and isomeric contraction. Eccentric loading involves the lengthening of the muscle-tendon unit during contraction (Figure 1.8). Concentric loading

involves shortening of the muscle-tendon unit during contraction (Figure 1.8), and isometric loading is strength training in which the joint angle and muscle length do not change. Use of these different loading modalities in exercising the muscle-tendon complex of a tendinopathic tendon have been compared against one another and against other treatments, with eccentric loading consistently reporting the most promising outcomes. Eccentric exercise training has thus been applied since the 1980's as a key component of tendon injury rehabilitation [Stanish et al., 1986].

A study by Rompe et al. [2007] compared the efficacy of eccentric exercise relative to no treatment (a wait-and-see approach) on chronic Achilles tendinopathy. The VISA-A success rates were 24% for the wait-and-see policy (with paracetamol offered when necessary), compared to 60% for eccentric loading exercises. By contrast, there have been a wide number of studies that have compared the efficacy of eccentric exercises relative to concentric exercises [Kaux et al., 2011; Allison and Purdam, 2009; Rees et al., 2008; Wasielewski et al., 2007]. Generally these studies have reported superior outcomes with eccentric exercise, reporting pain relief and patient satisfaction for 82% of patient participants while concentric training only reported patient satisfaction for 36% of participants [Mafi et al., 2001].

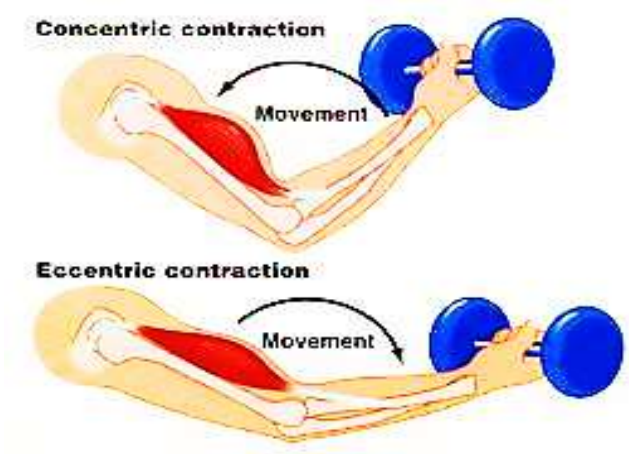

Concentric loading involves shortening of the muscle-tendon unit during contraction

Eccentric loading involves lengthening of the muscle-tendon unit during contraction

Figure 1.8: *Schematic of illustrating the protocol involved in eccentric and concentric contraction [Brady, 2012]*

Table 1.3 reports the results of different eccentric loading studies generally demonstrating good outcomes from a 12 week training programme. Some studies have suggested that eccentric loading is more successful in treating mid-portion tendinopathy, with the clinical evaluation satisfaction percentage for Achilles tendon showing 83.3±17.3 for mid-portion and 77.9±17.6 for insertional while the Visual Analogue Scale (VAS) decreased after an eccentric load

training programme from 66.8±19.8 to 10.2±13.7 for mid-portion and 68.3±7.0 to 13.3±13.2 for insertional tendon [Fahlstrom et al., 2003]. However, the satisfaction percentage between mid-portion and insertional Achilles tendon are hardly significant to confirm the efficacy and outcome of the study. Nonetheless, the statement of better clinical result in mid-portion than insertional tendon was supported by a later study in 2007 that evaluated the effects of non-surgical treatment option including eccentric exercise, which reported 90% clinical success for mid-portion Achilles tendon compared to 30% for insertional Achilles tendon [Alfredson and Cook, 2007]. However, the reasons behind this are unclear.

Table 1.3: Trial studies of eccentric exercise treatment protocols for tendinopathy and their outcome measures. Data from several sources have demonstrated success of eccentric loading using different time periods (12 and 52 weeks) and investigating tendinopathy in different tendon regions (mid-portion and insertional area).

Affected area	**Eccentric exercise protocol**	**Exercise prescription**	**Treatment period (**weeks**)**	**Outcome measures**	**References**
Insertional patellar tendon	Entire body on injured leg standing upright on a 25° decline board then knee slowly flexed to 70°	3 sets of 15 repetitions 2 times daily, 7 days a week	12	VAS decrease from 72.7±16.2 to 22.5±26.4	Jonsson and Alfredson, 2005
Insertional Achilles tendon	Entire body in upright position then heel raise with the non-injured leg, then transferred to injured leg. From heel raise to heel lowered slowly	3 sets of 15 repetitions 2 times daily, 7 days a week	12	VAS decrease from 69.9±18.9 to 21.0±20.6	Jonsson et al., 2008
Achilles tendon (location not defined)	Entire body on injured leg, forefoot on step, going from maximum heel lift to maximal dorsal flexion in ankle joint and using non-injured leg to lift back to start position	3 sets of 15 repetitions 2 times daily, 7 days a week	12	VAS decrease from 44±9 to 13±9	Langberg et al., 2007
Mid-portion Achilles tendon Insertional Achilles tendon	Entire body weight on injured leg, to all body weight on the forefoot with the ankle in plantar flexion. Then the calf muscles were loaded with knee straight and again with knee slightly bent	3 sets of 15 repetitions 2 times daily, 7 days a week	12	VAS decrease from 66.8±19.4 to 10.2±13.7 VAS decrease from 68.3±7 to 13.3±13.2	Fahlstrom et al., 2003

Achilles tendon (location not defined)	Entire body in upright position on small step hereafter the weight is transferred to injured leg and the heel slowly lowered as far as possible until maximal stretch of the calf muscles and/or the Achilles tendon.	3 sets of 15 repetitions	12 and 52	KOOS questionnaire reported marked improvements of score 0 after 52 weeks	Norregaard et al., 2007
Patellar tendon (location not defined)	Entire body on a 10cm at 25° inclined board and perform single leg squats on the injured leg	3 sets of 15 repetitions	12 and 52	VAS decrease from 30 to 18 (after 12 weeks) and 10 (after 52 weeks)	Young et al., 2005

Abbreviation: *VAS – Visual Analogue Scale from 0 (no pain) to 100 (severe pain)*
KOOS – Knee Injury and Osteoarthritis Outcome Score from 0 (mild pain) to 4 (extreme pain)

Initially it was believed that the improved efficacy of eccentric loading resulted from the tendon experiencing higher forces during eccentric than concentric exercise, resulting in more tendon remodelling in response to the higher strain. However, in vivo studies in healthy humans have reported no differences in peak Achilles tendon force during eccentric and concentric loading regimes [Chaudhry et al., 2015; Galloway et al., 2013]. However, while there are no difference in the peak forces experienced by the tendon when performing eccentric and concentric exercises, recent studies have demonstrated that eccentric training generates high frequency perturbations of between 8-12Hz in the muscle-tendon complex, which are not apparent in concentric training (Figure 1.9) [Chaudhry et al., 2015; Grigg et al., 2013; Henriksen et al., 2010; Semmler et al., 2007]. Data confirms that this 8-12Hz frequency is coming predominantly from medial soleus and medial gastrocnemius muscle activity where the force is generated and transferred to the tendon [Chaudhry et al., 2015]. As such, it has been hypothesised that these high frequency perturbations maybe the important driver of repair in tendinopathic tendon, as they may promote more stimulus for tendon remodelling and formation of new collagen [Chaudhry et al., 2015; Kaux et al., 2011; Tan and Chan, 2008].

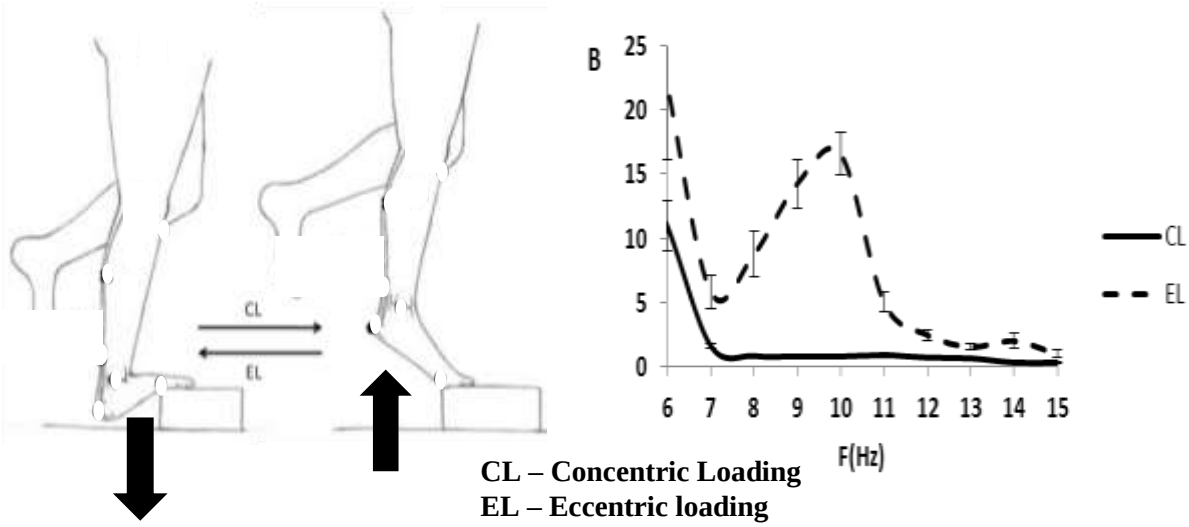

Figure 1.9: *Schematic of eccentric and concentric contraction of the triceps surae and a graph comparing the perturbation frequencies observed in the tendon from both exercise modalities [Chaudhry et al., 2015; Grigg et al., 2012]*

Based on these findings, one could hypothesis that the efficacy of both eccentric exercise and ESWT in treating tendinopathy is a result of the vibrations at approximate 10Hz applied to tendon during the treatment. Research by Yamamoto et al. [2005] demonstrated that the frequency and duration of cyclic stress application significantly affected the mechanical

properties of cultured collagen fascicles. However, very little is known about tendon perturbations and how they may influence tendon turnover or repair. Nevertheless, it is well established that tendon cells (tenocytes), like all connective tissue cells are mechano-responsive to varying magnitude and frequencies of applied strain [Khan and Scott, 2009].

1.6 CELLULAR MECHANOTRANSDUCTION

Tendons are dynamic mechanoresponsive tissues that adapt to loading and unloading [Andarawis-Puri and Flatow, 2011; Neviaser et al., 2012]. It is now well accepted that mechanical forces or deformations applied to cells lead to chemical cascades that crucially influence the form and function of cells in a process referred to as *mechanotransduction* [Orr et al., 2006; Jaalouk and Lammerding, 2009; Hoffman et al., 2011].

An example of the effect of mechanotransduction in tissue development has been described in bone [Jaalouk and Lammerding, 2009]. Compact bone consists of concentric layers of bone matrix, wherein small cavities called lacunae are distributed in regular intervals. These lacunae contain cells called osteocytes and are connected to one another and to the Haversian canal through a network of interconnecting canals called canaliculi. Weight bearing and muscle contraction during movement generates gravitational and compressive forces that result in small deformations of the poroelastic bone, resulting in pressure gradients that drive interstitial fluid flow through the lacunae–canalicular network. This load induced fluid flow is thought to stimulate localized bone remodelling and optimize the physical performance of the bone through mechanotransduction signalling [Orr et al., 2006; Jaalouk and Lammerding, 2009]. Studies also indicate frequency dependence to matrix metabolism in bone cells, specifically suggesting that higher frequencies may promote more rapid healing in bone tissues [Zhang et al., 2007]. Similarly, chondrocytes (the main cells that comprise cartilage) respond to mechanical loading with cell proliferation and an increase in cartilage matrix synthesis [Iqbai and Zaidi, 2005; Jaalouk and Lammerding, 2009].

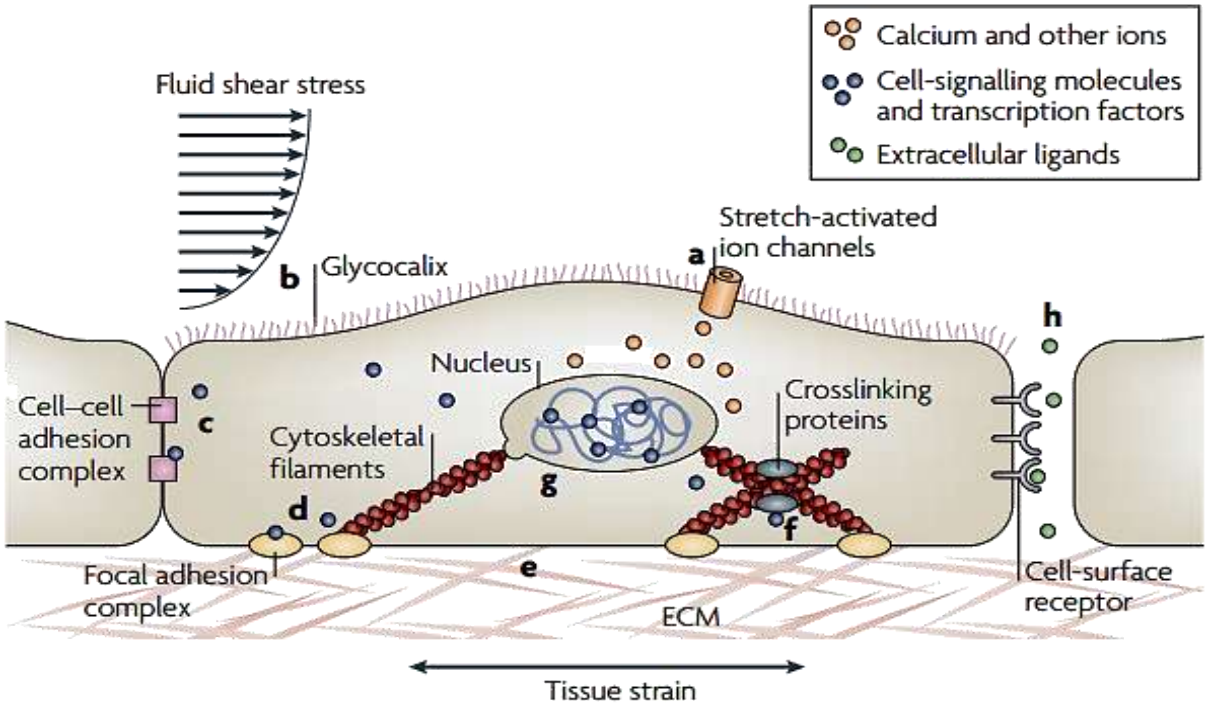

Figure 1.10: *Schematic depicting some of the known mechanisms of cellular mechanotranduction:* ***a)*** *applied load causes the* ***ion channels*** *in the membrane to open allowing the influx of calcium and other ions that initate further downstream signalling,* ***b)*** *glycocalix (a layer of carbohydrate-rich protein) mediate mechanotransduction signalling in response to fluid shear stress,* ***c) cell to cell*** *junctional receptors* ***d) Cell to ECM*** *junction central adhesion to the environment,* ***e)*** *force induced unfolding* ***ECM proteins such as fibronectin****, mediate mechanotransduction signalling outside the cell,* ***f)*** *activation of signalling pathways,* ***g) the nucleus*** *acts as a mechanosensor to sense mechanical signals,* ***h)*** *cell to surface adhesion to influence a change in the inter-cellular space [Jaalouk and Lammerding, 2009]*

Figure 1.10 gives a general overview of some of the mechanisms through which cellular mechanotransduction can occur. Mechanical stimuli creates an interaction between the ECM and cell adhesion molecules (integrins, cadherins, dystroglycans, proteoglycans or tyrosine kinase receptors) [Kjær, 2004]. The interaction leads to activation of a series of downstream secondary messenger / signalling pathways and cytoskeletal rearrangements [Cooper, 2000; Kjær, 2004]. The various signalling pathways results in changes in the nucleus in response to the mechanical stimuli.

Within tendon tissues, mechanical forces are transmitted by cell focal adhesion sites, composed primarily of integrins. Integrins play a vital role in tendon mechanotransduction because they are believed to be the main receptor between the cell and the ECM that sense tensile strain [Kjær, 2004]. Integrins are large cell surface receptors that link the ECM to the cell cytoskeleton via molecular bridges of actin-associated proteins such as talin, vinculin, zyxin

and paxillin [Schnatwinkel and Bryant, 2014; Wang et al., 2009]. Tension applied to tendon tissue, may lead to the activation of the stretch-sensitive ion channels (Ca^{2+}), depending on the integrins involved [Ingber, 2006]. Activation of the ion channels causes an influx of extracellular and intercellular Ca^{2+} from intercellular stores, through intracellular messengers such as inositol trisphosphate (IP_3) and diacylglycerol (DAG) [Wall and Banes, 2005]. The mechanical signals are then transferred to the nucleus via cytoskeletal filaments that connect to the nucleus to influence matrix production. In normal conditions, this process simply maintains tendon homeostasis, breaking down and replacing damaged molecules to maintain tissue structure and the mechanical properties of the extracellular matrix (ECM) that are fundamental to cellular and tissue health [Humphrey et al., 2014]. In tissue development, the change could be for cell proliferation, differentiation and migration [DuFort et al., 2011]. However, in the case of injury, the change could be for tissue development, regulating both anabolic (ECM, collagen and proteoglycan synthesis) and catabolic (MMPs and ADAMTs expression) matrix turnover [Popov et al., 2015].

1.7 TENOCYTE RESPONSE TO LOADING

Mechanical loading induces cell deformation which initiates changes in gene expression and growth factors responsible for catabolic and/or anabolic cellular and molecular responses (e.g. synthesis of collagen and matrix proteins). These initial responses may proceed to induce long-term tendon structural modifications that may affect tendon material and morphological properties [Galloway et al., 2013; Heinemeier and Kjaer, 2011; Wang, 2006]. In particular, studies have shown that collagen synthesis and procollagen expression are mediated by growth factors such as insulin-like growth factor 1 (IGF-I), transforming growth factor-ß-1 (TGFß-1) as well as interleukin-6, whose interstitial concentration increased with exercise [Heinemeier et al., 2012; Kjaer et al., 2009; Wang, 2006]. Consequently, collagen synthesis has been shown to increase from 1% at rest to 2-3% after exercise, and remained elevated for at least 3 days [Miller et al., 2005].

The increase of metabolic activities observed in tendon when subjected to mechanical loading like exercise shows that the tendon is not just a passive connector between muscles and bone, but is an active tissue that responds to applied mechanical loading [Kalliokoski et al., 2005; Kjaer et al., 2005]. However, whether different amounts of mechanical loading induce differential expression of tenocyte and non-tenocyte related genes, remains unknown. Furthermore, the mechanotransduction mechanisms, by which cells sense mechanical loading and translate them into the biochemical signals that induce tissue adaptive responses, are still not completely understood [Heinemeier and Kjaer, 2011; Wang, 2006].

While the mechanism of action of eccentric loading is poorly understood, the new studies demonstrate that the differential component of loading during eccentric loading and ESWT is the 10Hz vibrations, which may provide useful insight [Chaudhry et al., 2015; Sweeney et al., 2011; Rees et al., 2008]. However, no one has yet investigated how 10Hz loading may influence tendon cell mechanotransduction.

Therefore, this study is designed to further understand the effects of 10Hz mechanical loading on tenocyte metabolism, comparing cell response to that seen with 1Hz loading, as most commonly seen in other studies.

1.8 HYPOTHESES, AIMS AND OBJECTIVES

Hypotheses

Clinical data indicates that mechanical loading may be involved in tendon healing with eccentric loading and ESWT studies indicating that tendon vibrations at 10Hz might be important for repair, therefore this study hypothesise that:

1) Mechanical loading will initiate increased metabolic activity of tenocytes, upregulating anabolic and catabolic gene expression enabling increased matrix turnover.
2) Mechanical loading at 10Hz will lead to an augment tenocyte response relative to loading at 1Hz.
3) Cells response to mechanical loading will differ between healthy and tendinopathy tenocytes.

Aim

The study aims to measure tenocyte metabolic activity in response to mechanical loading, investigating a broad range of metalloproteinases and matrix genes as a basis for trying to understand cell response to mechanical loading. Secondly, it aims to further characterise tenocyte mechanotransduction behaviour, by probing the signalling pathways involved in the mechanoregulation of gene expression.

Objectives

1. Set up system(s) to enable the application of high frequency (10Hz) loading to tendon cells while maintaining cell viability (chapter 2).
2. Compare cell response to mechanical loading at low (1Hz) and high (10Hz) loading frequencies (chapter 3).
3. Compare the metabolic activity of healthy and tendinopathic tenocytes to mechanical loading (chapter 3).
4. Investigate the signalling pathways involved in the tenocyte response to mechanical loading (chapter 4).

CHAPTER TWO

IN VITRO MODELS

2.1 INTRODUCTION

It is well known that mechanical load promotes tissue remodelling in tendon [Rees et al., 2008]. A number of studies looking at the effects of cyclic strain on tendon cells have demonstrated that the strain magnitude, strain frequency, strain rate and duration of strain application can all influence the cellular biochemical responses [Arampatzis et al., 2007]. However, there is little consensus about how different load magnitudes or frequencies affects cell behaviour, and poor understanding of how available data relate to *in vivo* loading. To begin to address the associations between *in vivo* loading and cell response, several studies have developed methods to probe the loads on tendon *in vivo* and subsequently estimate the strains experienced by cells [Chaudhry et al., 2015; Henriksen et al., 2009; Rees et al., 2008]. There are then a number of methods through which tenocyte mechanobiology in response to these strains can be investigated using experimental set ups.

It is possible to simulate *in vivo* load conditions directly with *in vivo* animal models, in which tendons are subject to defined loading protocols. However, not only do such experiments require the use of animals, but the *in vivo* situation is also very complex. Factors such as the animal's age, gender, physiology, genetics, behaviour and nutrition may all have an effect on the study outcome, or be confounding variables in the research process. Research done *in vitro* allows for a single experimental variable to be manipulated, hence mechanobiology studies using *in vitro* models can offer great insights when analysing the effect of various physiological and pathological load conditions on cell behaviour. However, they are some shortcomings with *in vitro* models also.

An ideal *in vitro* system would need to fully replicate the mechanical environment of the cells *in vivo*. Tissue explant models are closest to achieving this, providing a normal cell matrix interface and more realistic physiological cues, but while the chemical environment is more easily controlled than *in vivo*, it remains a less defined and variable parameter [Devkota and Weinhold, 2005]. Complete environmental control can be achieved by isolating cells from a tissue and seeding them into a new fully defined material for further characterisation. However, such approaches lose the physiological cell-matrix interface and simplify the cell strain environment. The simplest of such approaches adopts two-dimensional (2D) models, in which cells are cultured on an elastic membrane and subjected to a variety of mechanical stimulation regimes [Bayer et al., 2014]. 2D models provide a uniform cell seeding platform and the capacity to apply well defined strains but do not create

an environment similar to the native tissue environment [Thomopoulos et al., 2013]. Tenocytes in situ are known to form a three-dimensional (3D) communicating network that can be subjected to tensile, compressive and shear strains [Maeda et al., 2009]. Therefore, a model that supports this 3D organisation has some advantages over 2D systems, as it may be able to maintain tenocyte morphology and intercellular network organization, thus providing a more physiologically relevant local strain environment for cells when the material is subjected to a variety of mechanical stimulation regimes [Phillips and Brown, 2011]. 3D models unlike 2D models provide uniform mechanical stimulation through the scaffold thickness, hence across the cell body, whilst in 2D systems, cell attachment occurs on one side of the cell (that which is in contact with the 2D surface) [Thomopoulos et al., 2013]. Nevertheless, whilst cell attachment may be more physiological, the structure of 3D scaffolds remain poorly matched to the complex hierarchical organisation of ECM in tissues.

This chapter provides a brief overview of the *in vitro* models that were developed and tested in this research. For each model, the rationale for, and pertinent findings concerning, its use in future work are discussed, before selecting an appropriate *in vitro* platform for the remaining experimental work.

2.2 EXPLANT MODELS

INTRODUCTION

The need for reliable *in vitro* models as alternatives to traditional *in vivo* studies has increasingly become imperative in basic research. As such, explant models have been used to both minimize the number of animal/human samples required (since numerous explants can be obtained from one animal/human) and also to prevent any suffering associated with *in vivo* animal work. In addition, tissue explants to some extent mimic the *in vivo* cell environment, by retaining cells *in situ* in their native matrix [Patterson-Kane et al., 2012]. Nevertheless, it must be recognised that *in vitro* explants are often not representative of the *in vivo* situation in terms of cell population, nutrient supply and mechanical loading [Fisher, 2005].

In tendon research, tissue explants have been used to understand the composition, properties and mechanics of tendon [Thorpe et al., 2014; Thorpe et al., 2013b; Wren et al., 2001], and to study how cyclic loading under creep or stress deprivation conditions alter cell and tissue mechanobiology [Weinhold et al., 2001]. Of particular interest to the current project, a number of studies have been successful in investigating cell response to strain in cultured tissue explants. In 2005, Screen and colleagues reported an upregulation in collagen production in response to cyclic tensile strain using rat fascicles, demonstrating that the application of cyclic tensile strain to isolated tendon fascicles would initiate anabolic matrix metabolism [Screen et al., 2005]. Tenocytes respond to mechanical stimulus by altering the balance between anabolic and catabolic processes. Maeda et al. [2010] showed increased anabolic cell response in rat tail tendon subjected to cyclic tensile strain (3% amplitude superimposed on a 2% static strain) for 1 or 24 hr. The anabolic response was more pronounced as the number of strain cycles was increased, with the 1hr of cyclic strain showing a significant upregulation in gene expression of growth factors including basic fibroblast growth factor (bFGF) and vascular endothelial growth factor, while the 24hr cyclic strain showing increased expression of types VI and VIII collagen, aggrecan, TGF-β1, vascular endothelial growth factor, and bone morphogenetic protein 2 expression [Maeda et al., 2010]. In the current study, the potential to use tendon explants to investigate cell response to 10Hz loading was explored.

2.3 BOVINE EXPLANT MODEL

2.3.1 METHODOLOGIES

2.3.1.1 SAMPLE COLLECTION AND PREPARATION

The feet of healthy bovines (male steers between 18 and 36 months) with no observed tendon injury were sourced from a local abattoir. The extensor tendons were removed within 24 hour of slaughter under sterile conditions, and wrapped in tissue paper dampened with sterile Dulbecco's Modified Eagle Medium (DMEM) ready for explant dissection (Figure 2.1). The extensor tendons of the bovine foot were selected in preference to the flexor tendons, as the extensor fascicles run in straight lines, and are visible to the naked eye, thus minimizing the likelihood of damage during dissection. During explant dissection, hydration was maintained with DMEM. Tissue explants (containing 5-8 fascicles; 0.4-0.6mm diameter and 20 mm length) were isolated from the bovine extensor tendons by cutting with a scalpel longitudinally through the tendon using previously established protocols [Legerlotz et al., 2013] . Hydration in isolated explants was maintained by storing them wrapped in tissue paper dampened with DMEM prior to testing.

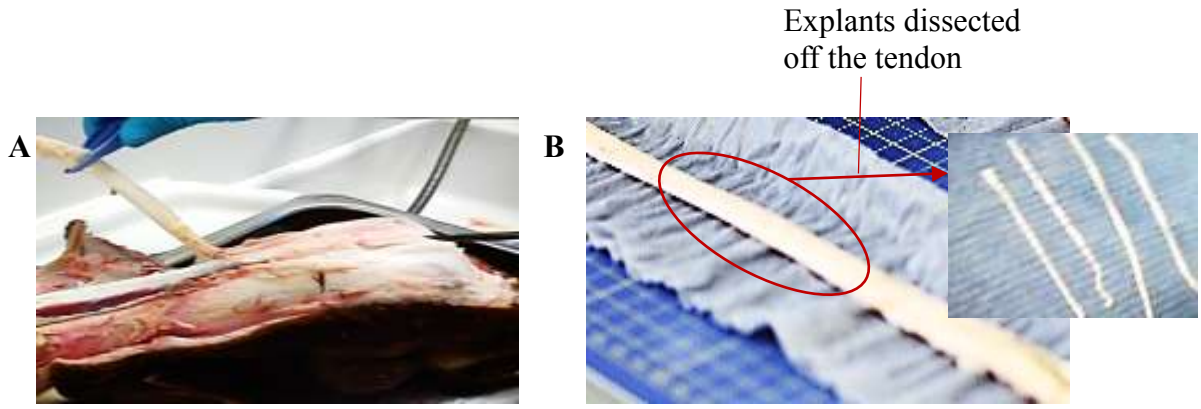

Figure 2.1: ***A.*** *Bovine hoof skinned to access the Extensor tendons,* ***B.*** *Extensor tendon dissected from the bovine hoof ready for dissection into explants (inset)*

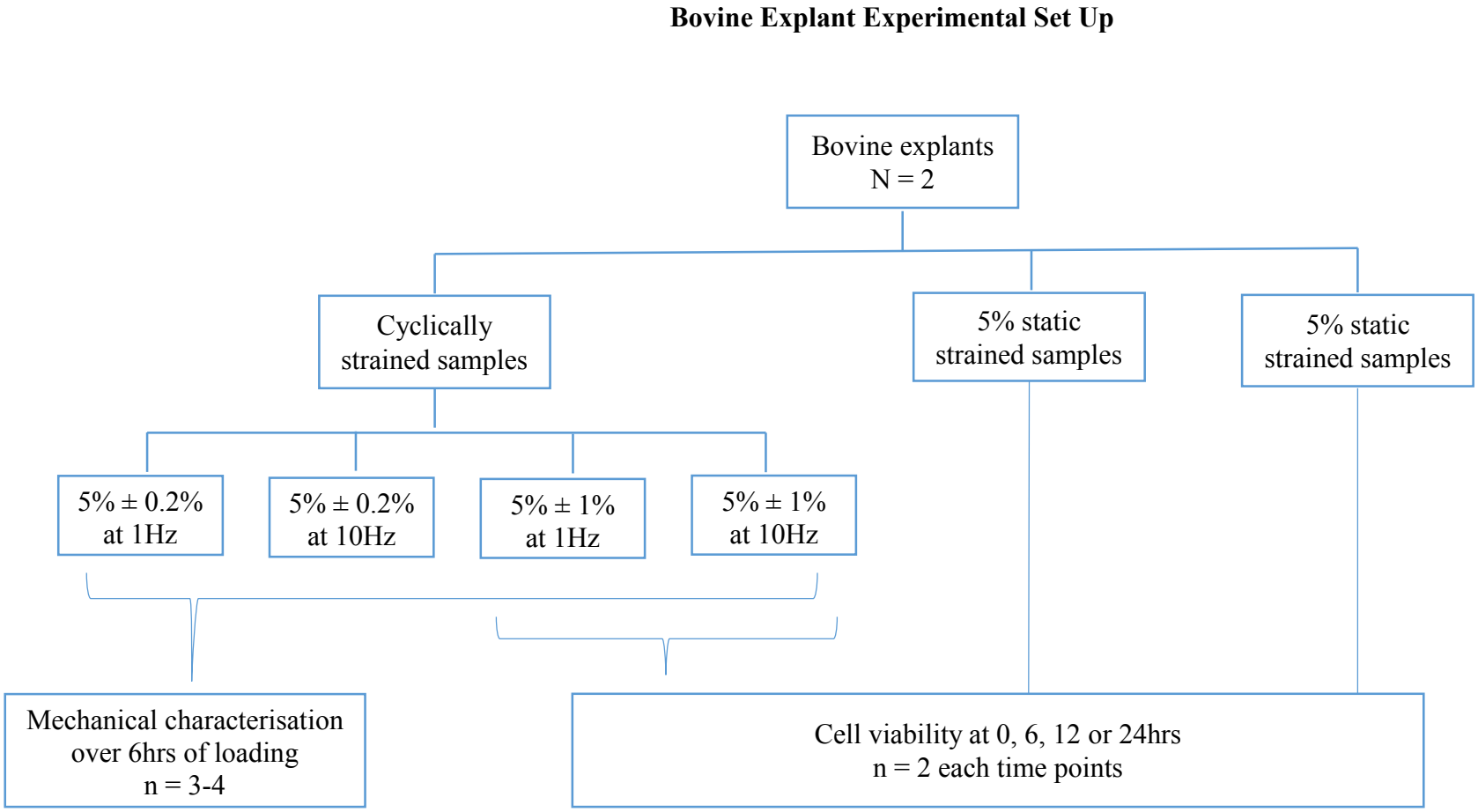

Figure 2.2: *Flow diagram of experiments performed on bovine explants to investigate their mechanical behaviour and cell viability over the duration of loading experiments. Four loading regimes are proposed for future studies; cyclic loading at 1Hz and 10Hz to strains of 5% ± 0.2% and 5% ± 1%. N (number of biological repeat) = 2, n (technical repeats).*

To establish if explants may be appropriate for mechanobiology studies, explant viability was investigated with and without the application of cyclic mechanical stimuli. In addition to viability assessment, the mechanical response of the explants to the required mechanical stimuli was assessed, to confirm if the cells will experience strain throughout any further experiments. A flow diagram outlining the experimental groups is shown in Figure 2.2.

2.3.1.2 BOVINE EXPLANTS MECHANICAL CHARCTERISATION

For mechanical characterisation explant diameters were measured using a non-contact laser micrometre (LSM-501, Mitotuyo, Japan; resolution = 0.5μm) following previously established protocol [Shepherd et al., 2014]. Each explant was moved through the laser beam taking 10 evenly spaced diameter measures along the 10mm length, of which the minimum value was recorded and used to calculate the cross sectional area of the explant, assuming a circular shape. Explants were secured in custom designed stainless steel loading chambers at a grip-to-grip distance of 10 mm (Figure 2.3). The chambers were filled with DMEM then sealed with the surrounding glass tube allowing full hydration at all times. Each chamber was secured in a mechanical loading frame (TA ElectroForce) with a 225N load cell, housed in an incubator to maintain samples in 5% CO_2 at 37°C as shown in Figure 2.3. The loading frame then applied the required mechanical stimuli to the sample for a 6hr period, recording displacement and maximum and minimum peak loads. The loading conditions and technical repeats assessed were:

- Low magnitude Low frequency: 5% ± 0.2% at 1Hz (n = 4)
- Low magnitude High frequency: 5% ± 0.2% at 10Hz (n = 3)
- High magnitude Low frequency: 5% ± 1% at 1Hz (n = 4)
- High magnitude High frequency: 5% ± 1% at 10Hz (n = 3)

A student's t-test was used to investigate significant differences in load relaxation between loading groups. Significance was defined as $p \leq 0.05$.

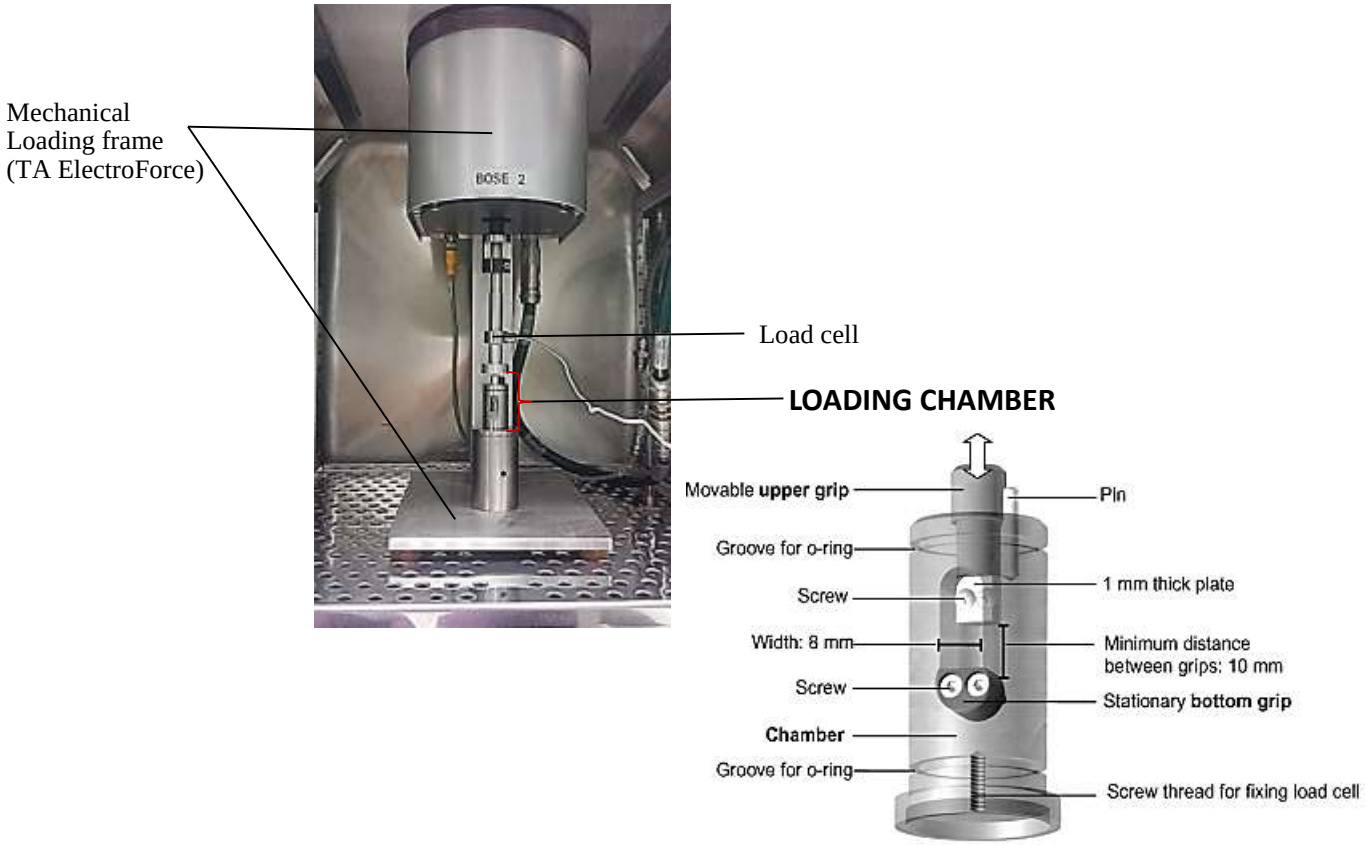

Figure 2.3: *Photograph of an explant secured in a loading chamber and within the incubator ready for testing. The schematic of the chamber highlights its components. The explant was secured between two metal plate grips tightened with screws, the chamber filled with medium and sealed with a Plexiglas cylinder. O-rings at the top and bottom of the chamber prevent the medium from leaking out. The chamber is then secure in the mechanical loading frame. Schematics of loading chamber [adapted from Legerlotz et al., 2013].*

2.3.1.3 BOVINE EXPLANT CELL VIABILITY ANALYSIS

Spatial assessment of cell viability in explant tissues was performed using visual live/dead staining on a confocal microscope, adopting a previously established protocol [Thorpe et al., 2014]. The stains used were Calcein AM and Ethidium homodier; the live cells metabolize Calcein AM and show green fluorescence, while the membranes of the dead cells are penetrated by Ethidium homodier and show red fluorescence.

After subjecting explants to the mechanical testing conditions of interest, explants were incubated in 2ml of DMEM, containing Calcein AM (0.01mg/ml) and Ethidium homodimer (3.75µM/ml) at 37^{o}C for 1 hour 30 minutes, to allow the dye penetrate the tissue. During incubation, the sample was covered with aluminium foil to protect the dye and sample from light and photo bleaching. After incubation, explants were washed in Dulbecco's Phosphate-Buffered Saline (DPBS) and transferred to a microscopy slide, covered with a coverslip, and mounted for viewing on a confocal laser scanning microscope (Perkin Elmer) at X10

magnification, where the laser line was excited at 488 nm for Calcein AM and 568mm for ethidium homodimer. Fluorescence was collected at 525 ± 10 nm for Calcein AM and at 620±10 nm for ethidium homodimer.

Cell viability was assessed as a percentage of live to dead cells. Two fields of view were randomly selected for each sample (one at the periphery and one in the core region), and the number of live cells and dead cells within each field of view counted to determine viability using equation 2.1.

$$\%\ cell\ viability\ in\ field\ of\ view = \frac{\text{Live cells}}{\text{Total number of cells (live + dead cells)}} x100 \quad - - - - Equation\ 2.1$$

Cell viability was analysed after the following loading conditions;

- Unstrained for 0, 6, 12, and 24hrs
- 5% Static strain for 6, 12, and 24hrs
- High magnitude Low frequency loading: 5% ± 1% at 1Hz for 6, 12, and 24hrs
  High magnitude High frequency loading: 5% ± 1% at 10Hz for 6, 12, and 24hrs

2.3.2 RESULTS

2.3.2.1 BOVINE EXPLANTS MECHANICAL TEST CHARACTERISATION

Typical stress relaxation curves for explants subjected to each cyclic strain condition are shown in Figure 3.4 with mean data for stress relaxation at 6hrs across samples (calculated using equation 2.2) shown in Figure 3.5. Data indicate significantly greater stress relaxation with low frequency (1Hz) loading compared with high frequency (10Hz) loading and relaxation was also greater when the applied strains were higher.

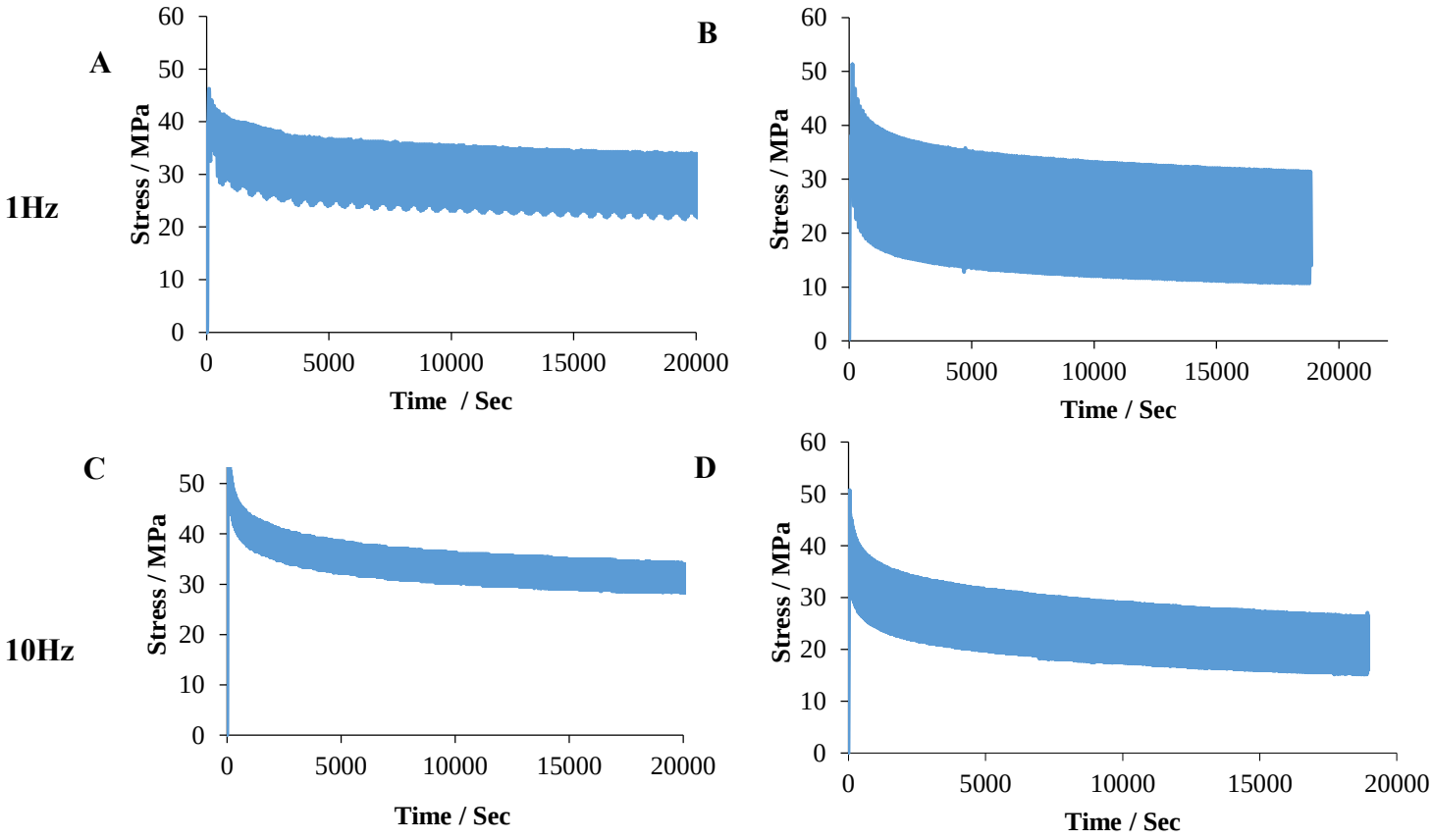

Figure 2.4: *Typical stress relaxation curves from bovine explants subject to cyclic strain.* ***A)*** *5%±0.2% strain at 1 Hz* ***B)*** *5%±1% strain at 1 Hz* ***C)*** *5%±0.2% strain at 10 Hz* ***D)*** *5%±1% strain at 10 Hz.*

$$\%\ Max\ stress\ relaxtion = \frac{\text{maximum peak stress} - \text{minimum peak stress}}{\text{maximum peak stress}}\ \text{X}\ 10 - -Equation\ 2.2$$

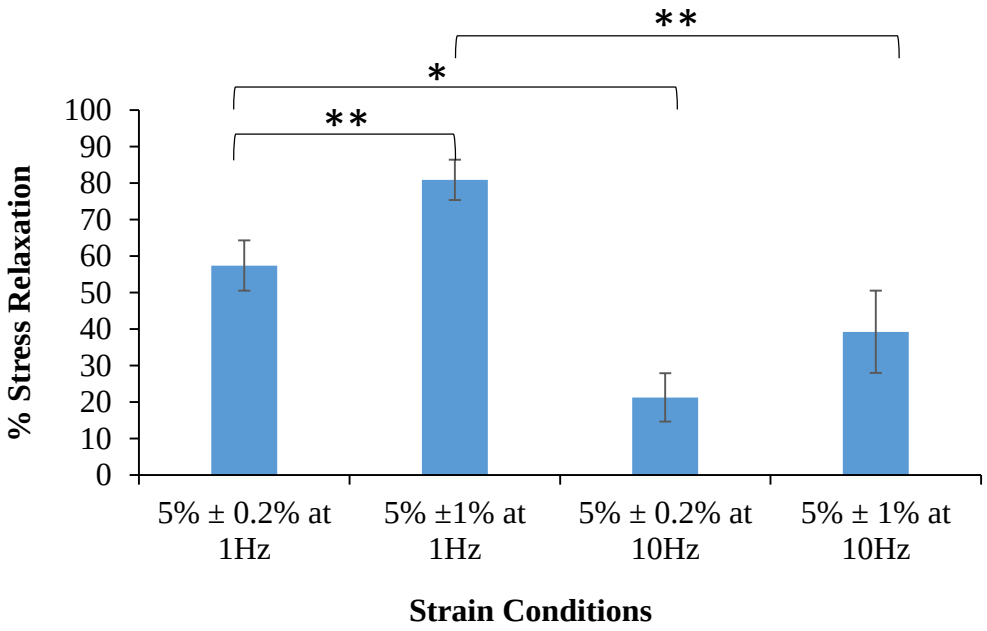

Figure 2.5: *Mean stress relaxation of bovine tendon explants after 6hrs of loading, comparing each loading condition. Stress relaxation was greatest with the higher magnitude of applied strain and the slower loading frequency. Error bars show standard deviation from the mean. * = p<0.05, ** = p<0.01.*

2.3.2.2 BOVINE EXPLANTS CELL VIABILITY

Live and dead cells were counted and viability expressed as percentage of the total cell number. Figure 2.6 show representative images of the cells after 24hrs of loading (strain of 5% ± 1% at 10Hz) whilst table 2.1 reports mean viability in the periphery and core across all samples. All sample groups showed below 50% cell viability.

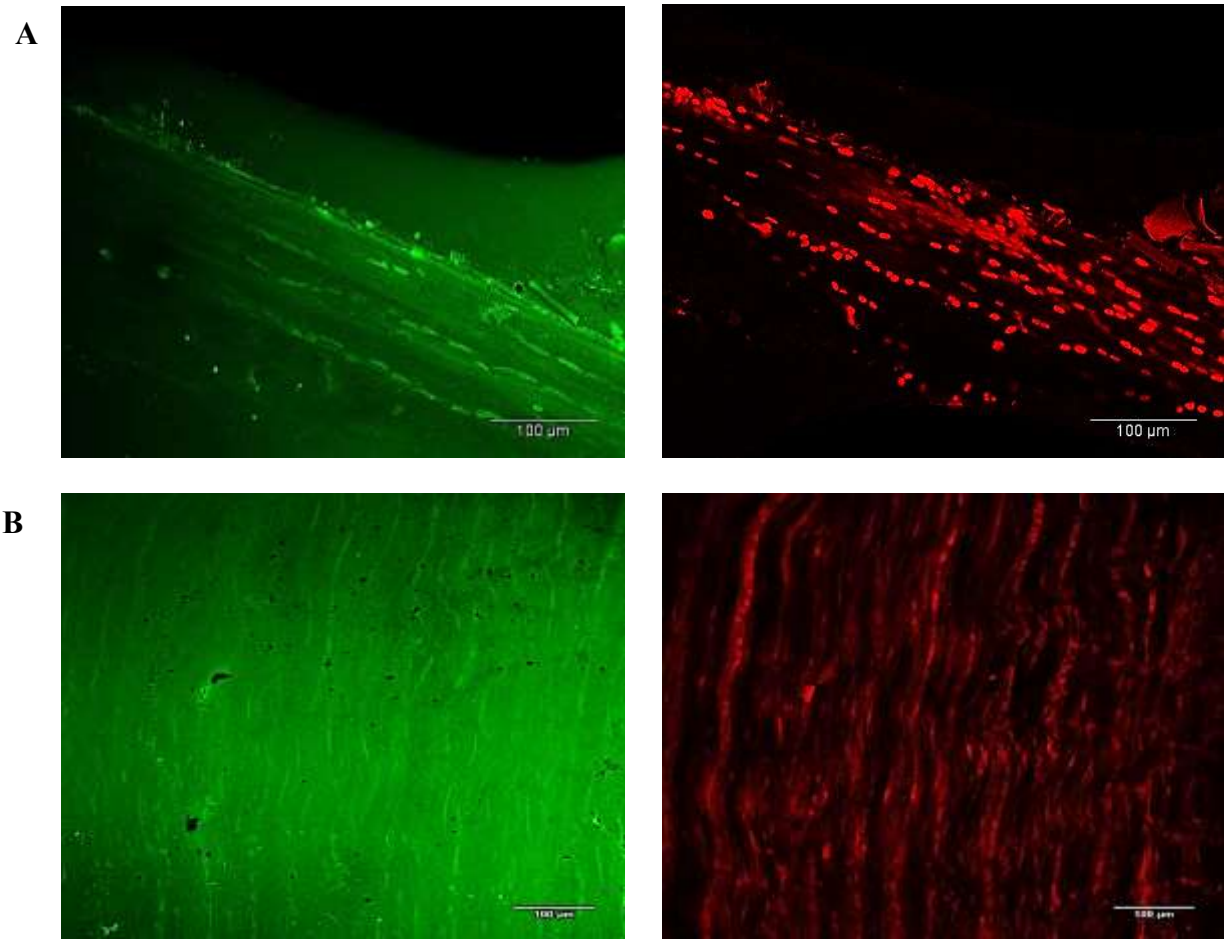

Figure 2.6: *Typical images of bovine explants subjected to strain of 5% ± 1% at 10Hz for 24hrs, stained to show live and dead cells after loading. Scale bar = 100µm. Live cells emits green fluorescence while dead cells emits red fluorescence.* ***A)*** *Representative images at the periphery of the explants,* ***B)*** *Representative images at the core of the explants.*

Table 2.1: Cell viability results, showing the mean percentage of live cells at the periphery (left-hand columns) and core (right-hand columns) of explants, comparing response in unloaded samples with those subject to different load conditions. Biological repeats, N = 2 with the number of optical viewpoints ranging from 3 to 5 for each repeat experiment.

	Percentage viability at the periphery of the fascicles [Mean (%) ± standard deviation]		**Percentage viability at the core of the fascicles [Mean (%) ± standard deviation]**			
Duration (hrs)	**Unloaded**	**Static**	**Unloaded**	**Static**	**High mag low freq**	**High mag high freq**
0	22 ± 1.2	-	44 ± 0.8	51 ± 18.4	-	-
6	18 ± 7.6	19 ± 2.9	39 ± 8.7	40 ± 6.3	21 ± 8.9	32 ± 10.5
12	9 ± 5.2	6 ± 1.6	29 ± 9	36 ± 1.7	0	0
24	0	0	27 ± 1.5	30 ± 8.8	0	0

Cell viability from 0 to 12hrs was between 9 and 22% at the periphery of explants and not influenced by the application of static strain. By 24hrs, the cell viability at the periphery was 0%. Viability was somewhat improved in the core of explants, but still low, ranging from 21-51% (see table 2.1). Whilst not affected by static loading, the cell viability at the core after 12hrs of cyclic loading was 0% indicating 100% cell death with cyclic loading.

2.3.3 DISCUSSION

This study has examined the efficacy of using bovine explants to test the hypothesis that high frequency loading differentially influence tenocyte mechanobiology. Tendon is known to be viscoelastic [Peltonen et al., 2013; Duenwald et al., 2009], hence to better understand the effects of cyclic loading on cells, the mechanical properties of explants must be characterised, to establish how the tendon will behave under the described loading conditions. Cell viability must also be analysed to ensure the cells within the explants remain viable.

The stress relaxation data (Figure 2.5) showed that all samples exhibited stress relaxation supporting existing literature [Shepherd et al., 2014; Screen et al., 2013; Duenwald, et al., 2010]. Stress relaxation was greatest under the higher strain and slower loading frequency conditions. Studies have shown that stress relaxation occur as a result of structural rearrangement within the samples thus, when load is applied more slowly, more time facilitates greater levels of stress relaxation [Shepherd et al., 2014]. It is important that the explant does not stress relax to the point where no strain is experienced by the cells, or their response to the desired loading regime cannot be examined. Data confirmed that samples experienced load throughout the test period. However, the magnitude of cell strains will be influenced by the stress relaxation behaviour.

Cyclic loading of explants can also result in damage, presenting as kinking of the collagen fibres and widening of the inter-fibre space. Such damage is likely to elicit a response from the resident cells, which may well take an active role in controlling further tendon behaviour and may affect later gene expression analysis [Shepherd et al., 2014]. In the current study, explants contained 0.3mm diameter of fascicles and were cyclically loaded to 5% strain at 1Hz or 10Hz for 21600 cycles. Shepherd et al. [2014] have previously established that cyclic stress relaxation of single fascicles from bovine extensor and flexor tendons, showed some degree of collagen matrix disorganisation after 1800 cycles of 14% strain at 1Hz. Whilst the loading conditions in the current study were notably less severe, it is feasible the loading may lead to some matrix disorganisation. It would be important to avoid this in the current study, where the goal is to investigate cell response to different loading frequencies.

However, as a result of cell viability data, this was not explored further. The cell viability data in Figure 2.6 and table 2.1 clearly showed that the bovine explants exhibited pronounced cell death with the applied loading conditions. Cell death at the periphery of an explant has been

reported previously, likely a result of the damage generated by the scalpel. However, previous studies had shown the core fascicles remain viable in the equine model [Thorpe et al., 2015b]. This was clearly not the case in the bovine model, possibly as explants had a slightly smaller diameter. Upon cell death, factors stored in the cytosol may be released causing inflammation [Kondratko-Mitttnacht et al., 2015], potentially affecting gene expression data and subsequent tissue remodelling and repair process. These findings highlighted that bovine explants could not be utilised for further studies. Owing to this major limitation, alternative explant sources were examined, in which dissection was less extensive.

2.4 RAT EXPLANT MODEL

2.4.1 METHODOLOGIES

Individual tendon explants can easily be removed from rats with no need for dissection, as they can simply be pulled out from the tendon sheath. It was therefore hypothesised the cell viability would not be affected by sample preparation using the rat model (either Achilles tendon or tail tendon fascicles). Samples were tested to confirm cell viability with and without loading and also to assess the effects of explant preparation on gene expression and determine how long explant gene expression takes to stabilise post removal. Further research into the potential mechanical stimuli generated by ESWT or eccentric loading identified that the magnitude of vibrations is likely to be very small. As such, the loading conditions have been altered to apply 1% ± 1% cyclic strain from this point onwards

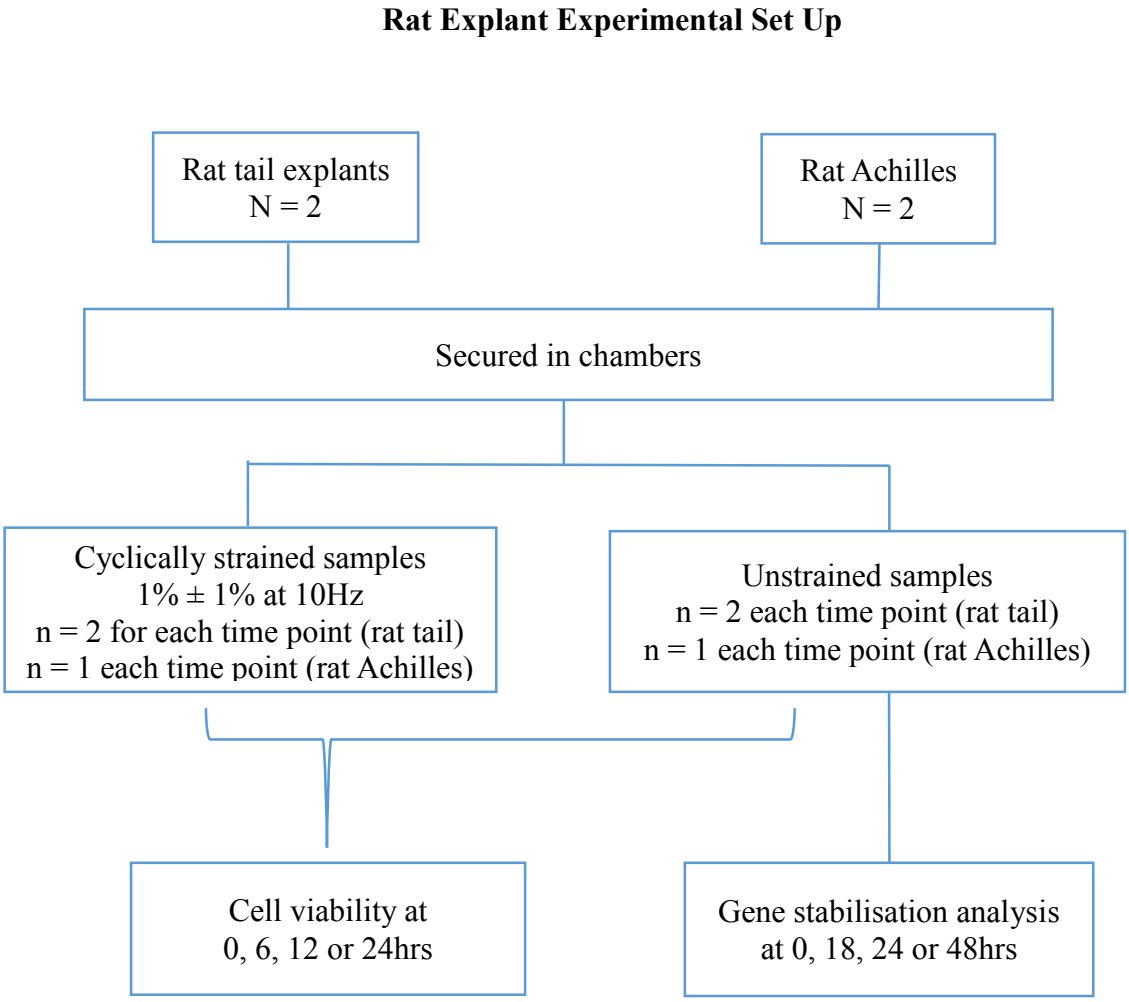

Figure 2.7: *Flow diagram of experiments performed on rat explants. Cell viability was investigated in cyclically strained samples, strained at 1% ± 1% strain while the unstrained samples were left unloaded in the incubator for the specified time. Number of biological repeats, N = 2, n is the number of technical repeats*

2.4.1.1 SAMPLE COLLECTION AND PREPARATION

Adult female *Sprague Dawley* rats, each weighing 200g, were used in this study. Tails and legs from the rats were obtained as waste tissue from an experiment that took place in the university medical campus in Whitechapel, carrying out a neurological experiment on the brain and spine, which had no effect on the tendons. Rat tail and Achilles tendon explant were obtained following a previously established protocol [Screen et al., 2004]

Rat Tendon Tail Explant

Individual fascicles of approximately 20mm length were carefully dissected from the proximal end of the tail within a sterile hood (n = 5). The rat tail has six tendons surrounding the tail vertebrae [Bruneau et al., 2010] (Figure 2.8) and fascicles are separate entities within each tendon, so can be removed with ease. During dissection, special care was taken not to load the fascicles while separating them from the bony attachments, and the main securing force was placed on the tail backbone itself, not on the tendon being dissected. Fascicles were obtained from each tendon by carefully pulling them out of their sheath, and placing them in DMEM-soaked blue paper roll to maintain hydration.

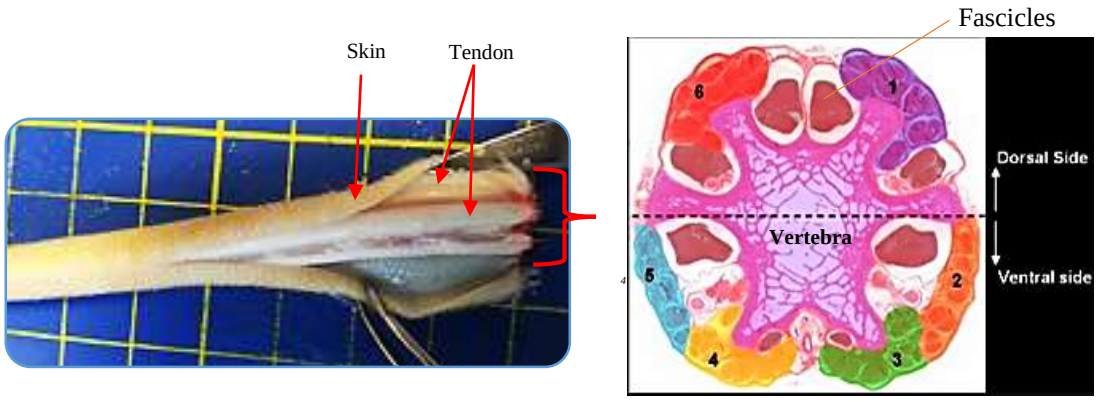

Figure 2.8: *The rat tail is a long cylinder consisting of three concentric layers. The innermost core of the tail is bone (vertebra). The bone is surrounded by a layer of tendons (labelled 1-6), and the tendons are surrounded by a layer of skin. Cross sectional image of a rat tail [adapted from Bruneau et al., 2010].*

Rat Achilles Tendon Explant

In a sterile hood, the rat Achilles tendon was carefully dissected from the muscle attachment points and the tuber calcanei, and maintained in paper towel soaked in DMEM in order to maintain hydration. The rat Achilles tendon is made up of three single separate strands; one

from each of the three tricep surae muscles (the medial head of the gastrocnemius muscle, the lateral head of the gastrocnemius muscle and the plantaris tendon) (Figure 2.9). At the muscle attachment end, the three single strands of the Achilles tendon are loosely connected to one another with a soft proteoglycan rich matrix, which is easily transected during dissection. However, the fusion between the individual parts of the Achilles tendon by the tuber calcanei is distinctly stronger and required the use of a scalpel. The individual parts of the Achilles tendon were separated to give three samples of which one was used as an unstrained control, the explant from the lateral head of the gastrocnemius muscle (the longest of the three).

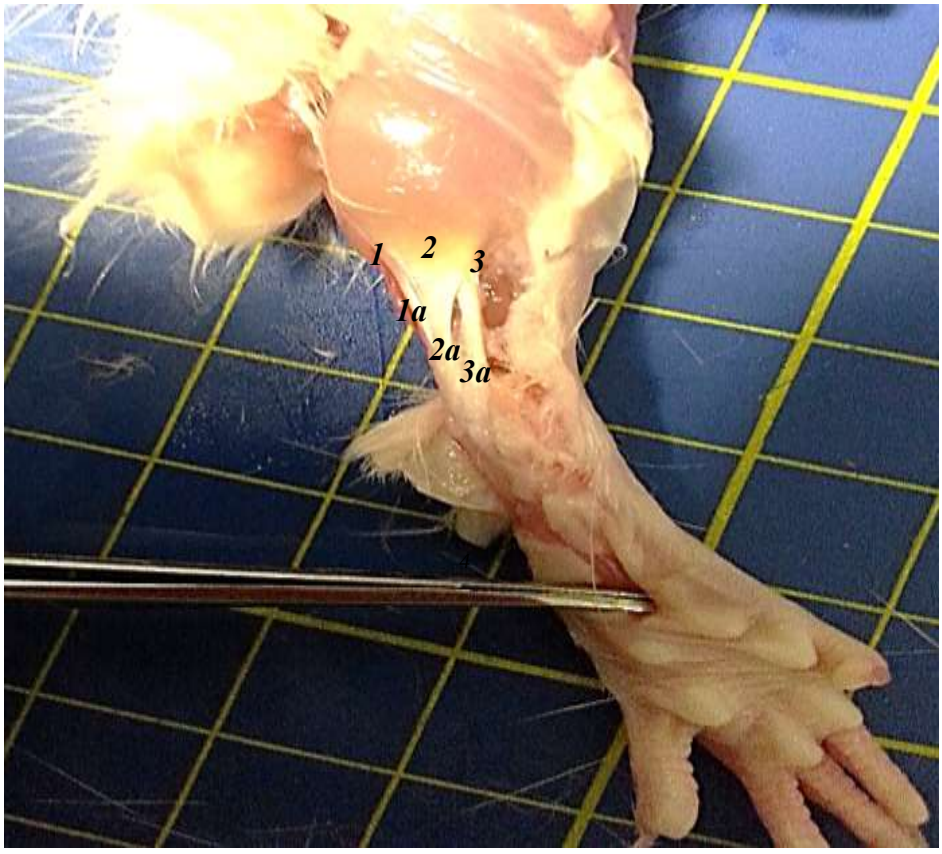

Figure 2.9: *The rat Achilles tendon joins the three tricep surae muscles and inserts at the tuber calcanei. Rat Achilles tendon from the right leg;* ***1*** *– the medial head of the gastrocnemius muscle;* ***1a*** *– the fascicle from the medial head of the gastrocnemius muscle;* ***2*** *– the lateral head of the gastrocnemius muscle;* ***2a*** *– the fascicle from the lateral head of the gastrocnemius muscle;* ***3*** *– the plantaris muscle;* ***3a*** *– the fascicle from the plantaris muscle;* ***4*** *– the tuber calcanei.*

Samples were secured in individual custom designed stainless steel loading chambers at a grip-to-grip distance of 10 mm (Figure 2.3). The chambers were filled with DMEM then sealed in the glass surround, maintaining full hydration. Rat tail explants secured in chambers (up to 6 at a time) were connected to a single actuator arm and secured within a BOSE loading frame housed in an incubator to maintain samples in 5% CO_2 at 37°C as shown in Figure 2.3 then

subjected to cyclic strain of 1% ± 1% at 10Hz for 24hrs. Unloaded controls from rat tail and rat Achilles explants were secured in chambers also but the chambers were simply housed in the 5% CO_2 at 37^{o}C incubator for 24hrs.

2.4.1.2 RAT EXPLANTS CELL VIABILITY ANALYSIS

For viability analysis, rat tail explants were placed in the Calcein AM / Ethidium homodimer dye mix described in chapter 2.2.1 at 37°C for 1 hour, while the rat Achilles samples were incubated at 37°C for 1 hour 30 minutes. All samples were removed from the dye, rinse in DMEM, and then placed on a coverslip to be viewed under the laser scanning confocal microscope (Perkin Elmer), using an X20 objective. Three images were collected across the length of the explant at a depth (z) of 0.2mm, with images of red and green fluorescence collected at each view point.

2.4.1.3 RAT EXPLANTS GENE STABILISATION CHECK

A time course analysis of selected genes (MMP3, MMP13, COL1A1, COL3A1, IL6, and Decorin) was carried out to investigate how sample dissection and preparation may influence gene expression, and the time period required for gene expression to stabilise prior to mechanical loading experiments. Samples were dissected, and immediately secured in chambers and maintained unloaded until the appropriate time points (0, 18, 24 or 48hrs) when they were removed, and immediately placed in a 1mm cryotube and immersed in liquid nitrogen for 3-5 minutes before storing at -80°C for later gene analysis.

RNA Extraction

RNA was isolated as described previously, using a tri-spin protocol [Ireland et al., 2001]. In detail, samples were removed from the -80°C freezer and homogenised using a Sartorius Mikro-Dismembrator (Figure 2.10). A ball was added to the cryotube and the sample was homogenised using a dismembrator set at 2000 RPM for one minute. The cryotube was removed from the dismembrator, 1ml Trizol reagent added to each tube and left to incubate at room temperature for 5 minutes to allow complete dissociation of nucleoprotein complexes. 125µg/ml (25µl) glycogen was then added to each cryotube, the tube inverted and incubated at room temperature for another 5 minutes. Glycogen binds to RNA and assists in visualising the RNA pellet obtained at a later stage of this protocol by making it cloudy.

Figure 2.10: *A dismembrator with cryotube attached, set at 2000 RPM for one minute to homogenise a sample into powder form, aiding complete homogenisation with Trizol.*

Empty phase lock gels tubes were centrifuged at 10000g for 1 minute to collect the gel at the bottom of the tube. After centrifugation, the sample solution (trizol + glycogen) was transferred to the phase lock gel tubes and 1/5 sample volume of chloroform was added to the samples, which were then shaken vigorously for 15 seconds and incubated at room temperature for 3 minutes. Samples were centrifuged at 12000g for 15 minutes at 4ºC. The phase lock gels allowed a clear separation of the phenol-chloroform organic phase and the interface material containing the nucleic acid. The interface material in the upper aqueous phase was transferred into a new tube (volume of the aqueous phase is about 60% of the volume of trizol reagent) for RNA precipitation while the phase lock gel tubes and remaining content were discarded.

Propan-2-ol was added to the fresh tube containing the colourless aqueous phase at a 1:1 ratio. For precipitation of the nucleic acid, the fresh tube was then inverted 5 times and the samples were incubated at room temperature for at least 10 minutes. Samples were centrifuged for 10 minutes at 12000g at 4ºC. RNA precipitate formed at the bottom of the tube as a cloudy gel-like pellet.

The supernatant was removed completely and RNA pellets washed twice with 1ml of 70% ethanol, centrifuging samples at 7500g for 5 minutes at 4ºC after each wash. Ethanol was then removed completely. This was repeated twice.

Samples were air dried for 15-20 minutes (until pellets appeared transparent) after which the RNA was dissolved and re-suspended in 30µl of nuclease free water. Samples were incubated at room temperature for 10 minutes and mixed by flicking tubes gently, before storing at -80ºC until ready for analysis.

Samples were removed from the -80ºC freezer, thawed at room temperature for 5 minutes and then centrifuged at 10000g for 1 minute. RNA concentration and quality was estimated using a nanodrop spectrophotometer. 1µl of sample was directly placed onto the fiber optic measurement surface of the nanodrop spectrometer where it was held in place by surface tension, eliminating the need for cuvettes or capillaries. When the upper fiber optic tip engages the sample, a liquid column of controlled path length is formed. A full-spectrum absorbance measurement is automatically made through the hourglass-shaped sample column at both a 1mm and 0.2mm path length. The absorbance (A) ratio of these measures is calculated as an indicator of RNA quality. A_{260}:A_{280} of ≥ 1.6 is considered acceptable with an optimum value of 2. After nanodrop analysis, samples were returned to -80ºC for later gene analysis.

Reverse Transcription and Quantitative Real Time PCR

Samples were removed from -80ºC freezer and thawed at room temperature for 5 minutes ready for gene transcription and qRT-PCR following previously described protocols [Jones, 2012]. All RNA samples were diluted in RNA free water, so all samples in an experimental set were at the same concentration. From each sample, 9.5µl was pipetted into separate wells of a 96 well plate and centrifuged at 2000g for 1 minute. RNA was primed with 1.5µl of random hexamers (concentration – 200ng/µl), centrifuged at 2000g for 10 seconds and incubated in a thermocycler at 70ºC for 10 minutes then held at 4ºC until removed. RNA was reverse transcribed with 9µl of reverse transcription master mix containing the component outlined in table 2.2. Samples were then centrifuged at 2000g for 10 seconds and incubated at 42ºC for 60 minutes, then 70ºC for 10 minutes and held at 4ºC until removed. The resulting cDNA for each sample was diluted to a concentration of 1ng/µl.

Table 2.2: Composition of reverse transcription master mix

Component (Supplier)	Amount (µl)
Superscript II at 200U/µl concentration (Life Technologies)	1
5x Sample buffer (Supplied in Superscript II kit)	4.5
DTT (Dithiothreitol) at 10mM concentration (Supplied in Superscript II kit)	2
dNTP's (Deoxy-nucleotide triphosphate) at 2.5mM concentration (Promega)	1
RNase inhibitor at 20U/µl concentration (Promega)	0.5
	Total volume = 9

A cDNA stock solution was made by taking 5µl cDNA from each sample. 5 serial dilutions of 1:5 were made from the cDNA stock solution (20µl cDNA + 80µl water) to create a 5 point standard curve. Standard curves for each assay were used to confirm primer probe efficiency. A slope of $-3.6 \geq \text{slope} \geq -3.3$ was expected, along with a correlation coefficient or R value of 1; only primers with similar values to this were accepted (slope ±0.5, R ±0.1).

10µl of each standard dilution was pipetted into the Taqman plate for a 10ng reaction. A gene master-mix was prepared for each gene of interest (table 2.3) and 15µl of gene master-mix was pipetted to the Taqman plate. The standard qRT-PCR programme was run using the Applied Biosystems 7500 real time PCR system (ThermoFisher Scientific) which took 90mins.

The thermal cycles were performed at 50°C for 2 minutes, 95°C for 10 minutes, followed by 40 cycles of 95°C for 15 seconds, and finally 60°C for 1 minute. Relative expression levels of each gene of interest were analysed by normalising to endogenous control genes GAPDH (ΔCt [endogenous control gene Ct-gene of interest Ct]) and linearising these data by expressing it as $2^{\Delta Ct}$. Data for loaded samples were then expressed as a fold change from the control ($2^{\Delta\Delta Ct}$ [strained condition $2^{\Delta Ct}$ / Control $2^{\Delta Ct}$]) while data for the vary time points were expressed as a fold change from the 0hr control ($2^{\Delta\Delta Ct}$ [unstrained time condition $2^{\Delta Ct}$ / 0hr unstrained control $2^{\Delta Ct}$]). Statistical analyses were performed using the student's t test (two tailed distribution, equal variance).

Table 2.3: Composition of gene master-mix

Component (Supplier)	Amount (µl)		
	Probe	**SYBR green**	**Prime probe mix**
Forward primer at 10µM concentration (Life Technologies)	0.5	0.5	-
Reverse primer at 10µM concentration (Life Technologies)	0.5	0.5	-
Probe at 0.1µM concentration (Life Technologies)	0.5	-	-
SYBR green (Life Technologies)	-	0.3	-
Prime-Probe mix (Life Technologies)			1
2x Master mix (Life Technologies)	8.33	8.33	8.33
Analytical grade water (Sigma Aldrich)	5.17	5.37	5.67
	Total volume = 15		

Table 2.4: Primer sequences (Forward and reverse) used for real-time polymerase chain reaction

Target Gene	Primer Sequence	Length of Product (bp)	GeneBank Accession no.	Reference
RAT				
GAPDH	GGAAAGCTGTGGCGTGAT AAGGTGGAAGAATGGGAGTT	1306	NM_017008	Zhang et al., 2011
MMP3	GACCAGGGACCAATGGAGATG TGAGCAGCAACCAGGAATAGG	1771	NM_133523	Zhang et al., 2011
MMP13	GGCCAGAACTTCCCAACCA ACCCTCCATAATGTCATACCC	2601	NM_133530	Zhang et al., 2011
COL1A1	CTACAGCACGCTTGTGGATG CAGATTGGGATGGAGGGAGT	5843	NM_053304	Zhang et al., 2011
COL3A1	ATCAAACACGCAAGGCCATG AAGCAAACAGGGCCAATGTC	4792	NM_032085	Gu et al., 2014
IL6	ACTTCACAAGTCGGAGGCTT AGTGCATCATCGCTGTTCAT	1045	NM_012589	Zhang et al., 2014
Decorin (DCN)	TGAAGGACTTGCATACCTG GTTACTTGTAGTTCCCAAGT	1639	NM_024129	Sasamura et al., 2001

2.4.2 RESULTS

2.4.2.1 RAT EXPLANTS CELL VIABILITY

Cell viability were analysed within rat tail fascicles over time. Figure 2.11 shows cell viability for a typical region within the core of the rat tail explant. The rat tail tendon explants maintained cell viability at around 70% even after loading for 24hrs. Unfortunately, the cell viability within the rat Achilles explants could not be analysed using fluorescent dyes, as the dyes were unable to penetrate to the tissue, hence could not dye the cells.

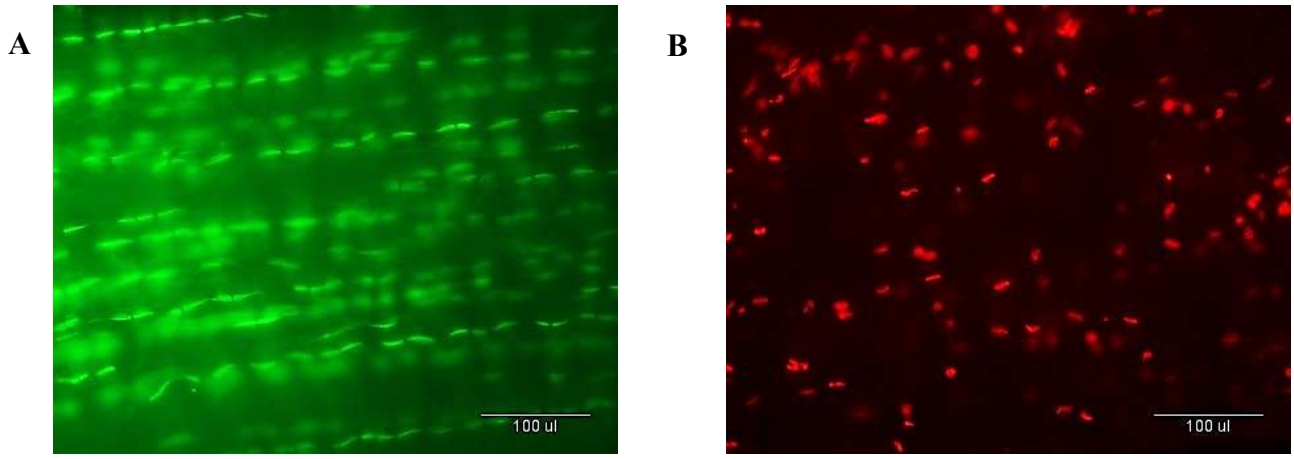

Figure 2.11: *Images from a typical region, showing calcein AM and ethidium homodimer emission from the same region of a rat tail explant after 24hrs of loading. A) Live cells emits green fluorescence* ***B)*** *Dead cells emits red fluorescence.*

Table 2.5: Cell viability results, showing the mean percentage of live cells in rat tail explants after different time periods. Biological repeats, N = 2 with the number of optical viewpoints ranging from 3 to 5 for each repeat experiment.

	Percentage viability (Mean (%) ± standard deviation)	
Duration	**Unloaded**	**Loaded at high freq.**
0hrs	90 ± 4.9	-
6hrs	83 ± 5.7	81 ± 1.4
12hrs	74 ± 2.8	71 ± 3.5
24hrs	71 ± 1.4	68 ± 3.5

2.4.2.2 RAT EXPLANTS GENE STABILISATION CHECK

Time Course Analysis of Selected Genes

A time course analysis of selected genes was carried out for the rat tail and Achilles tendon explants, comparing gene expression at 0, 18, 24 and 48 hours to see when it stabilised after explant dissection and preparation. Data is graphed in Figures 2.12 and 2.13, showing fold changes in gene expression at 18, 24 or 48hrs relative to the 0hr time point. Statistical analysis showed no significant differences in the expression of any gene between the 18, 24 or 48 hour groups but there was a notable change in expression from 0 hrs to 18 hrs across the majority of genes.

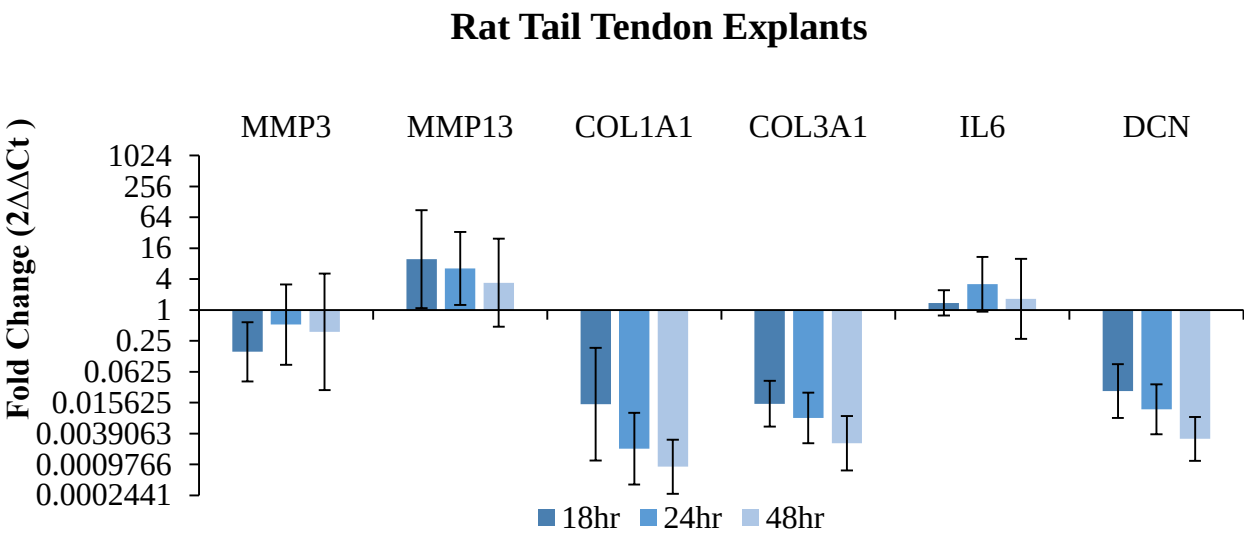

Figure 2.12: *Gene expression changes in dissected rat tail tendon fascicles over 48hrs. Explants were fixed in a custom-made chamber and maintained for 48hrs, assessing changes in gene expression over this time period using standard qRT-PCR. Data was normalised to GAPDH and presented as fold changes relative to the 0hr time point* ($2^{\Delta\Delta Ct}$) *[mean ± SD]. The greatest changes were seen in the first 18hrs, after which expression largely stabilised.*

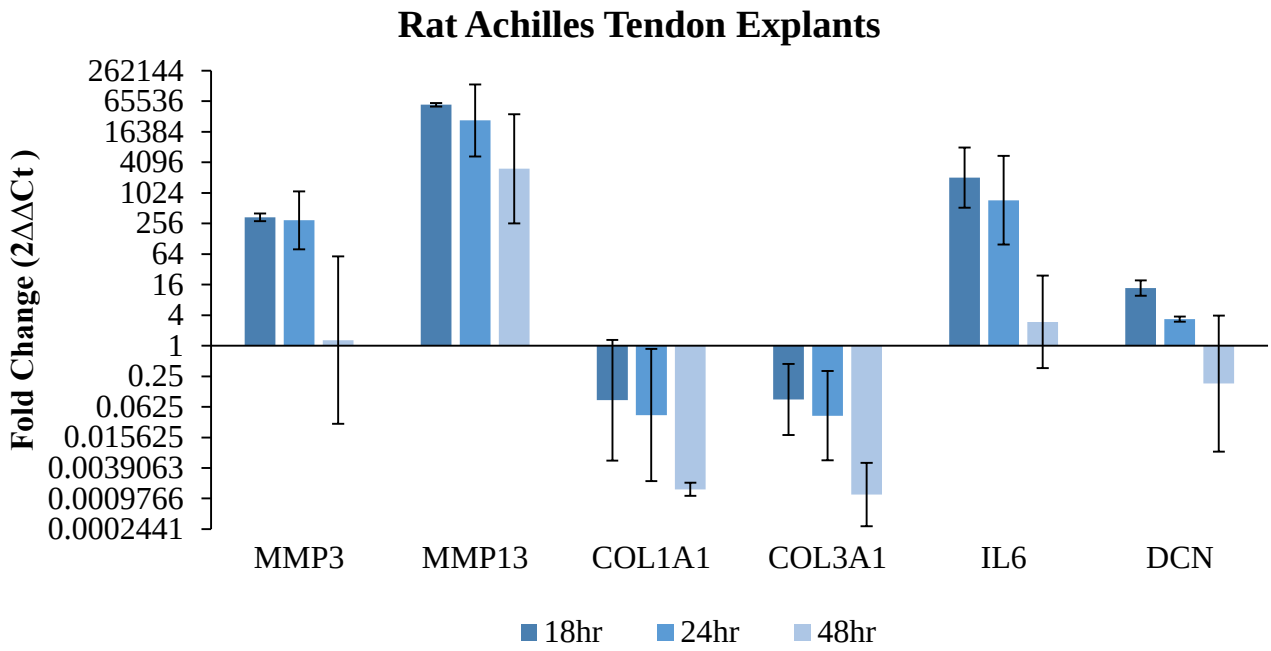

Figure 2.13: *Gene expression changes in dissected rat Achilles tendon over 48hrs. Explants were fixed in a custom-made chamber and maintained for 48hrs, assessing changes in gene expression over this time period using standard qRT-PCR. Data was normalised to GAPDH and presented as fold change relative to the 0hr time point* ($2^{\Delta\Delta Ct}$) *[mean ± SD]. The greatest changes were seen in the first 18hrs, after which expression largely stabilised.*

2.4.3 DISCUSSION

The result from this study demonstrated that cell viability was maintained at 70% or higher in rat tendon explants confirming the initial hypothesis, that viability is maintained in explants when there is no need for extensive dissection. Furthermore, viability was maintained under the different under loading conditions, even with the more mechanically extreme 10Hz loading. This result supports previous studies which have presented cell viability of over 95% in rat fascicles after loading [Kondratko-Mittnacht et al., 2015]. The slightly higher cell death observed with loading is possibly because the cells were not well adapted to the long periods of loading although they can generally withstand small amounts of normal strains [Kondratko-Mittnacht et al., 2015]. However, no significant differences in cell viability as a result of loading were evident. Therefore, it can be said that the mechanical loading applied in this study can be tolerated by the cells.

Having established a viable explant model, it was next necessary to explore gene expression. It is known that cells respond to abrupt environmental changes by altering gene expression levels, adjusting cellular physiology and metabolism to the new condition and possibly protecting the cells from damage or death [Lopez-Maury et al., 2008]. Changes in gene expression levels can be momentary even with tenacious stress, thus, gene expression levels can return to its steady-state levels that are close to those in unstressed cells after some time [Lopez-Maury et al., 2008]. As such, an initial investigation was carried out to examine gene stabilisation in response to dissecting samples and securing them in chambers. Figure 2.12 and 2.13 showed that gene expression altered notably between 0 and 18hrs, but no significant differences were seen between 18, 24 and 48 hours. Pahl and Brune, [2002] in their study of gene expression profiling in blood showed how the expression levels of IL-1β decreased 6hrs after phlebotomy but had returned to normal after day 1. They used these data to evidence the need for gene stabilization after sample preparation; neglecting gene stabilization may lead to over or under estimated results in gene expression profiling [Pahl and Brune, 2002]. An *in vitro* study on rat explants was used to investigate time course of gene expression changes associated with tissue harvest, mechanical unloading and culture [Leigh et al., 2006]. The study demonstrated that type I collagen and decorin stabilised at 24hrs which was seen in this current study (Figure 2.12 and 2.13). However, the study showed that MMP3 and MMP13 continued to increase throughout the 48hrs experimental period, which was not the case in this current study. But the differences in MMPs seen by Leigh and this current study is unknown.

Data from the current study demonstrate that rat tendon explants provide an appropriate system in which gene expression in response to loading could be further analysed, with viability maintained for 48hrs, allowing for a 24hr gene stabilisation period, followed by a 24hr experimental period, as proposed for further loading experiments.

2.5 RAT TENDON EXPLANT MODEL – CELL RESPONSE TO LOADING

2.5.1 METHODOLOGIES

Having validated the use of rat explants, a loading experiment was performed, to investigate gene expression in response to the differential loading protocols of interest.

19 rat tail tendon explants and 3 rat Achilles explants were collected from a single rat and prepared following the methods outlined in chapter 2.3.1. Samples were individually secured in the custom designed stainless steel loading chambers at a grip-to-grip distance of 10 mm, and the chambers filled with DMEM then sealed in the glass surround, maintaining sample hydration. All 22 chambers were incubated in a 5% CO_2 at 37°C incubator for 24hrs allowing time for gene stabilisation as established from previous experiments. After 24hrs, samples were split into 3 test groups, with 5-7 tail explants and 1 Achilles explant in each group.

- Unstrained control
- High magnitude low frequency loading: 1% ± 1% at 1Hz
- High magnitude high frequency loading: 1% ± 1% at 10Hz

The first control group of samples where left in the incubator for an addition 24hrs without load, while samples in the remaining 2 loading groups were connected to an electro force mechanical loading instrument and subjected to either high magnitude low frequency, or high magnitude high frequency loading for 24hrs.

Rat Explants Cell Response Experimental Set Up

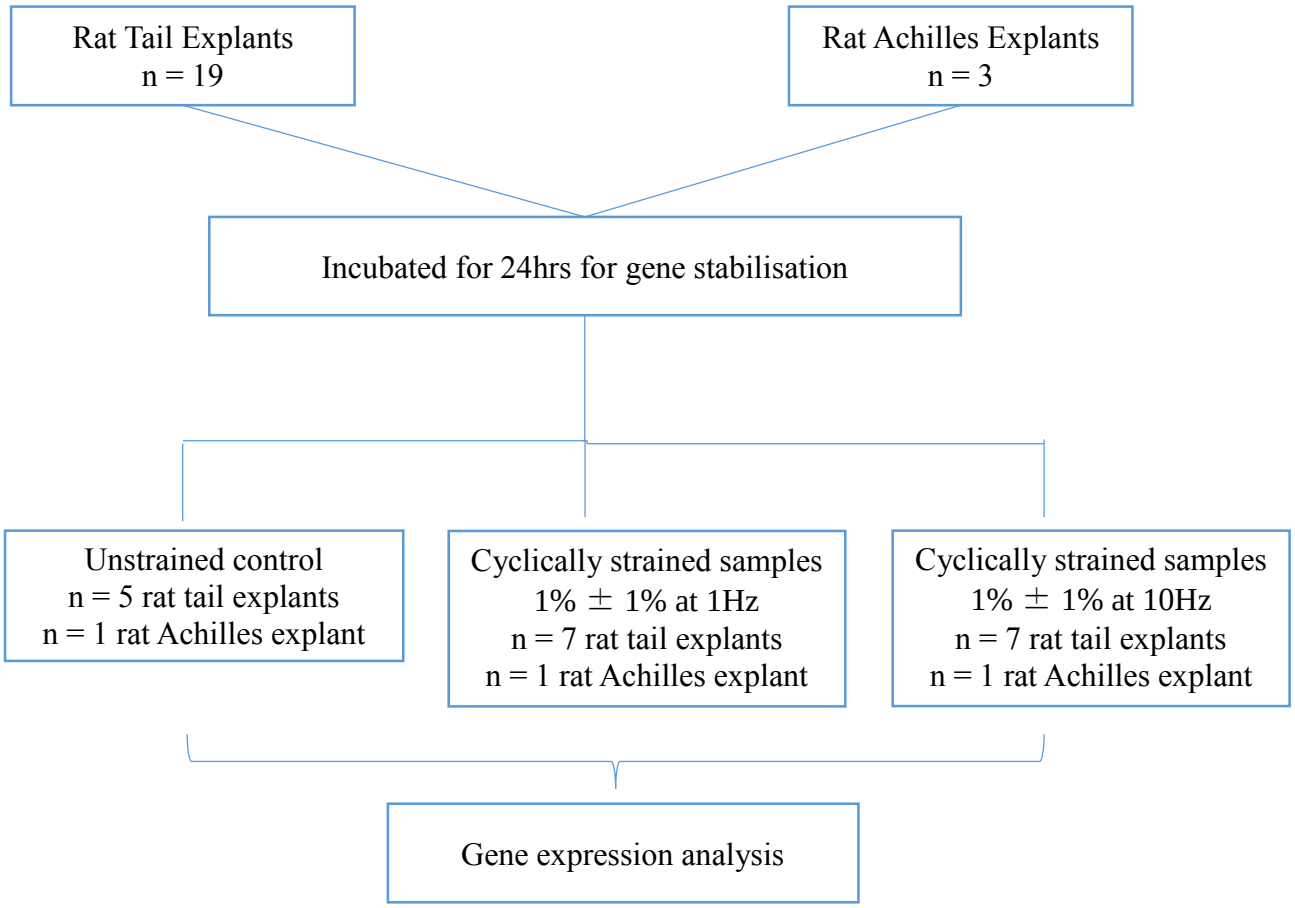

Figure 2.14: *Flow diagram of experiments performed from on rat explants to investigate the effect of loading on tenocyte gene expression. Biological repeat, N = 1.*

After 48hrs, samples were removed from the chambers and immediately placed in a 1mm cryotube and immersed in liquid nitrogen. After 3-5 minutes, the samples were removed from liquid nitrogen and stored at -80°C for later gene analysis. RNA extraction, reverse transcription and quantitative real time PCR was performed as detailed in chapter 2.3.1. The genes analysed are detailed in table 2.6.

Table 2.6: Primer sequences (Forward and reverse) used for real-time polymerase chain reaction

Target Gene	Primer Sequence	Length of Product (bp)	GeneBank Accession no.	Reference
RAT				
GAPDH	GGAAAGCTGTGGCGTGAT AAGGTGGAAGAATGGGAGTT	1306	NM_017008	Zhang et al., 2011
MMP3	GACCAGGGACCAATGGAGATG TGAGCAGCAACCAGGAATAGG	1771	NM_133523	Zhang et al., 2011
MMP13	GGCCAGAACTTCCCAACCA ACCCTCCATAATGTCATACCC	2601	NM_133530	Zhang et al., 2011
COL1A1	CTACAGCACGCTTGTGGATG CAGATTGGGATGGAGGGAGT	5843	NM_053304	Zhang et al., 2011
COL3A1	ATCAAACACGCAAGGCCATG AAGCAAACAGGGCCAATGTC	4792	NM_032085	Gu et al., 2014
IL6	ACTTCACAAGTCGGAGGCTT AGTGCATCATCGCTGTTCAT	1045	NM_012589	Zhang et al., 2014
Decorin	TGAAGGACTTGCATACCTG GTTACTTGTAGTTCCCAAGT	1639	NM_024129	Sasamura et al., 2001
Aggrecan (ACAN)	TCCAAACCAACCCGACAAT TCTCATAGCGATCTTTCTTCTGC	6939	NM_022190	Zhang et al., 2011
ADAMTS-5	CGACAAGAGTCTGGAGGTGAG CGTGAGCCACAGTGAAAGC	2787	NM_198761	Lai et al., 2012
TIMP-3	TCTGCAACTCCGACATCG GCGTAGTGTTTGGACTGATAGC	1778	NM_012886	Li and Curry, 2009

Data was normalised to the housekeeping gene GAPDH and changes with loading expressed as a fold change from the unstrained control ($2^{\Delta\Delta Ct}$).

2.5.2 RESULTS

In response to the loading bout, data from tail explants showed an upregulation of MMP13 and a downregulation of MMP3, COL1A1, COL3A1, DCN, ACAN, ADAMTS5 and TIMP3. There was no indication of significant differences in the response to high (10Hz) and low (1Hz) frequency loading, although the response to high frequency loading appeared more pronounced in the majority of genes.

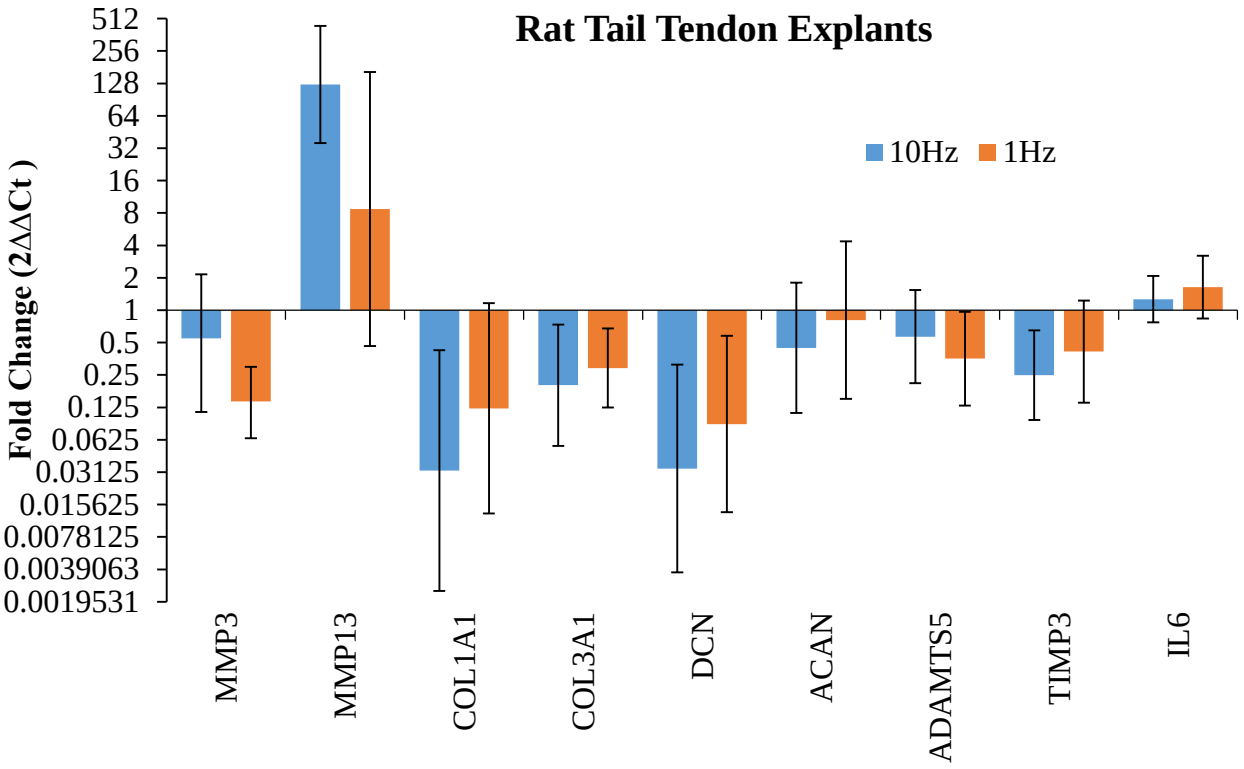

Figure 2.15: *Gene expression response in rat tail tendon explants subjected to 24hrs of high or low frequency loading shown relative to unstrained controls. Data was normalised to GAPDH and presented as a fold change from unstrained samples ($2^{\Delta\Delta Ct}$) [mean ± SD].*

Data from the rat Achilles explants showed a similar profile to that seen in rat tail explants, with the downregulation of the majority of genes, except for IL6 which was unchanged with loading. However, each data point is a single sample, so it is not possible to make definitive statements concerning this response.

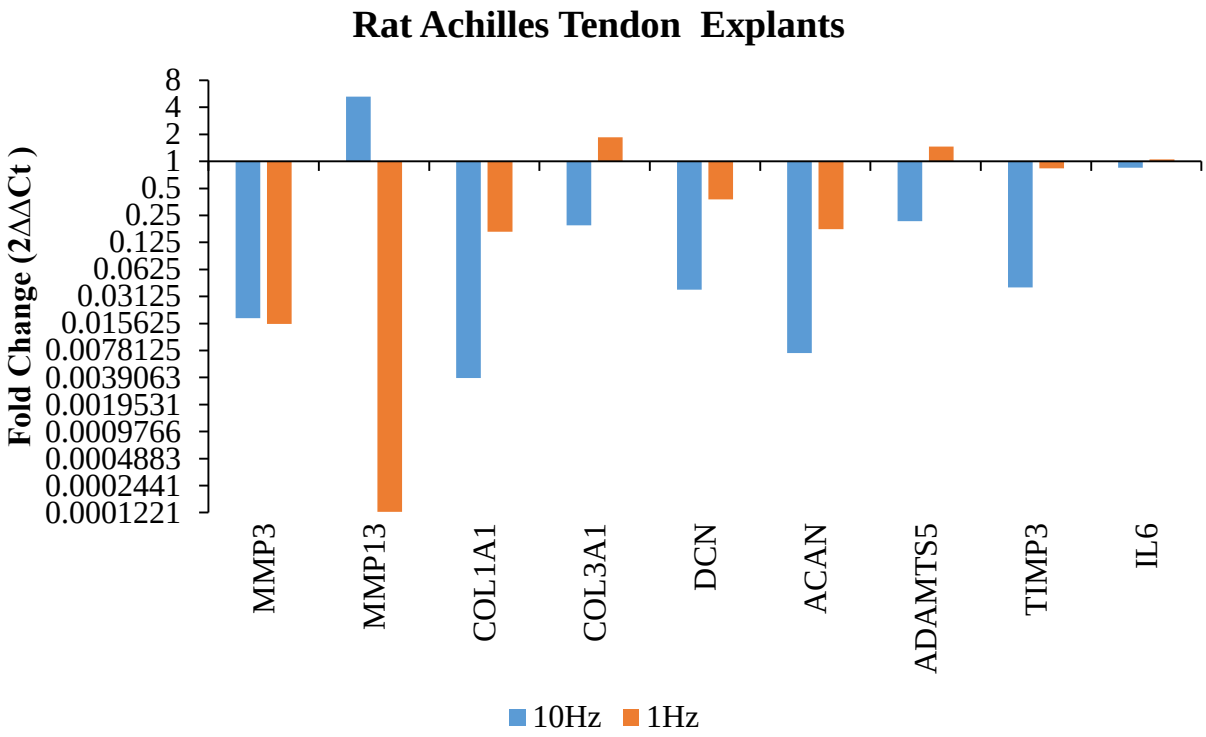

Figure 2.16: *Gene expression response in rat Achilles tendon explants subjected to 24hrs of high or low frequency loading shown relative to unstrained controls. Data was normalised to GAPDH and presented as a fold change from unstrained samples ($2^{\Delta\Delta Ct}$) [mean ± SD].*

2.5.3 DISCUSSION

In response to cyclic loading, rat tendon explants appear to downregulate the majority of analysed genes, with the exception of MMP13, in which a notable increase in expression was evident, particularly in response to high frequency (10Hz) loading and IL6 that displayed no change with loading. It is interesting to note that the downregulated genes included both collagens and MMPs. Matrix metalloproteinases (MMPs) belong to a diverse group of enzymes which are not only involved in restructuring the extracellular matrix, but also play a major role in various pathophysiological conditions by virtue of their complicated expression, activation, and regulation processes [Gardner et al., 2008]. MMP13 is a collagenase-3 that induces degradation of the extracellular matrix. The upregulation of MMP13 with high frequency (10Hz) loading may be indicative of active tissue remodelling, as degradation is important for healing and remodelling of connective tissues [Buono et al., 2013]. On the other hand, for biologic remodelling to occur, it is expected that there is high levels of changes in gene expression of a range of anabolic and catabolic genes [Iatridis et al., 2013; Riley, 2005], which is not seen from this data.

With mechanical loading conditions of 1% ± 1% at 1Hz or 10Hz for 24hrs, there is a possibility that the explants have been underloaded with a high expression of MMP13 and downregulation of various matrix proteins and proteoglycans. From the literature, underload or stress deprivation may contribute to the progression of tendinopathy [Lewis, 2010; Thornton et al., 2008]. These studies demonstrated upregulation of MMP13 [Lewis, 2010; Thornton et al., 2008] as well as MMP3 and TIMP2 [Thornton et al., 2008] in stress deprived tendons relative to cyclically strained tendons. A study by Wang et al. [2013] investigating the response of rat Achilles explants, performed cyclic strain at 0.25Hz to 3%, 6% and 9% strain for 6 days, loading for 8hrs a day. Data demonstrated that tendons experiencing the lowest strain (3% cyclic strain) had moderate matrix deterioration with the highest upregulation of MMP-1, 3, and 12, whilst those subjected to 9% strain reported massive rupture of the collagen bundles and a significant highest upregulation of COL3A1 [Wang et al., 2013]. The authors hypothesised that 3% strain was ‘underload’ whilst 9% strain was ‘overload’ as samples subjected to 6% cyclic strain maintained their tissue structure and showed the highest expression of COL1A1, lowest expression of MMP-1, 3, and 12 and no expression of COL3A1. Nonetheless, it is important to note that Wang and colleagues’ study looked at varying strain magnitude at the much lower frequency of 0.25Hz and also investigated longer loading periods, which may have differentially impacted the metabolic response of their cells.

In this current study, N = 1 is not enough to make any conclusions, therefore, further experiments need to be done to verify outcomes. However, these pilot experiments validate the potential to use rat explants for further work.

2.6 2D ISOLATED CELL MODEL

2.6.1 INTRODUCTION

Cells are anchorage-dependent and will grow and function only when adhered to physical surfaces, hence the interactions between cells and the extracellular matrix are at the core of tissue engineering [Plant et al., 2009]. Porous membranes coated in materials such as collagen type I, fibrin, fibronectin, laminin, or basement membrane extract (BME),, that promote cell adhesion, spreading and proliferation, are used as a platform on which to seed cells for *in vitro* studies to understand cell behaviour [Moore and Maitland, 2014]. Most mechanobiology studies have used traditional 2D systems, where cells are extracted from tissues, seeded on a surface of cell-derived matrix, and mechanically loaded on stretching devices like flexcell (Flexcell Corporation, FX-4000) [Colombo et al., 2008; Yang et al., 2005]. Collagen type I coated membranes are regularly selected, as collagen is a major component of most connective tissues.

A 2D membrane provides a simple, convenient and potentially highly controlled system for growing adhesive cells and mechanically loading them by simply stretching the membrane. Such systems have subsequently been very popular, however, there are some limitations to the use of 2D membranes, as the cells are not in an environment mimicking that seen physiologically.

2.6.2 METHODOLOGIES

2.6.2.1 SAMPLE COLLECTION AND PREPARATION

Bovine tenocytes were derived from bovine extensor tendons by explant outgrowth, following previously described protocols [Schulze-Tanzil et al., 2004]. The bovine hoof was washed, and transferred to a cell culture hood for aseptic dissection of the extensor tendon. Within the hood, the hoof was skinned and all muscle and tissues surrounding the tendon removed. The tendon was then extracted, ensuring constant irrigation with DPBS to maintain hydration. Small tendon explants, 3mm thick and up to 1mm length, were cut from the middle of the tendon away from the sheath. Three explants were placed into each plate of a six-well culture plate, evenly separated (Figure 2.17) and covered with a small drop of 50% fetal bovine serum (FBS) medium, the composition of which is detailed in table 2.7.

Table 2.7: Culture media component depending on percentage fetal bovine serum content

Component (Supplier)	**50% FBS Media (ml)**	**10% FBS Media (ml)**
Dulbecco's modified Eagle's medium (DMEM) (low glucose, pyruvate, no glutamine, no phenol red) (ThermoFisher Scientific)	500	500
FBS (Sigma Aldrich)	250	50
Penicillin streptomycin (PS) (Sigma Aldrich)	10	10
HEPES solution (Sigma Aldrich)	10	10
L-Glutamine solution (Sigma Aldrich)	5	5
MEM non-essential amino acid solution (NEAA) (Sigma Aldrich)	5	5
Sodium Bicarbonate (Sigma Aldrich)	1.85g	1.85g

A  **B** 

Figure 2.17: ***A.*** *Bovine hoof skinned to access the extensor tendon,* ***B.*** *Small pieces of tendon (explants) placed in a 6 well plate for culture*

The plate was placed in a humidified 37ºC, 5% CO_2 incubator. After 24hrs, an additional drop of 50% FBS medium was added and after 48hrs, further 50% FBS medium was applied to

cover the entire surface of the plate while ensuring that the tendon explants did not float. The additional medium increased the area for tenocyte growth, encouraging tenocyte proliferation and outgrowth across the well. 50% FBS medium was replaced every 2 to 3 days just covering the surface of the well each time until cells reached confluence. At this point, the explants were removed and disposed of, after which the cells were released from the surface of the culture plate, to reseed for further cell culture. Cells were released by removing the media and adding 0.25% trypsin-EDTA (trysinization) for 5mins. Released cells were pipetted into a corning flask, centrifuged at 2000 rpm for 5 minutes before the supernatant was removed, leaving cell pellets at the base of each tube. The cells were then re-suspended in 10% FBS culture medium, and divided into cell culture flasks for further growth. Cells were cultured for up to 3 passages before use.

At passage three, to avoid the cell differentiation observed with further passaging [Mazzocca et al., 2012], the cells were trysinized, centrifuged, re-suspended in fresh 10% FBS medium and counted. 15µl of the cell suspension and 15µl of trypan blue were added to a tube and mixed, then a small amounted pipetted into a haemocytometer. Trypan blue dyes dead cells blue while viable live cells are left unstained. Live cells were counted across the haemocytometer grid using a microscope and X10 objective (Figure 2.18).

Figure 2.18: *A haemocytometer – showing the grids in which cells are counted. All cells within the central grid, and those touching the top or left perimeter of the grid were counted, while those on the bottom or right perimeter were ignored.*

The number of live cells was calculated from the mean cell number multiplied by 2 (dilution in trypan blue), multiplied by 10^4 to obtain the number of cells per ml of each sample. The cell suspension was then adjusted (diluted or concentrated) to provide a final concentration of 1 million cells per ml.

Collagen coated membranes were prepared for cell straining experiments cutting 2mm wide, 14mm long strips from sheets of sterile collagen coated membrane (Flexcell International Incorporation, Burlington, NC 27215) using a custom made cutter (Figure 2.19). Five strips of

membrane were placed into each well of a six well plate, and 0.5ml (0.5 million cells) of the bovine tenocyte suspension was pipetted into each well to cover the membranes. Membrane were incubated at 37°C for 24hrs allowing the cells time to attach.

Figure 2.19: *Picture of the custom-made membrane cutter. Dimensions - width 2mm, and length 14mm*

After seeding membranes, any remaining cell suspension was frozen for long term storage. In more detail, cell suspension was centrifuged at 2000 rpm for 5 minutes and the supernatant disposed of. Cells were then re-suspended in 10% FBS media also containing 10% Dimethyl Sulfoxide (DMSO) (Sigma – Aldrich, 472301) then aliquoted at 1 ml per tube and incubated overnight in a Nalgene cryo-freezing container at -80^{o}C. Cells were then transferred to liquid nitrogen for longer term storage.

In order to validate the use of 2D membranes as a loading model, it was necessary to confirm the cells were attached to the membrane and remained viable after securing in chambers and after mechanical loading. 18 membranes were prepared to investigate attachment. Membranes were seeded with cells, and after a 24hr attachment period, were divided into four test groups;

- Unstrained, free swelling controls
- Secured in chambers unloaded for 0, 12 or 24 hrs
- Secured in chambers and loaded with high magnitude low frequency loading: 1% ± 1% at 1Hz for 12 or 24 hrs
- Secured in chambers and loaded with high magnitude high frequency loading: 1% ± 1% at 10Hz for 12 or 24 hrs

At the end of the test periods, samples were carefully placed on a coverslip for imaging with a X10 magnification lens under bright-field settings (Leica microscope).

2D Isolated cell model Experimental Set Up

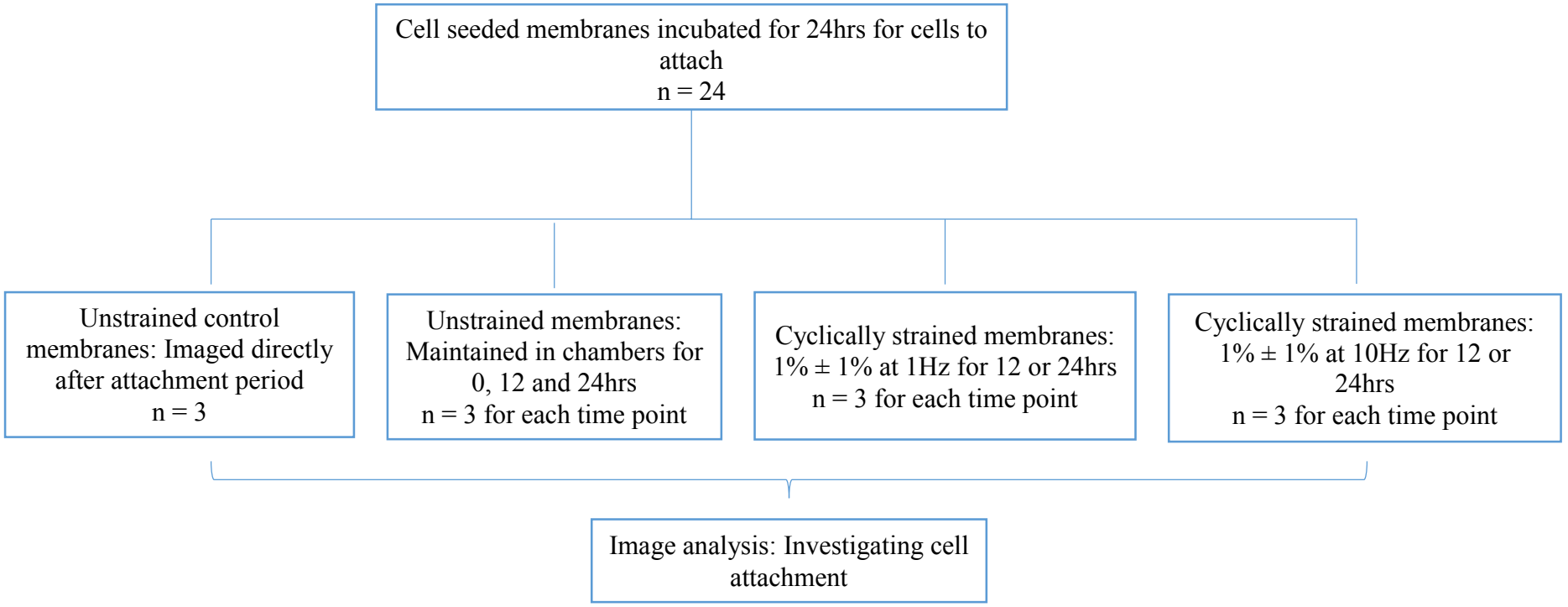

Figure 2.20: *Flow diagram of experiments performed on 2D isolated cell model to investigate cell adhesion to the membrane with and without loading*

2.6.3 RESULTS

Cells were well adhered 24hrs after seeding (Figure 2.21A). However, fixing samples into the loading chambers immediately resulted in some cells detaching from the membrane (Figure 2.21B). Over time, cell detachment from the membrane steadily progressed (Figures 2.21B-D). Mechanically loading the samples led to severe disruption of the cells, with clear detachment in Figures 2.20E-H.

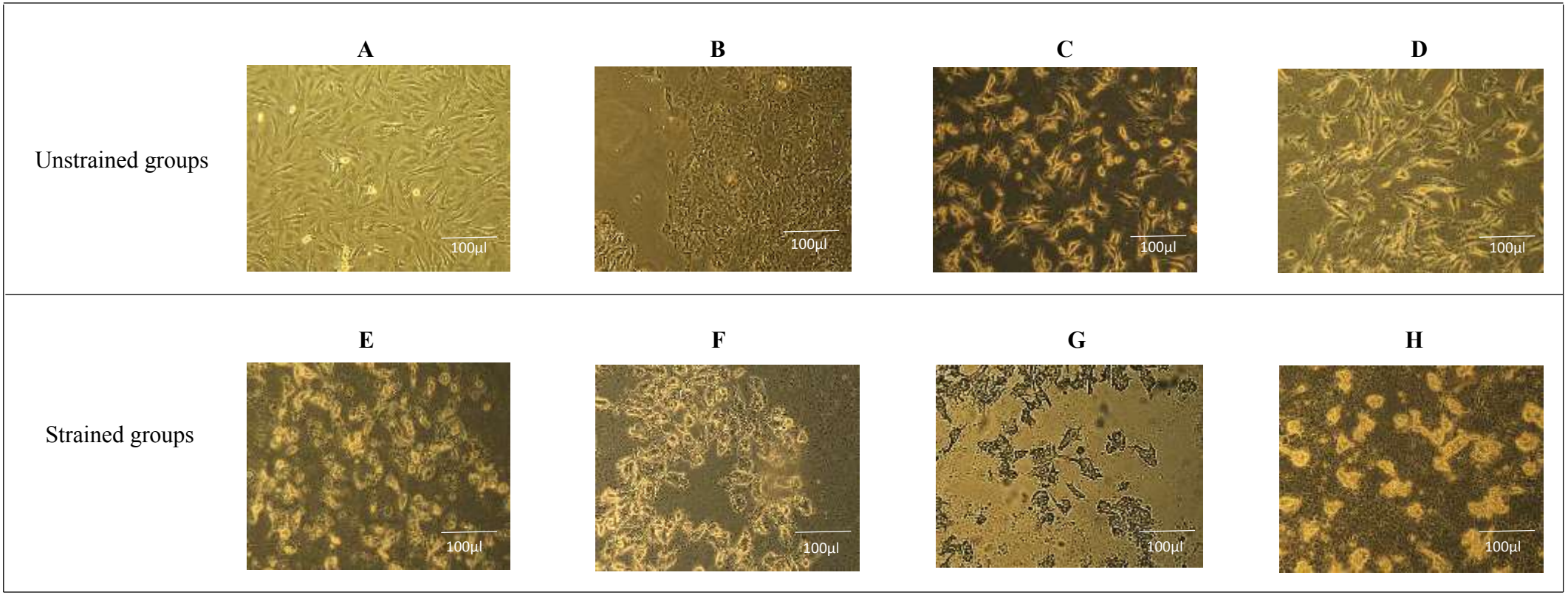

Figure 2.21: *Morphology of bovine cells in 2D collagen coated membrane at varying time points with and without loading observed using a Leica microscope at 10X optical zoom. After a 24hrs cell attachment period, cell were imaged immediately (A), or fixed into chambers and then removed and imaged after 0hr (B), 12hrs (C) or 24hrs (D). Additional samples were subjected to mechanical loading prior to imaging, comparing 1% ± 1% at 1Hz for 12hrs (E) or 24hrs (F) with 1% ± 1% at 10Hz for 12hrs (G) or 24hrs (H).*

2.6.4 DISCUSSION

The collagen membranes clearly facilitated cell adhesion, and cells were well adhered after 24hrs seeding, showing elongated cell processes. However, the act of gripping the membrane disrupted cell attachment, and the cells appeared more rounded as evident in Figure 2.20B-D. Loading further exacerbated the cell disruption showing highly disrupted and rounded cells, and possible evidence of apoptosis [Pullan et al., 1996]. The appearance of the cells becoming round following loading was also observed by Lavagnino et al. [2015] after they applied a 12% strain at 1Hz for 2hrs to rat tail tendon cells using a Flexcell system. The study went on to explain that the reason for the cells becoming rounded was possibly due to alteration of the cells' cytoskeletal structure from the tensile strain resulting in loss of tensional homeostatsis and change in cell shape [Lavagnino et al., 2015]. However, it is unclear why cells detach from the membranes so rapidly after fixing into chambers. Samples were handled carefully during preparation, nevertheless any handling disrupted the cells.

The upright orientation of membranes in chambers may have prompted the cell detachment. To reduce cell detachment, other methods of loading the 2D constructs, where samples were secured and loaded in a horizontal alignment, were explored. However, both our in-house loading system and the commercially available Flexercell system, cannot apply loading at sufficiently fast frequencies to test the desired hypotheses. In 2D culture environments, only a segment of the cell's membrane adheres to the collagen membrane, therefore the cell does not have the distributed adhesion experienced in a 3D environment (Figure 2.22). Therefore, a 3D model was explored.

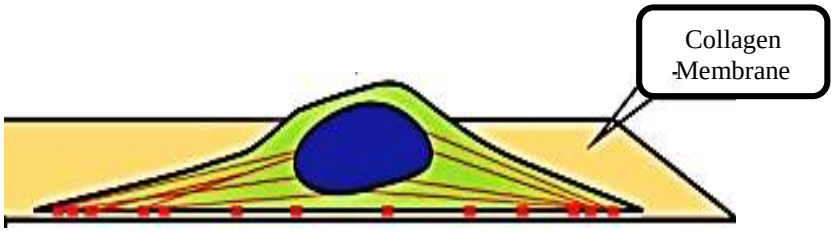

Figure 2.22: *Schematics showing cell adhesion on a 2D membrane. Adhesion is restricted to x-y plane [adapted from Baker and Chen, 2012]*

2.7 3D MODEL

2.7.1 INTRODUCTION

3D gel systems have been commonly used in tissue engineering and mechanotransducion studies for many years, across a broad range of tissues including bone, cartilage and tendon [Fisher et al., 2004; Sakiyama et al., 1999; Yu et al., 1999; Blackshaw et al., 1997]. 3D gels are generally made of cross-linked natural base materials like agarose, collagen, laminin, fibrin or hyaluronic acid, with collagen type I commonly selected as the substrate of choice. Collagen is an abundant and important part of the ECM across various connective tissues and the most abundant protein in tendon [Artym and Matsumoto, 2010]. Also, collagen can be obtained from animal sources in a reliable and pure form, unlike other 3D gel substrates that may be supplemented with mixtures of other bioactive ECM proteins and growth factors (like fibrin gel that is formed by thrombin cleavage of fibrinogen– a serine protease) which can complicate experimental tests and results [Cheema and Brown, 2013; Sakiyama et al., 1999].

Collagen gels take about 30 minutes to set at neutral pH and room temperature, giving the gel time to be moulded into the desired shape and/or seeded with cells. However, the method of 3D collagen gel preparation, the collagen concentration, and density of the collagen gel all influence the final characteristics of the 3D collagen gel matrix produced, which in turn can affect how cells interact with the gel and thus result in distinct cell morphology and cellular response [Artym and Matsumoto, 2010]. Thus to avoid possible heterogeneity in results due to changes in collagen fibril morphology, one needs to follow the same conditions for 3D collagen matrix assembly for all gels used within any particular experiment.

Collagen gels have a large amount of fluid (>99.5%) relative to collagen (0.5%), which is typically a considerably lower collagen density than seen in native connective tissues where collagen is about 25-30% of the wet weight [Cheema et al., 2007]. Collagen gels thus present poor mechanical properties relative to the tissues they mimic. However, Cheema and Brown, [2013] develop a method in which some fluid can be expelled from the gel, to increase the collagen density to >20% wet weight without cell damage. This process is called *the plastic compression* (PC) fabrication process. Plastic compression of collagen gels rapidly produces dense collagen sheets (100-200μm thick) with a tissue-like architecture, improved mechanical properties (approaching those of native tissue collagen) and biomimetic function (e.g. supporting high cell viability) [Cheema et al., 2012]. This process is versatile in terms of the volumes, densities, and shapes that can be produced (e.g. sheets can be layered or rolled up), thus creating the possibility to mechanically load the final scaffold structures.

2.7.2 METHODOLOGIES

This section describes the production, and analysis of a rectangular collagen gel model (seeded with bovine tenocytes) which has previously been used successfully to investigate the effect of mechanical loading applied to cells by Cheema and Brown, [2013].

2.7.2.1 CELL SEEDED COLLAGEN GEL

Collagen gels were prepared as described by Phillips and Brown [2011]. Briefly, for forming one gel, a mix of 4ml Type I collagen solution from rat tail (First Link - 2mg/ml chloroform treated) and 0.5ml of 10X Minimum Essential Medium with phenol red (MEM – Life Technologies) was placed on ice and neutralised by drop-wise addition of sodium hydroxide (NaOH, 5µl at a time up to 20µl), to reach a pH of 7 as shown by the colour change indicator from yellow to citrus pink.

Cells were cultured to P3, harvested by trypsinization, collected by centrifugation, and re-suspended in 10% FBS media at a volume of 1 million cells per ml. 0.5ml cell suspension was added to the 4.5ml of collagen solution and well mixed, giving 5ml of solution, sufficient for one gel. Five pieces of absorbent whatman paper (grade 1: 11µm, 185mm diameter) were placed in a petri dish and a rectangular sterile mould (22 x 10 x 33 mm) placed on them. The final gel solution was pipetted into the rectangular mould and allowed to incubate at room temperature for 30 minutes to solidify and form a collagen gel with 90% liquid.

Plastic Compression of collagen gels

Once formed, gels were compacted to expel liquid and increase their mechanical strength and compliance following a modified version of the process described by Cheema and Brown [2013]. The rectangular mould was removed and a second set of absorbent Whatman filter paper (5 pieces) were placed on top of the gel. A 120g metal block was then placed on top of the Whatman filter papers, loading the gel. After five minutes of loading, the gel had been compressed to form a collagen sheet (100-200µm thick) protected between the absorbent Whatman filter papers (Figure 2.23).

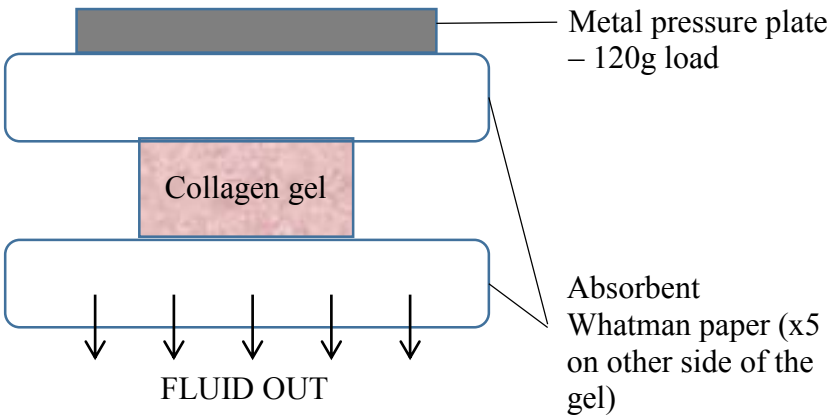

Figure 2.23: *A schematic showing the routine assembly for plastic compression of collagen gels. The collagen gel was compressed under fixed load so that rapid fluid removal (~99% fluid loss within five mins) was achieved. The compression produces collagen sheets of ~100-200µm thickness [procedure modified from Cheema and Brown, 2013].*

The compressed collagen gels were peeled away from the absorbent Whatman filter papers, then rolled up along their long axis, to form a cylindrical gel, roughly 33mm in length and 1mm in diameter. As a cylinder, it was then possible to grip the gels within the loading chambers (section 2.2.1) for further experimental analysis.

A series of experiments were carried out, to validate the 3D collagen gels for mechnobiology experiments. First, the mechanical behaviour of the gels during loading experiments was assessed, and cell viability for the duration of an experiment confirmed (Figure 2.24).

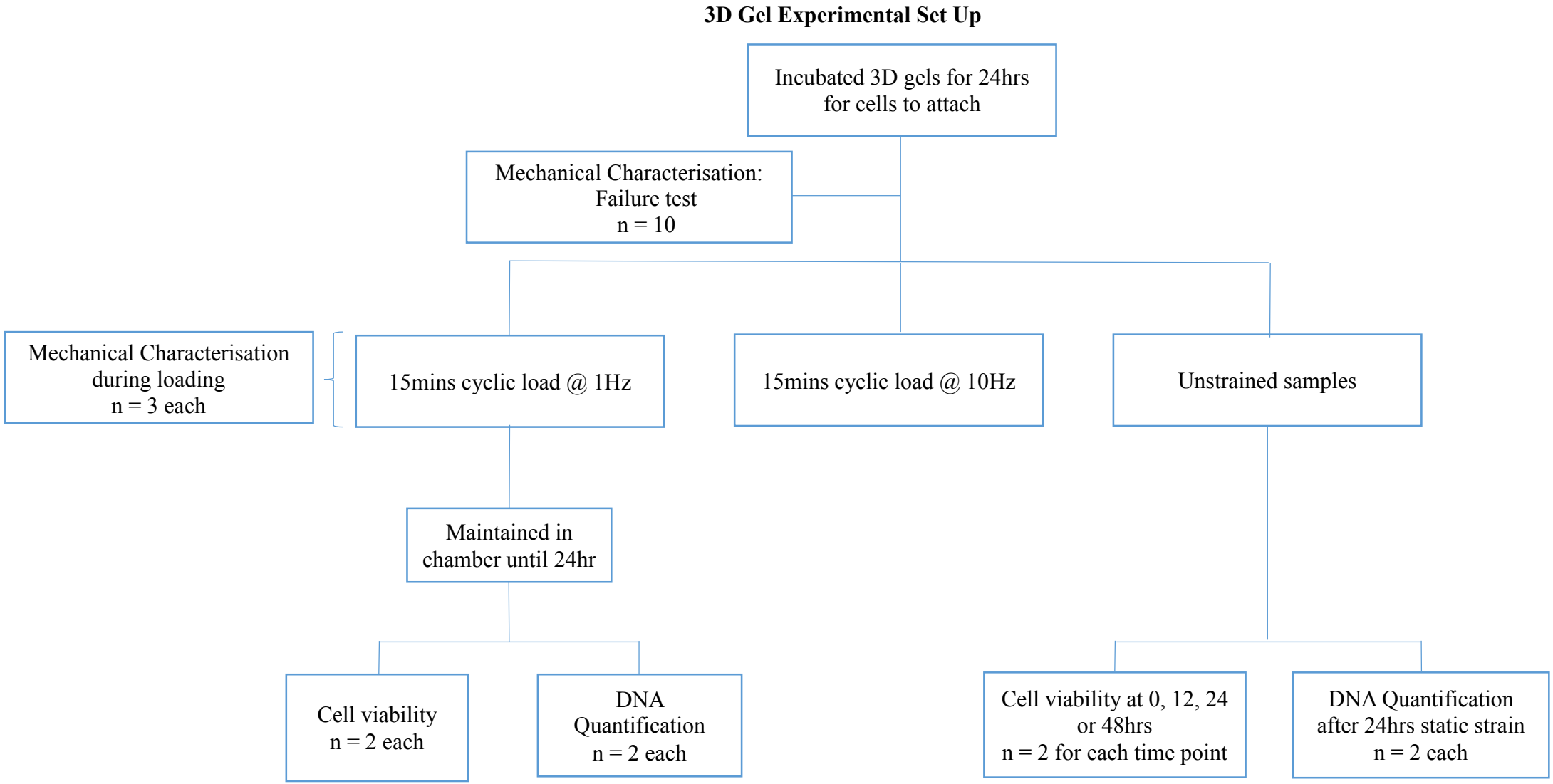

Figure 2.24: *Flow diagram of experiments performed on 3D collagen gels. Samples were incubated for 24hrs before a cyclic strain period of 15mins at 1% ± 1% followed by 24hrs of static strain period (24hrs at 1% strain) to allow for cell response.*

2.7.2.2 GEL MECHANICS

The purpose of this mechanical test was to characterize the mechanical response of the gel over the duration of a cell loading experiment, to ensure cells experienced strain for the duration of the test. In order to further mimic the load conditions seen during eccentric loading or ESWT, the duration of loading was reduced from 24 hours to a more physiologically representative 15 minutes, as seen in a typical exercise or ESWT bout [Langberg et al., 2007; Jonsson and Alfredson, 2005]

Load Relaxation

A cyclic loading experiment, replicating the experimental strain conditions was performed on cell seeded 3D gels to analyse the extent of relaxation during loading, and confirm if the cells will experience strain throughout the experiment.

The gels were then secured in the custom designed stainless steel loading chambers at a grip-to-grip distance of 10 mm. The chambers were filled with DMEM, then sealed with the glass surround, maintaining full hydration. Each chamber was secured in the electro force loading system housed in an incubator to maintain samples in 5% CO_2 at 37^{o}C as shown in Figure 2.3, and incubated for 24hrs to allow stabilisation. Loading was then applied, recording displacement, and maximum and minimum peak loads, throughout the period. The loading conditions assessed were:

- High magnitude low frequency loading: 15mins cyclic strain at 1% ± 1% at 1Hz
- High magnitude high frequency loading: 15mins cyclic strain at 1% ± 1% at 10Hz

Failure Test

A simple quasi-static failure test was also carried out on a number of samples, to determine if the loads experienced by the gel during the loading experiments were within the linear region of the gel stress-strain response.

10 cell seeded 3D collagen gels were prepared as cylinders and left in a sterile container filled with DMEM for 24hrs in an incubator, to maintain samples in 5% CO_2 at 37^{o}C, to allow for stabilisation. The gels were secured in chambers and were then pulled apart to failure at a speed

of 1 mm/s using the electro force loading system. Force and extension data were continuously recorded at 100 Hz.

2.7.2.3 CELL VIABILITY TESTING

In order to validate this model, it was essential to confirm that the cells in the 3D collagen gels remained viable, both in the presence or absence of mechanical load. Cell viability was assessed in cell seeded collagen gels in response to the following loading regimes:

- Initial control condition (0hr) – immediately after preparation
- Unstrained controls at 18, 24 and 48hrs
- High magnitude low frequency loading: 15mins at 1% ± 1% at 1Hz followed by 1% static strain until the 24hr time point
- High magnitude high frequency loading: 15mins at 1% ± 1% at 10Hz followed by 1% static strain until the 24hr time point

Two different methods of analysing cell viability were used: Calcein AM and ethidium homodimer staining was used to assess spatial viability within the gels, whilst a more quantitative count of cell viability was carried out with trypan blue.

Cell Viability – Spatial Analysis: Calcein AM and Ethidium Homodimer Staining

Tenocyte seeded 3D gels were stained using a Calcein AM and Ethidium homodimer dye mix, following the detailed protocol described in Chapter 2.2.1. Collagen gels were removed from the chambers, placed in a dye mix and incubated at 37°C for 30 minutes. After staining, the samples were rinsed in DMEM then unrolled so they were once again flat sheets, which could be placed on a microscope slide, ready to be viewed with a confocal microscope (Perkin Elmer). The sample was located and focused using bright field imaging, after which the live/dead stains were viewed using the fluorescence laser and a X10 optical lens. Live and dead cell numbers were counted in three regions across the width of the sample as shown in Figure 2.25, to assess viability throughout the sample.

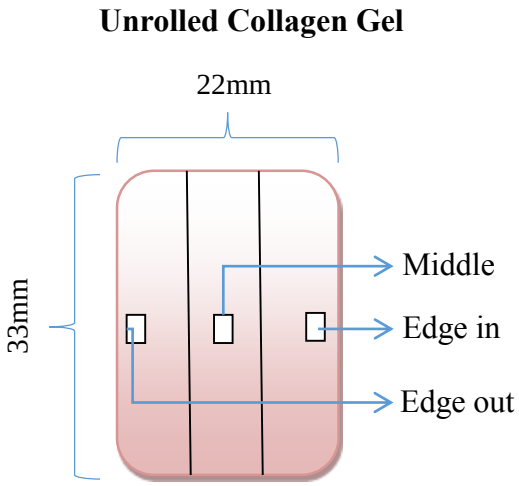

Figure 2.25: *Schematic of a collagen gel showing the positions where cell viability was taken for each sample. In the rolled state, 'edge out' is the outer exposed region whilst 'edge in' will be deep within the core of the sample.*

Note: An imaging depth of approximately 50-70µm was adopted, and was consistent across the three image locations for a particular sample, but may have varied slightly between samples.

Cell Viability – Quantitative Cell Count: Trypan Blue Staining

Tenocyte seeded 3D collagen gels were washed in PBS, then digested in DMEM containing collagenase type IV (0.125%) at 37°C for 30 – 45 minutes, until the gel had fully dissolved and the cells were left in suspension. The cells were collected by centrifugation and re-suspended in 10% FBS media. 15µl of the cell suspension was pipetted into a tube and 15µl of trypan blue added making a dilution factor of 2. The cell suspension and trypan blue mix was pipetted into a hemocytometer, which was then placed under a microscope and the cells counted following the cell count protocol detailed in Chapter 2.5.1.

Cell Viability – DNA Quantification

Cell numbers within the 3D collagen gels over the course of an experiment were assessed to ensure there was no cell proliferation, which may otherwise affect results. DNA levels were assayed fluorometrically with the Hoechst dye method.

After loading, collagen gels were digested to release the cells and DNA content measured fluorometrically. DNA standards were made from a DNA stock solution of known concentration of 20µg/ml, which was diluted to make the concentrations in table 2.8 using

digest buffer. The digest buffer was made from 5mM EDTA (0.731g) and 5mM Cysteine hydrochloride (0.439g) in 500ml PBS at pH 6. Serial dilutions were made as follows:

Table 2.8: Serial dilution for DNA standards, 1:6 dilution, for standard curve used to calculate the DNA concentration of a sample

Standard	**Concentration (µg/ml)**	**Concentration (µg/well)**	**Digest buffer (µl)**	**Diluted DNA standard (µl)**
S1	20	2000	980	20 µl of stock standard
S2	15	1500	250	750
S3	10	1000	500	500
S4	5	500	750	250
S5	1	100	800	200
S6	0	0	1000	0

100µl of either the test samples or standards were pipetted in duplicate into a 96 well plate to a planned layout. 100µl of Hoechst dye (stock of 1mg/ml of distilled water, previously prepared and sterilised by filtration through a 0.22µm filter and stored at 4^{o}C away from light, was diluted with the digest buffer to 1/1000) was then added to each well and mixed briefly using a pipette. The plate was transferred to a fluorescence spectrometer (Flurostar Galaxy Flourimeter) and the fluorescence intensity measured with excitation at 390nm and emission at 460nm.

2.7.3 RESULTS

2.7.3.1 GEL MECHANICS

Load Relaxation

Figure 2.26 shows the response of a typical sample subjected to 1% ± 1% cyclic strain at 10Hz over 900 loading cycles. Samples behaved elastically under all applied load conditions (1% ± 1% at 1Hz and 10Hz), with no stress relaxation behaviour, or changes to the stress-strain behaviour of the samples over the 15 minutes of loading. The 3D collagen gels showed a percentage load relaxation of zero in all instances.

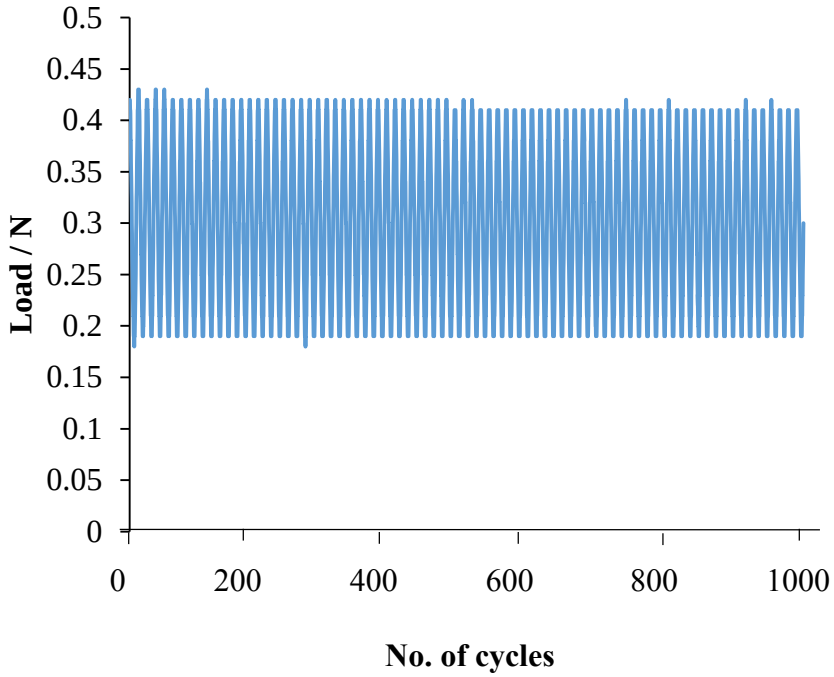

Figure 2.26: *Typical load behaviour during the loading period (1% ± 1% at 10Hz) monitored to ascertain the strains experienced by the cells. No stress relaxation of the gels was evident at any point during the 15mins loading period.*

Failure Test

The failure test data in Figure 2.27 showed that the collagen gels stretched to around 40% of their original length prior to failure and failed at stresses of around 2.5MPa. Gels showed non-linear stress-strain behaviour, similar to that seen in many soft tissues, with a toe region of lower stiffness at low applied strains.

Cyclic load conditions used in the cell straining experiments, loaded the gels in the initial, fully elastic toe region.

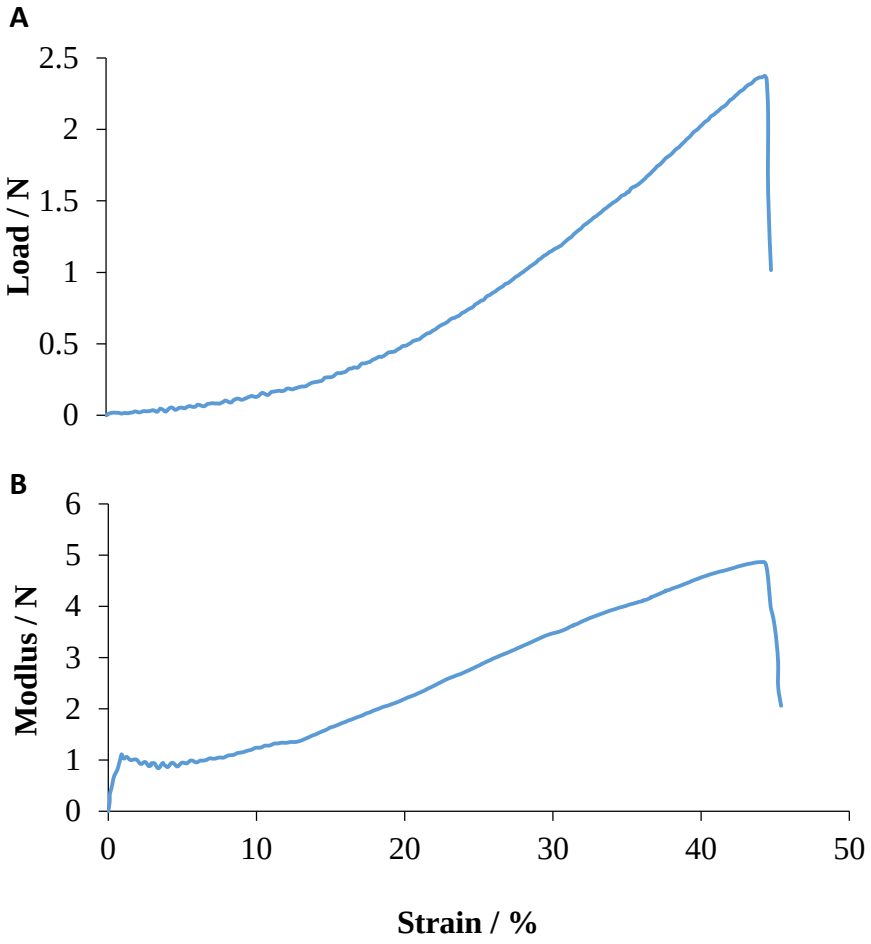

Figure 2.27: ***A)*** *Typical strain to failure graph for a tenocyte seeded 3D collagen gel. The low stiffness toe region is evident up to approximately 10% strain.* ***B)*** *The modulus-strain curve highlights a gradual increase in gel stiffness with increasing strain.*

Table 2.9: Failure test results showing the failure load and strain in 3D collagen gels seeded with bovine cells

Sample	Max Failure load / N	Failure Strain / %
1	1.60	34
2	2.24	49
3	2.34	36
4	2.65	45
5	2.16	37
6	1.96	44
7	2.20	40
8	2.96	55
9	1.49	37
10	2.18	45
Mean	2.18	42.20
STDEV	0.44	6.61

2.7.3.2 CELL VIABILITY TESTING

Cell Viability – Spatial Analysis: Calcein AM and Ethidium Homodimer Staining

The unloaded samples showed a cell viability of 79-93% across the gel, with no evident decrease in cell viability over time nor differences in cell viability between the regions (table 2.10).

The loaded samples showed a cell viability of 74-91% across the gel and whilst there was a trend towards improved viability in the ‘edge in’ region, there were no significant differences in cell viability between the regions (table 2.11).

Calcein AM staining of the cytoplasm of live cells also indicated that in strained cultures, the cells were predominantly aligned to the direction of loading (Figure 2.28B), whereas in non-strained cultures no primary cell orientation was evident (Figure 2.28A).

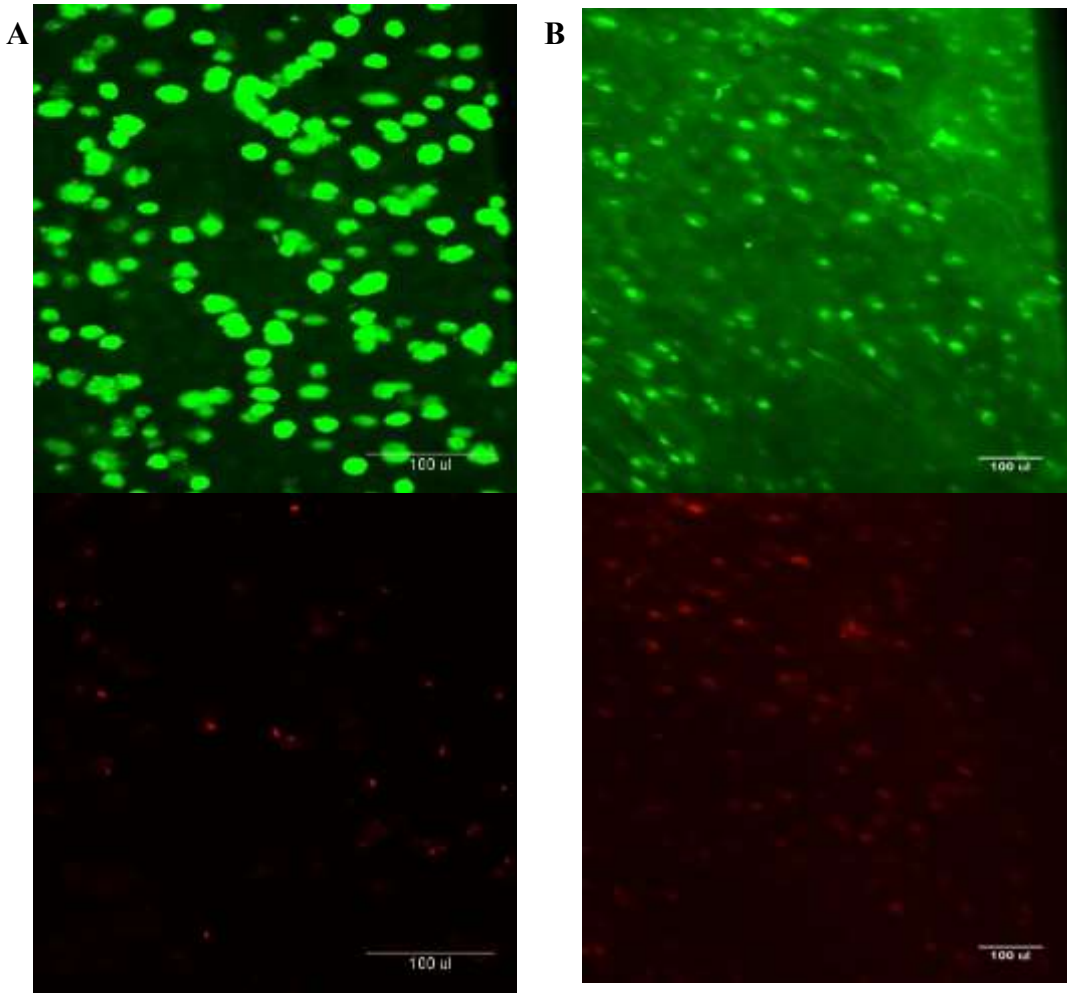

Figure 2.28: *Typical images showing the viability of bovine tenocytes seeded in collagen gels. Cells were stained using Calcein AM (live cells – green) and Ethidium Homodimer (dead cells – red) with paired images from both channels shown.* ***A)*** *Non-strained,* ***B)*** *strained (1% ± 1% at 10Hz)*

Table 2.10: Cell viability results showing the mean percentage of live cells in unloaded 3D collagen gels seeded with bovine cells at different time points as well as in loaded groups

		Percentage viability (%) Mean ±STDEV		
Duration		**Edge out**	**Middle**	**Edge in**
0hrs		84±7.1	88±0.7	91±10.6
12hrs		81±2.1	79±5.7	86±3.5
24hrs		86±3.5	87±2.1	93±7.8
48hrs		82±7.1	77±2.1	78±10.6
24hrs incubation; 15mins cyclic load, 1% static strain up to 24hr time point	1% ± 1% at 1Hz	88±1.7	87±2.3	81±2.9
	1% ± 1% at 10Hz	87±1.1	84±1.6	90±9.6

Cell Viability – Quantitative Cell Count: Trypan Blue Staining

To further confirm cell viability within the 3D gels, an additional means to measure cell viability in a more quantitative manner was adopted using trypan blue. Cell viability calculated in this manner ranged from 79-85%, consistent with the ethidium homodimer and Calcein AM staining results.

Table 2.11: Cell viability results showing the mean percentage of live cells in 3D collagen gels seeded with bovine cells after loading

		Percentage viability (%)
Duration	**Loading condition**	**Mean ±STDEV**
48hr incubation	No strain	79±0.7
24hrs incubation; 15mins cyclic load, 1% static strain up to 24hr time point	1% ± 1% at 1Hz	81±0.7
	1% ± 1% at 10Hz	85 ±0.0

Cell Viability – DNA Quantification

Changes in cell number during the course of an experiment were examined through quantification of DNA levels in samples.

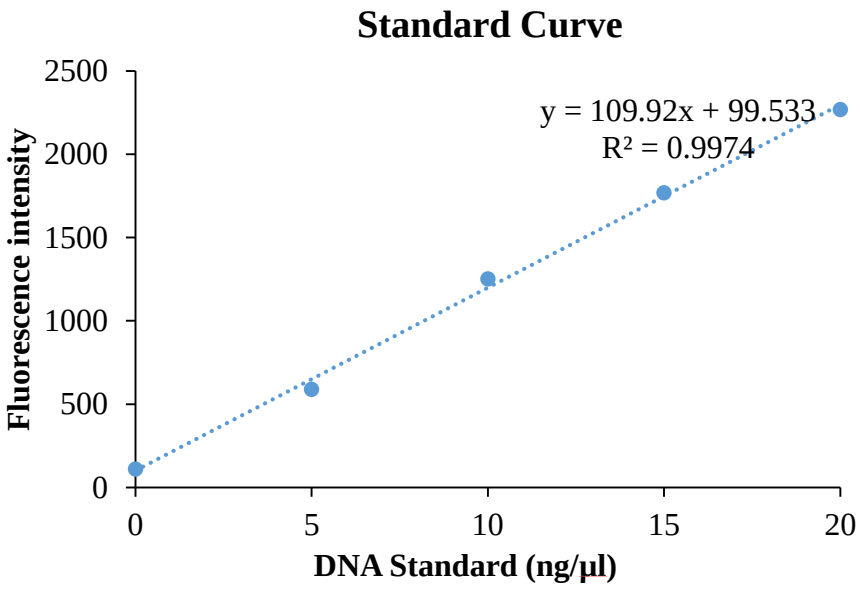

Figure 2.29: *Representative DNA assay standard curve*

No differences in DNA levels were seen in any of the control or loaded samples, indicating consistent cell numbers for the duration of the experiment.

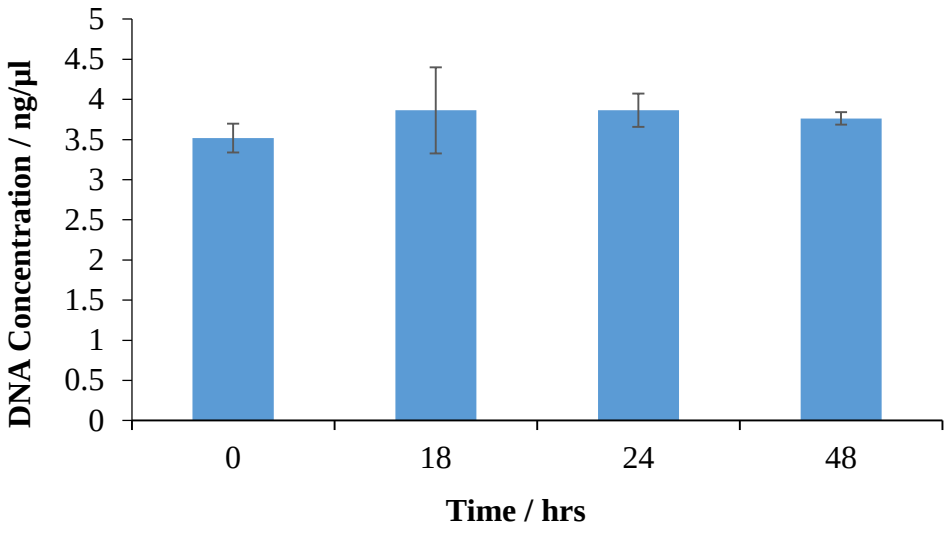

Figure 2.30: *DNA levels in unloaded samples at 0, 18, 24 and 48hrs showing no cell proliferation across the different samples and time points.*

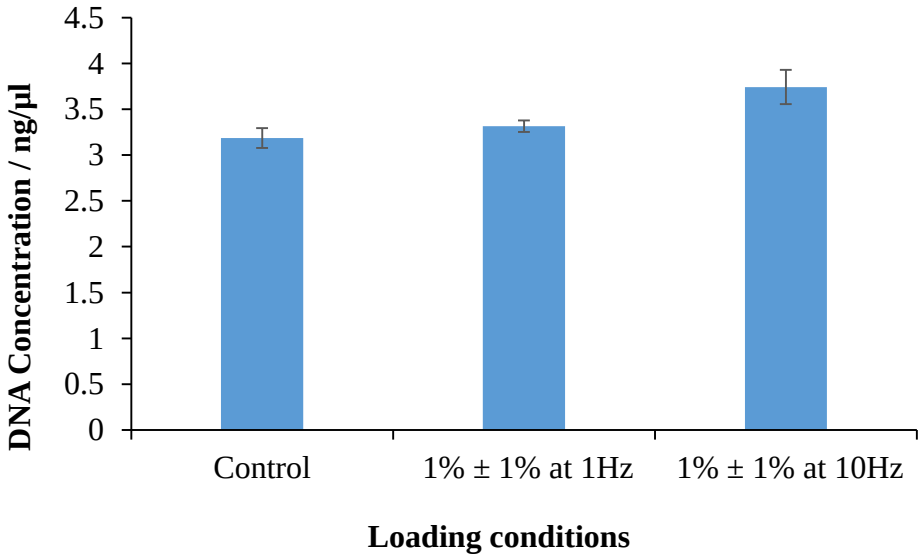

Figure 2.31: *DNA levels in loaded samples showing no cell proliferation across the different samples without and with loading.*

These data (Figure 2.30 and 2.31) in conjunction with the visual evidence of maintained cell viability provides confidence that viable cells are successfully maintained within the collagen gels throughout the experiment with no proliferation, irrespective of load application.

2.7.4 DISCUSSION

In these validation studies, the mechanical behaviour of the collagen gels was assessed, and cell viability throughout the construct was also confirmed. The mechanical response of the gel is important for elucidating cell matrix interactions at the microstructural level and hence to determine the overall mechanical environment experienced by the cells. The stress relaxation data in Figure 2.26, confirmed no stress relaxation in the gels during the applied cyclic strain period ensuring that the cells experienced consistent and easily defined strains throughout the loading experiments. A recent study on the mechanics of 3D collagen gels seeded with bone marrow stromal cells demonstrated stress relaxation in a range of different gel-cell materials [Chieh et al., 2014]. Collagen gels seeded with cells at concentrations of 0.1, 0.25, 0.5 or 1 x 10^6 cells/ml all demonstrated stress relaxation but also showed that stress relaxation behaviour is reduced in gels with a greater cell concentration [Chieh et al., 2014]. These tests used a static strain stress relaxation protocol (8.6% strain for 90 seconds). Such a strain protocol is more aggressive than the cyclic loading applied in the current study, and the higher strains may be responsible for the stress relaxation reported.

In order to confirm cell viability for the duration of the study, live/dead staining, trypan blue and DNA assay analyses were all conducted to give both a quantitative value and a spatial assessment of cell viability. The DNA assay combined with the trypan blue assay provided a quantitative confirmation that overall cell numbers did not change and that viability is maintained above 77%, while live/dead staining checked that viability was consistent across samples and confirmed that rolling the samples did not affect viability in the core. Table 2.10 and 2.11 as well as Figure 2.30 and 2.31 show cell viability data for different time points, with and without strain. The ability of 3D collagen gels to maintain cell viability with or without strain application over time was also validated by Galie and Stegemann [2011]. They investigated cell viability in 3D collagen gels seeded with cardiac fibroblasts, both unstrained for a 120hr period and mechanically strained at 5% strain at 1Hz for 48hrs, 24hrs after seeding. Using a live/dead viability kit, the study demonstrated a viability percentage of 85 – 90% [Galie and Stegemann, 2011]. These data suggest that cells can be maintained in 3D collagen constructs and that application of strain does not compromise cell viability.

These results are important for the use of this 3D collagen gel for the examination of cell response to loading under the proposed mechanical loading conditions.

2.7.5 MODEL SELECTION

Each *in vitro* model investigated within this chapter possessed both advantages and disadvantages when considering its use for the current research project. Although there was regular supply of bovine tissue from which to obtain tendon explants, dissecting these samples resulted in explants with poor cell viability, which diminished further in response to loading, making bovine explants clearly unsuitable for investigating the cell response to loading. Explants from the rat model (tail fascicles or Achilles tendon) demonstrated far better cell viability at around 70% even after cyclic strain. However, tissue supply was limited to the point that adopting this model became high risk for the future progress of the project.

Isolated cells were investigated in both 2D and 3D model systems, initially utilising the readily available bovine cell source. A 2D system was investigated owing to ease of set up and the simplicity of the resulting cell strain environment. However, it was established that cells were not able to survive the applied load regimes in this system, with cells detaching from the surface of the gel upon the application of cyclic strain. Accordingly, a 3D system was investigated, seeding isolated cells within a collagen gel. Cell viability was maintained in this system, even with the application of loading, and a mechanical characterisation of the gels confirmed that it was possible to confidently determine the local strain environment surrounding cells for further interpretation of data. Together, these data supported the use of 3D collagen gels for further cell mechanobiology studies.

Furthermore, while the different loading models were under investigation, potential loading conditions were also explored. The initial cyclic strain condition (5% ± 5% at 1Hz or 10Hz for 24hrs) used for the bovine tendon explant, was changed to 1% ± 1% at 1Hz or 10Hz for 24hrs for the rat tendon explant studies, as it was hypothesised that the strain used for stimulating the bovine tendon explants may have been too high and contributed to the cell death after strain application. Lower magnitude strains were maintained throughout the studies in isolated cells, reflecting research which has indicated that the strains experienced by tenocytes within tissues were of the order of 1-2% [Screen et al., 2014]. When working with isolated cells, the duration of 24hrs continuous loading was also changed to 15mins, a decision made when reflecting on the duration of loading experienced by cells or tissues during either ESWT or an eccentric rehabilitation program of 3 sets of 15 repetitions [Jonsson et al., 2008; Norregaard et al., 2007].

CHAPTER THREE

TENOCYTE RESPONSE TO LOADING

3.1 INTRODUCTION

Like other connective tissues, tendons experience varying loads in their natural environment and manage matrix metabolism accordingly. Under physiological loads, matrix metabolism is generally geared towards homeostasis but excess mechanical load or stress deprivation can both lead to a deleterious cell response [Gardener et al., 2008; Scott et al., 2005]. The mechanical loading variables (strain level, loading frequency, strain duration, repetition number) which determine cell response have been studied to some extent, but the optimal conditions to prevent injury or promote anabolic matrix response and repair are still unknown and likely differ across tendon types and species [Huisman, et al., 2014; Hsieh and Turner, 2001].

Increased knowledge of the mechanical loading parameters which promote an anabolic matrix response in tenocytes provides an important input towards optimising exercise prescription for tendinopathic patients, considering that mechanical stimulation of tendons through exercise is a cornerstone to the treatment of tendinopathy [Chaudhry et al., 2015; Henriksen et al., 2009]. A number of studies have investigated the regulation of metalloproteinase and matrix genes in response to mechanical load using rat tissue or cells, however, very few studies have done the same using human samples or cells [Sun et al., 2010; Szczodry et al., 2009; Legerlotz et al., 2007]. In addition, the majority of the studies have only been able to look at a few metalloproteinase and matrix genes, mainly focussing on MMP1, MMP2, MMP3, MMP13 and COL1A1 [Maeda et al., 2009; Asundi and Rempel, 2008].

A study by Legerlotz et al. [2013] investigated the effect of cyclically loading tendon explants *in vitro* using bovine fascicles. The tendon fascicles were subjected to cyclic tensile strain to 30% or 60% of the strain at failure at 1Hz for 0hr to 5hrs, with data demonstrating that mechanical loading reduced explant failure stress and increased the expression of COL1A1 and IL6 [Legerlotz et al., 2013]. A different study was also able to investigate the effect of cyclically loading isolated tenocytes cultured onto 0.05% collagen type I silicone flasks and strained to 6% at 1Hz or 2Hz for 48hrs [Zaman et al., 2013]. This study demonstrated that loading at 1Hz increased MMP1 and fibronectin expression, whilst loading at 2Hz increased cell proliferation [Zaman et al., 2013]. Furthermore, tendon cells seeded in a 3D scaffold of poly(L-lactide-co-ε-caprolactone)/collagen and cyclically strained to 2%, 4% or 8% at 0.3Hz, 0.5Hz or 1Hz for 3hrs per day demonstrated increased expression of COL1A1, tenascin-C, tenomodulin and scleraxis with loading [Xu et al., 2015]. These *in vitro* studies have concentrated on exploring the effects of low frequency and static mechanical loads using varied *in vitro* models, generally selected as

such loads are hypothesised to imitate those present in tendons during conventional physical activity (walking at ~1Hz).

Chaudhry et al. [2015] showed that completing an eccentric exercise regime for the Achilles tendon generated tremor within the tendon at a mean frequency of 10Hz. This high-frequency (10Hz) mechanical stimuli was hypothesised to stimulate tendon repair [Chaudhry et al., 2015]. In bone, high-frequency (5–100Hz) mechanical load has been shown to be capable of stimulating bone cells to promote bone growth, doubling bone formation rates relative to unstimulated controls [Bacabac et al., 2006]. Taken together with the knowledge that tendinopathy is effectively treated by eccentric loading, it could be hypothesised that 10Hz loading is stimulatory for tendon cells. However, no study have investigated the response of tenocytes to 10Hz loading. This research hypothesises that 10Hz loading may lead to an anabolic stimulation of tendon cells

The aim of this study was to determine the effects of 10Hz loading relative to the more commonly adopted 1Hz loading upon healthy and tendinopathic human tenocytes.

3.2 METHODOLOGIES

3.2.1 SAMPLE COLLECTION AND PREPARATION

Human tenocytes were collected from tendinopathic Achilles tendon [n = 3, Age: 21 ± 1 years] and healthy semitendinosus tendon (which will be referred to as hamstring tendon from here on, throughout this thesis) [n = 3, Age: 48 ± 3 years]. Cells were previously prepared by either explant outgrowth or collagenase digest respectively, and obtained from Dr. Graham Riley at the Bio-Medical Research Centre (BMRC) University of East Anglia (UEA). Cells were cultured in 10% FBS media, the components of which are detailed in Table 3.1. Medium was replaced every three days until cells reached 80% confluent. Cells were passaged as described in Chapter 2.5.1. Cells at passage four to six were used in this research.

Table 3.1: Component of 10% FBS media used for human cell culture

Component	10% FBS Media (ml)	Loading Media (ml)
DMEM (with sodium pyruvate, phenol red, glutamaxTM and low glucose) (ThermoFisher Scientific, 21885-025)	500	500
FBS (Sigma – Aldrich, F7524)	50	-
Penicillin streptomycin (PS) (Sigma – Aldrich, P4333)	5	5

When sufficient cells were available, cells were trysinized, centrifuged, re-suspended in fresh media and counted using a haemocytometer as described in Chapter 2.5.1. The cells were then seeded into a collagen gel as described in Chapter 2.6.1, and the gel fixed within the custom-made chambers and filled with 1.5ml of loading media as shown in Figure 2.3. The loading media contained no FBS because FBS is an uncharacterised, variable derivative of cow blood containing an array of growth factors, enzymes and other macromolecules and micronutrients, thus to maintain consistency within samples and experimental groups, a controlled, FBS free loading media was adopted.

In order to prepare for a loading study, comparing gene expression in response to 1Hz and 10Hz loading, a series of validation steps were carried out (Figure 3.1). First a stabilisation experiment was carried out using bovine tenocytes, to assess the time taken for gene expression to stabilise after samples were secured in the loading chambers. After this was ascertained, human tenocytes were used, to next review the time course for the load induced response of different genes, to determine the optimal time for carrying out gene expression analysis post loading.

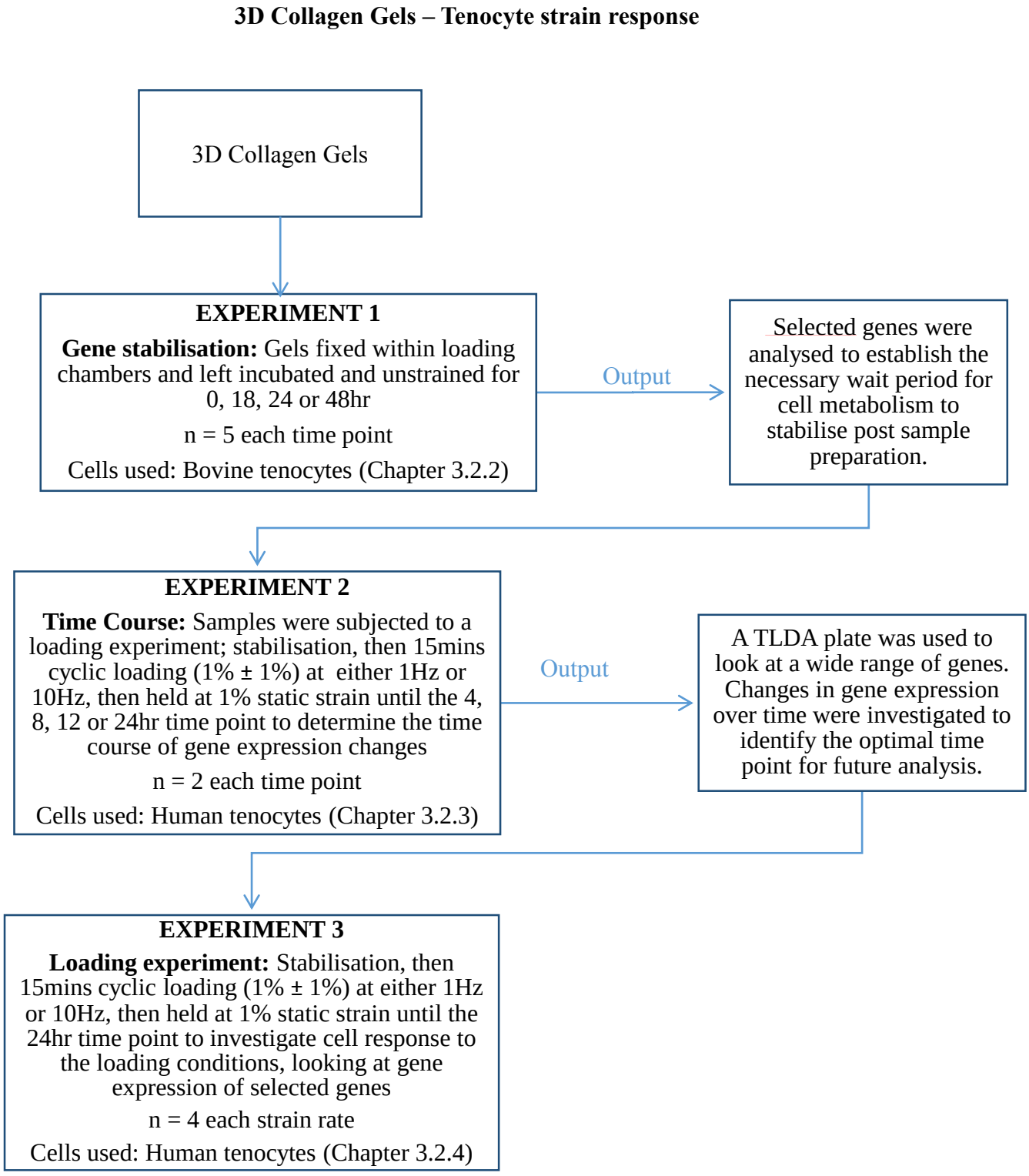

Figure 3.1: *Flow diagram of experiments performed on 3D collagen gels. Gene stabilisation was performed on unstrained samples using bovine tenocytes, followed by a time course experiment on human tenocytes seeded in collagen gel. Strained samples were left to incubate for 24hrs then cyclically strained. A loading experiment was then carried out on samples allowed to incubate for 24hrs and then cyclically strained. (TLDA – Taqman Low Density Array)*

3.2.2 3D COLLAGEN GEL GENE STABILISATION

A time course analysis of selected genes (detailed in Table 3.2) was carried out to investigate how sample preparation, including securing gels in the loading chambers, altered gene expression over a 48hr period and to establish when samples had stabilised in preparation for loading experiments. Bovine tenocyte seeded collagen gels (n=20) were fixed in loading chambers and placed in an incubator to maintain samples in 5% CO_2 at 37°C. 5 samples were removed from the chambers at each time point of 0, 18, 24 and 48hrs. The gripped ends of the collagen gels were removed using a sterile scalpel and the mid-portion of the gel (10mm long), was placed into a cryotube and immersed in liquid nitrogen. After 3-5 minutes, the samples were removed from liquid nitrogen and stored at -80°C for later gene analysis. RNA extraction, reverse transcription and qRT-PCR was then carried out as detailed in Chapter 2.3.1.

Table 3.2: Bovine primer sequences (Forward and Reverse) used for real-time polymerase chain reaction

Target Gene	Primer / Probe Type	Sequence
18s	Forward Reverse Probe	TGCGGCTTAATTTGACTCAACA CGAGAAAGAGCTATCAATCTGTCAAT AAACCTCACCCGGCCCGGAC
MMP3	Forward Reverse Probe	CCTTGTCCTTCGATGCAATCA ATGAAATTCAGGTTCGAATGTCCT TTTCCGCCAAAAATGTCTGCCTTTAAAGAA
MMP13	Forward Reverse Probe	CGCGGAGAAACACTGATCTTT GTTAAAAACAGCTCYGCWTCAACCT AGATTCTTCTGGCGSCTGCATCCTC
COL1A1	Forward Reverse Probe	GCCTGGTCAGAGAGGAGAAAGA CCTTGTTTGCCGGGTTCAC TTCCCTGGTCTTCCTG
IL6	Forward Reverse Probe	CCAGAGAAAACCGAAGCTCTCA CTCATCATTCTTCTCACATATCTCCTTT AGCGCATGGTCGACAAAATCTCTGC

3.2.3 TIME COURSE ANALYSIS FOR GENE EXPRESSION CHANGES POST-LOADING

A second time course analysis involving a wide range of genes was carried out, this time to investigate the time course for peak gene expression changes in response to loading. Healthy human hamstring tenocytes were seeded into collagen gels (n=18), fixed in loading chambers and placed in an incubator to maintain samples in 5% CO_2 at 37°C for 24hrs allowing gene

expression to stabilise. Samples were then subjected to one of the three different loading conditions and stopped at different times:

- Unstrained (24hrs only) – Control group
- High magnitude low frequency loading: 15mins cyclic loading (1% ± 1% at 1Hz) followed by 1% static strain until the 4, 8, 12 or 24hrs time points
- High magnitude high frequency loading: 15mins cyclic loading (1% ± 1% at 10Hz) followed by 1% static strain until the 4, 8, 12 or 24hrs time points

After loading, collagen gels were removed from the chambers and the gripped ends of the gels were removed using a sterile scalpel. The mid-portion of the gel was frozen and stored for later gene analysis as previously described (for full details see Chapter 2.3.1).

RNA was quantitated, reverse transcribed and analysed using a Taqman Low Density Array (TLDA) qRT-PCR. A TLDA is a microfluidic card with 384-wells across eight ports, each port containing 48 connected wells. The primers and probe for each assay are preloaded and dried onto the designated duplicate wells, hence the TLDA card is useful to analysis a wide range of genes (48 genes) in 8 different samples in one single run, rather than running single PCR assays (significantly less sample is needed for a TLDA analysis). The TLDA (Life Technologies, Paisley, UK) was specifically designed to investigate tendon matrix genes, and covered 7 of the 23 MMP genes as well as 8 of the 19 ADAMTS genes, all 4 TIMP genes, 4 interleukin genes, 12 key proteoglycans and 10 collagen genes, as well as 3 endogenous control genes 18s, GAPDH and TOP1 (see Table 3.3 for the TLDA gene selection).

Table 3.3: Cytokines, matrix genes, metalloproteinases & TIMPs selected for the Taqman Low Density Array primer sets

Primer Probe Set	Gene Abbreviation	Full Name
Hs00223332_m1	TNMD	Tenomodulin
Hs03054634_g1	SCXB;SCXA	Scleraxis
Hs01115665_m1	TNC	Tenascin C
Hs00164359_m1	COMP	Cartilage Oligomeric Protein
Hs00365052_m1	FN1	Fibronectin
Hs01555410_m1	IL1B	Interleukin 1
Hs00174114_m1	IL2	Interleukin 2
Hs00985639_m1	IL6	Interleukin 6
Hs00174103_m1	IL8	Interleukin 8
Hs00199608_m1	ADAMTS1	A Disintegrin and Metalloproteinase with Thrombospondin Motifs 1

Hs01029111_m1	ADAMTS2	A Disintegrin and Metalloproteinase with Thrombospondin Motifs 2
Hs00610744_m1	ADAMTS3	A Disintegrin and Metalloproteinase with Thrombospondin Motifs 3
Hs00192708_m1	ADAMTS4	A Disintegrin and Metalloproteinase with Thrombospondin Motifs 4
Hs00199841_m1	ADAMTS5	A Disintegrin and Metalloproteinase with Thrombospondin Motifs 5
Hs01058097_m1	ADAMTS6	A Disintegrin and Metalloproteinase with Thrombospondin Motifs 6
Hs00229594_m1	ADAMTS12	A Disintegrin and Metalloproteinase with Thrombospondin Motifs 12
Hs01548449_m1	ADAMTS14	A Disintegrin and Metalloproteinase with Thrombospondin Motifs 14
Hs00899658_m1	MMP1	Matrix Metalloproteinase 1
Hs01548727_m1	MMP2	Matrix Metalloproteinase 2
Hs00968305_m1	MMP3	Matrix Metalloproteinase 3
Hs01042796_m1	MMP7	Matrix Metalloproteinase 7
Hs01029057_m1	MMP8	Matrix Metalloproteinase 8
Hs00234579_m1	MMP9	Matrix Metalloproteinase 9
Hs00233992_m1	MMP13	Matrix Metalloproteinase 13
Hs00171558_m1	TIMP1	Tissue Inhibitor of Metalloproteinase 1
Hs00234278_m1	TIMP2	Tissue Inhibitor of Metalloproteinase 2
Hs00165949_m1	TIMP3	Tissue Inhibitor of Metalloproteinase 3
Hs00162784_m1	TIMP4	Tissue Inhibitor of Metalloproteinase 4
Hs00195140_m1	PRG4	Proteoglycan 4
Hs00153936_m1	ACAN	Aggrecan
Hs00156076_m1	BGN	Biglycan
Hs00171642_m1	VCAN	Versican
Hs00370384_m1	DCN	Decorin
Hs00157619_m1	FMOD	Fibromodulin
Hs00300550_m1	LAMA1	Laminin
Hs00164004_m1	COL1A1	Collagen I
Hs00264051_m1	COL2A1	Collagen II
Hs00943809_m1	COL3A1	Collagen III
Hs00266237_m1	COL4A1	Collagen IV
Hs00609133_m1	COL5A1	Collagen V
Hs01095585_m1	COL6A1	Collagen VI
Hs00932129_m1	COL9A1	Collagen IX
Hs01097664_m1	COL11A1	Collagen XI
Hs00189184_m1	COL12A1	Collagen XII
Hs00964045_m1	COL14A1	Collagen XIV
Hs99999905_m1	GAPDH	Glycoraldehyde 3-phosphate Dehydrogenase
Hs99999901_s1	18S	18s rRNA
Hs00243257_m1	TOP1	Topoisomerase 1

Ct values were collected for each gene, with undetected samples given a Ct value of 40. Relative expression levels of each gene of interest were analysed by normalising to the endogenous

control gene 18s (ΔCt [endogenous control gene Ct–gene of interest Ct]) and expressing the data as $2^{\Delta\Delta Ct}$. All data were normalised to the control group, which is represented by the baseline value of 1. 18s was chosen as the house keeper of choice over GAPDH or TOP1 because it had the most stable Ct values across the different groups. It is also less sensitive to strain than GAPDH and more sensitive to RNA degradation, making it a good marker of sample quality [Kuchipudi et al., 2012]. Statistical analysis was not performed as only a single exploratory TLDA analysis was carried out. The TLDA was analysed to select genes of interest for a more extensive investigation of tenocyte response to strain, and establish the most appropriate time point for a more detailed analysis utilising standard RT-PCR.

3.2.4 TENOCYTE RESPONSE TO LOADING

The tenocyte response to high frequency (10Hz) and low frequency (1Hz) loading was compared to investigate gene expression changes that may shed light on the efficacy of eccentric loading in treating tendinopathy (Figure 3.2).

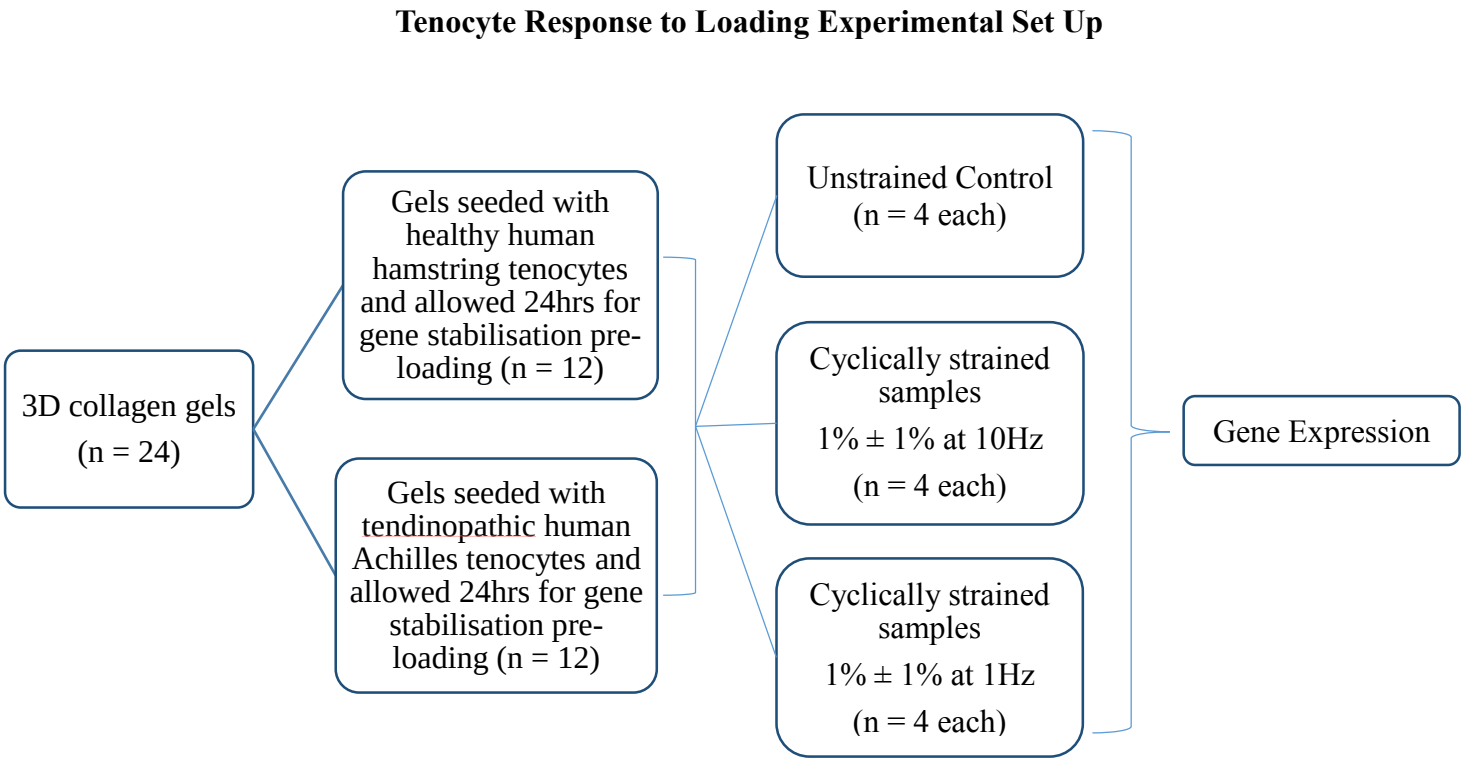

Figure 3.2: *Flow diagram depicting the experiments performed using 3D collagen gels, comparing the cell response to 10Hz and 1Hz loading.*

Collagen gels were seeded with either healthy hamstring tenocytes (n = 12) or tendinopathic Achilles tenocytes (n = 12). Gels were fixed into loading chambers and incubated for 24hrs to allow gene expression to stabilise, after which they were subjected to one of the three different loading conditions;

- Unstrained (24hrs) – Control group
- High magnitude low frequency loading: 15mins cyclic loading (1% ± 1% at 1Hz) followed by 1% static strain until the 24hrs time point
- High magnitude high frequency loading: 15mins cyclic loading (1% ± 1% at 10Hz) followed by 1% static strain until the 24hrs time point

After loading, collagen gels were frozen and stored for later gene analysis as described in Chapter 2.3.1.

Table 3.4: Human primer sequences (forward and reverse) used for real-time polymerase chain reaction

Target Gene	Primer / Probe Type	Sequence
18s	Forward Reverse Probe	GCCGCTAGAGGTGAAATTCTTG CATTCTTGGCAAATGCTTTCG ACCGGCGCAAGACGGACCAG
MMP1	Forward Reverse Probe	TTTGATGTACCCTAGCTACACCTTCA AAAGGTTAGCTTACTGTCACATGCTTT CCAAGCCATATATGGACGTTCCCAAAATCC
MMP2	Forward Reverse Probe	TACGACCGCGACAAGAAGTATG TTGTTGCCCAGGAAAGTGAAG CCCTGAGACCGCCATGTCCACTGTT
MMP13	Forward Reverse Probe	CCGAGGAGAAACMATGATCTTT GTTAAAAACAGCTCYGCWTCAACCT AGATTCTTCTGGCGSCTGCATCCTC
COL1A1	Forward Reverse Probe	CGCACGGCCAAGAGGAA CATGGTACCTGAGGCCGT TCT CCAAGACGAAGACATCCCACCAATCACC
COL3A1	Forward Reverse Probe	AATAAACTTCAACACTCTTTATGATAACAA CA ACTGGTGAGCACAGTCATTGCT TGTGTTATATTCTTTGAATCCTAGCCCATCT GCA
COL5A1	Primer/Probe Mix	Hs00609133_m1 – Life Technologies
ADAMTS5	Forward Reverse Probe	AGGAGCACTACGATGCAGCTATC CCCAGGGTGTCACATGAATG TGCCCACATAAATCCTCCCGAGTAAAC A
IL6	Forward Reverse SYBR Green	GGTACATCCTCGACGGCATCT GTGCCTCTTTGCTGCTTTCAC
IL8	Forward Reverse SYBR Green	AAGAGAGCTCTGTCTGGACC GATATTCTCTTGGCCCTTGG
TIMP-3	Forward Reverse Probe	GCTGACAGGTCGCGTCTATGA GTAGCAGGACTTGATCTTGCAGTT AGCTGGTCCCACCTCTCCACGAAGTT

3.2.5 STATISTICAL ANALYSIS

Statistical analysis was performed using a one way analysis of variance (one way ANOVA) looking for significant differences in the responses of tendinopathic and healthy cell types, when exposed to the different loading conditions. Tukey's Honest Significant Difference (HSD) pot-hoc tests were adopted when significant differences were identified, with P values < 0.05 considered significant.

3.3 RESULTS

3.3.1 3D COLLAGEN GEL GENE STABILISATION CHECK

A time course analysis of selected genes was carried out on bovine seeded 3D collagen gels, looking 0, 18, 24 and 48 hours after cells were secured in loading chambers, to determine when gene expression stabilised after gel preparation. 18s was confirmed stable throughout the experimental period, and gene expression changes were normalised to this house keeping gene. There was a notably large change in gene expression between 0 and 18hrs after which no further significant differences in gene expression were evident from 18 to 48 hours after sample preparation (Figure 3.3).

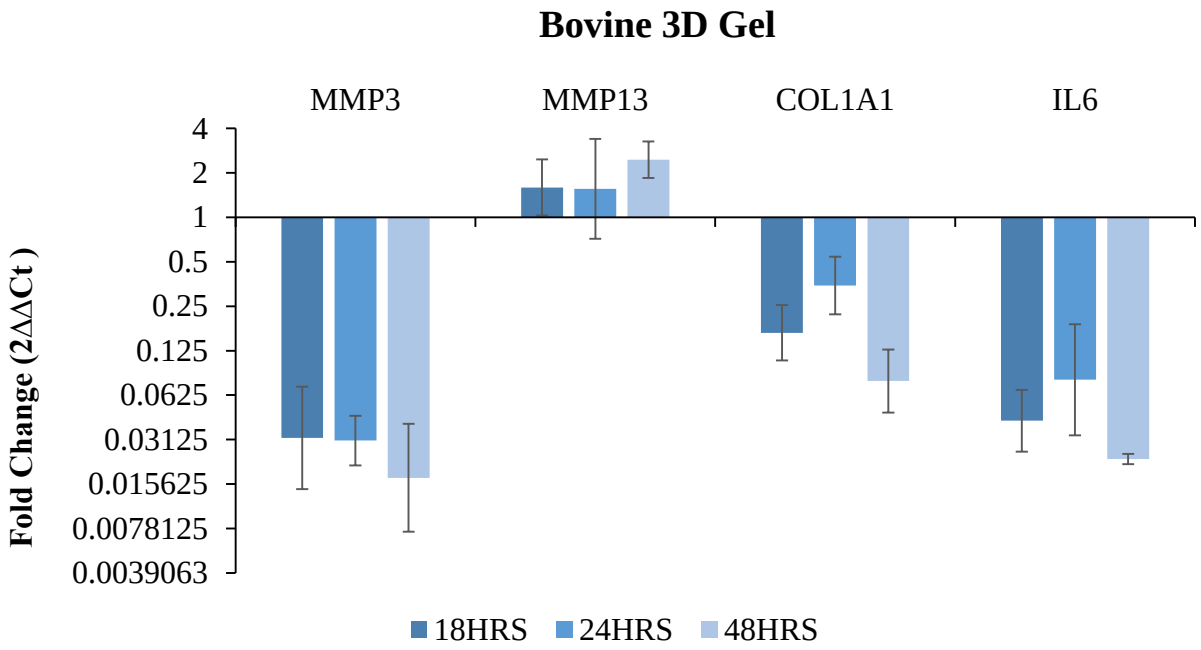

Figure 3.3: *Gene expression changes in bovine tenocytes after cells were seeded in 3D collagen gels and secured into loading chambers. Data was normalised to 18s and presented as fold changes relative to the 0 hour start of the experiment ($2^{\Delta\Delta Ct}$) [mean ± SD]. The greatest changes were seen in the first 18hrs, after which expression largely stabilised.*

3.3.2 TAQMAN LOW DENSITY ARRAY (TLDA) ANALYSIS

A TLDA was carried out to ascertain a broad spectrum gene expression response to 1Hz and 10Hz loading, to establish the peak response time across a range of relevant matrix genes. Of the analysed genes, MMP7, MMP8, ADAMTS3, COL2A1 and COL9A1 were not detected. The remaining genes showed a steady increase in gene expression for most genes with both high frequency (10Hz) and low frequency (1Hz) loading, with peak expression seen at 24hrs. Of

particular note, the greatest upregulations of gene expression with loading were seen in MMP1 (7.3 fold), MMP2 (4.1 fold), MMP13 (5.1 fold), ADAMTS1 (7.0 fold), ADAMTS5 (10 fold), ADAMTS12 (27.8 fold), TIMP2 (4.9 fold), TIMP3 (13.2), TIMP4 (9.1 fold), IL6 (8.1 fold), IL8 (5.4 fold), COL1A1 (6 fold), COL3A1 (5.4), and COL5A1 (566.3), for all other fold changes see Figure 3.4A and B.

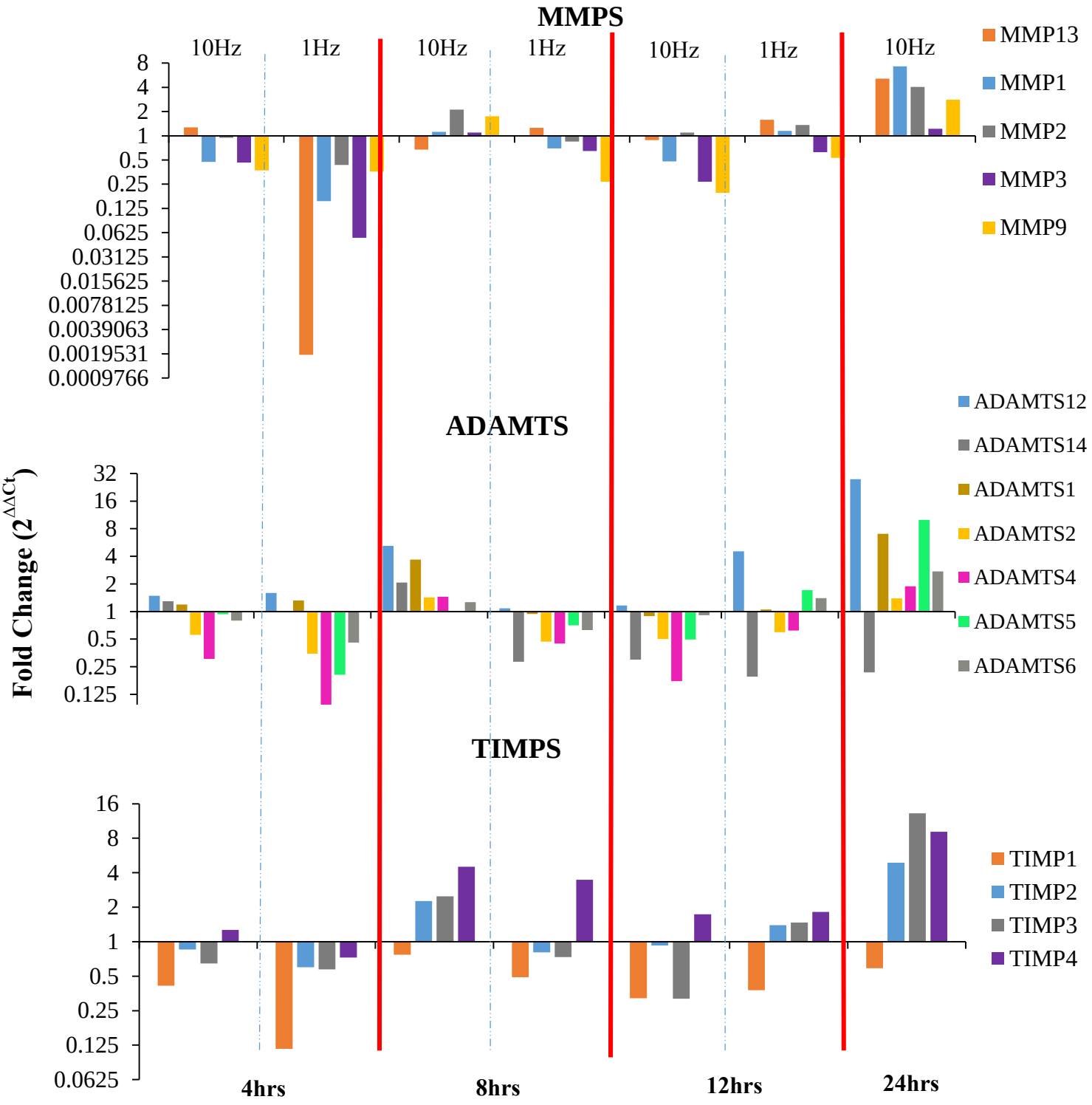

Figure 3.4A: *Regulation of gene expression with mechanical load over the 24hrs loading period using human healthy tenocytes. Collagen gels were fixed to a custom-made chamber and subjected to a cyclic load of 1% ± 1% for 15mins then statically strained at 1% until the 4, 8, 12 or 24hrs time point. Matrix genes expression levels were measured using a Taqman Low Density Array. Data was normalised to 18s and expressed relative to the 0hr unstrained samples. The greatest changes in gene expression were seen at 24hrs.*

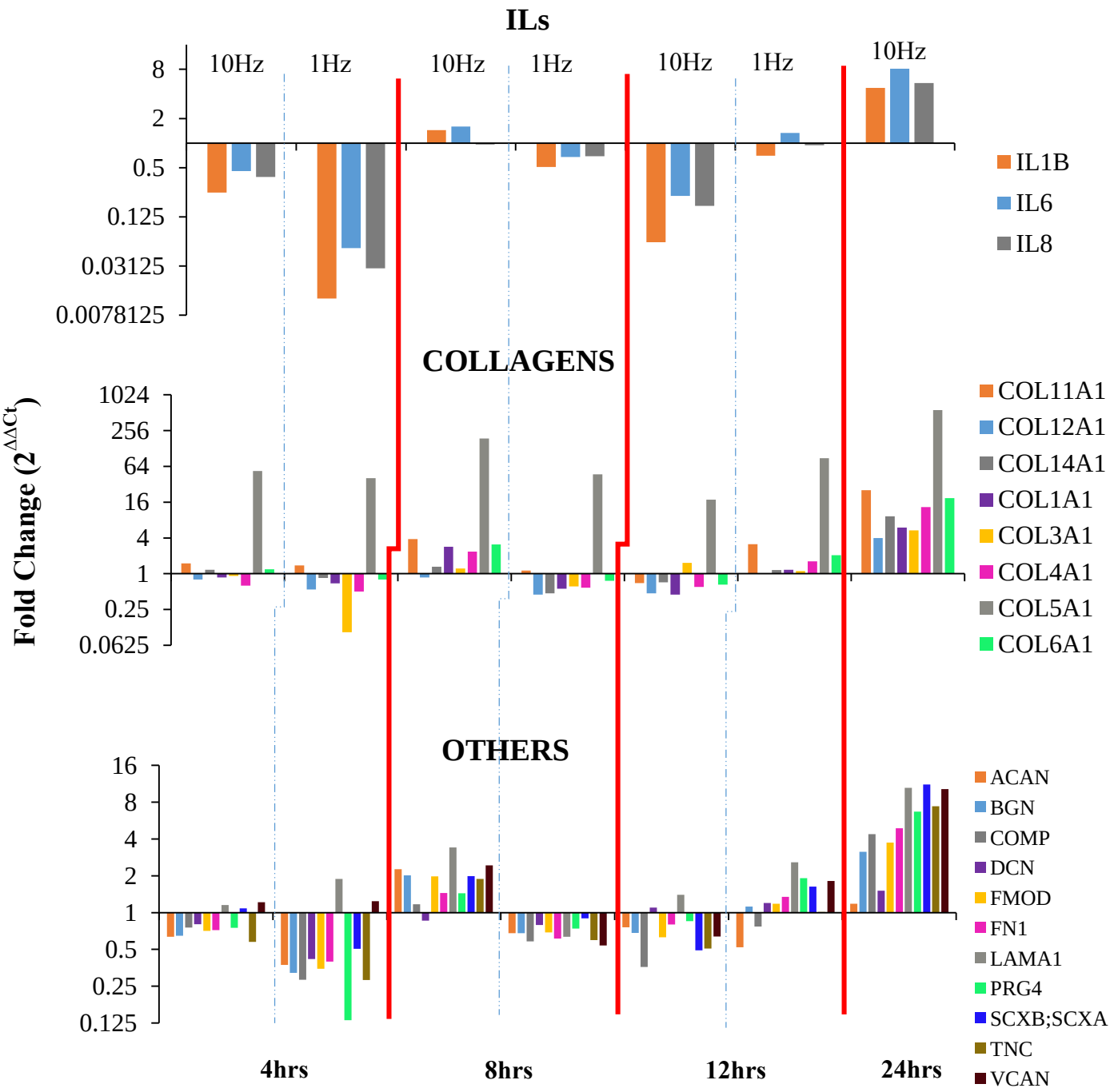

Figure 3.4B: *Regulation of gene expression with mechanical load over the 24hrs loading period using human healthy tenocytes.. Collagen gels were fixed to a custom-made chamber and subjected to a cyclic load of 1% ± 1% for 15mins then statically strained at 1% until the 4, 8, 12 or 24hrs time point. Matrix genes expression levels were measured using a Taqman Low Density Array. Data was normalised to 18s and expressed relative to the 0hr unstrained samples. The greatest changes in gene expression were seen at 24hrs.*

3.3.3 CELL RESPONSE TO LOADING

A comparison of cell response to 1Hz and 10Hz loading for selected genes demonstrated that gene expression changes were consistently more pronounced with loading at 10Hz compared to loading at 1Hz for both cell types (healthy and tendinopathic tenocytes) (Figure 3.5 and 3.6). Large error bars highlight the notable variability between biological replicates. However, paired analyses of data indicated significant differences only evident in the healthy tenocyte response, where MMP1 ($p = 0.039$), IL6 ($p = 0.026$) and IL8 ($p = 0.043$) were all significantly more responsive to 10Hz than 1Hz loading, demonstrating consistent trends in cell behaviour. The gene expression profile of tendinopathic cells showed an upregulation of COL3A1 and downregulation of COL1A1 and COL5A1, while the healthy hamstring tenocytes showed upregulation of all analysed genes, highlighting the different cell phenotypes. It was also notable that substantially higher gene expression levels were seen in the healthy hamstring tenocytes compared to the tendinopathic Achilles tenocytes, suggesting that the healthy cells are maybe more mechano-responsive to these loading conditions. However, age and tendon type may also play a role in this response.

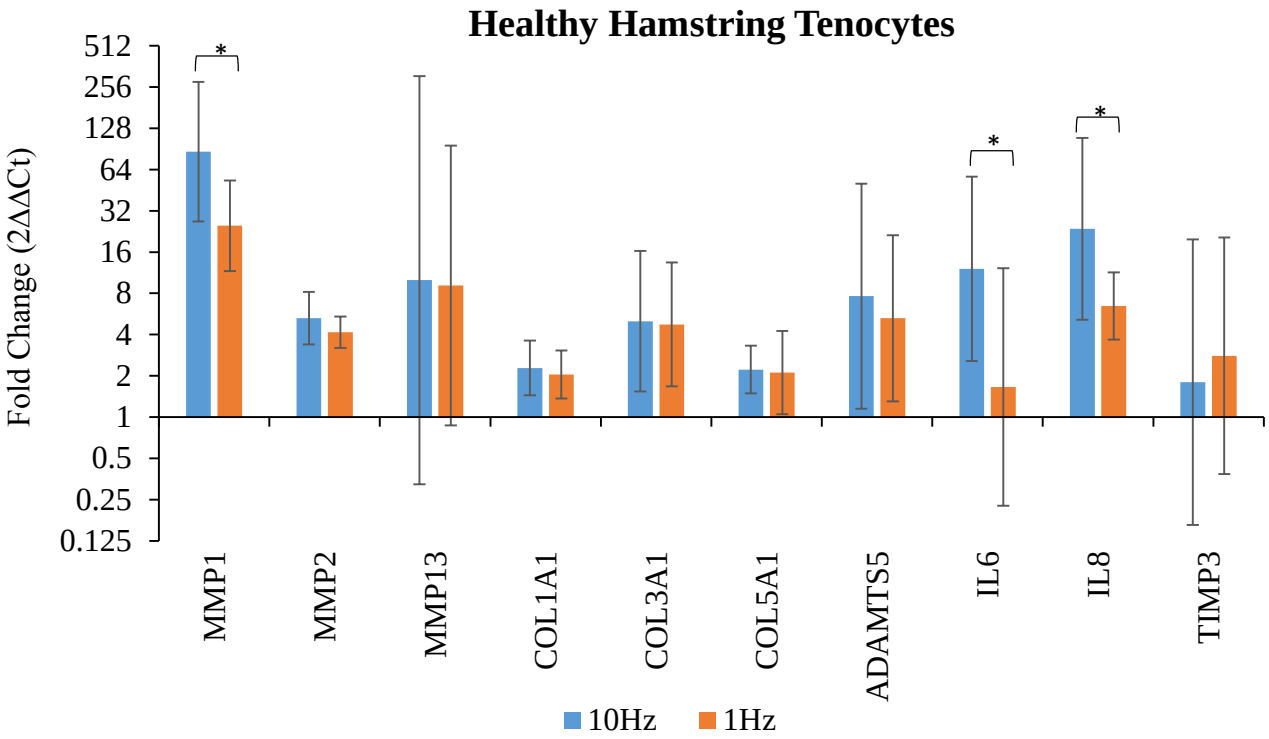

Figure 3.5: *Gene expression changes in healthy human hamstring tenocytes seeded in 3D collagen gels subjected to a cyclic load of 1% ± 1% for 15mins then held at 1% strain for 24hrs. Matrix genes were measured using standard qRT-PCR. Data was normalised to 18s and presented as a fold change relative to the 24hr control (unloaded) samples* ($2^{-\Delta\Delta Ct}$) *[mean ± SD]. * mean $p < 0.05$*

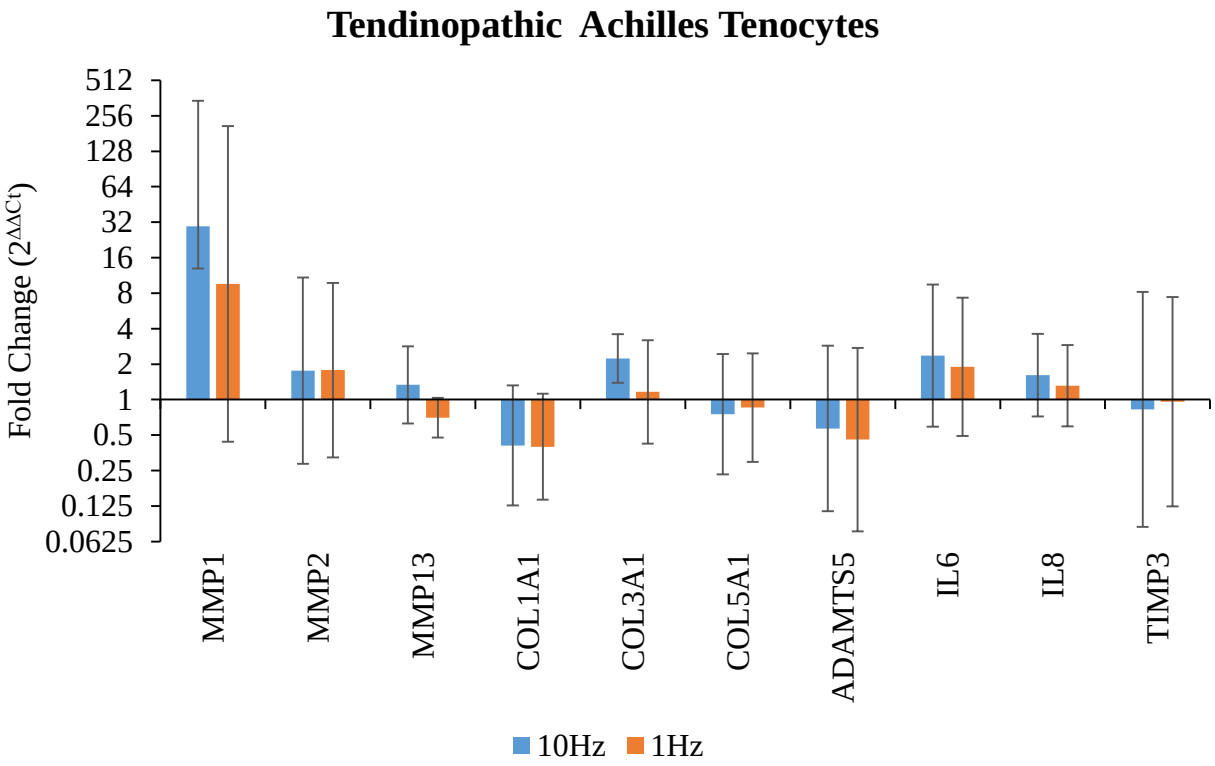

Figure 3.6: *Gene expression changes in tendinopathic human Achilles tenocytes seeded in 3D collagen gels subjected to a cyclic load of 1% ± 1% for 15mins then held at 1% strain until the 24hrs time point. Matrix genes were measured using standard qRT-PCR. Data was normalised to 18s and presented as a fold change relative to the 24hr control (unloaded) samples ($2^{\Delta\Delta Ct}$) ⌈mean ± SD].*

3.4 DISCUSSION

In Chapter 2, it was evident that preparing and securing explants within chambers altered their gene expression, therefore it was important to investigate the timeframe required for gene changes to stabilise within cells seeded with a 3D collagen gel prior to carrying out loading experiments. Figure 3.3 showed that gene expression was altered notably over the first 18hrs after sample preparation, but no significant differences were seen in the expression of any analysed gene after this point. Previous data (Tables 2.9, 2.10 and 2.11), confirmed that cell viability was maintained in constructs for 48hrs, hence a gene expression stabilisation period of 24hrs followed by an experimental period of 24hrs was deemed appropriate to proceed to further experimental analysis.

Studies have shown that the time frame over which different genes respond to loading is variable [Jones et al., 2013; Lesur et al., 2010], making it difficult to establish the most appropriate time point at which to investigate cell response to the applied loading conditions. In order to address this, a broad spectrum TLDA analysis of the time course of gene expression in response to the load regime of interest was carried out, helping to identify those genes most responsive to the applied strain and the most appropriate time at which to measure them for a future, more detailed analysis. Overall, the response to loading increased over time, peaking at 24hrs. However, it was notable that tenocytes initially appeared to respond more rapidly to 1Hz loading at 4hrs, but with a general trend towards downregulating gene expression before expression levels rose. The gene expression profile of this pilot study showed a general upregulation of ADAMTS and collagen relative to MMPs which may indicate a more anabolic response to mechanical load. Further experimental repeats with selected genes were then repeated using standard qRT-PCR analysis to investigate cell response to loading more closely. A tendinopathic cell group was also added, enabling a comparison of the metabolic response of these two populations.

It is difficult to determine the actual load that human tenocytes undergo within the tendon matrix during eccentric loading or ESWT due to lack of human studies in this area. However, the loading condition applied (strain at 1% ± 1%) in this study may be deemed physiological. Data from Screen, et al. [2004] that used microscopic examination to visualise rat tail fascicles during strain, demonstrated that tenocyte strain is limited to less than 2%, and it can be expected that the vibrations caused by ESWT or eccentric loading are likely to be small magnitude.

In this current study, genes were chosen for more detailed qRT-PCR analysis on the basis that they were more responsive to the loading conditions from the TLDA study. Other studies have also pointed out that the selected genes are reportedly modified by mechanical load or tendinopathy [Jones et al., 2013; Legerlotz et al., 2012]. The data from the TLDA experiment could not be combined with standard qRT-PCR analysis because the target the amplicons of primer and probe sets were different on the TLDA compared to those used for standard qRT-PCR. However, whilst gene expression levels with the TLDA and qRT-PCR were at variance, the changes and patterns were consistent, which increases confidence in the gene changes.

Data from Figures 3.5 and 3.6 indicate that healthy and tendinopathic derived tenocytes respond to mechanical loading in a similar manner. Whilst substantial error bars are evident in the data, these were primarily a product of variability between biological repeats particularly in the tendinopathic cells, which is indicative of the inconsistency in tendiniopathic cells. It was also evident that healthy tendon derived cells showed a more marked pattern of response, suggesting that cells derived from tendinopathic tissues may be less responsive to mechanical load. Tendinopathic tenocytes showing a less responsive pattern to loading in comparison to healthy tencocytes was also observed by Jones [2012], where healthy and tendinopathic tenocytes were cyclically strain to 5% in collagen gels using a flexcell system. It is possible this is a contributing factor to why tendinopathy does not get better with other treatment options, as the cells do not respond to load. However, a contradictory pattern was observed by Patel [2015]. Here healthy and tendinopathic human tenocytes were seeded into a fibre composite construct made of polyethylene glycol (PEG) with cells seeded onto stiff PEG fibres and surrounded by a softer PEG matrix, so on loading, cells experienced both tension and shear. Under these conditions, a more responsive pattern was seen in the tendinopathic tenocytes compared to the healthy tenocytes [Patel, 2015]. The differences between both the studies could be a result of the scaffold material in which the cells were seeded on or the type of loading applied, with direct mechanical shear differentially stimulating the cells.

The healthy hamstring tendon cells showed an upregulation of all genes analysed, which may indicate an anabolic response to mechanical loading [Sun et al., 2010], while the tendinopathic Achilles tendon cells showed a downregulation of COL1A1, the primary structural protein of tendon. The preferential upregulation of COL3A1 relative to COL1A1 and COL5A1 has previously been reported to denote an early healing response [Sun et al., 2010]. Type III collagen

has been identified as a major component of newly synthesized ECM in early tendon healing [Erisksen et al., 2002].

The cell response to 10Hz loading was constantly more marked than that seen with 1Hz loading, perhaps indicating a greater capacity for matrix turnover in response to the vibrations caused by eccentric loading. The difference in response to 10Hz and 1Hz loading was significant for MMP1, MMP2, IL6 and IL8 but only in the healthy cell population. The significantly greater response of these collagenases and cytokines with 10Hz loading may suggest that higher loading frequencies are better able to initiate matrix breakdown. However, when considered in conjunction with evidence of the upregulation of gene expression for collagen synthesis also in these samples, it may represent a greater capacity for matrix turnover, ultimately supporting repair. MMP1 and MMP13 are said to promote degradation of the ECM [Thorpe et al., 2014; Buono et al., 2013]. But, degradation can be important for healing and remodelling of damaged collagen fibres within the matrix. Therefore, increased MMP1 and MMP13 levels may induce active tissue remodelling or a healing response after injury [Hellio Le Graverand et al., 2000] especially when paired with new collagen production.

IL-6 is a multifunctional inflammatory cytokine, which exhibits both pro- and anti-inflammatory actions, and is released in response to mechanical loading [Legerlotz et al., 2012; Skutek et al., 2001]. IL-6 has also been shown to stimulate fibroblasts to induce collagen synthesis, with and without the presence of a mechanical stimulus, suggesting that IL-6 may be important for connective tissue health [Andersen et al., 2011]. In contrast, there are many studies reporting the role of IL-6 in tendon adaptation, suggesting it may promote negative effects [Nakama et al., 2006; Mihara et al., 1995]. These conflicting arguments reveal the need for further research into healing pathways before extensive conclusions can be made. IL8 on the other hand, is generally considered a pro-inflammatory cytokine induced by mechanical loading, however, not many studies have looked into the effects IL8 in tenocytes in response to loading [Waugh et al., 2015]. Waugh et al. [2015] showed an upregulation of IL8 after mechanical loading provided by ESWT at 8Hz, and although no significant difference existed between healthy and tendinopathic patients, IL8 production was more pronounced within the patient group. The study also demonstrated increased expression of IL-1 and IL-2 which was not analysed by the current study but suggests an inflammatory response to ESWT.

The TLDA demonstrated that IL8 expression begun to rise 24hrs after loading confirmed by further PCR. The application of cyclic strain has been shown to increase the production of IL6

and IL1β [Jelinsky, et al., 2011]. IL1β in turn increases the production MMPs [Waugh et al., 2015; Tsuzaki et al., 2003b]. In addition, IL1 not only increases expression of MMPs but IL6 also [Tsuzaki et al., 2003b; Archambault et al., 2002], suggesting that the IL1 signalling may be involved in the mechanotransduction pathways associated with load response.

In conclusion, these findings have demonstrated for the first time that loading at a frequency of 10Hz may enhance metabolic response in healthy tenocytes relative to loading at 1Hz. However, this response appears to be less pronounced in tendinopathic tenocytes. Further studies are needed to establish if the enhanced response to 10Hz loading is a result of the higher loading frequency or simply the increased overall mechanical stimulus, and additionally to investigate the mechanisms by which 10Hz loading stimulates increased gene expression.

CHAPTER FOUR

FURTHER CHARACTERISATION OF TENOCYTE STRAIN SENSITIVITY

4.1 INTRODUCTION

Cells detect and respond to mechanical loading by altering their metabolic response through a variety of pathways [Lavagnino et al., 2015]. The deformation of tendon cells initiates the expression of genes responsible for catabolic and/or anabolic cellular and molecular responses, which affect tissue development and also homeostasis. Data from this study have shown that 10Hz loading resulted in a significantly higher metabolic response in tenocytes than 1Hz loading. This Chapter aims to explore the mechanisms associated with the difference in cell response to the two frequencies, and the mechanotransduction pathways associated with the metabolic response.

From a mechanobiological point of view, four factors of the applied strain may affect the adaptive response of tenocytes: magnitude, frequency, number of cycles and duration [Bohm et al., 2014]. In the experiments described in Chapter 3, the magnitude and duration of loading were the same for the different loading groups, whilst the loading frequency and total number of loading cycles were both altered. Indeed, a clear limitation of experiments investigating different loading frequencies is that it is not possible to keep all other factors constant between groups. Either the loading period or total number of cycles must be at variance. Data from Rubin and Lanyon [1984] suggests that number of cycles may play an important role in tissue remodelling. This study investigated the effect of applying 4, 26, 360 and 1800 loading cycles to isolated rooster ulna, showing that with more cycles, the bone mass was further increased in a turkey ulna model [Rubin and Lanyon, 1984]. An increase in tenocyte differentiation was also seen with increased number of cycles, on tenocytes seeded in a 3D collagen gel and mechanically strained from 0-10% at 0.1Hz for 10, 100 or 1000 cycles once a day for two weeks [Scott et al., 2011]. This study also demonstrated increased expression of scleraxis with increasing number of cycles of loading [Scott et al., 2011]. In the current study, it is difficult to determine if it is loading frequency or total number of cycles responsible for the differential response of test groups. However, this can be explored by repeating the experiment, but including a test group with a constant number of cycles.

Tendon cells subjected to mechanical loading, activate mechanotransduction signalling pathways that are not fully understood. In normal conditions, these processes balance and maintain tissue homeostasis [Popov et al., 2015]. During mechanical loading, load is transmitted through the extracellular matrix to the cytoskeleton of the mechanosensitive tendon cells via

focal adhesion sites (such as integrins, ion channels, or growth factors) activating downstream proteins kinases [Lavagnino et al., 2015; Wang, 2006].

Cell culture studies have shown that tenocytes respond to mechanical loading by increasing the production and secretion of certain genes such as growth factors and IL-1, which in turn act on the cell to induce expression of other genes [Bouchard, 2015]. Some of the other genes reported to respond to mechanical loading include collagens, MMPs and interleukins, seen across a range of experiments on human and animal cells [Gumucio et al, 2015; Wang et al., 2007; Heinemeier et al., 2007; Olesen et al., 2006].

In general, the healing process of an injured or compromised tendon passes throughout three main phases containing distinctive cellular and molecular cascades (figure 4.1). Growth factors have been demonstrated to increase in response to mechanical loading which in turn increases metabolic activity essential to tendon healing [Zhang and Wang, 2013]. The tendon healing process is complexly orchestrated by a variety of secreted molecules [Docheva et al., 2015]. Initially, certain inflammatory cytokines, such as interleukin (IL)-6 and IL-1β, are produced by the invading inflammatory cells. Later, tissue repair is facilitated by a number of growth factors, which are released by cells located at the injury site [Docheva et al., 2015]. In particular, growth factors like transforming growth factor beta (TGFβ), connective tissue growth factor (CTGF), insulin-like growth factor (IGF), vascular endothelial growth factor (VEGF), platelet-derived growth factor (PDGF) and basic fibroblast growth factor (bFGF) are upregulated in different phases of the healing process, with diverse molecular effects during healing (figure 4.1) [Molloy et al., 2003]. TGFβ is upregulated in both gene expression and in protein form in all stages of tendon healing and is responsible for stimulating cell migration, regulation of proteinases, fibronectin binding interactions, termination of cell proliferation via cyclin-dependent kinase inhibitors, and stimulation of collagen production [Jones et al., 2013; Molloy et al., 2003]. A study by Jones et al. [2013] indicated that mechanical loading induces the TGFβ signalling pathway, and much of the strain induced mRNA expression in tenocytes occurred through this pathway. Therefore, in this thesis, TGFβ was investigated to establish if it was involved in the tenocyte strain response, and to investigate which genes may be associated with TGFβ expression.

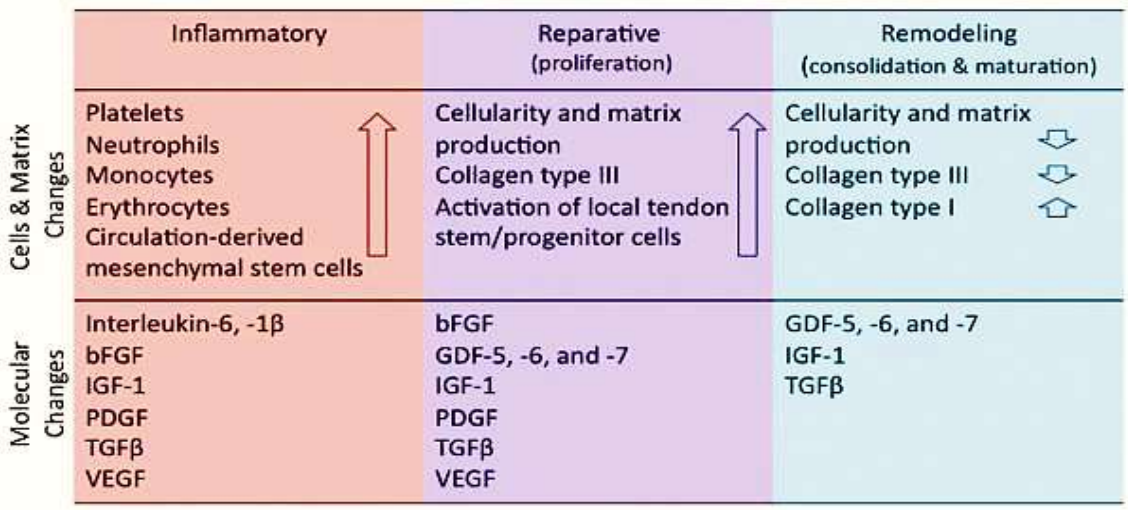

Figure 4.1: *Key molecular, cellular and matrix changes occurring during the three main phases of tendon repair. Each healing stage is characterized by involvement of different growth factors, activation of certain cell types and production of essential matrix proteins, which collectively contribute to the replacement of the initial fibrous tissue with more a tendinous regenerate [Adaptaed from Docheva et al., 2015]*

IL-1 family members have been intensely studied (especially IL-1α and IL-1β), unravelling their roles as proinflammatory cytokines in diseased tissues [Dinarello, 1996; Sun et al., 2008]. Studies that have investigated IL-1 in tissue healing suggest that IL-1 might contribute to stimulating expression and accumulation of MMPs and IL-6 in tendon matrix [Sun et al., 2008; Tsuzaki et al., 2003a]. IL-1 is secreted by macrophages and monocytes, and it is well known that MMPs are a group of enzymes released from macrophages [Tsuzaki et al., 2003a], Previous data from this thesis showed an upregulation of MMPs and IL-6 in healthy hamstring tenocytes subjected to cyclic load. Therefore, in this present study, IL-1 will also be investigated to establish if it may be involved in stimulating human tendon cells to express mRNA for MMPs and IL-6 in response to loading.

A review of current understanding of the TGFβ and IL-1 signalling pathways is now provided.

TGFβ Secretion and Activation

Mature TGFβ is secreted by a cell after intracellular proteolytic cleavage of the TGFβ protein by the endopeptidase furin, that yields a dimer protein from the N-terminal called latency associated peptide (LAP) and a dimer protein from the C-terminal called mature TGFβ [Horiguchi et al., 2012; Khalil, 1999]. The LAP protein facilitates the transit of TGFβ from the cell while also ensuring the TGFβ remains biologically inactive, also referred to as latent TGFβ protein (LTBP) [Khalil, 1999]. TGFβ and LAP together form small latent complex (SLC) but are not covalently

bonded [Horiguchi et al., 2012]. Within the endoplasmic reticulum (ER), SLC binds to LTBP via a disulphide bond through LAP to form large latent complex (LLC) which is released into the ECM for future activation (Figure 4.2) [Horiguchi et al., 2012].

The LLC, contains a convenient store of TGFβ within the ECM which can easily be activated. Activation has been reported to occur by a variety of mechanisms which include proteases (such as MMP2, MMP3, MMP9, MMP13, MMP14, thrombin and plasmin) [Krstic and Santibanez, 2014; Jenkins, 2008], thrombospondin-1 (TSP-1) [Murphy-Ullrich and Poczatek, 2000], ionizing radiation and reactive oxygen species (ROS) [Jobling et al., 2006] and mechanical stimulation via integrins [Jones, 2012; Shi et al., 2011; Wipff and Hinz, 2008]. These activators release active TGFβ either by degrading the LAP and/or LTBPs, or by modifying the conformation of the latent complex or by mechanical pulling of the LAP by integrins [Horiguchi et al., 2012]. The active TGFβ homodimer binds to TGFβ receptors III, II, and I to initiate the intracellular signalling cascade of SMAD phosphorylation (Figure 4.3).

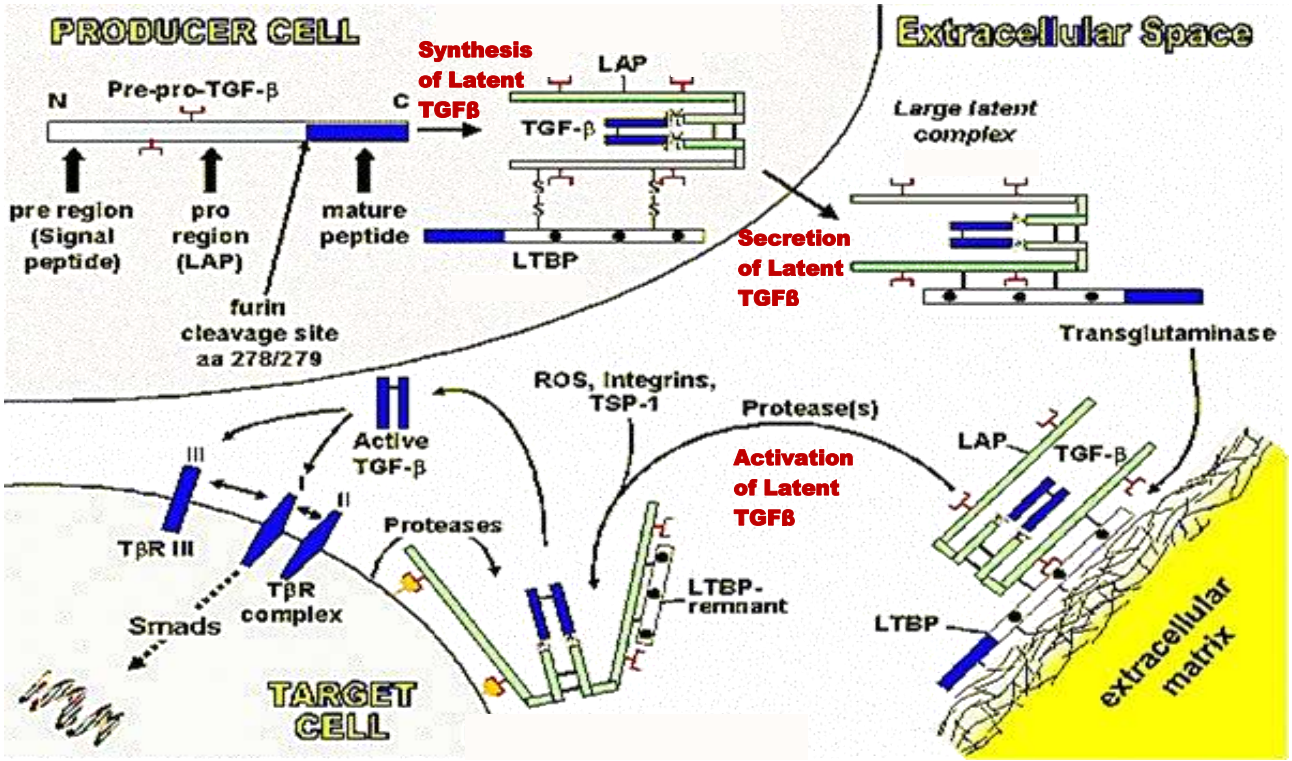

Figure 4.2: *Schematic presentation of intracellular TGFβ synthesis, secretion and activation. TGFβ precursor contains N-terminal pro-region (LAP), and a C-terminal region TGFβ protein. Both LAP and TGFβ exist as homodimers within the cell but remain non-covalently bonded forming the SLC. LLC containing a third component, LTBP, is linked to LAP by a single disulphide bond, is released into the ECM. The latent TGFβ can be activated by many factors to form free active TGFβ that binds to TGFβ receptors to initiate the intracellular signalling cascade of SMAD phosphorylation. [Adapted and modified from Gressner et al., 2007].*

TGFβ Signalling Pathway

TGFβ is crucial in regulating cell physiology during tissue development. It stimulates and/or inhibits cell proliferation, differentiation, motility, adhesion or death, depending on cell type [Javeland and Mauviel, 2004; Shi and Massagne, 2003]. TGFβ is active in all cell types, functioning to regulate ECM proteins like collagens and fibronectin, and prevent ECM degradation by inhibiting MMPs through the upregulation of TIMPs [Heinemeier et al., 2009; Javeland and Mauviel, 2004]. It is considered a potent anabolic factor in the deposition and repair of connective tissue. Fenwick et al. [2001] showed that chronically injured tendon increased expression of TGFβ.

TGFβ family ligands like bone morphogenetic proteins (BMPs), growth and differentiation factors (GDFs), anti-mullerian hormone (AMH), activins, nodal and TGFβ, signal by assembling to a heterodimer receptor complex [Weiss and Attisano, 2012]. The heterodimer receptor consist of a type I and type II receptor which are serine/threonine kinases, meaning they have a catalytic portion which adds a phosphate group to serine/threonine residues [Weiss and Attisano, 2012]. A third TGFβ receptor (TGFβRIII) enhances binding of active TGFβ to TGFβRII. When ligands bind to the receptors, activating the serine/threonine kinase of the type II receptor, they then add a phosphate group onto the serine/threonine domain of the type I receptor, propagating TGFβ signalling [Massague, 2012]. Consequently, R-SMAD protein (SMAD 2/3) is recruited. The SMAD 2/3 protein is phosphorylated by the serine/threonine kinase of the type I receptor. Receptor-phosphorylated SMAD 2/3 protein cleaves off the type I receptor to form a transcriptional complex with SMAD 4 that goes to the nucleus of the cell. The SMAD complex or transcription factor interacts with the DNA in the nucleus where transcription occurs.

TGFβ signalling can also activate other SMAD-independent signalling pathways including mammalian target of rapamycin (mTORC), phosphoinositol 3-kinase (PI3K), SH2 domain-containing transforming protein (SHC), extracellular signal-regulated kinase (ERK) and Rho/Rho associated protein kinase (ROCK), although the biochemical and structural bases for many of these links remain unknown [Massague, 2012].

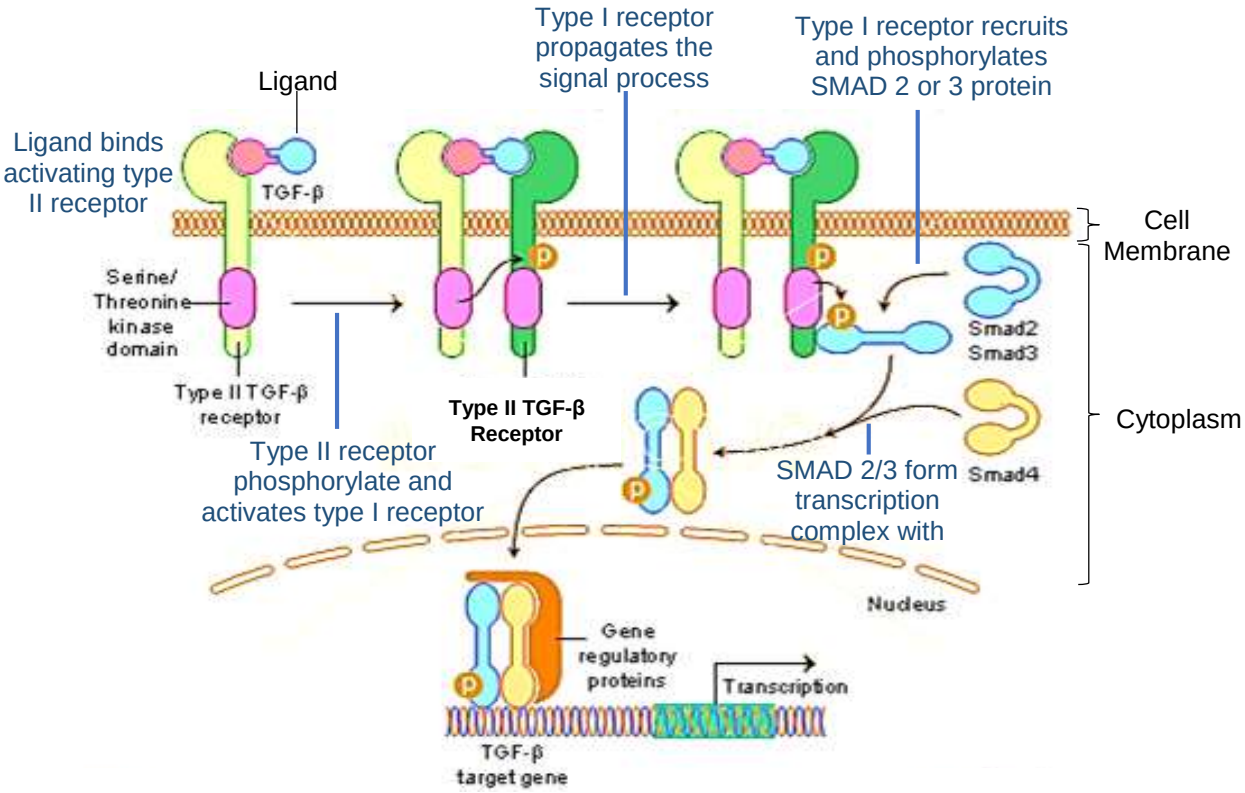

Figure 4.3: *Overview of TGFβ receptor signalling through SMAD-dependent pathway [Adapted and motified from Motifolio, 2016]*

IL-1 Signalling Pathway

The IL-1α or IL-1β ligand binds to the type 1 receptor (IL-1R1), initiating the signalling process with the help of a co-receptor (Figure 4.4), IL-1 receptor accessory protein (IL-1RAP), to form a trimeric complex [Ozbabacan et al., 2014]. The Toll-/IL-1R (TIR) domains of the IL-1R1 and IL-1RAP receptors interact together, recruiting cytoplasmic adaptor proteins like myeloid differentiation primary response gene 88 (MYD88), Toll-interacting protein (TOLLIP) and IL-1 receptor-associated kinase 4 (IRAK4) to form a stable complex [Ozbabacan et al., 2014]. The presence of MYD88 triggers the phosphorylation of IL-1 receptor-associated kinases 1/2/4 which in turn recruits and oligomerizes tumor necrosis factor receptor-associated factor 6 (TRAF6). TRAF6 and phosphorylated IRAK1/2 dissociate and migrate to the membrane to associate with TGFβ-activated kinase 1 (TAK1) and TAK1-binding proteins TAB1 and TAB2 [Ozbabacan et al., 2014]. The TAK1-TAB1-TAB2-TRAF6 complex migrates back to the cytoplasm, where TRAF6 is ubiquitinated and TAK1 is phosphorylated. From this point, the signal can propagate via two main paths: IKK – IkB – NF-kB and/or MKK – MAPK/JNK/ERK. In the first path, phosphorylated TAK1 activates the inhibitor of nuclear factor kappa-B kinase subunit beta

(IKKb). The activated IKKb phosphorylates the nuclear factor kappa-B inhibitor (IkB) which gets degraded so that nuclear factor kappa-B kinase (NFkB) (p65 and p50 subunits) are released and migrate to the nucleus to act as a transcription factor [Weber et al., 2010]. In the second path, phosphorylated TAK1 activates mitogen-activated kinases (MAPK) p38, c-Jun N-terminal kinases (JNK) (a subunit of AP-1) and extracellular signal-regulated kinases (ERK1/2) by interacting with MAP kinase kinase (MKK) proteins [Risbud and Shapiro, 2014]. Downstream in this path, are transcription factors such as c-Jun, c-Fos, c-Myc and ATF2 [Ozbabacan et al., 2014].

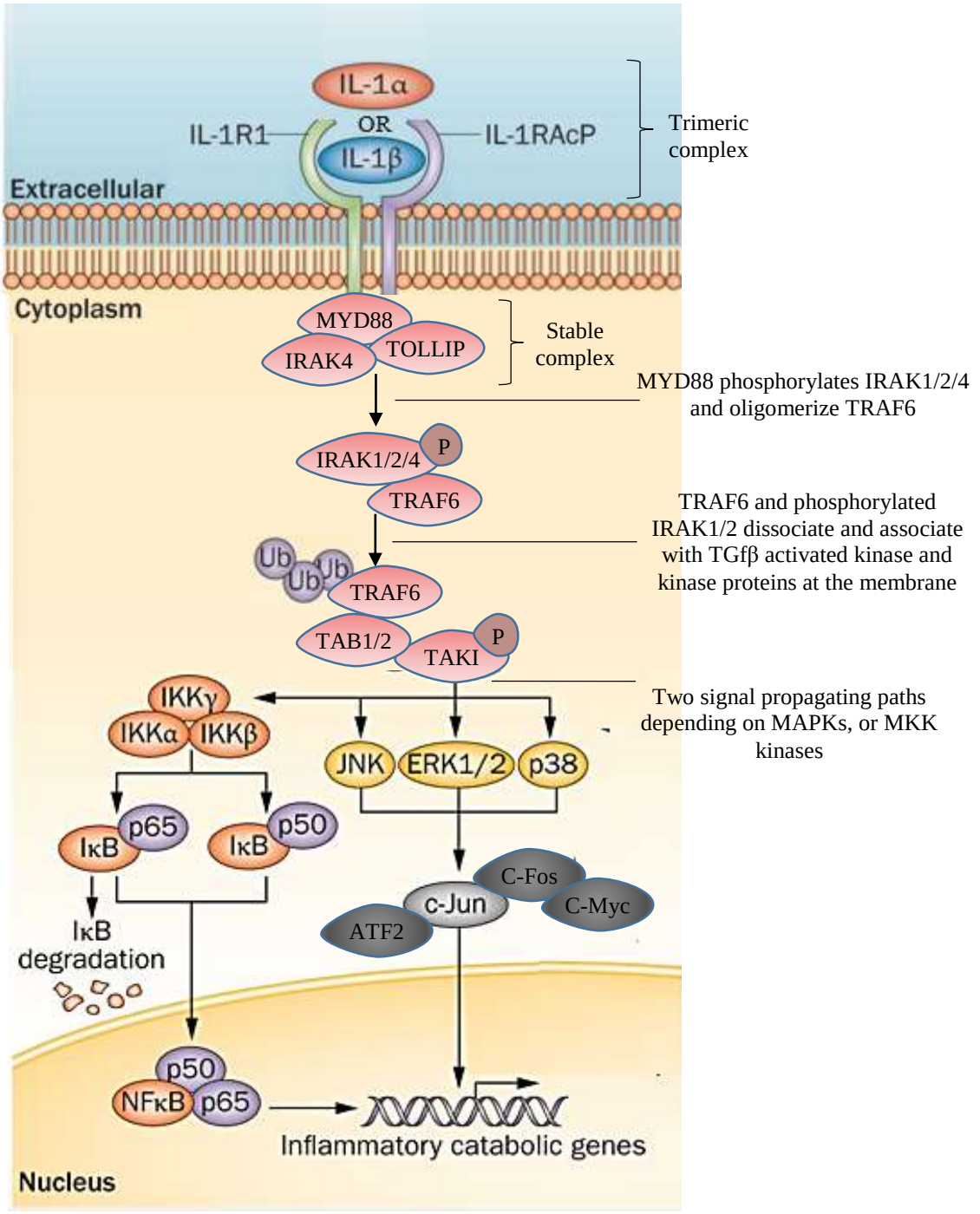

Figure 4.4: *Overview of IL-1 signalling pathway [Adapted and modified from Risbud and Shapiro, 2014; Ozbabacan et al., 2014]*

The aim of this current study is to further investigate the mechanosensitivity and mechanotransduction of tendon cells in 3D collagen gels, to determine the signalling pathways activated by load and the downstream matrix gene expression changes. The following specific hypotheses were investigated:

1. The increased metabolic activity seen in tenocytes subjected to high frequency (10Hz) loading relative to low frequency (1Hz) loading is a response to the difference in loading frequency and not the number of loading cycles.
2. The TGFβ signalling pathway is responsible for initiating an overall metabolic tenocyte response to both high and low frequency strain.
3. The IL-1 signalling pathway is responsible for initiating a catabolic and inflammatory tenocyte response to both high and low frequency strain.

4.2 METHODOLOGIES

In this Chapter, healthy human hamstring tenocytes were seeded into collagen gels and secured within custom-made chambers filled with loading media, with or without TGFβ or IL-1 inhibitor, depending on the experiment.

Table 4.1: Component of the different media used for incubating the 3D gel before and during loading

Component	Loading media (ml)	Loading media with inhibitor of TGFβR1 (ml)	Loading media with inhibitor of IL-1R (ml)
DMEM (with sodium pyruvate, phenol red, glutamaxTM and low glucose) (ThermoFisher Scientific, 21885-025)	500	500	500
Penicillin streptomycin (PS) (Sigma – Aldrich, P4333)	5	5	5
Inhibitor		1 in 1000	1 in 100

4.2.1 CYTOKINE ARRAY

In order to first investigate the cytokine response to loading, 8 collagen gels were prepared, secured within custom-made chambers and filled with standard loading media in preparation for loading as outlined in figure 4.5.

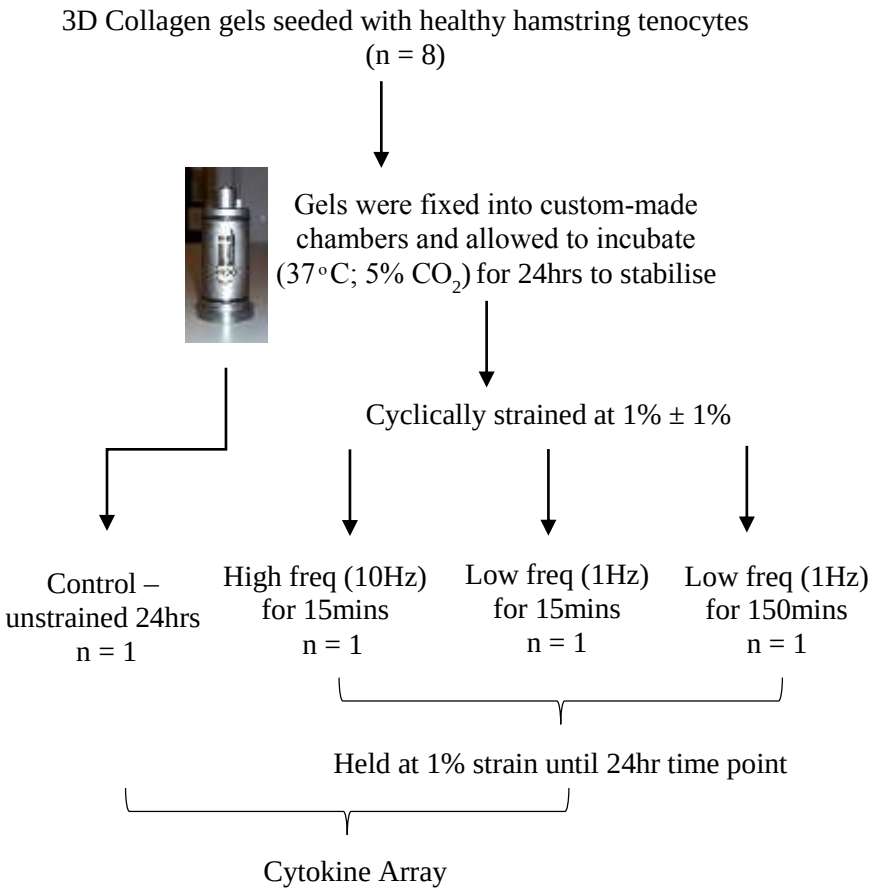

Figure 4.5: *Flow diagram depicting the experiments performed on 3D collagen gels to investigate the cytokine response to the applied loading conditions of interest*

Two gels were assigned to each loading condition, to examine the cytokine response, utilising a cytokine array following previously described protocols [Khalfaoui et al., 2016]. However, these were immediately combined post-loading to ensure sufficient protein for the array. Firstly, the protein concentration for each group was determined using semi-quantitative western blot analysis in order to normalise protein expression across samples for cytokine analysis. A bicinchoninic acid (BCA) assay kit was used to quantify the protein in each group by colorimetric detection and quantification of total protein. Assay standards were made using a stock solution of 2mg/ml of Albumin and lysis buffer. To get a broad range of concentrations necessary to plot a standard curve, serial dilutions were made as follows:

Table 4.2: Serial dilution of protein standards for BCA assay, 1:7 dilutions for standard curve used to calculate the protein concentration of a sample

Standard	Protein standard (µg/ml)	Volume of 2mg/ml Albumin (µl)	Volume of lysis buffer (µl)
Blank	0	0	100
S1	20	1	99
S2	100	5	95
S3	250	12.5	87.5
S4	500	25	75
S5	900	45	55
S6	1400	70	30
S7	2000	100	0

Following the manufacturer's instructions, the BCA working reagent that reacts with protein, was prepared at a ratio of 50:1 of BCA reagent A and BCA regent B respectively. 25µl of protein standards or samples were pipetted into the wells of a 96-well microplate in duplicate, and 200µl of BCA working reagent was added to each well and mixed thoroughly using a plate shaker for 30 seconds. Subsequently, the plate was incubated for 30 minutes at 37^{o}C. After 30 minutes, the plate was removed from the incubator and allowed to cool at room temperature. Protein concentration was measured using a plate reader at an absorbance of 562nm. In order to ensure a consistent protein concentration across all samples, samples were then diluted in order to match the lowest concentration.

For cytokine expression analysis, the cytokine human membrane antibody array ab133998 (Abcam, Cambridge, UK) was used, performed predominantly according to the manufacturer's instructions. Cytokine antibody array membranes were placed into 4 of the 8-well trays provided in the kit, and incubated for 30 minutes at room temperature with 2ml 1X blocking buffer also provided in the kit. The blocking buffer was aspirated, then 1ml of sample was pipetted into each well containing a membrane. Samples were incubated over night at 4^{o}C then washed thrice with 2ml wash buffer I, and twice with 2ml wash buffer II; both proprietary wash buffers provided in the kit. Cytokine detection was carried out by adding 1ml biotin-conjugated antibody to each well, and incubated for 1 hour, after which the antibody was pipetted out and the membranes

washed thrice with 2ml wash buffer I, and twice with 2ml wash buffer II. 2ml IRDye-labelled streptavidin solution was pipetted into each well and incubated for 45 minutes, after which the dye solution was removed and the membranes washed thrice with 2ml wash buffer I, and twice with 2ml wash buffer II. Membranes were scanned using an Odyssey imager with the following scanning parameters; resolution – 84µm, quality – medium, focus offset – 0.0mm, and intensity – 5. Evaluation was made by densitometry for a semi-quantitative comparison using image studio lite 5.0, which calculated signal intensity proportional to the amount of analyte bound. Samples signal were normalisation to the positive control, and the overall protein concentration of each loaded sample group was compared relative to the unstrained control. The method detects the following cytokines:

Table 4.3: Cytokines array (ab13398, Abcam, UK)

Cytokine Abbreviation	Full Name
ENA-78	Epithelial neutrophil-activating protein 78
GCSF	Granulocyte colony stimulating factor
GM-CSF	Granulocyte macrophage colony stimulating factor
GRO	Growth regulated oncogene
GRO-α	Growth regulated oncogene-alpha
I-309	Inflammatory cytokine
IL-1α	Interleukin-1 alpha
IL-1β	Interleukin-1 beta
IL-2	Interleukin-2
IL-3	Interleukin-3
IL-4	Interleukin-4
IL-5	Interleukin-5
IL-6	Interleukin-6
IL-7	Interleukin-7
IL-8	Interleukin-8
IL-10	Interleukin-10
IL-12	Interleukin-12
IL-13	Interleukin-13
IL-15	Interleukin-15
IFN-y	Interferon-gamma
MCP-1	Monocyte chemoattractant protein-1
MCP-2	Monocyte chemoattractant protein-2
MCP-3	Monocyte chemoattractant protein-3
MCSF	Macrophage colony-stimulating factor
MDC	Macrophage -derived chemokine
MIG	Monokine induce by interferon
MIP-1b	Macrophage inflammatory protein-1 beta
MIP-1δ	Macrophage inflammatory protein- 1 gamma
RANTES	Regulated on Activation, Normal T Cell Expressed and Secreted)

SCF	Stem cell factor
SCDF-1	Stromal cell-derived factor 1
TARC	Thymus and activation-regulated chemokine
TGF-β1	Transforming growth factor-beta 1
TNF-α	Tumour necrosis factor alpha
TNF-β	Tumour necrosis factor beta
EGF	Epidermal growth factor
IGF-1	Insulin-like growth factor
Angiogein	
Oncostatin M	
Thrombopoietin	
VEGF	Vascular endothelial growth factor
PDGF-BB	Platelet-derived growth factor
Leptin	
BDNF	Brain-derived neutrophic factor
BLC	B-Lymphocyte chemoattractant
Ck β 8-1	Chemokine-beta 8-1 / Chemokine (C-C motif) ligand 23
Eotaxin-1	Chemokine (C-C motif) ligand 11
Eotaxin-2	Chemokine (C-C motif) ligand 24
Eotaxin-3	Chemokine (C-C motif) ligand 26
FGF-4	Fibroblast growth factor – 4
FGF-6	Fibroblast growth factor – 6
FGF-7	Fibroblast growth factor – 7
FGF-9	Fibroblast growth factor – 9
Flt-3 Ligand	Flt-3 Ligand
Fractalkine	Fractalkine / Chemokine 3 (C-X-C motif) ligand 1
GCP-2	Granulocyte chemoattractant protein-2 / Chemokine (C-X-C motif) ligand 6
GDNF	Glial cell-line derived neurotrophic factor
HGF	Hepatocyte growth factor
IGFBP-1	Insulin-like growth factor binding protein - 1
IGFBP-2	Insulin-like growth factor binding protein - 2
IGFBP-3	Insulin-like growth factor binding protein - 3
IGFBP-4	Insulin-like growth factor binding protein - 4
IL-16	Interleukin-16
IP-10	Interferon gamma-induced protein 10 / Chemokine (C-X-C motif) ligand 10
LIF	Leukaemia inhibitory factor
LIGHT	LIGHT / tumour necrosis factor superfamily member 14 (TNFSF14)
MCP-4	Monocyte chemoattractant protein - 4
MIF	Macrophage migration inhibitory factor
MIP-3α	Macrophage Inflammatory Protein-3 / Chemokine (C-C motif) ligand 20
NAP-2	Neutrophil-activating protein-2
NT-3	Neurotrophin-3
NT-4	Neurotrophin-4
Osteopontin	Osteopontin
Osteoprotegerin	Osteoprotegerin (OPG)
PARC	Pulmonary and Activation-Regulated Cytokine

PIGF	Placenta growth factor
TGF-β2	Transforming growth factor-beta 2
TGF-β3	Transforming growth factor-beta 3
TIMP-1	Tissue inhibitor of metalloproteinases - 1
TIMP-2	Tissue inhibitor of metalloproteinases - 2

4.2.2 GENE EXPRESSION ANALYSIS

The effects of number of loading cycles and also possible signalling pathways initiated by the loading conditions were investigated. In preparation for testing, 30 type I collagen gels were made and secured within custom-made chambers in preparation for loading. In order to investigate the TGFβ and IL-1 pathway involvement in the strain response, inhibitors of these cytokines were included within the media of some samples, as outlined in Figure 4.6, before samples were subjected to different loading conditions.

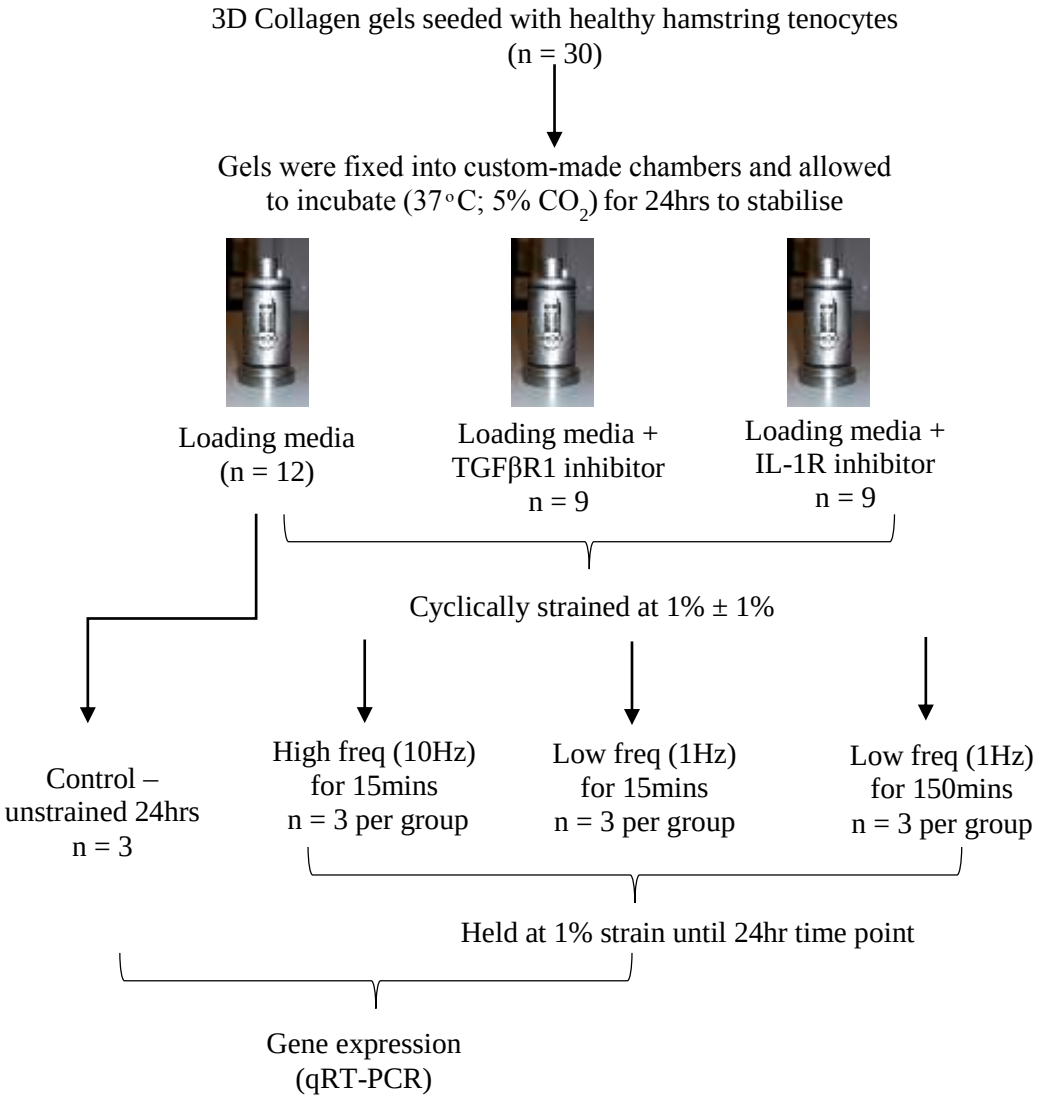

Figure 4.6: *Flow diagram depicting the experiments performed on 3D collagen gels to investigate the gene expression changes to the applied loading conditions with and without the addition of an inhibitor*

Selected genes were analysed in samples, subjected to the different load conditions and inhibitors, with selection based on previous results and literature [Jones et al., 2013; Tsuzaki et al., 2003b] (table 4.4).

Table 4.4: Genes analysed for the different sample groups

Target Gene	Samples with loading media	Samples with loading media + TGF β Inhibitor	Samples with loading media + IL-1 Inhibitor
HUMAN			
18s	√	√	√
MMP1	√		√
MMP13	√		√
COL1A1	√	√	√
COL3A1	√	√	
COL5A1	√	√	
ADAMTS5	√		
IL6	√	√	√
IL8	√		

4.2.3 STATISTICAL ANALYSIS

Statistical analysis was performed using a one way analysis of variance (one way ANOVA) looking for significant differences in the response of healthy cell types to different loading conditions and to the effects of the inhibitors. Tukey's Honest Significant Difference (HSD) pot-hoc tests were adopted where significant differences were identified, with P values < 0.05 were considered significant.

4.3 RESULTS

4.3.1 CYTOKINE ARRAY

For each sample, data were displayed as western spots blots (Figure 4.7) which were subjected to digital densitometry to determine the differences in cytokine expression in each sample relative to the unstrained control. Positive controls are labelled by blue frames, while negative controls are labelled by red frames (Figure 4.7).

Signal intensity for each cytokine under each loading condition was plotted relative to the control in log base 10, so as to respond to skewness towards large values (where a few points are much larger than the bulk of the data), making it easier to identify the changes between groups (Figure 4.8). However, a few of the cytokine patterns, where the control sample had no signal, were set to 1, in order to directly compare each cytokine.

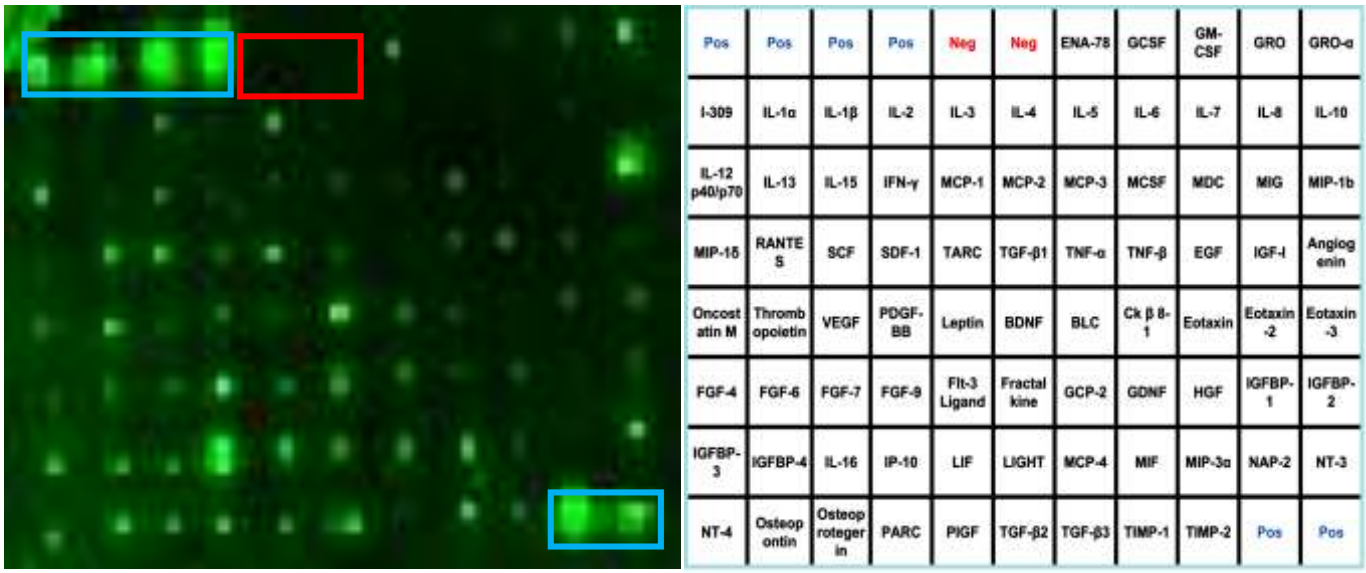

Figure 4.7: *Typical overview of the cytokine panel and the locations of the 80 cytokines including the internal assays controls and representative spot blots for the control group. Blue letters and boxes indicate the positive controls, red letters and boxes indicate the negative controls.*

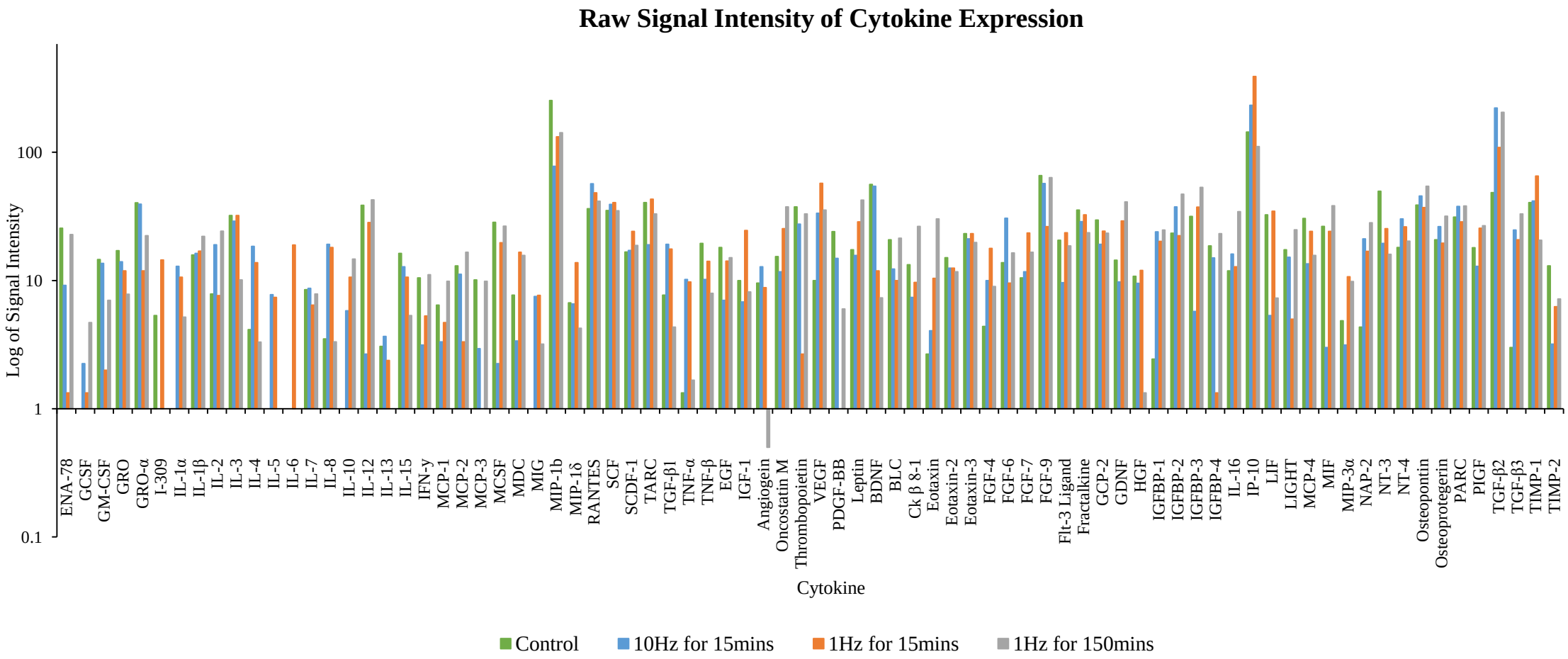

Figure 4.8: *Raw data of a semi-quantitative analysis of cytokine expression patterns across the different loading groups, expressed in* log_{10}.

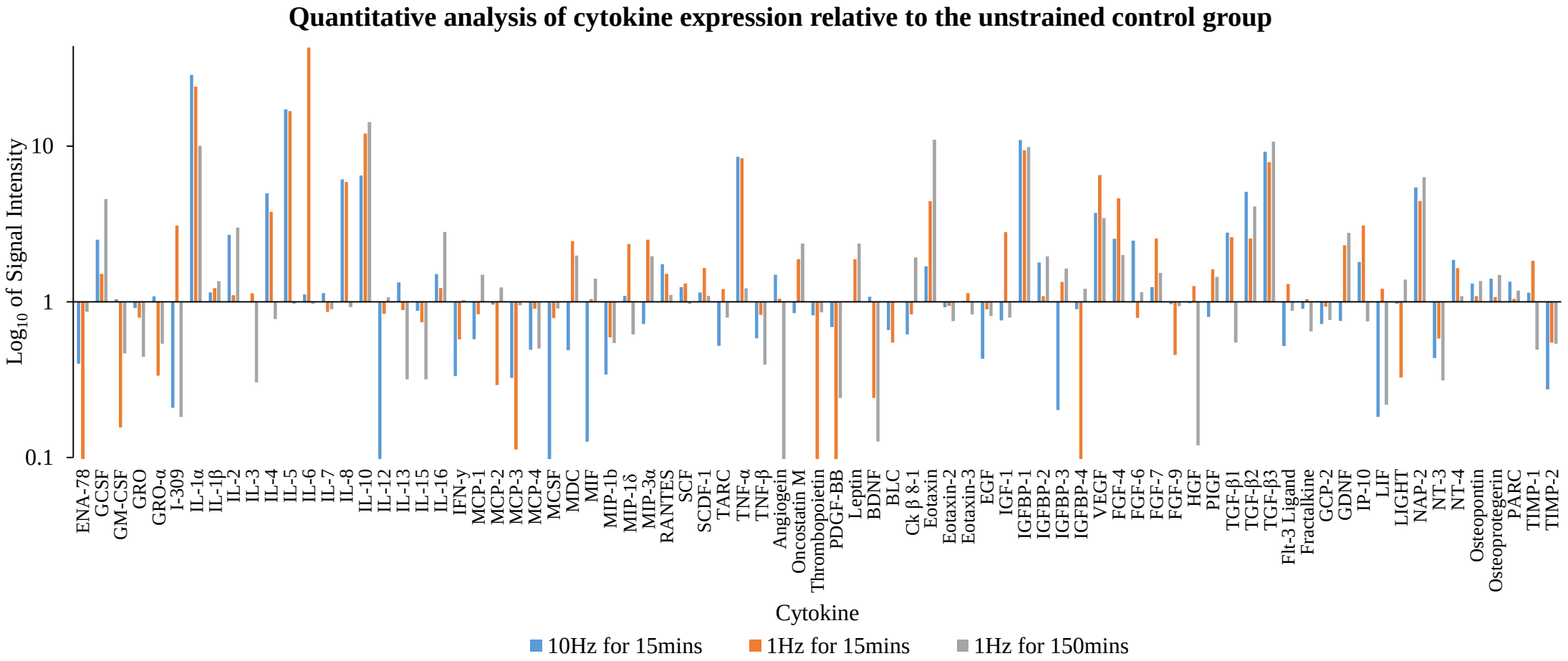

Figure 4.9: *Semi-quantitative analysis of cytokine expression patterns across the different loading groups, expressed in log_{10} relative to unstrained controls. Normalisation was performed against the assay internal controls and compared to the total protein content relative to the unstrained control.*

The cytokine array reflects pathway activity patterns with the upregulation of the different cytokines with loading (Figure 4.8 and 4.9). Some cytokines were upregulated exclusively in the presence of mechanical loading, and not present in unloaded controls, this include IL-1α, IL-5, IL-6, IL-10 and MIG.

Of the listed cytokines, some showed a similar response comparing 10Hz loading for 15mins and 1Hz loading for 150mins, including, GCSF, IL-2, IL-16, MCP-2, IGF-1, IGFBP-2, TGFβ2, TGFβ3 and NAP-2. However, the expression of some cytokines seem to be triggered specifically by high frequency (10Hz) loading, for example GCSF, IL-2, IL-4, IL-16, MCP-2, Angiogein, IGFBP-2, FGF-6, TGFβ2, TGFβ3 and NAP-2. There were also a few genes that were more expressed with increased number of cycles at low frequency (1Hz) loading, relative to both other conditions, for example IL-10, MIF, Eotaxin, Oncostatin M, and Leptin, and some that were more expressed specifically with 1Hz loading at 15mins, including I-309, IL-6, MDC, MIP-1δ, MIP-3α, and TIMP1.

Overall, data indicates that 10Hz loading differentially alters gene expression relative to either 1Hz loading group. However, this was investigated further by additional experimental repeats, using standard RT-PCR, to compare the effects of loading cycles and loading frequency on some of those genes seen in Chapter 3 to respond differentially to 10Hz.

Furthermore, to investigate the possible involvement of the IL-1 and TGFβ signalling pathways in the tenocyte response, inhibitors were introduced to the loading media to determine their effect on cell response to loading. Of the interleukins, IL-1α was most highly expressed with the different loading conditions. For the growth factors, of the IGFBPs, IGFBP-1 was most responsive to the loading conditions irrespective of the frequency or loading cycles applied; of the FGFs, FGF-4 was most responsive to the loading conditions; EGF, HGF and PIGF were not very responsive to the loads; of the TGFβ, all the three isoforms, TGFβ1, TGFβ2 and TGFβ3, were all responsive to the different loading conditions. In addition, the data from Chapter 3 (Figure 3.5) gene expression profiling of healthy hamstring tendon cells also showed an increase in genes related to IL-1 and TGFβ signalling. Therefore, IL-1 and TGFβ were selected for the signalling pathway analysis.

4.3.2 GENE EXPRESSION

Hypothesis 1: Effect of number of loading cycles on cell response

Selected genes were analysed to provide a thorough investigation into the effect of loading on cell response looking at different number of cycles of loading relative to loading frequencies.

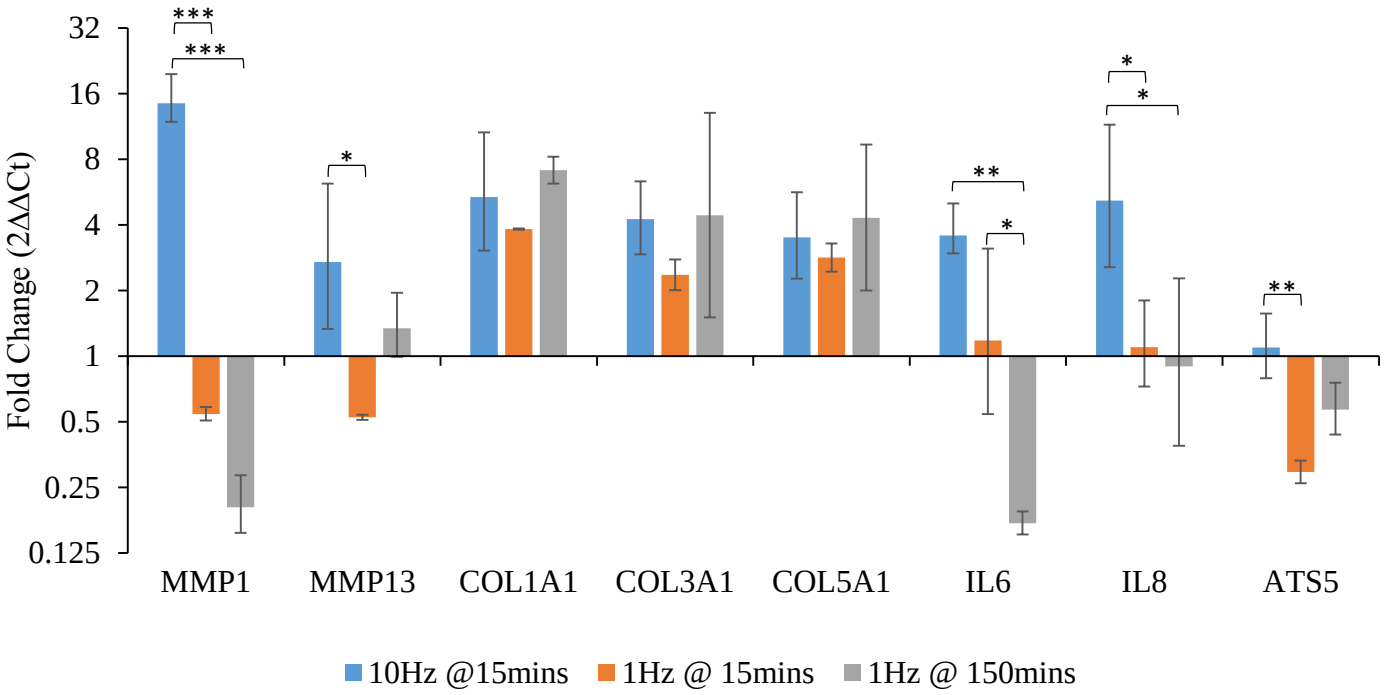

Figure 4.10: *Gene expression changes in healthy human hamstring tenocytes seeded in 3D collagen gels subjected to a cyclic load of 1% ± 1% for 15mins then held at 1% strain until the 24hr time point. The response to 10Hz and 1Hz loading is compared with number of cycles of loading. Matrix genes were measured using standard qRT-PCR. Data was normalised to 18s and presented as a fold change relative to unloaded controls ($2^{\Delta\Delta Ct}$) ⌈mean ± SD]. * means p < 0.05, ** means p < 0.01, *** means p < 0.001.*

The data showed no significant difference between 10Hz and 1Hz loading for collagen genes (COL1A1, COL3A1, COL5A1) and also demonstrated no significant or notable difference with number of cycles. However, considering the genes that were significantly different between 10Hz and 1Hz loading in Chapter 3 (MMP1, IL6, and IL8), these genes also showed significant differences between 10Hz loading for 15mins and 1Hz loading for 150mins.

Hypothesis 2 and 3: TGFβ and IL-1 signalling pathway involvement

A few genes were selected to investigate the response to loading with and without TGFβ or IL-1 cytokine inhibitors, to determine their likely involvement in tenocyte response to the applied loading conditions.

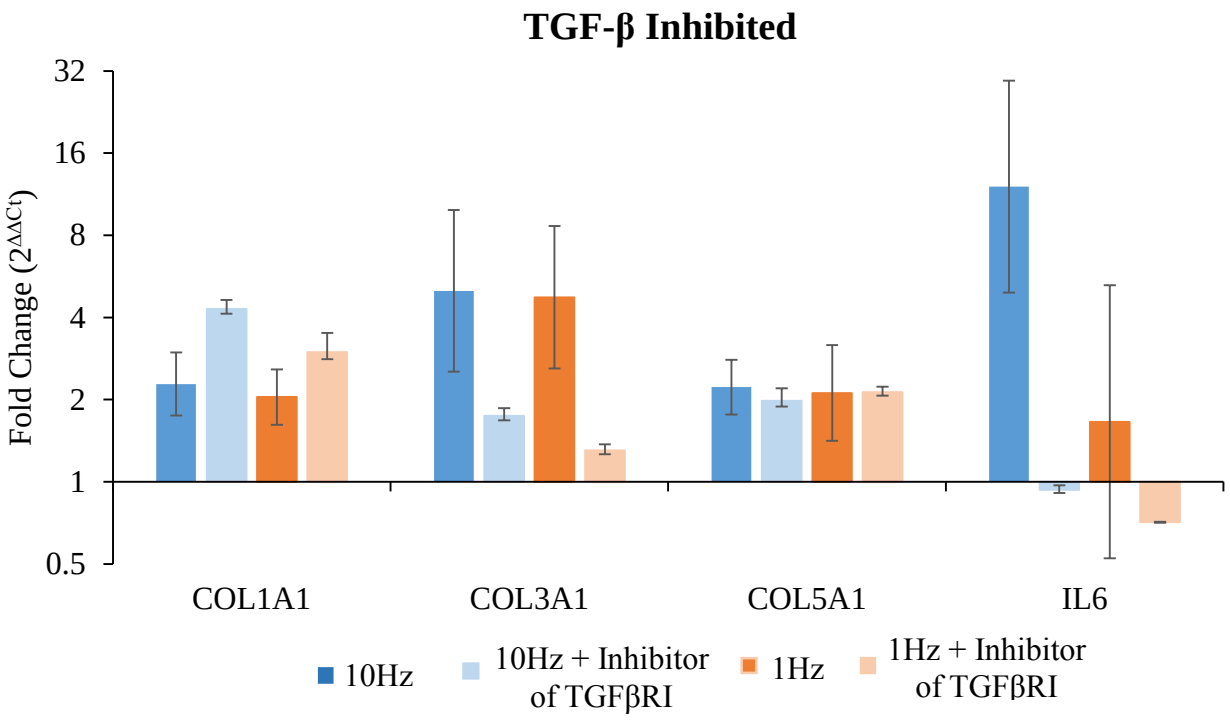

Figure 4.11: *Gene expression changes in healthy human hamstring tenocytes seeded in 3D collagen gels subjected to a cyclic load of 1% ± 1% for 15mins then held at 1% strain until the 24hr time point. The response to 10Hz and 1Hz loading is compared with and without the addition of an inhibitor of TGFβRI. Matrix genes were measured using standard qRT-PCR. Data was normalised to 18s and presented as a fold change relative to unloaded controls ($2^{\Delta\Delta Ct}$) [mean ± SD].*

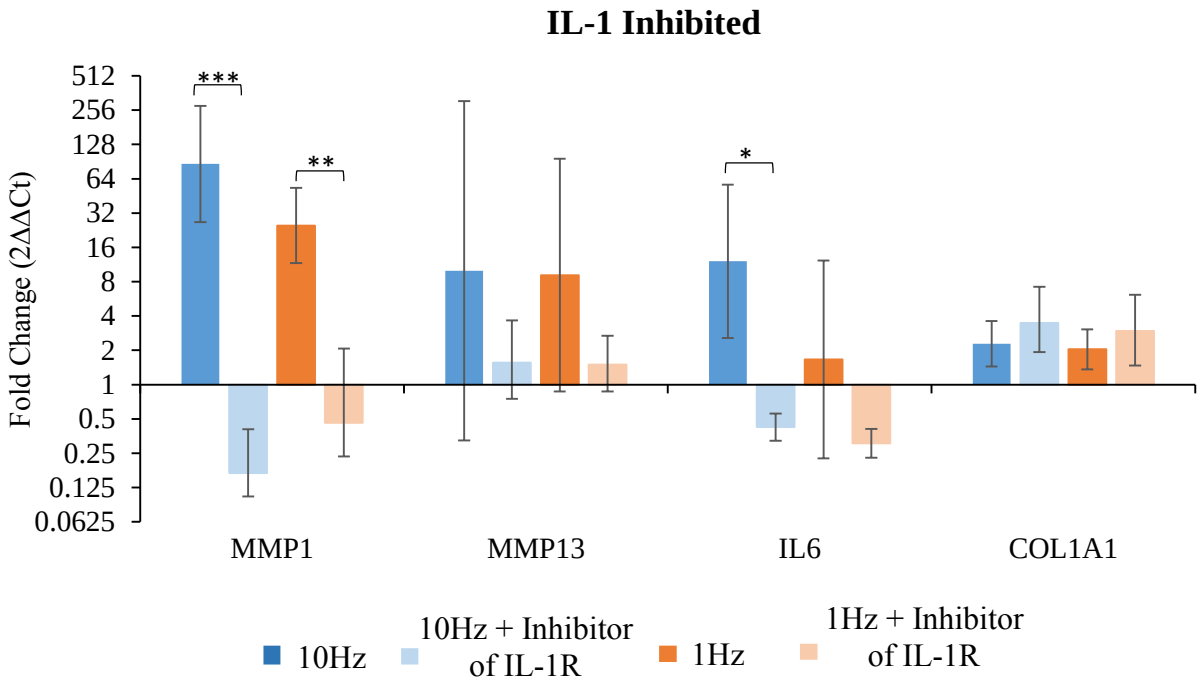

Figure 4.12: *Gene expression changes in healthy human hamstring tenocytes seeded in 3D collagen gels subjected to a cyclic load of 1% ± 1% for 15mins then held at 1% until the 24hr time point. The response to 10Hz and 1Hz loading is compared with and without the addition of an inhibitor of IL-1R. Matrix genes were measured using standard qRT-PCR. Data was normalised to 18s and presented as a fold change relative to unloaded controls ($2^{\Delta\Delta Ct}$) [mean ± SD]. * means p < 0.05, ** means p < 0.01, *** means p < 0.001.*

The addition of the TGFβR1 inhibitor made no significant difference to the load induced upregulation of collagen genes, COL1A1, COL3A1 and COL5A1. However, a notable reduction in IL-6 expression, with a p value of 0.0513 seen in TGFβR1 inhibited samples at 10Hz frequency.

Inhibiting IL-1 resulted in a pronounced downregulation of the load induced MMP expression, (MMP1 and MMP13) in addition to a reduction in IL-6 expression. Differences were significant for MMP1 in both loading conditions (p = 0.001 for 10Hz loading and p = 0.016 for 1Hz loading) and IL-6 (p = 0.049) with high frequency (10Hz) loading.

With the addition of the inhibitor, the expression of some genes fell below the control demonstrating a reduction in gene expression relative to the unloaded control.

4.4 DISCUSSION

Based on the findings in Chapter 3, which demonstrated that high frequency (10Hz) loading initiated a greater metabolic response in tenocytes seeded in 3D collagen gels than low frequency (1Hz) loading, it was necessary to investigate further, to determine whether the response observed with 10Hz loading was as a result of the frequency of loading or the fact that loading at 10Hz applied 10 times the number of cycles to the cells compared to 1Hz loading. Figure 4.10 explores the effect of number of cycles of loading relative to frequency of loading, showing that 10Hz loading of tenocytes resulted in greater expression of metabolic genes irrespective of the number of loading cycles. This was also the case with the cytokine data in Figure 4.9, which demonstrated that although some cytokine expression levels were similar for 10Hz loading for 15mins and 1Hz loading for 150mins, in general 10Hz loading for 15mins resulted in greater expression of interleukins, growth factors and angiogein expressed compared to 1Hz loading for 150mins. Overall, a greater metabolic response appear to preferentially take place at higher frequency (10Hz) loading, in parallel with an enhanced inflammatory effect. This may reflect the wound healing environment *in vivo* whereby early events of tenocyte proliferation and matrix deposition take place in a mechanically unstable environment prior to tendon healing [Yu et al., 2015]. Other studies have also demonstrated that higher frequency loading (4Hz compared to 1Hz and 0.2Hz compared to 0.02Hz) relative to number of cycles of loading maintained tendon tissue biomechanical properties [Yamamoto et al., 2005] and accelerated tendon healing response [Takai et al., 1991] respectively. Therefore, these studies are supportive of the current data that higher frequency loading induces a metabolic response in tenocytes that may play a role in improving matrix turnover.

This Chapter, additionally adopted a cytokine array, to investigate the effects of 10Hz and 1Hz loading conditions on a wide range of cytokines and matrix proteins. The data in Figure 4.8 and 4.9 demonstrated that cytokine expression was upregulated in response to load. The data presented endogenous expression of cytokine molecules such as GCSF, IL-1α, IL-2, IL-4, IL-5, IL-6, IL-8, IL-10, IL-16, MCP-2, TNF-α, VEGF, Eotaxin, FGF-4, IGFBP-1, NAP-2, TGFβ1, TGFβ2, and TGFβ3 *in vitro*, in tenocytes seeded in 3D collagen gels in response to the applied load. It was observed that different cytokines responded differently to different loading conditions. However, overall, it was also notable that high frequency (10Hz) loading for 15mins upregulated expression of substantially more cytokines than seen in response to low frequency (1Hz) loading for either 15mins or 150mins, perhaps indicating both a more

inflammatory response and a greater upregulation of growth factors responsible for stimulating angiogenesis, cell migration, proliferation and tissue remodelling [Molloy et al., 2003]. Whether these cytokines play a role in the early proliferative phase of tendon healing with the applied loading conditions in this study is presently unknown. However, in human tendon repair, the local signalling events surrounding inflammation and early proliferative activity remain poorly defined [Ackermann et al., 2013].

Figure 4.8 showed that of the growth factors explored, four were highly expressed with loading (TGFβ, VEGF, FGF and IGFBP). Numerous *in vitro* studies have indicated that growth factors like TGFβ, VEGF and FGF are associated with tendon remodelling and increase with loading, however they have also been correlated with tendinopathy [Andarawis-Puri et al., 2015]. Growth factors have previously been reported to influence expression of TIMP3, collagens [Zhang et al., 2013], and of the growth factors, TGFβ is likely the most important factor in tendon pathology, since it plays a major role in tissue repair [Fenwick et al., 2001]. TGFβ expression in human Achilles cells was upregulated in response to increased mechanical loading or loading frequency with increases of 7%, 49% and 14% seen in TGFβ1, TGFβ2, and TGFβ3 respectively [Zhang et al., 2013]. Another study also demonstrated strain dependency in the TGFβ response to loading, showing that high strains of 10% – 12% at 0.1 Hz for 24 h stimulated TGFβ upregulation which in turn promote collagen synthesis for tissue healing [Yu et al., 2015]. These studies have hypothesised that mechanical strain may regulate TGFβ signalling and promote differentiation responses to TGFβ via a mechanotransduction pathway. However, Jones et al. [2013] investigated the relationship between load and TGFβ in greater detail, observing no increase in TGFβ expression with load, but more specifically significant upregulation in TGFβ activity after 48hrs loading. A number of TGFβ mediated cell and molecular changes have been documented in tendinopathy and TGFβ has also been shown to promote collagen synthesis important during the early stages of tissue repair [Gumucio et al., 2015; Corps et al., 2004; Fenwick et al., 2001]. A study by Fenwick et al. [2001] demonstrated that TGFβ isoforms have differential roles in tissue healing. The study evaluated the expression of the different TGFβ isoforms in healthy and pathological Achilles tissues and found a high expression of TGFβ2 and TGFβRII in pathological tissues with the absent of TGFβI. However, TGFβ requires both type I and type II receptors to propagate its signal as discussed in the introduction [Massague, 2012]. Therefore, this study concluded that chronic tendon lesions fail to resolve due to the absent of TGFβI and suggests that the addition of exogenous TGF-β would have little effect on chronic tendinopathy [Fenwick et al., 2001].

To determine the effect of TGFβ in this current study, a TGFβRI inhibitor was used. The inhibition of the TGFβ signalling pathway not only abrogated the strain-induced changes in mRNA for IL-6 but led to levels below the basal level, indicating the presence of TGFβ signalling in non-strained cultures. This may be due to the tensional forces present across the tenocyte seeded collagen gel in the absence of cyclic loading. By contrast, the collagen mRNA levels were unchanged with the addition of TGFβRI inhibitor. This demonstrated that TGFβ may not be involved in collagen expression in this study. However, this result may simply be due to the period of applied strain or time point for investigating cell response. A study by Zhang et al. [2004] demonstrated that inhibiting TGFβ by the addition of a neutralizer in rabbit cells cultured for three days, reduced the expression levels of collagen I. Further, a recent study by Jones et al. [2013] demonstrated that TGFβ abrogated the strain response of COL1A1 after 48hrs of strain application on isolated human Achilles cells. The contradiction between the current experimental data and the literature may be attributed to difference in *in vitro* experimental conditions and models.

Figure 4.8 and 4.9 also demonstrated an upregulation of a number of interleukins and TNF-α. From the literature, it is known that TNF-α induces production of IL-1β, IL-6, IL-8, and IL-10 [John et al., 2010]. In the current data set, IL-1α is the most expressed of all the interleukins in all loading conditions, as seen in Figure 4.9 with response to loading. IL-1 is a pro-inflammatory cytokine that can cause matrix destruction and loss of tendon biomechanical properties by inducing inflammatory mediators such as cytosolic phospholipase A2 (cPLA2), cyclooxygenase-2 (COX-2) and prostaglandin E2 (PGE2) [Zhang et al., 2015]. There have been reports of a synergistic effect of mechanical load and IL-l [Yu et al., 2015; Tsuzaki et al., 2003b], which supports current data that inflammatory mediators like IL-1 were upregulated with loading. IL-1 is thought to contribute to the positive metabolic activity necessary for tissue repair by stimulating increased expression of matrix metalloproteinases (MMPs) such as MMP1, MMP3 and MMP13 in tenocytes [Zhang et al., 2015; Tsuzaki, et al., 2003a]. Furthermore, IL-1 may induce secondary interleukins like IL-6. Therefore, IL-1 was evaluated in this study to determine if it is a contributing factor to the upregulation of MMPs and interleukins observed in healthy hamstring tenocytes with loading. IL-1Ra regulates both IL-1α and IL-1β pro-inflammatory activity by competing with them for binding sites of the receptor. Therefore, IL-1Ra was used to inhibit IL-1 signalling and its subsequent gene changes.

Inhibiting IL-1, demonstrated its relationship with MMP1, MMP13 and IL-6, abrogating the expression of the genes in response to loading. Although, the enzyme activity itself was not evaluated, this study provides initial evidence of possible catabolic behaviour in tendon cells in response to loading through IL-1. It also confirms the literature that IL-1 stimulates MMPs and IL-6 [Sun et al., 2008; Nagase and Woessner, 1999]. In summary, this study has shown that tenocytes respond to loading, particularly high frequency (10Hz) loading, by regulating inflammatory and matrix turnover related genes, suggesting that the IL-1 signalling pathway is at least in part involved in the beneficial adaptations to eccentric loading.

CHAPTER FIVE

GENERAL DISCUSSION, CONCLUSIONS AND FUTURE WORK

5.1 GENERAL DISCUSSION

Tendons are subjected to high mechanical loads during daily activities, and must undergo continuous repair to maintain their functional properties. When subjected to mechanical stimuli, tendons are known to undergo endogenous changes in cell morphology, tissue remodelling, and mechanical properties, with effects shown in animal models and in humans [Wang, 2006]. Mechanical stimuli are necessary for appropriate tendon development and maintenance, modulating the extracellular environment through the formation and degradation of matrix proteins [Popov et al., 2015; Galloway et al., 2013].

Given the importance of mechanical stimulation to maintain tendon functional properties, investigators have shown that exposure to either excess loading, or load deprivation can result in tendinopathy [Wang et al., 2006]. Over the years, eccentric exercise has stood out as one of the most effective treatment option for tendinopathy [Rees et al., 2008; Alfredson and Cook, 2007]. However, despite evidence supporting the efficacy of eccentric exercise for its treatment, the mechanism through which this is achieved remains unknown [Chaudhry et al., 2015; Rompe et al 2007]. Chaudhry [2012] showed that perturbation occurred within the Achilles tendon at 8-12Hz during eccentric loading, leading to a hypothesis that these perturbations may provide a repair stimulus for tendon. Indeed, one of the other treatments shown to be effective for treating tendinopathy is ESWT, in which shockwave are administered at around at 8Hz. ESWT leads to an immediate inflammatory and catabolic response in the tendon [Waugh et al., 2015; Mani-Babu et al., 2014], suggesting that mechanical stimuli in the region of 8-12Hz might aid tendon remodelling by promoting degradative processes that are associated with removing damaged matrix constituents.

This study aimed at investigating the underlying effects of high frequency (10Hz) loading on tendon cells (chapter 3) as well as two possible mechanotransduction pathways involved in the tenocyte response (chapter 4). These data may provide further indication if the 10Hz vibration seen in tendon during eccentric loading is an important driver of tendon repair.

5.1.1 LOAD FREQUENCIES

The current study hypothesised that high frequency (10Hz) loading might facilitate repair in tendinopathic tissue. A loading frequency of 10Hz was explored as the typical frequency seen across the range of eccentric exercise or ESWT studies which have measured this parameter

[Chaudhry et al., 2015; Waugh et al., 2015; O'Neil et al., 2015; Galloway et al., 2013; Lorenz and Reiman, 2011; Alfredson and Cook, 2007]. The current study investigated both rat explant tissue (Figures 2.15 and 2.16) and isolated cells seeded in a 3D collagen gels (Figures 3.5 and 3.6), showing that gene expression levels were higher in response to 10Hz loading than they were in response to low frequency (1Hz) loading. This relationship was consistent across all experimental work, and was also seen in Figure 3.4A and B where the response of a broad spectrum of genes was investigated over time using a TLDA analysis and additionally in chapter 4, where 80 cytokines were explored, showing that substantially more genes were further upregulated with 10Hz loading relative to the 1Hz loading condition.

Whilst the response to loading was consistently more pronounced, it was interesting to note that there was downregulation of most genes with load in the explant models contrary to the isolated cells seeded in 3D collagen gels. The underlying reason for such an outcome remains unknown requiring further investigation. However, this may be a result of the load magnitude, as only small deformations were applied, and previous studies have indicated that low loaded explants may perceive stress deprivation conditions [Thornton et al., 2008], which can lead to a catabolic cell response and even tendinopathy.

By contrast, the data from the cells seeded in 3D collagen gels points in the direction of Waugh et al. [2015] findings, in which the cell response to ESWT was examined *in vivo*. Both studies demonstrated inflammatory and catabolic cell responses, which are generally associated with removing damaged matrix constituents. The isolated cell study highlighted significant upregulation of MMPs and interleukins with 10Hz loading relative to 1Hz loading. Markers of anabolism were not investigated in the ESWT study. However, the current data additionally suggested a possible anabolic process for the synthesis of new ECM with the upregulation of COL3A1. The symmetry between the *in vivo* ESWT and *in vitro* collagen gel study gives confidence that this model offer some benefit for probing cell mechanobiology in this simplified manner.

Previous studies on bone have shown high frequency loading regimes (between 10–50 Hz) to be effective in promoting bone anabolic effects [Wehrle et al., 2015; Ozcivici et al., 2010; Torcasio et al., 2008; Rubinacci et al., 2008]. By contrast, very few studies have investigated the effects of loading frequency in tendon.

Explant studies on rat tendon fascicles investigated the effect of varying frequency (0.017, 0.17 or 1Hz) on tendon cell response. The study demonstrated that cyclically straining tendon can maintain the tissue homeostasis depending on the applied frequency [Lavagnino et al., 2003]. Low amplitude (1%) cyclic strain at 0.017 Hz was found to significantly inhibit, but not completely eliminate MMP1 expression but increasing the frequency to 0.17Hz or 1Hz completely eliminated MMP1 expression [Lavagnino et al., 2003]. The mechanical properties of tendon fascicles were also maintained with higher frequency loading, of 4Hz relative to 1Hz, when rabbit patellar tendon fascicles were cyclically stressed to 2MPa for 1hr or 24hrs at 1Hz or 4Hz [Yamamoto et al [2005]. These studies highlight that not only the amplitude, but also the frequency of strain is also important in instigating a healing response in tendon cells. However, the exact mechanism for this improvement (i.e. inhibition of catabolism or stimulation of anabolism) was not determined. Two studies have investigated tendon response to higher frequency loading. However, these studies investigated response at a single frequency, so can only be considered in isolation. Nevertheless, cyclic loading of 0.06 ± 0.01N at 20Hz over a five day period (1hr a day), increased the mechanical properties and elastic moduli of rat fascicles after a 2 day rest [Adekanmbi et al., 2013]. A similar effect was observed when 30Hz sinusoidal vibrations were applied to intact flexor carpi ulnaris tendons in rats using a whole-body vibration table and electromagnetic shaker [Sandhu et al., 2011]. In this study, the authors reported increased tendon cross-section area and stiffness after vibration simulation for 20 mins per day for 5 days a week for 5 weeks. These findings suggest that the increased metabolic activity seen with higher frequency loading may be beneficial for increased matrix turnover, to improve the mechanical properties of tendinopathic tendons.

Considering isolated cell studies, Xu et al. (2015) seeded tendon derived stem cells (TDSCs) from rat Achilles tendons on poly(L-lactide-co-ε-caprolactone)/collagen (P(LLA-CL)/collagen) scaffolds (1×10^5 cells/scaffold) for 3D culture in a bioreactor, and cyclically strained them with different parameters [strains (2, 4 or 8%) and frequencies (0.3, 0.5 or 1Hz)] for 3hrs/day over a 7 day loading period. They demonstrated increased cell proliferation and increased expression of type I collagen, tenascin-C, tenomodulin and scleraxis at 4% strain with an optimal frequency at 0.5Hz. Tenascin-C is used as a tendon marker as it is expressed in embryonic tendon as well as in developed tendon during repair/remodelling [Midwood and Orend, 2009]. Expressions of scleraxis and tenomodulin are frequently analysed to confirm differentiation towards a tenocyte lineage as they lead to the eventual formation of tendon tissue [Shukunami et al., 2006]. Increased cell proliferation and increased type I collagen expression with loading was also

observed in human patellar tendon fibroblasts cultured on microgrooved silicone surface (2 x 10^5 cells/surface) and subjected to 4% or 8% cyclic strain at 0.5Hz for 4hrs followed by 4hrs rest [Yang et al., 2004]. The study also demonstrated increased expression of type III collagen and TGFβ1 with the loading conditions [Yang et al., 2004].

However, in contrary data, Jones et al. [2013] demonstrated that human Achilles tenocytes seeded in 3D collagen gels (3 x 10^5 cells/gel) and strained from 0-5% at 1Hz for 24hrs or 48hrs reported increased expression of ADAMTS2/4/16, MMP24, TIMP3 and type I collagen at both 24 or 48hrs loading time period. A pilot study investigating the effects of cell density on loading response indicated that metabolism depended on cell density, as it demonstrated that scaffold with a higher cell density had a greater response [Jones et al., 2013]. These findings suggest that the effects of frequency on the isolated tendon cell response is dependent on cell density, duration of loading and possibly the applied strain. Nonetheless, why higher frequencies have not been explored for isolated cells models cannot be explained. However, such studies are more technically challenging to perform, with many experimental set ups unable to operate this rapidly. Therefore, this study is the first to investigate the effect of frequency as high as 10Hz on isolated cells using 3D collagen gels.

Overall, the studies demonstrated that loading at 1Hz and above stimulated a more anabolic response in tendon *in vitro* models, explants and isolated cell models (with cell density over 3 x 10^5 cells/gel), which was consistent with the hypothesis and findings of this study that high frequency loading initiated increase metabolic activity.

5.1.2 DIFFERENT STRAIN MODALITIES

Tendon cells are able to detect mechanical signals from deformation of their cellular membrane, irrespective of the frequency at which strain is applied [Ingber, 2006]. A wide range of *in vitro* studies using explants or isolated cells, have investigated cell response to different strain modalities or magnitudes, and changes in tenocyte gene expression have been demonstrated following exposure to mechanical strains ranging from 1 to 20% [Xu et al., 2015; Mousavizadeh et al., 2014; Huisman et al., 2014; Scott et al., 2005; Goodman et al., 2004; Lavagnino et al., 2003]. In the current study, preliminary work applied strains of 5% ± 5% to bovine tendon explants. However, the magnitude of vibrations caused by eccentric loading or ESWT is likely smaller than this, so a perturbation of 1% ± 1% was adopted. Considering *in vitro* work investigating local tendon strains and the likely cell strain environment in situ, tenocytes are

known to experience tensile strains of around 1-2% within a loaded tissue, so a strain protocol of 1% ± 1% strain was adopted for future studies. Initial validation studies adopting this protocol confirmed that cell viability was maintained at over 70% for both rat tendon explants (table 2.5) and isolated cells seeded within 3D collagen gels (table 2.10). Whilst this protocol lead to a general upregulation of gene expression in isolated cells, it was noted that loading explants to 1% ± 1% lead to the downregulation of the majority of genes after loading, perhaps indicative of a tendinopathic response.

The different response of the cells in these two model systems is not fully understood. An explant study on bovine tendon fascicles suggested tendon adaptation to loading with increased gene expression of type I collagen and IL6 following a 7% cyclic strain at 1Hz for 1hr followed by 2% cyclic strain at 1Hz for a further 6hrs [Legerlotz et al., 2013]. Another study demonstrated that cyclic strain at 0.17Hz to 1, 3 or 6% strain, all inhibited catabolism and supported tissue homeostasis with increased ratio of TIMP1/MMP13 in rat tail fascicles [Gardner et al., 2008]. These data would suggest that any magnitude of cyclic applied strain would initiate an anabolic tenocyte response. However, other studies have indicated that gene expression is modulated by magnitude of cyclic tensile strain [Lavagnino et al., 2003]. In this study, 1% strain inhibited MMP1 gene expression at a frequency of 0.017Hz but the expression was completely eliminated when the strain was increased to 3 or 6% at the same frequency of 0.017Hz [Lavagnino et al., 2003]. However, this study also demonstrated an interrelationship between strain magnitude and frequency, as when strain frequency was increased to 0.17Hz, 1% cyclic strain completely eliminated MMP1 expression. By contrast, other studies have investigated cell response to very high strains [Scott et al., 2005]. Cyclic strains of 20% at 1Hz for 6hrs resulted in cell apoptosis. Taken together, these data highlight the complexity associated with testing explants, but suggest that applied strains need to be of a minimum magnitude to ensure a homeostatic or anabolic response, but excess strain can lead to catabolism and matrix breakdown.

Studies in isolated cells also show considerable variability in response. Isolated cells from a chicken flexor digitorum tendon, seeded in a 3D construct and strained to 1% at 1Hz, 1hr/day for 7 days, demonstrated increased expression of type I/III/XII collagen, aggrecan, and tenascin [Garvin et al., 2003]. Another study on human Achilles tenocytes, cultured in 2D on a polystyrene dish, and cyclically strained to 1, 5 or 8% strain at 1Hz for 60min/day for 3 days demonstrated increased gene expression of MMP9/13/14, fibromodulin, lumican and versican independent of the applied strain [Popov et al., 2015]. This study suggested the optimal strain

was 8%, with higher upregulation of collagen-binding integrins (α1, α2 and α3) and activation of downstream kinases p38 and ERK1/2 [Popov et al., 2015]. Yet by contrast, Xu et al. [2015], investigating cyclic strain response on tendon derived stem cells (TDSCs), seeded in 2D on P(LLA-CL)/collagen scaffolds, demonstrated the highest anabolic cell response with 4% cyclic strain comparing 2, 4 or 8% strain at 0.3, 0.5 or 1Hz for 3hrs/day over a 7days. The difference in ultimate strain between the two studies [Popov et al., 2015 and Xu et al., 2015] may be attributed to the different scaffold materials used and other varied experimental conditions, but suggest more strain is not necessarily better. Micro-mechanics experiments in explants indicate that few of the strain conditions adopted are physiologically relevant, as tenocyte strains rarely exceed 2% seen *in vivo* [Screen, et al., 2004]. Nevertheless, some researchers applied even larger strains such as 10% at 1Hz for 24hrs, applied to healthy human hamstring tenocyte [Mousavizadeh et al., 2014]. Although the authors demonstrated that such high strain can be tolerated by the cells, the cells responded with an inflammatory signature, and increased expression of angiogenic genes (COX2, VEFG, FGF2) in the first 4hrs of loading after which, by extending the time course of cyclic strain, the expression of these same genes was subsequently downregulated [Mousavizadeh et al., 2014]. The data suggest that at such high strain at short burst of cyclic strain may initiate cell proliferation and tissue formation while prolong cyclic strain potentially contribution to the progression of tendon degeneration.

The current study demonstrated that a cyclic strain of 1% might be low for explants but was probably more physiological for isolated cells.

5.1.3 DURATION OF LOADING AND NUMBER OF CYCLES

Gene expression changes in response to loading can be assessed at varying time points, ranging from hours to days to weeks. A standardised appropriate time point for investigating gene expression post loading cannot be defined, not least because response time will be influenced by the load protocol adopted, but also as the time course for the upregulation of different genes can be highly variable. Selecting a time point for analysis is always a compromise, and it is too complex and expensive to do multiple time points in all experiments generally. The most appropriate time to investigate gene expression changes post-loading was investigated for both the explant model and the isolated cell model, and found to be 24hrs.

As the collagen gel model was selected for further study, it was additionally characterised more fully, and the gene stabilisation post sample preparation was examined, using a TLDA analysis

at 4, 8, 12 and 24hrs time points after a 15mins loading episode relative to 24hr unloaded control (Figure 3.4A and B). The data in Figure 3.4A and B demonstrated fluctuations in gene response with time. At the first time point of 4hrs, on average, gene expression levels were reduced in loaded samples relative to unloaded samples, particularly with 1Hz loading. Levels steadily increased to around basal levels at 8hrs, with most genes upregulated relative to controls by 12hrs. Owing to insufficient wells to run all sample groups, the response to 1Hz loading at 24hrs was unfortunately not investigated. However, based to the steady increase in expression and maximum response with 10Hz loading at 24hrs, this was selected as the time point for analysis in future experiments.

In a study by Eliasson et al. [2012], the gene expression changes in rat Achilles tendon after a 30mins single burst of loading were strongly regulated at 3hrs after loading, compared to 12, 24 and 48hrs after loading. 86 genes were strongly upregulated, mainly wound healing associated genes, and 64 genes were strongly downregulated, mainly proteoglycans, COLVIII and COLXI. This could also possibly explain why the rat explants showed downregulation of all the analysed gene except for MMP13 to loading after 24hrs. There is also the possibility that the loading time was not enough for peak gene response.

The gene expression profile in Figure 4.10 demonstrated cycle-independent tenocyte response to the applied loading condition. This study was carried out to determine if the increased metabolic response seen in tenocytes in response to 10Hz loading was driven by increased cycle number, but the findings highlighted that this was not the case. Such a result is at odds with some other studies, which showed that increased number of loading led to increased total collagenase content when an avian flexor digotorum profundus (FDP) was loaded at either 12MPa or 3MPa at 1Hz for 0, 7200, 43200, 79200 or 86400 cycles [Devkota et al., 2007]. Sun et al [2010] findings on *in vivo* rat patellar tendon loaded at 50% maximal load at 1Hz also demonstrated a higher response in high-cycle fatigue loading (7,200 cycles of loading), with magnified changes in gene expression in MMPs, TIMPs, and collagens associated with healthy response, compared to low-cycle fatigue loading (100 cycles of loading). However, it is likely in samples subjected to more cycles, these studies are generating damage within the tendon and the increased cell response may be associated with this.

These findings provide evidence that an appropriate strain duration and repetitive loading are essential components for an efficient adaptive stimulus for tendons cell response.

5.1.4 DIFFERENT CELL TYPES

This current study showed increased metabolic activity with 10Hz loading relative to 1Hz loading, which is attributed to the loading frequency specifically. Of note, the upregulation of gene expression with load, and the relative differences between 1Hz and 10Hz loading were both greater in healthy than tendinopathic cells. This could be because of the cells phenotypic differences, but could also be due to the tissue source, as healthy tenocytes were obtained from hamstring tendons while tendinopathic tenocytes were obtained from Achilles tendons. In addition, some of the differences observed could also be associated to changes seen with tendinopathy. It is well known that cell culture can result in changes in cell phenotypic, as demonstrated by a study on human tenocytes, where there was a reduction in collagen type I and collagen type III gene expression after passage 3 and protein content after passage 4, and tenascin-C gene expression after passage 5 [Mazzocca et al., 2012]. The current study used cells between passage 3 and passage 5, so as to limit cell phenotypic changes. However, it is notable that clear metabolic differences between the cells remained evident at this point, indicating that not all phenotypic differences between the cell types have been lost through culture.

Considering other studies looking specifically at injured tendon, a recent study explored the effects of cyclic mechanic load of 0-0.06N at either 20Hz or 1Hz, relative to static load, for 1hr/day for 5 days. Data demonstrated increased metabolic activity with high frequency load [Adekanmbi et al., 2016]. However, the study only looked at damaged rat tail tendon fascicles, where a cut was made along the length of the fascicles using a needle. The study demonstrated significantly higher tangent modulus and increase in metabolic activity with 20Hz loading, relative to the unloaded damaged controls, the 1Hz loaded group, and the static load. However, it is difficult to clarify the load effects without an uninjured control [Adekanmbi et al., 2016].

Another study directly comparing healthy and tendinopathic tenocytes was performed by Patel et al. [2014], who seeded the cells into a specially designed fibre composite construct and applied cyclic multi-modal tensile and shear load to the cells for 24hrs. The study showed tendinopathic tenocytes to be more mechano-sensitive than healthy tenocytes under shear-tension load contrary to this current study [Patel et al., 2015; Patel et al., 2014]. Interestingly, these studies utilised exactly the same cells as the current study, suggesting that either the material, how the cell interacted with the material or the shear loading condition could contribute to the difference seen between the studies. Application of tension and shear load *in vivo* is determined by the tendon

tissue solid (collagen matrix) and fluid components between fascicles in the IFM [Lavagnino et al., 2008], therefore exposing tenocytes to both tension and shear during tendon loading might initiate a different response. So, to obtain a comprehensive understanding of tenocyte mechanobiology, a combined stimulus of tenocytes response to fluid shear stress and cyclic tensile strain is needed.

The application of controlled shear has been achieved in some studies through the use of fluid shear. A study by Lavagnino et al. [2008] was able to create a multiscale computational tendon model composed of both matrix and fluid phases to examine how tensile and shear loading may affect stresses and strains at the cellular level. The study was able to generate a simplified model of tendon able to demonstrate that both fluid-flow induced shear stress and matrix-induced cell deformation are able to independently alter rat interstitial collagenase gene expression at varying strain rate and amplitudes. A recent study by Maeda et al. [2013] developed a system to apply simultaneously, tensile strain and fluid shear stress to tenocytes. The system applied tension to a flexible cell seeded microgrooved membrane, with the microgrooves present to keep cells isolated in rows. Fluid was then moved across the surface of the cells at a controlled speed, with both tension and fluid flow applied in a uniaxial direction. The study pointed out that the combination of shear and tensile strain significantly increased tenocytes mechanotransduction response relative to unloaded controls [Maeda et al., 2013].

These findings suggest that the difference in response in cell types might be linked to the loading condition applied, stimulating a more or less mechanosensitive response from the cells.

5.1.5 PATHWAY INVESTIGATIONS

Chapter 4 presented preliminary evidence to indicate that the IL-1 signalling pathway was activated with mechanical strain. This correlates with the mRNA data from chapter 3, which showed high levels of expression of MMPs and interleukins (Figure 3.4A and B) from a TLDA analysis and high expression of MMP1, MMP2, MMP13, IL6 and IL8 (Figure 3.5) from qRT-PCR analysis. The current study also provides some evidence (Figure 4.12) that collagens are not regulated through this IL-1 pathway, as there was no significant difference between the non-inhibited and IL-1 inhibited samples when COL1A1 gene expression was analysed. Interestingly, collagens did not appear to be regulated through the TGFβ pathway either, as there was no change in the gene response for COL1A1, COL3A1, and COL5A1 in Figure 4.11.

The current study made use of inhibitors developed to block signalling at the receptor level (IL-1Ra and TGFβR1) thereby interfering with the binding of the protein to its receptor thus blocking intracellular signalling. Many other TGFβ pathway inhibitors have been investigated in the preclinical setting, while some are still in clinical development and can be sub-divided into three groups.

a. Inhibition at the ligand level – involves an antisense oligonucleotide delivered into the immune cells intravenously, targeting TGFβ2 to prevent TGFβ synthesis [Neuzillet et al., 2015].
b. Inhibition at the ligand-receptor level – involves a monoclonal antibody targeting different signalling receptors (for example TGFβRII) to prevent ligand-receptor interaction [Nagaraj and Datta, 2010].
c. Inhibition at the intracellular level - used in this study, to target the kinase domain of TGFβRI thereby interfering with the binding of TGFβ to its receptors, blocking intracellular signalling, and antisense oligonucleotides [Nagaraj and Datta, 2010].

To fully investigate genes that may be regulated through TGFβ pathway, further investigations would be required, adopting the other two forms of inhibitors to confirm findings.

The data from Figure 4.11 indicates that whilst the inhibition of TGFβ might not have directly influenced collagen gene expression, it did mediated IL6 gene expression, with the gene expression level falling below the basal level on addition of the TGFβ inhibitor. This may suggest that the TGFβ signalling pathway regulated IL6 expression, whilst collagen gene expression might be regulated by another pathway. On the other hand, although Figure 4.12 demonstrate that MMPs and IL6 are regulated by IL-1 pathway, this can be further clarified by using other IL-1 inhibitors with similar function as the IL-1Ra used in this study. IL-1 pathway inhibitors have been investigated using Anakinra, an IL-1 receptor blocking antibody, which function in the same manner as the IL-1 receptor antagonist (IL-1Ra) to block the activity of both IL-α and IL-1β [Dinarello et al., 2012]. This will provide further confirmation to the data.

Studies have stated that cell signalling pathways depend on the initiate trigger and extensive communication with other signalling pathways either directly or indirectly or as part of a feedback loop, leading to synergistic or antagonistic effects and eventually desirable biological outcomes [Guo and Wang, 2009]. However, the nature of such signalling cross-link is overwhelmingly complex and context-dependent. Therefore, in-depth mechanistic studies are

necessary to distinguish the cause from the consequence and to identify the specific convergence point of possible pathways.

5.1.6 LIMITATIONS

Although this research provided some insight into the response of healthy and tendinopathic tenocytes to 10Hz loading, there are a number of limitations which should be kept in mind when interpreting the results.

Firstly, the healthy and tendinopathic cells were from two different tendon types, hamstring and Achilles tendons respectively, so may have phenotypic differences associated with their functions. However, evidence suggests that both the tendons of the musculotendon hamstring system and the Achilles tendon exhibit energy-storing capability, making them a reasonable functional match [Shepherd et al., 2014]. However, the cell extraction method for both populations were also different (Chapter 3), which may also have had an impact on the results. The healthy hamstring tendon cells were isolated via enzymatic digestion (collagenase digest) while the tendinopathic Achilles tendon cells were obtained via explant outgrowth. Enzymatic digestion involves subjecting finely chopped tendon tissue to proteolysis using an enzyme - collagenase, whereas explant outgrowth involves placing a fragment of tendon tissue, a tendon explant, on a solid interface with culture media, and allowing it to adhere, and the outgrowth of cells from the explant collected by trypsinization and subcultured. Cells isolated by explant outgrowth would contain selective cells from the tissue, depending on their ability to migrate out of the explant and adhere which is not the case for collagenase digest [Lanza et al., 2007]. Studies have demonstrated that cell extraction method can affect cell yield, proliferation rate and gene expression [Gittel et al., 2013; Souza et al., 2010]. Extraction of mesenchymal stromal cells (MSCs) from equine subcutaneous adipose tissue, superficial digital flexor tendon, and umbilical cord matrix by enzymatic digestion or explant outgrowth resulted in significantly higher MSC yields and higher expression levels of scleraxis with enzymatic digestion compared to explant outgrown MSCs [Gittel et al., 2013]. Although Gittel et al. [2013] showed no significant differences in cell proliferation, studies comparing cells from the two cell isolation methods have found that cells digested from tissue generally exhibit higher proliferation rates [Souza et al., 2010; McDuffee, 2012]. However, findings have indicated that both extraction methods are effective in isolating cells and that cell passaging favours cell proliferation and each passage

increases growth fraction until the third passage where it exceeds 90% [Lanza et al., 2007; Jing et al., 2011].

Furthermore, there was age difference between the healthy hamstring tendon cells (21 ± 1) and the tendinopathic Achilles tendon cells (48 ± 3) used in this study. Studies have highlighted that tendon mechanical and structural properties diminish with age, demonstrating matrix damage, increased fibre sliding, and reduced matrix turnover making them more prone to injury [Thorpe et al., 2014; Thorpe et al., 2016c]. A number of studies have explored the mechanical properties of human tendons with age, considering 27-33 years as young and 65-80 years as old [Stenroth et al., 1985; Birch et al., 2001; Carroll et al., 2008; Magnusson et al., 2008]. These studies reported reduced ultimate tensile strength, reduced viscoelastic properties, lower tendon stiffness and increased cross-sectional area with aging. Although these changes observed in the tendon matrix with age are similar to changes observed in degenerated tendon, the age of the tendinopathic cells used in this study are referred to as middle-aged by Lewis and Shaw, [1997], making the data comparable as the changes expected to be observed from the tendinopathic cells will likely be due to tendinopathy and not age.

5.2 CONCLUSION

Published work has focused on exploring the effects of mechanical loading at frequencies between 0.017 to 1Hz in tendon, at both *in vivo* and *in vitro* levels. In Chapter 2, this study explore various *in vitro* models for mechanically loading tenocytes. The 3D collagen gel stood out as the most effective model for this study, as it provided a 3D environment for cell to cell communication, and an elastic material for loading the cells. It also maintained cell viability at above 74%, and did not promote cell proliferation over the 48hr time period required for both gene stabilisation and subsequent loading.

In Chapter 3, this study documented mechanical regulation of a wide range of matrix related genes a using TLDA analysis. The time course of gene expression changes was investigated (4-48 hours) under 1% ± 1% cyclic loading at 1Hz and 10Hz. The data showed that mechanical loading regulates a wide range of metalloproteinase, matrix genes, TIMPs and cytokines. Gene responses were more pronounced in cells subjected to 10Hz loading, indicating that 10Hz loading prompted a more responsive effect in the cells. This observation lead to a focus on few genes to further analysis the effect of frequencies on healthy and tendinopathic cells. The findings demonstrated that not only do cells respond more to 10Hz loading, but the effects were more pronounced in the healthy cells, perhaps indicating why tendinopathy is so difficult to treat.

These generated questions concerning the mechanotransduction signalling pathways involved in the cellular response to the applied mechanical loading. In Chapter 4, a broad spectrum cytokine array was first carried out to explore potential pathways. A number of cytokines were increased with loading, particularly with 10Hz loading, but of these, TGFβ and IL-1 stood out. Therefore, this study went further to look specifically at the potential role of the TGFβ and IL-1 signalling pathways in the mechanoregulation of gene expression. The result suggested that the mechanoregulation of tenocyte gene expression in this system is mediated via the IL-1 signalling pathway, which involves NFkB or c-Jun translocation to the nucleus and consequent transcriptional regulation.

Overall, the results obtained from this study provided more insight on tenocyte metabolism and response to loading, confirming that the application of 10Hz loading to tenocytes within the 3D collagen gel model may promote or initiate a healing response, and that tendinopathic tenocytes respond differently to healthy tenocytes. It also shows that the mechanical loading induced the

IL-1 signalling pathway. Moreover, inflammation, might be influenced by loading in a way that leads to improved healing.

5.3 FUTURE WORK

Whilst this study has indicated that 10Hz loading, adopted as a model of eccentric loading, resulted in a more pronounced cell response, the research has raised additional questions for future work.

1. **Verification of cell response to 10Hz loading by**
    a. Exposing the cells to 2 sets of 15mins cyclic strain over the 24hrs (more closely replicating a typical eccentric loading response)
    b. Evaluating the protein expression

2. **Mechanical loading**
    a. To determine the effect of an increased strain magnitude, as explored by other studies, at 10Hz frequency to determine how this may impact cell response
    b. To determine the effect of combined shear and tensile strain at 10Hz on the cell response

3. **IL-1 characterisation**: Validation of the role of IL-1 in the mechanoregulation of gene expression to strain, and how it is affected by alteration of loading frequency, thereby providing more insight into the role of this cytokine in inflammation and its relevance to tendon healing by:
    a. Adding IL-1 to determine its effect to the cells in response to loading
    b. Inhibiting the IL-1 pathway by blocking IRAK1 phosphorylation using curcumin [Jurrmann et al., 2005], or by inhibiting the processes that regulate IL-1 maturation and release by blocking the plasma membrane receptor for extracellular ATP, the $P2X_7$ receptor, thereby inhibiting the triggering of IL-1 maturation and exteriorization [Christopher et al., 2006].

4. **TGFβ characterisation**: Validation of the role of TGFβ in the mechanotransduction of gene expression to strain and frequency by exploring it effects on other genes aside from the selected genes in this study. As discussed in Chapter 4, TGFβ is generally secreted in a biologically latent form called either small or large latent-TGFβ. Therefore, the most relevant information reported on TGFβ is TGFβ activity, which is based on whether or not TGFβ is biologically active or latent.

REFERENCES

Adekanmbi, I., Franklin, S. and Thompson, M. S. (2013) 'A Novel *In Vitro* Loading System for High Frequency Loading of Cultured Tendon Fascicles'. *Medical Engineering and Physics*, 35(2): 205-210.

Adekanmbi, I., Zargar, N. and Hulley, P. (2016) 'An *in Vitro* Scratch Tendon Tissue Injury Model: Effects of High Frequency Low Magnitude Loading'. *Connective Tissue Research*, 1-10.

Al-Abbad, H. and Simon, J. V. (2013) 'The Effectiveness of Extracorporeal Shock Wave therapy on Chronic Achilles Tendinopathy: A Systematic Review'. *American Orthopaedic Foot and Ankle Society*, 34(1): 33-41.

Alfredson, H. and Cook, J. (2007) 'A Treatment Algorithm for Managing Achilles Tendinopathy: New Treatment Options'. *Br J Sports Med*, 41: 211-216.

Allison, G.T. and Purdam, C. (2009) 'Eccentric Loading for Achilles Tendinopathy - Strengthening or Stretching?'.'*Br J Sports Med'*, 43: 276–279.

Anckermann, P.W., Domeij-Arverud, E., Leclerc, P., Amodrouz, P. and Nader, G. A. (2013) 'Anti-Inflammatory Cytokine Profile in Early Human Tendon Repair'. *Knee Surgery, Sports Traumatology, Arthroscopy*, 21(8): 1801-1806.

Andarawis-Puri, N. and Flatow, E. L. (2011) 'Tendon Fatigue in Response to Mechanical Loading'. *J Musculoskelet Neuronal Interact*, 11: 106-14

Andarawis-Puri, N., Flatow, E. L. and Soslowsky, L. J. (2015) 'Tendon Basic Science: Development, Repair, Regeneration, and Healing'. *J Orthop Res*, 33(6): 780-784.

Andersen, M. B., Pingel, J., Kjaer, M. and Langberg H (2011) 'Interleukin-6: A Growth Factor Stimulating Collagen Synthesis in Human Tendon'. *J Appl Physiol*, 110(6):1549-1554.

Ansorge, H. L., Meng, X., Zhang, G., Veit, G., Sun, M., Klement, J. F., Beason, D. P., Soslowsky, L. J., Koch, M. and Birk, D. E. (2009) 'Type XIV Collagen Regulates Fibrillogenesis: Premature Collagen Fibril Growth and Tissue Dysfunction in Null Mice'. *J Biol Chem*, 284(13): 8427-8438.

Arampatzis, A., Karamanidis, K. and Albracht, K. (2007) 'Adaptational Responses of the Human Achilles Tendon by Modulation of the Applies Cyclic Strain Magnitude'. *The Journal of Experimental Biology*, 210: 2743-2753.

Archambault, J., Tsuzaki, M., Herzog, W. and Banes, A. J. (2002) 'Stretch and Interleukin-1β Induce Matrix Metalloproteinases in Rabbit Tendon Cells *In Vitro*'. *Journal of Orthopaedic Research*, 20:36-39.

Arnoczky, S. P., Lavagnino, M. and Egerbacher, M. (2007) 'The Mechanobiological Aetipathogenesis of Tendinopathy: Is it the Over-Stimulation or the Under-Stimulation of Tendon Cells?'. *Int J Exp Path, 88: 217-226*

Artym, V. V. and Matsumoto, K. (2010) 'Imaging Cells in Three-Dimensional Collagen Matrix'. *Curr Protoc Cell Biol.*, 10: 1-23.

Arya, S. and Kulig, K. (2010) 'Tendinopathy Alters Mechanical and Material Properties of the Achilles Tendon'. *Journal of Applied Physiology*, 108(3): 670-675.

Astrom, M., Rausing A., (1995) 'Chronic Achilles Tendinopathy. A Survey of Surgical and Histopathologic Findings'. *Clin Orthop Relat Res*, 316: 151–64.

Asundi, K. R. and Rempel, D. M. (2008) 'Cyclic Loading Inhibits Expression of MMP-3 but not MMP-1 in an *In Vitro* Rabbit Flexor Tendon Model'. *Clinical Biomechanics*, 23:117-121.

Bacabac, R. G., Smit, T. H., Van Loon, J. J. W. A., Doulabi, B. Z., Helder, M. and Klein-Nulend, J. (2006) 'Bone Cell Responses to High-Frequency Vibration Stress: Does the Nucleus Oscillate within the Cytoplasm?'. *The FASEB Journal*, 20: 858-864.

Baker, B. M. and Chen, C. S. (2012) 'Deconstructing the Third Dimension – How 3D Culture Microenvironments Alter Cellular Cues'. *Journal of Cell Science*, 125(13): 3015-3024.

Bayer, M. L., Schjerling, P., Herchenhan, A., Zeltz, C., Heinemeier, K. M., Christensen, L., Krogsgaard, M., Gullberg, D. and Kjaer, M. (2014) 'Releaze of Tensile Strain on Engineered Human Tendon Disturbs Cell Adhesions, Changes Matrix Architecture, and Induces an Inflammatory Phenotype'. *PLoS One*, 9(1): e86078.

Birch, H.L. (2007) ‘Tendon Matrix Composition and Turnover I Relation to Functional Requirements’. *Int J Exp pathol*, 88(4): 241-248.

Birch, H.L., Bailey, A.J. and Goodship, A.E. (1998) ‘Macoscopic ‘Degeneration’ of Equine Superfical Digital Flexor Tendon id Accompanied by a Change in Extracellular Matrix Composition’. *Equnie Vet J*, .30(6): 534-539.

Birch, H., Smith, T., Tasker, T. and Goodship, A. (2001) ‘Age Related Changes to Mechanical and Matrix Properties in Human Achilles Tendon’. *47th Annual Meeting, Orthopaedic Research Society*, Poster 0713.

Blackshaw, S. E, Arkison, S., Cameron, C. and Davies, J. A. (1997). ‘Promotion of Regeneration and Axon Growth Following Injury in an Invertebrate Nervous System by the Use of Three Dimensional Collagen Gels’. *Proc Biol Sci*, 264(1382): 657-61.

Bohm, S., Mersmann, F., Tettke, M., Kraft, M. and Arampatzis, A. (2014) ‘Human Achilles Tendon Plasticity in Response to Cyclic Strain: Effect of Rate And Duration’. *Journal of Experimental Biology*, 217: 4010-4017.

Borchiellini, C., Coulon, J. and Parco, Y. L. (1996) 'The Function of Type IV Collagen during Drosophila Muscle Development’. *Mechanisms of Development*, 58(1-2): 179-191.

Bosch, G., De Mos, M., Van Binsbergen, R., Van Schie, H. T. M., Van De Lest, C. H. A. and Van Weeren, P. R. (2009) ‘The Effect of Focused Extracorporeal Shock Wave Therapy on Collagen Matrix and Gene Expression in Normal Tendons and Ligaments’. *Equine Veterinary Journal*, 41(4): 335-341.

Bouchard, C. (2015) *Progress in Molecular Biology and Translational Science: Molecular and Cellular Regulation of Adaptation to Exercise*. Vol 135, London: Elsevier Inc, Academic Press.

Brown, R. A., Wiseman, M., Chuo, C. B., Cheema, U. and Nazhat, S. N. (2005) ‘Ultrarapid Engineering of Biomimetic Materials and Tissues: Fabrication of Nano- and Microstructures by Plastic Compression’. *Advanced Functional Materials*, 15(11): 1762-1770.

Bruneau, A., Champagne, N., Cousineau-Pelletier, P., Parent, G. and Langelier, E. (2010) 'Preparation of Rat Tail Tendons for Biomechanical and Mechanobiogical Studies'. *Journal of Visualized Experiments*, 41: 2176.

Buchner, J. and Moroder, L. (2009) 'Oxidative Folding of Peptides and Proteins'. London: RSC.

Bullied, N.J., Dalley, J.A. and Lees, J.F. (1997) 'The C-Propeptide Domain of Procollagen can be Replaced with a Transmembrane Domain without Affecting Trimer Formation or Collagen Triple Helix Folding during Biosynthesis'. *Tumour Microenvironment and Signalling*, 16(22): 6694-6701.

Buono, A. D., Oliva, F., Osti, L. and Maffulli, N. (2013) 'Matalloproteases and Tendinopathy'. *Ligaments and Tendon Journal*, 3(1): 51-57.

Canty, E. G. and Kadler, K. E. (2005) 'Procollagen Trafficking, Processing and Fibrillogenesis'. *Journal of Cell Science*, 118: 1341-1353.

Carroll, C. C., Dickinson, J. M., Haus, J. M., Lee, G. A., Hollon, C. J., Aagaard, P., Magnusson, S. P. and Trappe, T. A. (2008) 'Influence of Aging on the *In Vivo* Properties of Human Pattellar Tendon'. *Journal of Applied Physiology*, 105(6): 1907-1915.

Cassel, M., Baur, H., Hirschmuller, A., Carlsohn, A., Frohlich, K. and Mayer, F. (2014) 'Prevalence of Achilles and Patellar Tendinopathy and their Association to Intratendinous Changes in Adolescent Athletes' *Scandinavian Journal of Medicine and Science in Sports*, 25(3): e310-e318.

Chaudhry, S. (2012) 'A Biomechanical Characterisation of Eccentric and Concentric Loading of the Triceps Surae Complex'. PhD Thesis. Queen Mary University of London: School of Engineering and Material Science.

Chaudhry, S., Morrissey, D., Woledge, R. C., Bader, D. L. and Screen, H. R. C. (2015) 'Eccentric and Concentric Exercise of the Triceps Surae: An In Vivo Study of Dynamic Muscle and Tendon Biomechanical Parameters'. *Journal of Applied Biomechanics*, 31: 69-78.

Cheema, U. and Brown, R. A. (2013) 'Rapid Fabrication of Living Tissue Models by Collagen Plastic Compression: Understanding Three-Dimensional Cell Matrix Repair'. *In Vitro. Advances in Wound Care*, 2(4): 176-184.

Cheema, U., Nazhat, S. N., Alp, B., Foroughi, F., Anandagoda, N., Mudera, V. and Brown, R. A. (2007) 'Fabricating Tissues: Analysis of Farming Versus Engineering Strategies'. *Biotechnology and Bioprocess Engineering*, 12: 9-14.

Cheema, U., Rong, Z., Kirresh, O., Macrobert, A. J., Vadgama, P. and Brown, R. A. (2012) 'Oxygen Diffusion Through Collagen Scaffolds at Defined Densities: Implications for Cell Survival in Tissue Models'. *J Tissue Eng Regen Med.*, 6(1): 77-84.

Cheng, V. W. T. and Screen, H. R. C. (2007) 'The Micro-Structural Strain Response of Tendon. *J. Mater. Sci*. 42: 8957–8965.

Chen, Y. J., Wang, C.J., Yang, K. D., Kuo, Y. R., Huang, H. C., Huang, Y. T., Sun, Y. C. and Wang, FS. (2004) 'Extracorporeal Shock Waves Promote Healing of Collagenase-Induced Achilles Tendinitis and Increase TGF-β1 and IGF-1 Expression'. *Journal of Orthopaedic Research*, 22: 854-861.

Chhabra, N. (2013) 'Collagen Synthesis, Types and Composition'. *Biochemistry for Medics.*

Chieh, H. F., Sun, Y., Liao, J. D., Su, F. C., Zhao, C., Amadio, P. C. and An, K. N. (2014) 'Effects of Cell Concentration and Collagen Concentration Kinetics and Mechanical properties in a Bone Marrow Stromal Cell-Collagen Construct'. *J Biomed Mater Res A.*, 93(3): 1132-1139.

Clark, R. A. F. (2006) *The Molecular and Cellular Biology of Wound Repair*. 2nd Edition, New York: Plenum Press.

Clancy, S. and Brown, W. (2008) 'Translation: DNA to mRNA to Protein'. *Nature Education*, 1(1): 101.

Colombo, A., Cahill, P. A. and Lally, C. (2008) 'An Analysis of the Strain Field in Biaxial Flexcell Membranes for Different Waveforms and Frequencies'. *Proc Inst Mech Eng H*, 222(8): 1235-45.

Cook, J. L. and Purdam, C. R. (2009) 'Is tendon Pathology a Continuum? A Pathology o Explain the Clinical Presentation of Load Induced Tendiopathy'. *Br J Sports Med*, 43: 409-416.

Cooper, G. M. (2000) *The Cell: A Molecular Approach* 2nd Edition. Sunderland (MA): Sinauer Associates. Pathways of Intracellular Signal Transduction. Available from: http://www.ncbi.nlm.nih.gov/books/NBK9870/.

Corps, A. N., Robinson, A. H., Harrall, R. L., Avery, N. C., Curry, V. A., Hazleman, B. L. and Riley, G. P. (2012) 'Changes in Matrix Protein Biochemistry and the Expression of mRNA Encoding Matrix Proteins and Metalloproteinases in Posterior Tibalis Tendinopathy'. *Ann Rheum Dis*, 71(5):746-752.

Corps, A. N., Robinson, A. H., Movin, T., Costa, M. L., Ireland, D. C., Hazleman, B. L. and Riley, G. P. (2004) 'Versican Splice Variant Messenger RNA Expression in Normal Human Achilles Tendon and Tendinopathies'. *Rheumatology*, 43: 969-972.

Cowin, S. C. and Doty, S. B. (2007) *Tissue Mechanics*. New York: Springer.

Cribb, A. M. and Scott, J. E. (1995) 'Tendon Response to Tensile Stress: An Ultrastructural Investigation of Collagen: Proteoglycan Interactions in Stressed Tendon'. *J. Anat.*, 187: 423-428.

Dakin, S. G., Dudhia, J. and Smith, R. K. W. (2014) 'Resolving an Inflammatory Concept: The Importance of Inflammation and Resolution in Tendinopathy'. *Veterinary Immunology and Immunopathology*, 158(3-4):121-127.

Devkota, A. C. (2006) 'An *In Vitro* Explant Model of Overuse Tendinopathy. The Effects of Cyclic Loading and Inflammatory Mediators on Mechanical and Compositional Properties of Tendons'. PhD Thesis. University of North Carolina at Chapel Hill.

Devkota, A. C., Tsuzaki, M., Almekinders, L. C., Banes, A. J. and Weinhold, P. S. (2007) 'Distributing a Fixed Amount of Cyclic Loading to Tendon Explants over Longer Periods Induces Greater Cellular and Mechanical Responses'. *Journal of Orthopaedic Research*, 25: 1078-1086.

Devkota, V. and Weinhold, P. S. (2005) 'A Tissue Explant System for Assessing Tendon Overuse Injury'. *Med Eng Phys*, 27(9): 803-808.

Dinarello, C. A. (1996) 'Biologic Basis for Interleukin-1 in Disease'. *Blood*, 15;87(6): 2095-2147.

Dinarello, C. A., Simon, A. and Van Der Meer, J. W. M. (2012) 'Treating Inflammation by Blocking Interleukin-1 in a Broad Spectrum of Diseases'. *Nat Rev Drug Discov*, 11(8): 633-652.

Docheva, D., Muller, S. A., Majewski, M. and Evans, C. H. (2015) 'Biologics for Tendon Repair'. *Adavanced Drug Delivery Reviews*, 84: 222-239.

Docking, S., Samiric, T., Scase, E., Purdam, C. and Cook, J. (2013) 'Relationship Between Compressive Loading and ECM Changes in Tendons'. *MLTJ Muscles, Ligaments and Tendons Journal*. 3(1): 7-11.

Doral, M. N., Alam, M., Bozkurt, M., Turhan, E., Atay, O. A., Donmez, G. and Maffulli, N. (2010) 'Functional Anatomy of the Achilles Tendon'. *Knee Surgery, Sports Traumatology, Arthroscopy*, 18(5): 638-643.

Duenwald, S. E., Vanderby, R. and Lakes, R. S. (2009) 'Viscoelastic Relaxation and Recovery of Tendon'. *Annals of Biomedical Engineering*, 37(6): 1131-1140.

Duenwald, S. E., Vanderby, R. and Lakes, R. S. (2010) 'Stress Relaxation and Recovery in Tendon and Ligament: Experiment and Modeling'. *Biorheology*, 47: 1-14.

DuFort, C. C., Paszek, M. J. and Weaver, V. M. (2011) 'Balancing Forces: Architectural Control of Mechanotransduction'. *Nature Reviews: Molecular Cell Biology*, 12: 308-319.

Dyment, N. A., Hagiwara, Y., Matthews, B. G., Li, Y., Kalajzic, I. and Rowe, D. W. (2014) 'Lineage Tracing of Resident Tendon Progenitor Cells during Growth and Natural Healing'. *PLoS One*, 9(4): e96113.

Eliasson, P., Andersson, T. and Aspenberg, P. (2012) 'Influence of Single Loading Episode on Gene Expression in Healing Rat Achilles Tendon' *Journal of Applied Physiology*, 112(2): 279-288.

Elsdale, T. and Bard, J. (1972) 'Collagen Substrata for Studies on Cell Behaviour'. *The Journal of Cell Biology*, 54: 626-687.

Eriksen, H. A., Pajala, A., Leppilahti, J. and Risteli, J. (2001) 'Increased Content of Type III Collagen at the Rupture Site of Human Achilles Tendon'. *J Orthop Res*. 20(6):1352–1357.

Fahlstrom, M., Jonsson, P., Lorentzon, R. and Alfredson, H. (2003) 'Chronic Achilles Tendon pain Treated with Eccentric Calf-Muscle Training'. *Knee Surg Sports Traumatol Arthrosc*, 11(5): 327-333.

Fenwick, S. A., Curry, V., Harrall, R. L., Hazleman, B. L., Hackney, R. and Riley, G. P. (2001). 'Expression of Transforming Growth Factor-Beta Isoforms and their Receptors in Chronic Tendinosis'. *J Anat*, 199(Pt 3): 231-240.

Fisher, J. P. (2006) *Tissue Engineering: Advances in Experimental Medicine and Biology*. New York: Springer Science and Business Media.

Fisher, J. P., Jo, S., Mikos, A. G. and Reddi, A. H. (2004). 'Thermoreversible Hydrogel Scaffolds for Articular Cartilage Engineering'. *J Biomed Mater Res A*, 71(2): 268-74.

Franchi, M., Trire, A., Quaranta, M., Orsini, E. and Ottani, V. (2007) 'Collagen Structure of Tendon Relates to Function'. *The Scientific World Journal*, 7: 404-420.

Freedman, B. R., Gordon, J. A. and Soslowsky, L. J. (2014) 'The Achilles Tendon: Fundamental Properties and Mechanisms Governing Healing'. *Muscle, Ligaments and Tendons Joural*, 4(2): 245-255.

Frizziero, A., Trainito, S., Olivia, F., Aldini, N. N., Masiero, S. and Maffulli, N. (2014) 'The Role of Eccentric execise in Sport Injuries Rehabilitation'. *British Medical Bulletin*, 110: 47-75.

Fugle-Meyer, A. R., Nordin, G., Sjöström, M. and Vahlby, L. (1979) 'Achilles Tendon Injury: A Model for Isokinetic Strength Training using Biofeedback'. *Scand J Rehab Med*, 11:37-44.

Fung, D. T., Wang, V. M., Andarawis-Puri, N., Basta-Pljakic, J., Li, Y., Laudier, D. M., Sun, H. B., Jepsen, K. J., Schaffler, M. B. and Flatow, E. L. (2010) 'Early response to tendon fatigue damage accumulation in a novel in vivo model'. *Journal of Biomechanics*. 43, 274–279.

Henriksen, M., Aaboe, J., Biddal, H. and Langberg, H. (2009) 'Biomechanical Characteristics of the Eccentric Achilles Tendon Response'. *Journal of Biomechanics*, 42: 2702-2707.

Gaida, J.E. and Cook, J. (2011) 'Treatment Options for Patellar Tendinopathy: Critical Review'. *Current Sport medicine Reports*, 10(5): 255-270.

Galie, P. A. and Stegemann, J. P. (2011) 'Simultaneous Application of Intestitial Flow and Cyclic Mechanical Strain to a Three-Dimensional Cell-Shaped Hydrogel'. *Tissue Engineering*, 17(5): 527-537.

Galloway, M. T., Lalley, A. L., Shearn, J. T. (2013) 'The Role of Mechanical Loading in Tendon Development, Maintenance, Injury, and Repair'. *J. Bone Joint Surg Am*, 95(17): 1620-1628.

Gardner, K., Arnoczky, S. P., Caballero, O. and Lavagnino, M. (2008) 'The Effect of Stress-Deprivation and Cyclic Loading on the TIMP/MMP Ratio in Tendon Cells: An *In Vitro* Experimental Study'. *Disabil Rehabil*. 30:1523–1529.

Garrett, W. E. Jr., Califf, J. C. and Bassett, F. H. (1984) 'Histochemical Correlates of Hamstring Injuries'. *Am J Sports Med*, 12: 98-103.

Garvin, J., Qi, J., Maloney, M. and Banes, A. J. (2003) 'Novel System for Engineering Bioartifical Tendons and Application of Mechanical Load'. *Tissue Engineering*, 9(5): 967-979.

Gelse, K., Poschl, E. and Aigner, T. (2003) 'Collagens – Struucture, Function, and Biosynthesis'. *Advanced Drug Delivery Reviews*, 55: 1531-1546.

Gittel, C., Brehm, W., Burk, J., Juelke, H., Staszyk, C. and Ribitsch, I. (2013) 'Isolation of Equine Multipotent Mesenchymal Stromal Cells by Enzymatic Tissue Digestion or Explant Technique: Comparison of Cellular Properties'. *BMC Veterinary Research,* 9(221): 3-14.

Godoy, P., Hewitt, J. N., Albrecht, U. et al., (2013) 'Recent Advances in 2D and 3D in vitro Systems Using Primary Hepatocytes, Alternatives Hepatocyte Sources and Non-Parenchymal Liver Cells and their Use in Investigating Mechanisms of Hepatotoxicity, Cell Signalling and ADME'. *Arch Toxicol,* 87: 1315-1530.

Goodman, S. A., May, S. A., Heinegard, D. and Smith, R. K. W. (2004) 'Tenocyte Response to Cyclical Strain and Transforming Growth Factor Beta is Dependent upon Age and Site of Origin'. *Biorheology,* 41(5): 613-628.

Grant, T. M., Thompson, M. S., Urban, J. and Yu, J. (2013) 'Elastic Fibres are Broadly Distributed in Tendon and Highly Localized aroud Tenocytes'. *Journal of Anatomy,* 222: 573-579.

Gressner, O. A., Weiskirchen, R. and Gressner, A. M. (2007) 'Evolving Concepts of Liver Fibrogenesis Provide New Diagnostic and Therapeutic Options'. *Comp Hepatol*, 6(7): 1-13.

Grigg. N.L., Wearing, S.C., O'Toole, J.M. and Smeathers, J.E. (2012) 'Achilles Tendinopathy Modulates Force Frequency Characterised of Eccentric Exercise'. *Medicine and Science in Sports and Exercise,* 520-526.

Gu, Y., Li, X., He, T., Jiang, Z., Hao, P. and Tang, X. (2014) 'The Antifibrosis Effects of Peroxisome Proliferator – Activated Receptor ɡ on Rat Corneal Wound Healing after Excimer Laser Keratectomy'. *PPAR Research,* 2014: 1-11.

Gumucio, J. P., Sugg, K. B. and Mendias, C. L. (2015) 'TGF-β Superfamily Signaling in Muscle and Tendon Adaptation to Resistance Exercise'. *Exerc Sport Sci Rev,* 43(2): 93-99.

Guo, X. and Wang, X. F. (2009) 'Signaling Cross-Talk Between TGF-β/BMP and Other Pathways'. *Cell Res,* 19(1): 71-88.

Gupta, G. S. (2012) *Animal Lectins: Form, Function and Clinical Application*, In Collaboration with Gupta, A. and Gupta, R. K. New York: Springer.

Heinemeier, K. M. and Kjaer, M. (2011) '*In Vivo* Investigation of Tendon Responses to Mechanical Loading'. *J. Musculoskelet. Neuronal Interact*, 11: 115-123.

Heinemeier, K. M., Olesen, J. L., Haddad, F., Schjerling, P., Baldwin, K. M. and Kjaer, M. (2009). 'Effect of Unloading Followed by Reloading on Expression of Collagen and Related Growth Factors in Rat Tendon and Muscle'. *J Appl Physiol*, 106(1): 178-186.

Heinemeier, K. M., Olesen, J. L., Schjerling, P., Haddad, F., Langberg, H., Baldwin, K. M. and Kjaer, M. (2007) 'Short-term Strength Training and the Expression of Myostatin and IGF-1 Isoforms in Rat Muscle and Tendon: Differential Effects of Specific Contraction Types'. *J Appl Physiol*, 102(2): 573-581.

Heinemeier, K. M., Schjerling, P., Heinemeier, J., Magnusson, S. P. and Kjaer, M. (2013) 'Lack of Tissue Renewal in Human Adult Achilles Tendon is Revealed by Nuclear Bomb ^{14}C'. *The FASEB Journal*, 27(5): 2074-2079.

Heinemeier, K. M., Skovgaard, D., Bayer, M. L., Qvortrup, K., Kjaer, A., Kjaer, M., Magnusson, S. P., Kongsgaard, M. (2012) 'Uphill Running Improves Rat Achilles Tendon Tissue Mechanical Properties and Alters Gene Expression without Inducing Pathological Changes'. *J Appl Physiol*, 113: 827-836.

Hellio Le Graverand, M. P., Eggerer, J., Sciore, P., Reno, C., Vignon, E., Otterness, I. and Hart, D. A. (2000) 'Matrix Metalloproteinase-13 Expression in Rabbit Knee Joint Connective Tissues: Influence of Maturation and Response to Injury'. *Matrix Biol*, 19(5):431-441.

Henriksen, M., Aaboe, J., Bliddal, H. and Langberg, H. (2009) 'Biomechanical Characteristics of the Eccentric Achilles Tendon Exercise. *J Biomech*., 42(16):2702–2707.

Hoffman, B. D., Grashoff, C. and Schwartz, M. A. (2011) 'Dynamic Molecular Processes Mediate Cellular Mechanotransduction'. *Nature*, 475: 316-323.

Holmes, D. F., Graham, H. K., Trotter, J. A. and Kadler, K. E. (2001) 'STEM/TEM Studies of Collagen Fibril Assembly'. *Micron*, 32(3): 273-285.

Horiguchi, M., Ota, M. and Rifkin, D. B. (2012) 'Matrix Control of Transforming Growth Factor-β Function'. *J Biochem*, 152(4): 321-329.

Hsieh, Y. F. and Turner, C. H. (2001) 'Effects of Loading Frequency on Mechanically Bone Formation'. *Journal of Bone and Mineral Research,* 16(5): 918-924.

Huisman, E., Lu, A., McCormack, R. G. and Scott, A. (2014) 'Enhanced Collagen Type I Synthesis by Hunan Tenocytes Subjected to Periodic *In Vitro* Mechanical Stimulation'. *BMC Musculoskeletal Disord,* 15(386): 1-8.

Humphrey, J. D., Dufresne, E. R. and Schwarts, M. A. (2014) 'Mechanotransduction and Extracellular Matrix Homeostasis'. *Nature Reviews Molecular Cell Biology,* 15: 802-812.

Huston, M. and Speed, C. (2011) '*Sports Injuries'*. New York: Orford University Press.

Iatridis, J. C., Maclean, J. J., Roughley, P. J. and Alini, M. (2013) 'Effects of Mechanical Loading on Intervertebral Disc Metabolism *In Vivo*'. *J Bone Joint Surg Am*, 88(0 2): 41-46.

Ingber, D. E. (2006) 'Cellular Mechanotransduction: Putting all the Pieces Together Again'. *The FASEB Journal*, 20: 811-827.

Ireland, D., Harrall, R., Curry, V., Holloway, G., Hackney, R., Hazleman, B. and Riley, G. (2001) 'multiple Changes in Gene Expression in Chronic Human Achilles Tendinopathy'. *Matrix Biol*, 20(3): 159-169.

Jaalouk, D. E. and Lammerding, J. (2009) 'Mechanotransduction Gone Awry'. *Molecular Cell Biology,* 10: 63-73.

Javelaud, D. and Mauviel, A. (2004) 'Mammalian Transforming Growth Factor-Betas: Smad Signaling and Physio-Pathological Roles'. *Int J Biochem Cell Biol*, 36(7): 1161-1165.

Jelinsky, S. A., Rodeo, S. A., Li, J., Gulotta, L. V., Archambault, J. M. and Seeherman, H. J. (2011) 'Regulation of Gene Expression in Human Tendinopathy'. *BMC Musculoskeletal Disorders,* 12(86):1-12.

Jenkins, G. (2008) 'The Role of Proteases in Transforming Growth Factor Beta Activation'. *Int J Biochem Cell Biol*, 40(6-7): 1068-1078.

Jing, W., Xiao, J., Xiong, Z., Yang, X., Huang, Y., Zhou, M., Chen, S., Lin, Y. and Tian, W. (2011) 'Explant Culture: An Efficient Method to Isolate Adipose-Derived Stromal Cells for Tissue Engineering'. *Artifical Organs*, 35(2): 105-112.

Jobling, M. E., Mott, J. D., Finnegan, M. T., Jurukovski, V., Erickson, A. C., Walian, P. J., Taylor, S. E., Ledbetter, S., Lawrence, C. M., Rifkin, D. B. and Barcellos-Hoff, M. H. (2006) 'Isoform-Specific Activation of Latent Transforming Growth Factor Beta (LTGF-Beta) by Reactive Oxygen Species'. *Radiat Res*, 166(6): 839-848.

Jones, E. R. (2012) 'Investigation of the Effects of Mechanical Strain in Human Tenocytes'. PhD Thesis. University of East Anglia, Biological Sciences.

Jones, E. R., Jones, G. C., Legerlotz, K. and Riley, G. P. (2013) 'Cyclical Strain Modulates Metalloprotease and Matrix Gene Expression Human Tenocytes via Activation of TGFβ'. *Biochim Biophys Acta*, 1833(12):2596-2607.

Jones, G. C., Corps, A. N., Pennington, C. J., Clark, I. M., Edwards, D. R., Bradley, M. M., Hazeleman, B. L. and Riley, G. P. (2006) 'Expression Profiling of Metalloproteinases and Tissues Inhibitors of Metalloprteinases in Normal and Degenerate Human Achilles Tendon'. *Arthritis Rheum*, 54(3):832-842.

Jonsson, P. and Alfredson, H. (2005) 'Superior Results with Eccentric Compared to Concentric Quadriceps Training in Patients with Jumper's Knee: A Prospective Randomised Study'. *Br J Sports Med*, 39: 847-850.

Jozsa, L. and Kannus, P. (1997) *Human Tendons: Anatomy, Physiology and Pathology*. Champaign-Urbana: Human Kinetics Publisher.

Juneja, S. C. and Veillette, C. (2013) 'Defects in Tendon, Ligament, and Enthesis in Response to Genetic Alterations in Key Proteoglycans and Glycoproteins: A Review'. *Arthritis*, 2013: 1-30.

Jurrmann, N., Brigelius-Flohe, R. and Bol, G. F. (2005) 'Curcumin Blocks Interleukin-1 (IL-1) Signalling by Inhibiting the Recruitment of the IL-1 Receptoe-Associated Kinase IRAK in Murine Thymoma EL-4 Cells'. *J Nutr,* 135(8): 1859-1864.

Kader, D., Saxena, A. Movin, T. and Maffulli, N. (2002) 'Achilles Tendinopathy: Some Aspects of Basic Science and Clinical Management'. *Br J Sports,* 36: 239-249.

Kadler, K.E., Holmes, D.F., Trotter, J.A. and Chapman, J.A. (1996) 'Collagen Fibril Formation'. *Biochem,* 316: 1-11.

Kalliokoski, K. K., Langberg, H., Ryberg, A. K., Scheede-Bergdahl, C., Doessing, S., Kjaer, A., Boushel, R., Kjaer, M. (2005) 'The Effect of Dynamic Knee-Extension Exercise on Patellar Tendon and Quadriceps Femoris Muscle Glucose Uptake in Humans Studied By Positron Emission Tomography'. *J Appl Physiol*, 99: 1189–1192.

Kannus, P. (2000) 'Structure of the Tendon Connective Tissue'. *Scand J Med Sci Sports*, 10: 312-320.

Kastelic, J., Galeski, A. and Baer, E. (1978) 'The Multicomposite Structure of Tendon'. *Connect Tissue Res*, 6(1): 11-23.

Kaux, J.F., Drion, P., Libertiaux, V., Colige, A., Hoffmann, A., Nusgens, B., Besancon, B., Forthomme, B., Le-Goff, C., Franzen, R., Defraigne, J.O., Cescotto, S., Rickert, M., Criellaard, J.M. and Croisier, J.L. (2011) 'Current Options of Tendinopathy'. *Journal of Sport Science and Medicine*, 10: 238-253.

Khalfaoui, S., Eichhorn, V., Karagiannidis, C., Bayh, I., Brockmann, M., Pieper, M., Windisch, W., Schildgen, O. and Schildgen, V. (2016) 'Lung Infection bt Human Bocavirus Induces the Release of Profibrotic Mediator Cytokines *In Vivo* and *In Vitro*'. *PLoS One*, 25;11(1): e0147010.

Khalil, N. (1999) 'TGF-β form Latent to Active'. *Microbes and Infection*, 1(15): 1255-1263.

Khan, K.M., Cook, J.L. Bonar, F., Harcourt, P. and Astrom, M. (1999) 'Histopathology of Common Tendinopathies: Update and Implcations for Clinical Management'. *Sports Med*, 27(6): 393-408.

Killian, M.L., Cavinatto, L., Galatz, L.M. and Thomopoulos, S. (2012) 'The Role of Mechanobiology in Tendon Healing'. *Journal of Shoulder and Elbow Surgery / American Shoulder and Elbow Surgeons*, 21(2): 228-237.

Kingma, J. J., De Knikker, R., Wittink, H. M. and Takken, T. (2007). 'Eccentric Overload Training in Patients with Chronic Achilles Tendinopathy: A Systematic Review'. *Br J Sports Med*, 41(6): e1-e5.

Kjær, M. (2004) 'Role of Extracellular Matrix in Adaptation of Tendon and Skeletal Muscle to Mechanical Loading'. *Physiological Review*, 84(2): 649-698.

Kjær, M., Langberg, H., Heinemeier, K., Bayer, M. L., Hansen, M., Holm, L., Doessing, S., Kongsgaard, M., Krogsgaard, M. R. and Magnusson, S. P. (2009) 'From Mechanical Loading to Collagen Synthesis, Structural Changes and Function in Human Tendon.' *Scandinavian Journal of Medicine and Science in Sports*, 19: 500–510.

Kjær, M., Langberg, H., Miller, B.F., Boushel, R., Crameri, R., Koskinen, S., Heinemeier, K., Olesen, J. L., Dossing, S., Hansen, M., Pedersen, S. G., Rennie, M. J. and Magnusson, P. (2005) 'Metabolic Activity and Collage Turnover in Human Tendon in Response to Physical Activity'. *J Musculoskelet Neuronal InteractI*, 5(1): 41-52.

Kondratko-Mittnacht, J., Duenwald-Kuchi, S., Lakes, R. S., Vanderby Jr., R. (2015) 'Shear Loads Induce Cellular Damage in Tendon Fascicles'. *Journal of Biomechanics*, 48: 3299-3305.

Kountouris, A. and Cook, J. (2007) 'Rehabilitation of Achilles and Patella Tendinopathies'. *Best Practice & Research Clinical Rheumatology*, 21(2):295-316.

Krstic, J. and Santibanez, J. E. (2014) 'Transforming Growth Factor-Beta and Matrix Metalloproteinases: Functional Interactions in Tumor Stroma-Infiltrating Myeloid Cells'. *The Scientific World Journal*, 2014: 1-14.

Kuchipudi, S. V., Tellabati, M., Nelli, R. K., White, G. A., Perez, B. B., Sebastian, S., Slomka, M. J., Brookes, S. M., Brown, I. H., Dunham, S. P. and Chang, K. C. (2012) '18s rRNA is a Reliable Normalisation Gene for Real Time PCR Based on Influenza Virus Infected Cells'. *Virol J*, 8(9): 230.

Lai, A., Simonaro, C. M., Schuchman, E. H., Ge, Y., Laudier, D. M. and Latridis, J. C. (2012) 'Structural, Composition, and Biomechanical Alterations of the Lumbar Spine in Rats with Mucopolysaccharidosis Type VI (Maroteaux-Lamy Syndrome)'. *Journal of Orthopaedic Research*, 31(4): 621-631.

Lairson, L. L., Henrissat, B., Davies, G. J. and Whithers, S. G. (2008) 'Glycosyltransferases: Structure, Function and Mechanisms'. *Annual Review of Biochemistry*, 77: 521-555.

Lamande, S. R. and Bateman, J.F. (1999) 'Procollagen Folding and assembly: The Role of Endoplasmic Reticulum Enzymes and Molecular Chaperones'. *Semin Cell Dev Biol*, 10(5): 455-64.

Langberg, H., Ellingsgaard, H., Madsen, T., Jansson, J., Magnusson, S. P., Aagaard, P. and Kjaer, M. (2007) 'Eccentric Rehabilitation Exercise Increase Peritendinous Type I Collagen Synthesis in Humans with Achilles Tendinosis'. *Scand J Med Sci Sports*, 17(1): 61-66.

Lanza, R., Langer, R. and Vacanti, J. (2007) *Principles of Tissue Engineering*. 3rd Edition. USA: Elsevier Academic Press.

Lavagnino, M., Arnoczky, S. P., Kepich, E., Caballero, O. and Haut, R. C. (2008) 'A Finite Element Model Predicts the Mechanotransduction Response of Tendon Cells to Cyclic Tensile Loading'. *Biomech Model Mechanobiol*, 7: 405-416.

Lavagnino, M., Arnoczky, S. P., Tian, T. and Vaupel, Z. (2003) 'Effect of Amplitude and Frequency of Cyclic Tensile Strain on the Inhibition of MMP-1 mRNA Expression in Tendon Cells: An *In Vitro* Study'. *Connect Tissue Res*, 44(3-4):181-187.

Lavagnino, M., Gardner, K. L. and Arnoczky, S. P. (2015) 'High Magnitude, *In Vitro*, Biaxial, Cyclic Tensile Strain Induces Actin Depolymerization in Tendon Cells'. *MLTJ Muscle, Ligaments and Tendons Journal CIC Edizioni Internazionali*, 5(2): 124-128.

Lavagnino, M., Wall, M. E., Little, D., Banes, A. J., Guilak, F. and Arnocsky, S. P. (2015) 'Tendon Mechanobiology: Current Knowledge and Future Research Opportunities'. *Journal of Orthopaedic Research*, 33(6): 813-822.

Legerlotz, K., Jones, E. R., Screen, H. R. C. and Riley, G. (2012) 'Increased Expression of IL6 Family Members in Tendon Pathology'. *Rheumatology*, 51:1161-1166.

Legerlotz, K., Jones, G. C., Screen, H. R. C. and Riley, G. P. (2013) 'Cyclic loading of Tendon Fascicles using a Novel Fatigue Loading System Increases Interleukin-6 Expression by Tenocytes'. *Scand J Med Sci Sports*, 23: 31-37.

Legerlotz, K., Schjerling, P., Langberg, H., Bruggemann, G. P. and Niehoff, A. (2007) 'The Effect of Running, Strength, and Vibration Strength Training on the Mechanical, Morphological, and Biochemical Properties of the Achilles Tendon in Rats'. *J Appl Physiol*, 102(2):564-572.

Leigh, D. R., Abreu, E. L. and Derwin, K. A. 'Changes in Gene Expression of Individual Matrix Metalloproteinases Differ in Response to Mechanical Unloading of Tendon Fascicles in Explant Culture'. *Journal of Orthopaedic Research,* 26: 1306-1312.

Lesur, I., Textoris, J., Loriod, B., Courbon, C., Garcia, S., Leone, M. and Nguyen, C. (2010) 'Gene Expression Profiles Charaterize Inflammation Stages in the Acute Lung Injury in Mice'. *PLoS One*, 5(7):1-14.

Lewis, J. S. (2010) 'Rotator Cuff Tendinopathy: A Model for the Continuum of Pathology and Related Management'. *Br J Sport Med,* 44: 918-923.

Lewis, G. and Shaw, K. M. (1997) 'Tensile Properties of Human Tendon Achilles: Effects of Donor Age and Strain Rate'. *J Foot Ankle Surg*, 36(6): 435-445.

Li, F. and Curry, T. E. (2009) 'Regulation and Function of Tissue Inhibitor of Metalloproteinase (TIMP) 1 and TIMP3 in Periovulatory Rat Granulosa Cells'. *Endocrinology*, 150(8): 3903-3912.

Lian, O.B., Engebretsen, L. and Bahr, R., (2005) 'Prevalence of Jumper's Knee among Elite Athletes from Different Sports: A Cross-Sectional Study'. *Am J Sports Med*, 33: 561-567.

Lichtwark, G. A. and Wilson, A. M. (2005) 'In vivo Mechanical Properties of the Human Achilles Tendon during One-Legged Hopping'. *The Journal of Experimental biology*, 208: 4715-4725.

Liu, X., Wu, H., Byrne, M., Krane, S. and Jaenisch, R. (1997) 'Type III Collagen is Crucial for Collagen Fibrillogenesis and for Normal Cardiovascular Development. *Proc. Natl. Acad Sci.*, 94: 1852-1856.

Lodish, H., Berk, A., Zipursky, S. L., Matsudaira, P., Baltimore, D. and Darnell, J. (2000) *Molecular Cell Biology*, 4th Edition, New York: W. H. Freeman and Company.

Lohrer, H., David, S. and Nauck, T. (2016) 'Surgical Treatment for Achilles Tendinopathy – A Systematic Review'. *BMC Musculoskeletal Disorder*, 17(207): 1-10.

Lopez-Maury, L., Marguerat, S. and Bahler, J. (2008) 'Tuning Gene Expression to Changing Environments: From Rapid Responses to Evolutionary Adaptation'. *Natural Reviews Genetics:* 9: 583-593.

Lorenz, D. and Reiman, M. (2011) 'The Role and Implementation of Eccentric Training in Athletic Rehabilitation: Tendinopathy, Hamstring Strains, and ACL Reconstruction'. *The International Journal of Sports Physical Therapy*, 6(1): 27-44.

Maeda, E., Fleischmann, C., Mein, C. A., Shelton, J. C., Bader, D. L. and Lee, D. A. (2010). Functional Analysis of Tenocytes Gene Expression in Tendon Fascicles Subjected to Cyclic Tensile Strain. *Connective Tissue Research*, 51(6): 434-444.

Maeda, E., Shelton, J. C., Bader, D. L. and Lee, D. A. (2009) 'Differential Regulation of Gene Expression in Isolated Tendon Fascicles Exposed to Cyclic Tensile Strain *In Vitro*'. *J Appl Physiol*, 106: 506-512.

Maffulli, N., Sharma, P. and Luscombe, K. L. (2004) 'Achilles Tendinopathy: Aetiology and Management'. *Journal of the Royal Society of Medicine*, 97: 472-476.

Maffulli, N., Renstrom, P. and Leadbetter, W. B. (2005) *Tendon Injuries: Basic Science and Clinical Medicine*, London: Springer.

Mafi, N., Lorentzon, R. and Alfredson, H. (2001) 'Superior Shor-Term Results with Eccentric Calf Muscle Training Compared to Concentric Training in a Randomised Prospective Multicenter Study on Patients with Chronic Achilles tendinosis'. *Knee Surg, Sports Traumatol, Arthrose*, 9: 42-47.

Maganaris, C. N., Narici, M. V. and Maffulli, N. (2008) 'Biomechanics of the Achilles Tendon'. *Disabil. Rehabil*, 269:1542-7.

Maganaris, C. N. and Paul, J. P. (2000) 'In vivo Human Tendinous Tissue Stretch upon Maximum Muscle Force Generation'. *Journal of Biomechanics*, 33(11): 1453-1459.

Maganussen, R. A., Dunn, W. R. and Thomson, A. B. (2009) 'Nonoperative Treatment of Midportion Achilles Tendinopathy: A Systematic Review'. *Clin J Sport Med*, 19(1): 54-64.

Magnusson, S. P., Narici, M. V., Maganaris, C. N. and Kjaer, M. (2008) 'Human Tendon Behaviour and Adaptation, *In Vivo*'. *J Physiol*, 586(1): 71-81.

Mani-Babu, S., Morrissey, D., Waugh, C., Screen, H. and Barton, C. (2014) 'The Effectiveness of Extracorporeal Shock Wave Therapy in Lower Limb Tendinopathy: A Systematic Review'. *The American Journal of Sports Medicine*. 1-9.

Massague, J. (2012) 'TGFβ Signalling in Context'. *Nature Reviews Molecular Cell Biology*, 13: 616-630.

Matuszewski, P.E., Chen, Y.L., Szczesny, S. E., Lake, S. P., Elliot, D. M., Soslowsky, L. J. and Dodge, G. R. (2012) 'Regional Variation in Human Supraspinatus Tendon Proteoglycans: Decorin, Biglycan, and Aggrecan'. *Connective Tissue Research*, 1-7.

Mazzocca, A. D., Chowaniec, D., McCarthy, M. B., Beitzel, K., Cote, M. P., McKinnon, W. and Arciero, R. (2012) 'In Vitro Changes in Human Tenocyte Cultures Obtained from Proximal Biceps Tendon: Multiple Passages Result in Changes in Routine Cell Markers'. *Knee Surg Sports Traumatol Arthrosc*, 20**:** 1666-72.

McCulloch, C. A., Downey, G. P. and El-Gabalwy, H. (2006) 'Signalling Platforms that Modulate the Inflammatory Response: New Targets for Drug Development'. *Nature Reviews Drug Discovery*, 5: 864-876.

McDuffee, L. A. (2012) 'Comparison of Isolation and Expansion Techniques for Equine Osteogenic Progenitor Cells from Periosteal Tissue'. *Can J Vet Res*, 76(2): 91-98.

Meada, E., Hagiwara, Y., Wang, J. H. C. and Ohashi, T. (2013) 'A New Experimental System for Simultaneous Application of Cyclic Tensile Strain and Fluid Shear Stress to Tenocytes *In Vitro*'. *Biomedical Microdevices*, 14(6): 1067-1075.

Merline, R., Schaefer, R. M. and Schaefer, L. (2009) 'The Matricellular Functions of Small Leucine-Rich Proteoglycans (SLRPs)'. *J Cell Commun Signal*, 3(3-4): 323-325.

Midwood, K. S. and Orend, G. (2009) 'The Role of Tenascin-C in Tissue Injury and Tumorigenesis'. *J Cell Commun Signal*, 3(3-4): 287-310.

Mihara, M., Moriya, Y., Kishimoto, T. and Ohsugi, Y. (1995) 'Interleukin-6 (IL-6) Induces the Proliferation of Synovial Fibroblastic Cells in the Presence of Soluble IL-6 Receptor'. *Br J Rheumatol*, 34:321-325.

Milan, A. M., Sugars, R. V., Embery, G. and Waddington, R. J. (2005) 'Modulation of Collagen Fibrillogenesis by Dentinal Proteoglycans'. *Calcif Tissue Int.*, 76(2): 127-135.

Millar, N. L., Hueber, A. J., Reilly, J. H., Xu, Y., Fazzi, U. G., Murrell, G. A. C. and Mclnnes, L. B. (2010) 'Inflammation is Present in Early Human Tendinopathy'. *The American Journal of Sports Medicine*, 38(10): 2085-2091.

Miller, B. F., Olesen, J. L., Hansen, M., Dossing, S., Crameri, R. M., Welling, R. J., Langberg, H., Flyvbjerg, A., Kjaer, M., Babraj, J. A., Smith, K., Rennie, M. J. (2005) 'Coordinated Collagen and Muscle Protein Synthesis in Human Patella Tendon and Quadriceps Muscle after Exercise'. *J. Physiol*, 567(Pt 3): 1021-33.

Mofrad, M. R. K. and Kamm, R. D. (2010) *Cellular Mechanotransduction: Diverse Perspectives from Molecules to Tissues*. New York: Cambridge University Press.

Molloy, T., Wang, Y. and Muurrell, G. (2003) 'The Roles of Growth Factors in Tendon and Ligament Healing'. *Sports Med*, 33(5): 381-394.

Moore, J. E. and Maitland, D. J. (2014) *Biomedical Technology and Devices*. 2nd edition, Boca Raton: CRC Press.

Mousavizadeh, R., Khosravi, S., Behzad, H., McCormack, R. G., Duronio, V. and Scott, A. (2014) 'Cyclic Strain Alters the Expression and Release of Angiogenic Factors by Human Tendon Cells'. *PLoS ONE*, 9(5): e97356.

Murphy-Ullrich, J. E. and Poczatek, M. (2000) 'Activation of Latent TGF-Beta by Thrombospondin-1: Mechanism and Physiology'. *Cytokine Growth Factor Rev*, 11(1-2): 59-69.

Nagaraj, N. S. and Datta, P. K. (2010) 'Targeting the Transforming Growth Factor-β Signalling Pathway in Human Cancer' *Expert Opin Investig Drugs*, 19(1): 77-91.

Nagase, H. and Woessner, Jr. J. F. (1999). 'Matrix Metalloproteinases'. *J Biol Chem*, 274(31): 21491-21494.

Nakama, K., Gotoh, M., Yamada, T., Mitsui, Y., Yasukawa, H., Imaizumi, T., Higuchi, F. and Nagata, K. (2006) 'Interleukin-6 Induced Activation of Signal Transducer and Activator of Transcription-3 in Ruptured Rotator Cuff Tendon'. *J Int Med Res*, 34:624-631.

Neuzillet, C., Tijeras-Raballand, A., Cohen, R., Cros, J., Faivre, S., Raymond, E. and De Gramont, A. (2015) 'Targeting the TGFβ Pathway for Cancer Therapy'. *Pharmacology and Therapeutics*, 147: 22-31.

Nordin, M. and Frankel, V.H. (2001) *Basic Biomechanics of the Musculoskeletal System*. 3rd Edition, Maryland, USA: Lippinocott Williams & Wikins.

Norregaard, J., Larsen, C. C., Bieler, T. and Lanberg, H. (2007) 'Eccenttric Exercise in Treatment of Achilles Tendinopathy'. *Scand J Med Sci Sports*, 17: 133-138.

Nunley, J. A. (2009) *The Achilles Tendon: Treatment and Rehabilitation*. New York: Springer.

O'Brien, M. (1997) 'Structure and Metabolism of Tendons'. *Scand J Med Sci Sports*, 7: 55-61.

Ogden, J. A., Toth-Kischkat, A. and Schultheiss, R. (2001) 'Principles of Shock Wave Therapy'. *Clinical Orthopaedics and Related Research*, 387: 8-17.

Olesen, J. L., Heinemeier, K. M., Haddad, F., Langberg, H., Flybjerg, A., Kjaer, M. and Baldwin, K. M. (2006) 'Expression of Insulin-like Growth Factor I, Insulin-like Growth Factor Binding Proteins, and Collagen mRNA in Mechanically Loaded Plantaris Tendon'. *J Appl Physiol*, 101(1): 183-186.

Omelyanenko, N. and Slutsky, L. *Editor: Mironov, S.* (2014) *Connective Tissue: Histophysiology, Biochemistry, Molecular Biology*. Boca Raton, Florida: CRC Press

O'Neill, S., Watson, P. J. and Berry, S. (2015) 'Why are Eccentric Exercises Effective for Achilles Tendinopathy?'. *Int J Sports Phys Ther*, 10(4): 552-562.

Orr, A. W., Helmke, B. P., Blackman, B. R. and Schwartz, M. A. (2006) 'Mechanisms of Mechanotransduction'. *Developmetal Cell*, 10: 11-20.

Ozbabacan, S. E. A., Gursoy, A., Nussinov, R. and Keskin, O. (2014) 'The Structural Pathway of Interleukin 1 (IL-1) Initiated Signaling Reveals Mechanism of Oncogenic Mutations and SNPs in Inflammation and Cancer'. *PLoS Computation Biology*, 10(2): e1003470.

Ozcivici, E., Luu, Y. K., Alder, B., Qin, Y. X., Rubin, J., Judex, S. and Rubin, C. T. (2010) 'Mechanical Signals as Anabolic Agents in Bone'. *Nat. Rev. Rheumatol.*, 6: 50-59.

Pahl, A. and Brune, K. (2002) 'Gene Expression Changes in Blood after Phlebotomy: Implications for Gene Expression Profilling'. *Blood*, 100: 1094-1095.

Patel, D. (2015) 'A Novel Fibre Composite System to Investigate Tenocyte Metabolism under Physiological and Pathological Loading Conditions'. PhD Thesis. Queen Mary University of London, School of Engineering and Material Science.

Patel, D., Bryant, S. J., Riley, G., Jones, E. andScreen, H. R. C. (2014) 'Human Tenocyte Metabolism Under Pathological And Physiological Loading Conditions'. *British Journal of Sports Medicine*, 48: A51.

Patterson-Kane, J. C., Becker, D. L. and Rich, T. (2012) 'The Pathogenesis of Tendon Microdamage in Athletes: The Horse as a Natural Model for Basic Cellular Research'. *J Comp Path*, 147: 227-247.

Peltonen, J., Cronin, N. J., Stenroth, L., Finni, T. and Avela, J. (2013) 'Viscoelastic Properties of the Achilles Tendon *In Vivo*'. *Springerplus*, 2(212): 1-8.

Perrimon, n. and Bernfield, M. (2001) 'Cellular Function of Proteoglycans – An Overview'. *Cell and Development Biology*, 12: 65-67.

Phillips, J. B. and Brown, R. (2011) 'Micro-Structured Materials and Mechanical Cues in 3D Collagen Gel'. *Molecular Biology*, 695: 183-198.

Pingel, J., Fredberg, U., Mikkelsen, L. R., Schjerling, P., Heinmeier, K. M., Kjaer, M., Harrison, A. and Langberg, H. (2013) 'No Inflammatory Gene-Expression Response to Acute Exercise in Human Achilles Tendinopathy'. *Eur J Appl Physiol*, 113: 2101-2109.

Plant, A. L., Bhadriraju, K., Spurlin, T. A. and Elliott, J. T. (2009) 'Cell Response to Matrix Mechanics: Focus on Collagen'. *Molecular Cell Research*, 1793(5): 893-902.

Popov, C., Burggraf, M., Kreja, L., Ignatius, A., Schieker, M. and Docheva, D. (2015) 'Mechanical Stimulation of Human Tendon Stem / Progenitor Cells Results in Upregulation of Matrix Proteins, Integrins and MMPs, and Activation of p38 and ERK1/2 Kinases'. *BMC Molecular Biology*, 16(6): 1-11.

Pullan, S., Wilson, J., Metcalfe, A., Edwards, G. M., Goberdham,N., Tilly, J., Hickman, J. A., Dive, C. and Streuli, C. H. (1996) 'Requirement of Basement Membrane for the Suppression of Programmed Cell Death in Mammry Epithelium'. *Journal of Cell Science*, 109: 631-642.

Puxkandi, R., Zizak, I., Paris, O., Keckes, J., Tesch, W., Bernstorff, S., Purslow, P. and Fratzl, P. (2002) 'Viscoelastic Properties of Collagen: Synchrotron Radiation Investigation and Structural Model'. *Philos Trans. Roy. Soc. B.*, 357: 191-197.

Ranson, C. and Young, M. (2011) 'The Role of Targeted Exercises in the Management of Achilles and Patellar Tendinopathy in Sport'. *European Musculosketal Review,* 6(2):131-136.

Rees, J.D., Lichtwark, G.A., Wolman, R.L. and Wilson, A.M. (2008) 'The Mechanism for Efficacy of Eccentric Loading in Achilles Tendon Injury; An *in vivo* Study in Humans'. *Rheumatology*, 47: 1493-1497.

Rees, J. D., Stride, M. and Scott, A. (2013) 'Tendon – Time to Revisit Inflammation'. *Br J Sports Med,* 1-7.

Rigozzi, S., Muller, R., Stemmer, A. and Snedeker, J. G. (2012) 'Tendon Glycosaminoglycan Proteoglycan Sidechain Promote Collagen Fibril Sliding – AFM Observations at the Nanoscale'. *Journal of Biomechanics*, 46(4): 813-8.

Riley, G. (2005) 'Chronic Tendon Pathology: Molecular Basis and Therapeutic Implication'. *Expert Reviews in Molecular Medicine*, 7(5): 1-25.

Riley, G. P., Curry, V., DeGroot, J., Van El, B., Verzijl, N., Hazleman, B. L. and Bank, R. A. (2002) 'Matrix Metalloproteinase Activities and their Relationship with Collagen Remodelling in Tendon Pathology'. *Matrix Biol*, 21(2):185-195.

Risbud, M. V. and Shapiro, I. M. (2014) 'Role of Cytokines in Intervertebral Disc Degeneration: Pain and Disc Content'. *Nature Reviews Rheumatology*, 10: 44-56.

Rompe, J.D., Nafe, B., Furia, J.P. and Maffulli, N. (2007) 'Eccentric Loading, Shock-Wave Treatment, or a Wait-and-See Policy for Tendinopathy of the Main Body of Tendo Achillis: A Randomized Controlled Trial'. *American Journal of Sports Medicine*, 35(3): 374-383.

Root, M. L., Orien, W. and Weed, J. H. (1977), *Normal and Abnormal Function of the Foot,* Vol 2, Los Angeles: Clinical Biomechanics Corporation.

Rossert, J. and De Crombrugghe, B., (2002), *Type I Collagen: Structure, Synthesis and Regulation*, In: Bilezkian, J. P., Raisz, L. G. and Rodan, G. A. (Eds.), *Principles in Bone Biology*, pp. 189–210, Orlando: Academic Press.

Rubin, C. T. and Lanyon, L. E. (1984) 'Regulation of Bone Formation by Applied Dynamic Loads'. *J Bone Joint Surg Am*, 66(3): 397-402.

Rubinacci, A., Marenzana, M., Cavani, F., Colasante, F., Villa, I., Willnecker, J., Moro, G. L., Spreafico, L. P., Ferretti, M., Guidobono, F. and Marotti, G. (2008) 'Ovariectomy Sensitizes Rat Cortical Bone to Whole-Body Vibration'. *Calcif Tissue Int*, 82: 316-326.

Rumian, A.P., Wallace, A.L., and Birch, H.L., 2007, 'Tendon and Ligament Are Anatomically Distinct But Overlap in Molecular and Morphological Features-A Comparative Study in an Ovine Model', *Journal of Orthopaedic Reasearch*, **25,** 458-464.

Sandhu, E., Miles, J. D., Dahners, L. E., Keller, B. V., Weinhold, P. S. (2011) 'Whole Body Vibration Increase Area and Stiffness of the Flexor Carpi Ulnaris Tendon in the Rat'. *Journal of Biomechanics*, 44(6): 1189-1191.

Sakiyama, S. E., Schense, J. C. and Hubbell, J. A. (1999). 'Incorporation of Heparin-Binding Peptides into Fibrin Gels Enhances Neurite Extension: An Example of Designer Matrices in Tissue Engineering'. *FASEB J*, 13(15): 2214-24.

Samiric, T., Parkinson, J., Ilic, M.Z., Cook, J., Feller, J.A. and Handley, C.J. (2009) 'Changes in the Composition of the Extracellular Matrix in Patellar Tendinopathy'. *Matrix Biology*, 28: 230-236.

Sasamura, H., Shimizu-Hirota, R., Nakaya, H. and Saruta, T. (2001) 'Effects of AT1 Receptor Antagonist on Proteoglycan Gene Expression in Hypertensive Rats. *Hypertens Res*, 24: 165−172.

Schechtman, H. and Bader, D. L. (1997). '*In Vitro* Fatigue of Human Tendons'. *Journal of Biomechanics*. 30:829-835.

Schnatwinkel, C. and Bryant, S. J. (2014) 'The Role of Integrin-Alpha2 Signaling during Mechanotransduction in Tenocytes Tissue Homeostasis'. *ORS Annual Meeting*.

Schulze-Tanzil, G., Mobasheri,, A., Clegg, P. D., Sendzik, J., John, T. and Shakibaei, M. (2004) 'Cultivation of Human Tenocytes in High Density Culture'. *Histochem Cell Biol*, 122(3): 219-228.

Scott, A., Danielson, P., Abraham, T., Fong, G., Sampaio, A. V. and Underhill, T. M. (2011) 'Mechanical Force Modulates Scleraxis Expression in Bioartifical Tendons'. *J Musculoskelet Neuronal Interact*, 11(2): 124-132.

Scott, A., Docking, S., Vicenzino, B., Alfredson, H., Zwerver, J., Lundgreen, K., Finlay, O., Pollock, N., Cook, J. L., Fearon, A., Purdam, C. R., Hoens, A., Rees, J. D., Goetz, T. J. and Danielson, P. (2013) 'Sports and Exercise-Related Tendinopathies: A Review of Selected Topical Issues by Participants of the Second International Scientific Ttendinopathy Symposium (ISTS) Vancouver 2012'. *Br J Sports Med*, 00: 1-12.

Scott, A., Khan, K. M., Heer, J., Cook, J. L., Lian, O. and Duronio, V. (2005) 'High Strain Mechanical Loading Rapidly Induces Tendon Apoptosis: An *Ex Vivo* Rat Tibialis Anterior Model'. *Br J Sports Med*., 39:1–4.

Screen, H. R. C., Lee, D. A., Bader, D. L. and Shelton, J. C. (2004) 'An Investigation into the Effects of the Hierarchical Structure of Tendon Fascicles on Micromechanical Properties'. *Proc Inst Mech Eng H*, 218(12): 109-119.

Screen, H. R. C., Shelton, J. C., Bader, D. L. and Lee, D. A. (2005) 'Cyclic Tensile Strain Upregulates Collagen Synthesis in Isolated Tendon Fascicles'. *Biomechanical and Biophysical Research Communications*, 336(2): 424-429.

Screen, H. R. C., Toorani, S. and Shelton, J. C. (2013) 'Microstructural Stress Relaxation Mechanics in Functionally Different Tendons'. *Medical Engineering and Physics*, 35(1): 96-102.

Semmler, J.G., Tucker, K.J., Allen, T.J. and Proske, U. (2007) 'Eccentric Exercise Increases EMG Amplitude and Force Fluctuations during Submaximal Contractions of Elbow Flexor Muscles'.*Journal of Applied Physiology*, 103(3): 979-989.

Sems, A., Dimeff, R. and Lannotti, J.P. (2006) 'Extracorporeal Shock Wave Therapy in the Treatment of Chronic Tendinopathy'. *Jounrnal of the American Academy of Orthopaedic Surgeons*, 14(4): 195-205.Schechtman, H. and Bader, D. L. (1997) "In vitro fatigue of human tendons." *Journal of Biomechanics*. 30: 829–835.

Sharma, P. and Maffulli, N. (2006) 'Biology of tendon Injury: healing, modelling and Remodeling'. *J Musculoskelet Neuronal Interact*, 6(2): 181-190.

Shepherd, J. H., Legerlotz, K., Demirci, T., Klemt, C., Riley, G. P. and Screen, H. R.C. (2014) 'Functionally Distinct Tendon Fascicles Exhibit Different Creep and Stress Relaxation Behaviour'. *Proc Inst Mech Eng H: Journal of Engineering in Medicine*, 228(1): 49-59.

Shi, Y. and Massague, J. (2003). 'Mechanisms of TGF-beta Signaling from Cell Membrane to the Nucleus'. *Cell*, 113(6): 685-700.

Shi, M., Zhu, J., Wang, R., Chen, X., Mi, L., Waiz, T. and Springer, T. A. (2011) 'Latent TGF-β Structure and Activation'. *Nature*, 474: 343-349.

Shukunami, C., Takimoto, A., Oro, M. and Hiraki, Y. (2006) 'Scleraxis Positively Regulates the Expression of Tenomodulin, a Differentiation Marker of Tenocytes'. *Dev Biol*, 1;298(1): 234-247.

Skutek, M. Van Griensven, M. Zeichen, J., Brauer, N. and Bosch, U. (2001) 'Cyclic Mechanical Stretching Enhances Secretion of Interleukin 6 in Human Tendon Fibroblasts'. *Knee Suurg Sports Traumatol Arthrosc*, 9(5):322-326.

Smidt, N., Van de Windt, D. A. W. M., Assendelft, W. J. J., Deville, W. L. J. M., Korthals-de Bos, I. B. C. and Bouter, L. M. (2002) 'Corticosteroid Injections, Physiotherapy, or a Wait-and-See Policy for Lateral Epicondylitis: A Randomised Controlled Trial'. *The Lancet*, 339: 657-662.

Souza, L. M. D., Bittar, J. D., Silva, I. C. R. D., Toledo, O. A. D., Birigido, M. D. M. and Pocas-Fonseca, M. J. (2010) 'Comparative Isolation Protocols and Characterization of Stem Cells from Human Primary and Permanent Teeth Pulp'. *Braz. J. Oral Sci.*, 9: 427-433.

Stanish, W. D., Rubinovich, R. M. and Curwin, S. (1986) 'Eccentric Exercise in Chronic Tendinitis'. *Clin Orthop Relat Res*, 208: 65-68.

Stanton, H., Melrose, J., Little, C. B. and Fosang, A. J. (2011) 'Proteoglycan Degradation by the ADAMTS Family of Proteinases'. *Biochimica et Biophysica Acta*, 1812: 1616-1629.

Stenroth, L., Peltonen, J., Cronin, N. J., Sipila, S. and Finni, T. (1985) 'Age-Related Differences in AAchilles Tendon Properties and Triceps Surae Muscle Architecture *In Vivo*'. *J Appl Physiol*, 113(10): 1537-1544.

Sun, H. B., Andarawis-Puri, N., Li, Y., Fung, D.T., Lee, J. Y., Wang, V. M., Basta-Pljakic, J., Leong, D. J., Serevsky, J. B., Ros, S. J., Klug, R. A., Braman, J., Schaffler, M. B., Jepsen, K. J. and Flatow, E. L. (2010) 'Cycle-Dependent Matrix Remodelling Gene Expression Response in Fatigue-Loaded Rat Patellar Tendons'. *J Orthop Res*, 28(10):1380-1386.

Sun, H. B., Yonghui, L., Fung, D. T., Majeska, R. J., Schaffler, M. B. and Flatow, E. L. (2008) 'Coordinate Regulation of IL-1β and MMP-13 in Rat Tendons Following Subrupture Fatigue Damage'. *Clin Orthop Relat Res,* 466(7): 1555-1561.

Sutmuller, T., Brujin, J. A. and De Heer, E. (1997) 'Collagen Types VII and X, Two Non-Fibrillar Short-Chain Collagens. Structure Homologies, Functions and Involvement in Pathology'. *Hitology and Histopathology*, 12: 557-566.

Sweeney, E., Chaudhry, S., Screen, H., Woledge, R., Bader, D., Maffulli, N. and Morrissey, D. (2011) 'The Effect of Eccentric and Concentric Loading Speed on the Normal Achilles Tendon: An *In Vivo* Biomechanical Study'. *Br J Sports Med*, 45(2): e1.

Szczodry, M., Zhang, J., Lim, C. T., Davitt, H. L., Yeager, T., Fu, F. and Wang, J. H-C. (2009) 'Treadmill Running Exercise Results in the Presence of Numerous Myofibroblasts in Mouse Patellar Tendons'. *J Orthop Res,* 27(10):1373-1378.

Takai, S., Woo, S. L. Y., Horibe, S., Tung, D. K. L. and Gelberman, R. H. (1991) 'The Effects of Frequency and Duration of Controlled Passive Mobilization on Tendon Healing'. *Journal of Orthopaedic Research*, 9(5): 705-713.

Tan, S.C. and Chan, O. (2008) 'Achilles and Patellar Tendinopathy: Current Understanding of Pathophysiology and Management'. *Disability and Rehabilitation*, 30(20-22): 1608-1615.

Teitz, C. C., Garrett, W. E., Minaci, A., Lee, M. H. and Mann, R. A. (1997) 'Tendon Problems in Athletic Individuals'. *J Bone and Joint Surg*, 79:138-152.

Thomopoulos, S., Birman, V. and Genin, G. M. (2013) *Structural Interfaces and Attachments in Biology*. New York: Springer.

Thornton, G. M., Shao, X., Chung, M., Sciore, P., Boorman, R. S., Hart, D. A. and Lo, I. K. Y. (2008) 'Changes in Mechanical loading lead to Tendon-Specific Alteration in MMP and TIMP expression: Influence of Stress Deprivation and Intermittent Cyclic Hydrostatic Compression on Rat Supraspinatus and Achilles Tendons'. *Br J Sports Med*, 44: 698-703.

Thorpe, C. T., Birch, H. L., Clegg, P. D. and Screen, H. R. C. (2013c) 'The Role of the Non-Collagenous Matrix in Tendon Function'. *International Journal of Experimental Pathology*, 94(4): 248-259.

Thorpe, C. T., Chaudhry, S., Lei, I. I., Varone, A., Riley, G. P., Birch, H. L., Clegg, P. D. and Screen, H. R. C. (2014) 'Tendon Overload Results in Alterations in Cell Shape and Increased Markers of Inflammation and Matrix Degradation'. *Scand J Med Sci Sports*, 1-12.

Thorpe, C. T., Chaudhry, S., Lei, I. I., Varone, A., Riley, G. P., Birch, H. L., Clegg, P. D. and Screen, H. R. C. (2015b) 'Tendon Overload Results in Alterations in Cell Shape and Increased markers of Inflammation and matrix Degradation'. *Scand J Med Sci Sports*, 25(4): e381-e391.

Thorpe, C. T., Godinho, M. S. C., Riley, G. P., Birch, H. L., Clegg, P. D. and Screen, H. R. C. (2015a) 'The Interfascicular Matrix Enables Fascicle Sliding and Recovery in Tendon, and Behaves more Elastically in Energy Storing Tendons'. *J Mech Behav Biomed Mater*, 52: 85-94.

Thorpe, C. T., Karunaseelan, K. J., Chieng Hin, J. N., Riley, G. P., Birch, H. L., Clegg, P. D. and Screen, H. R. C. (2016b) 'Distribution of Proteins within Different Compartments of Tendon Varies According to Tendon Type'. *Journal of Anatomy*, 1-9.

Thorpe, C.T., Klemt, C., Riley, G.P., Birc, H.L., Clegg, P.D. and Screen, H. R. C. (2013a) 'Helical Sub-Structure in Energy-Storing Tendons Provide a Possible Mechanism for Efficient Energy Storage and Return'. *Acta Biomater*, 9(8): 7948-7956.

Thorpe, C. T., Peffers, M. J., Simpsson, D., Halliwell, E., Screen, H. R. C. and Clegg, P. D. (2016c) 'Anatomical Heterogeneity of Tendon: Fascicular and Interfascicular Tendon Compartments have Distinct Proteomic Composition'. *Scientific Reports,* 1-12.

Thorpe, C. T., Riley, G. P., Birch, H. L., Clegg, P. D. and Screen, H. R. C. (2014) 'Fascicles from Energy-Storing Tendons Show an Age-Specific Response to Cyclic Fatigue Loading'. *J R Soc Interface,* 11(92): 1-10.

Thorpe, C. T., Riley, G. P., Birch, H. L., Clegg, P. D. and Screen, H. R. C. (2016a) 'Fascicles and the Interfascicular Matrix Show Adaptation for Fatigue Resistance in Energy Storing Tendons'. *Acta Biomater*, 15(42): 308-315.

Thorpe C. T., Udeze, C. P., Birch, H. L., Clegg, P. D. and Screen, H. R. C. (2012) 'Specialization of Tendon Mechanical Properties Results from Interfascicular Differences'. *J. R. Soc. Interface,* 9:3108–3117.

Thorpe, C. T., Udeze, C. P., Birch, H. L.,, Clegg, P. D. and Screen, H. R. C. (2013b) 'Capacity for Sliding between Tendon Fascicles Decreases with Ageing Injury Prone Equine Tendons: A Possible mechanism for Age-Related Tendinopathy?'. *European Cells and Materials,* 25: 48-60.

Tibbitt, M. W. and Anseh, K. S. (2009) 'Hydrogels as Extracellular Matrix Mimics for 3D Cell Culture'. *Biotechnol Bioeng.,* 103(4): 655-663.

Tol, J. L., Spiezia, F. and Maffuli, N. (2012) 'Neovascularization in Achilles Tendinopathy: Have we been Chasing a Red Herring?'. *Knee Surg Sports Traumatol Arthrosc*, 1-4.

Torcasio, A., Van Lenthe, G. H. and Van Oosterwyck, H. (2008) 'The Importance of Loading Frequency, Rate and Vibration for Enhancing Bone Adaptation and Implant Osseointegration'. *European Cells and Materials,* 16: 56-68.

Tsuzaki, M., Bynum, D., Almekinders, L., Yang, X., Faber, J. and Banes, A. J. (2003b) 'ATP Modulates Load-Inducible IL-1beta, COX 2, and MMP-3 Gene Expression in Human Tendon Cells'. *J Cell Biochem,* 89(3):556-562.

Tsuzaki, M., Guyton, G., Garrett, W., Archambault, J. M., Herzog, W., Almekinders, L. C., Bynum, D., Yang, X. and Banes, A. J. (2003a) 'IL-1β Induces COX2, MMP-1, -3, and -13, ADAMTS-4, IL-1β and IL-6 in Human Tendon Cells'. *Journal of Orthopaedic Research*, 21: 256-264.

Varki, A., Cummings, R. D., Esko, J. D., Freeze, H. H., Stanley, P., Bertozzi, C. R., Hart, G. W. and Etzler, M. E. (2009) *Essentials of Glycobiology*. 2nd Edition, New York: Cold Spring Harbor Laboratory Press.

Wall, M. E. and Banes, A. J. (2005) 'Early Responses to Mechanical Load in Tendon: Role for Calcium Signaling, Gap Junctions and Intercellular Communication'. *J Musculoskelet Neuronal Interact*, 5(1): 70-84.

Wang, C. J. (2012) 'Extracorporeal Shockwave Therapy in Musculoskeletal Disorders'. *Journal of Orthopaedic Surgery and Research*, 7(11): 1-8.

Wang, J. H.C. (2006) 'Mechanobiology of Tendon', *Journal of Biomechanics*, **39,** 1563-1582.

Wang, J. H., Iosifidis, M. I. and Fu, F. H. (2006) 'Biomechanical Basis for Tendinopathy'. *Clin Orthop Relat Res*, 443: 320-322.

Wang, T., Lin, Z., Day, R. E., Gardiner, B., Landao-Bassonga, E., Rubenson, J., Kirk, T. B., Smith, D. W., Lloyd, D. G., Hardisty, G., Wang, A., Zheng, Q. and Zheng, M. H. (2013) 'Programmable Mechanical Stimulation Influences Tendon Homeostasis in a Bioreactor System'. *Biotechnology and Bioengineering*, 1-13.

Wang, C. J., Wang, F. S., Yang, K. D., Weng, L. H., Hsu, C. C., Huang, C. S. And Yang, L. C. (2003) 'Shock Wave Therapy Induces Neovascularization at the Tendon-Bone Junction: A Study in Rabbits'. *Journal of Orthopaedics Research*, 21: 984-989.

Wang, N., Tytell, J. D. and Ingber, D. E. (2009) 'Mechanotransduction at a Distance: Mechanically Coupling the Extracellular Matrix with the Nucleus'. *Nature Reviews: Molecular Cell Biology*, 10: 75-82.

Wasielewski, N. J. and Kotsko, K. M. (2007) 'Does Eccentric Exercise Reduce Pain and Improve Strength in Physically Active Adults with Symptomatic Lower Extremity Tendinosis? A Systematic Review'. *Journal of Athletic Training*, 42(3): 409-421.

Watanabe, T., Imamura, Y., Suzuki, D., Hosaka, Y., Ueda, H., Hiramatsu, K. and Takehana, K. (2012) 'Concerted and Adaptive Alignment of Decorin Dermatan Sulfate Filamnets in the Equine Organization of Collagen Fibrils in the Equine Superficial Digital Flexor Tendon'. *Journal of Anatomy*, 220(2): 156-163.

Waugh, C. M., Morissey, D., Jones, E., Riley, G. P., Langberg, H. and Screen, H. R. C. (2015) '*In Vivo* Biological Response to Extracorporeal Shockwave Therapy in Human Tendinopathy'. *European Cells and Materials*, 29: 268-280.

Weber, A., Wasiliew, P. and Kracht, M. (2010) 'Interleukin-1 (IL-1) Pathway'. *Science Signalling*, 19;3(105): cm1.

Wehrle, E., Liedert, A., Heilmann, A., Wehner, T., Bindl, R., Fischer, L., Haffner-Luntzer, M., Jakob, F., Schinke, T., Amling, M. and Ignatius, A. (2015) 'The Impact of Low – Magnitude high-Frequency Vibration on Fracture Healing is Profoundly Influenced by the Oestrogen Status in Mice'. *Dis Model Mech*, 8(1): 93-104.

Weinhold, P, Hill, J. and Banes, A. J. (2001) 'A Tissue Explant Model for Investigating Tendon Overuse Injury'. *Trans Orthop Res Soc*. 47:702.

Weiss, A. and Attisano, L. (2012) 'The TGFbeta Superfamily Signalling Pathway'. *Wiley Interdisciplinary Reviews: Developmental Biology*, 2(1): 47-63.

Wenstrup, R. J., Florer, J. B., Brunskill, E. W., Bell, S. M., Chervoneva, I. and Birk, D. E. (2004). 'Type V Collagen Controls the Initiation of Collagen Fibril Assembly'.*The Journal of Biological Chemistry*. 279(51): 53331-53337.

Wheeler, P. C. (2014) 'The Use of High-Volume Image-Guide Injections (HVIGI) for Achilles Tendinopathy – A Case Series and Pilot Study'. *Internation Musculoskeletal Medicine*, 36(3): 96-103.

Wilde, B., Havill, A., Priestley, L., Lewis, J. and Kitchen, S. (2011) 'The Efficacy of Sclerosing Injections in the Treatment of Painful Tendinopathy'. *Physical Therapy Reviews*, 16(4): 244-260.

Wilson, M. and Stacy, J. (2011) 'Shock Wave Therapy for Achilles Tendinopathy'. *Currents Reviews in Musculoskeletal Medicine,* 4(1): 6-10.

Wipff, P. J. and Hinz, B. (2008) 'Integrins and the Activation of Latent Transforming Growth Factor Beta1 - An Intimate Relationship'. *Eur. J. Cell Biol*, 87: 601-615.

Witvouw, E., Mahieu, N., Roosen, P. and McNair, P. (2007) 'The Role of Stretching in Tendon Injuries'. *Br J Sports Med*, 1: 224-226.

Wong, M. W. N., Lui, W. T., Fu, S. C. and Lee, K. M. (2009) 'The Effect of Glucocorticoids on Tendon Cell Viability in Human Tendon Explants'. *Acta Orthop,* 80(3): 363-367.

Wren, T. A. L., Yerby, S. A., Beaupre, G. S. and Carter, D. R. (2001) 'Mechanical Properties of the Human Achilles Tendon'. *Clinical Biomechanics,* 16: 245-251.

Xu, Y., Wang, Q., Li, Y., Gan, Y., Li, S., Zhou, Y. and Zhou, Q. (2015) 'Cyclic Tensile Strain Induces Tenogenic Differentiation of Tendon-Derived Stem Cells in Bioreactor Culture. *BioMed Research International,* 2015: 1-15.

Yamamoto, E., Kogawa, D., Tokura, S. and Hayashi, K. (2005) 'Effects of the Frequency and Duration of Cyclic Stress on the Mechanical Properties of Cultured Collagen Fascicles from the Rabbit Pattelar Tendon'. *J Biomech Eng,* 127(7): 1168-1175.

Yan, G., Im, H. J. and Wang, J. H. (2005) 'Repetitive Mechanical Stretching Modulates IL-1beta Induced COX-2, MMP-1 Expression, and PEG2 Production in Human Patellar Tendon Fibroblasts'. *Gene,* 19(363):166-172.

Yan, J. Stringer, S. E., Hamilton, A., Charlton-Menys, V., Gotting, C., Miller, B., Aeschlimann, D. and Alexander, M. Y. (2011) 'Decorin GAG Sysnthesis and TGF-β Signalling Mediate Ox-LDL-Induced Mineralization of Human Vascular Smooth Muscle Cells'. *Arteriosclerosis, Thrombosis and Vascular Biology, Journal of the American Heart Association*, 31: 608-615.

Yang, G., Crawford, R. C. and Wang, H. H. C. (2004) 'Proliferation and Collagen Production of Human Patellar Tendon Fibroblast in Response to Cyclic Uniaxial Stretching in Serum-Free Conditions'. *Journal of Biomechanics*, 37(2004): 1543-1550.

Yang, G., Im, H. J. and Wang, J. H. C. (2005) 'Repetitive Mechanical Stretching Modulates IL-1β Induced COX-2, MMP-1 Expression, and PGE_2 Production in Human Patellar Tendon Fibroblasts'. *Gene*, 363: 166-172.

Yin, M., Yeung, E., Li, B., Li, W., Lui, M. and Tsoi, C. (2003). 'Sonographic Evaluation of the Size of Achilles: The Effect of Exercise and Dominance of the Ankle'. *Ultasound in Medicine & Biology*. 29(5): 637-642.

Yoon, J. H. and Halper, J. (2005) 'Tendon Proteoglycans: Biochemistry and Function'. *J Musculoskelet Neuronal Interact*, 5(1): 22-34.

Young, M. (2012) 'Stem Cell Applications in Tendon Disorder: A Clinical Perspective'. *Stem Cells International*, 2012, 1-10.

Young, M. A., Cook, J. L., Purdam, C. R. Kiss, Z. S. and Alfredson, H. (2005) 'Eccentric Decline Squat Protocol Offers Superior Results at 12 Months Compared with Traditional Eccentric Protocol for Patellar Tendinopathy in Volleyball Players'. *Br J Sports Med*, 39: 102-105.

Yu, H. S., Kim, J. J., Kim, H. W., Lewis, M. P. and Wall, I. (2015) 'Impact of Mechanical Stretch on the Cell Behaviors of Bone and Surrounding Tissues'. *Journal of Tissue Engineering*, 7: 1-24.

Yu, X., Dillon, G. P. and Bellamkonda, R. B. (1999). 'A Laminin and Nerve Growth Factor-Laden Three-Dimensional Scaffold for Enhanced Neurite Extension'. *Tissue Eng*, 5(4): 291-304.

Zaman, T. K., Roebuck, M. M., Williams, R. L. and Frostick, S. P. (2013) 'Effects of Cyclical Loading on Tendon Fibroblast Metabolism *In Vitro*'. *56th Annual Meeting of the Orthopaedic Research Society*, Poster No. 886.

Zhang, A. Y., Pham, H., Ho, F., Teng, K., Longaker, M. T. and Chang, J. (2004) 'Inhibition of TGFβ Induced Collagen Production in Rabbit Flexor Tendons'. *The Journal of Hand Surgery*, 29(2): 230-235.

Zhang, G., Young, B. B., Ezura, Y., Favata, M., Soslowsky, L. J., Chakravarti, S. and Birk, D. E. (2005) 'Development of Tendon Structure and Function: Regulation of Collagen of Collagen Fibrillogenesis'. *J Musculoskelet Neuronal Interact*, 5(1): 5-21.

Zhang, J. and Wang, J. H. C. (2013) 'The Effects of Mechanical Loading on Tendons – An *In Vivo* and *In Vitro* Model Study'. *PLoS One*, 8(8): e71740.

Zhang, J., Li, Y., Shan, K., Wang, L., Qiu, W., Lu, Y., Zhao, D., Zhu, G., He, F. and Wang, Y. (2014) 'Sublytic C5b-9 Induces IL-6 and TGF-1 Production by Glomerular Mesangial Cells in Rat Thy-1 Nephritis Through p300-Mediated C/EBP Acetylation'. *The FASEB Journal*, 28(3): 1511-1525.

Zhang, K., Asai, S., Yu, B. and Enomoto-Iwamoto, M. (2015) 'IL-1β Irreversibly Inhibits Tenogenic Differntiation and Alters Metabolism in Injured Tendon-Derived Progenitor Cells *In Vitro*'. *Biochenical and Biophysical Research Communications*, 463(4): 667-672.

Zhang, L., David G. and Esko, J. D. (1995) 'Repetitive Ser-Gly Sequences Enhances Heparan Sulfate Assembly in Proteoglycans'. *The Journal of Biological Chemistry*, 270(45): 27127-27135.

Zhang, P., Tanaka, S. M., Sub, Q., Turner, C. H. and Yokota, H. (2007) 'Frequency-Dependent Enhancement of Bone Formation in Murine Tibiae and Femora with Knee Loading'. *Journal of Bone and Mineral Metabolism*. 25(6): 383-391.

Zhang, Y. H., Zhao, C. Q., Jiang, L. S. and Dai, L. Y. (2011) 'Substrate Stiffness Regulates Apoptosis and the mRNA Expression of Extracellular Matrix Regulator Genes in the Rat Annular Cells'. *Matrix Biology*, 30: 135-144.

APPENDIX

MATERIALS

2-Propanol	Sigma – Aldrich, I9516
Anti-IL1 alpha antibody	Abcam, ab9614
Calcein AM	Cambridge Bioscience, BT80011
Collagenase from Clostridium histolyticum	Sigma – Aldrich, C5138
Corning CellBIND surface cell culture flasks:	
150cm^2	Sigma – Aldrich, CLS3291
75cm^2	Sigma – Aldrich, CLS3290
25cm^2	Sigma – Aldrich, CLS3289
Corning CellBIND cell culture multiwall plates (6 well culture plate)	Sigma – Aldrich, CLS3335
Corning 15ml centrifuge tubes	Sigma – Aldrich, CLS430791
Corning 50ml centrifuge tubes	Sigma – Aldrich, CLS430291
Corning costar stripette serological pipetes, individually paper/plastic wrapped:	
5ml	Sigma – Aldrich, CLS4487
10ml	Sigma – Aldrich, CLS4488
25ml	Sigma – Aldrich, CLS4489
Chloroform	Sigma – Aldrich, C2432
Collagen gel	First Link UK, 6030810
Cytokine antibody array (Membrane, 80 targets)	Abcam, ab133998
DMEM (1X)	Life Technologies, 11880-036
DMEM, low glucose	ThermoFisher Scientific, 21885-108
dNTPs, 10mM	Promega, U1515
Dulbecco's phosphate buffered saline	Sigma – Aldrich, D8537
Ethanol, 200 proof	Sigma – Aldrich, E7023
Foetal Bovine Serum	Sigma – Aldrich, F7524, Batch number: 111M3395
Glycogen (5mg/ml)	Life Technologies, AM9510
HEPES Solution (1M)	Sigma – Aldrich, H0887

L-Glutamine Solution (200mM)	Sigma – Aldrich, G7513
MEM (10X)	Life Technologies, 11430-030
MEM Non-essential amino acid solution (100X)	Sigma – Aldrich, M7145
Nuclease-Free water (not DEPC-Treated)	Life Technologies, AM9937
Penicillin-Streptomycin 10000 units penicillin and 10mg streptomycin per ml	Sigma – Aldrich, P4333
Phase lock gel heavy (2ml)	5 Prime, 2302830
Pipette filter tips sterilised (1000ul)	Gilson, F171803
RNaseZap RNase decontamination wipes refill	Life Technologies, AM9788
RNaseZap RNase decontamination solution	Life Technologies, AM9780
Sodium bicarbonate	Sigma – Aldrich, S8875
Sodium hydroxide pellets	Sigma – Aldrich, S8045
SuperScript II Reverse Transcriptase	Life Technologies, 18064-014
Taqman Universal PCR Master Mix No AmpErase UNG	Life Technologies, 4324018
TGFβ inhibitor	Sigma – Aldrich, SB431542
Trizol Reagent	Sigma – Aldrich, T9424
Trypsn Blue	Sigma – Aldrich, T8154
Trypsin-EDTA solution (1X concentration)	Sigma – Aldrich, T4049
Whatman filter paper	Lab shop, 1001-25

PUBLICATIONS AND PRESENTATIONS

Paper in Draft:

- Response of tenocytes seeded in 3D collagen gel to high frequency loading. C. P. Udeze-Jyambere, E. R. Jones, G. P. Riley, D. Morrissey, H. R. C. Screen

Abstract Publications:

- The effect of loading frequency on tenocyte metabolism. C. P. Udeze, E. R. Jones, G. P. Riley, D. Morrissey, H. R. C. Screen. (2015) *The bone and joint journal*, 97-B(SUPP 11), 26.

Poster Presentations:

- The effect of loading frequency on tenocyte metabolism. Advances in tendon research: From bench to bedside. BSMB satellite conference 2015, London UK.
- The role of high frequency loading in the treatment of tendinopathy. Orthopaedic research UK furlong Christmas lecture 2015, London UK.
- The effect of loading frequency on tenocyte metabolism. Summer Biomechanics, Bioengineering and Biotransport Conference (SB^3C) 2016, Maryland, USA.